ANALYSIS OF NEURONAL SURVIVAL IN THE PRESENCE OF VARIOUS STRESS CONDITIONS AND TARGETED DELIVERY

Thesis submitted to the

University of Hyderabad for the award of the degree

DOCTOR OF PHILOSOPHY

in

BIOTECHNOLOGY

by

ATHMAKUR HARI KIRAN

Enrollment No: 11LTPH05

Department of Biotechnology and Bioinformatics

School of Life Sciences

University of Hyderabad

Hyderabad 500 046

India

June 2019

Department of Biotechnology & Bioinformatics
School of Life Sciences
University of Hyderabad
Hyderabad-500046. Telangana, India.

CERTIFICATE

This is to certify that thesis entitled **"Analysis of neuronal survival in the presence of various stress conditions and targeted delivery"** is a record of bonafide work done by **Mr. Athmakur Hari Kiran Goud**, a research scholar for the Ph.D. programme in the Department of Biotechnology and Bioinformatics, University of Hyderabad under my guidance and supervision. The thesis has not been submitted previously in part or full to this or any other University or Institution for the award of any degree or diploma. I recommend his thesis for submission towards the partial fulfillment of 'Doctor of Philosophy' degree in Biotechnology.

Supervisor	Head Department of Biotechnology and Bioinformatics	Dean School of Life Sciences

Department of Biotechnology & Bioinformatics
School of Life Sciences
University of Hyderabad
Hyderabad-500046. Telangana, India.

CERTIFICATE

This is to certify that the thesis entitled **"Analysis of neuronal survival in the presence of various stress conditions and targeted delivery"** submitted by **Mr. Athmakur Hari Kiran Goud** bearing registration number 11LTPH05 in partial fulfilment of the requirements for award of 'Doctor of Philosophy' in the Department of Biotechnology and Bioinformatics, School of Life Sciences is a bonafide work carried out by him under my supervision and guidance.

This thesis is free from plagiarism and has not been submitted previously in part or in full to this or any other University or Institution for the award of any degree or diploma.

Further, the student has the following publication before submission of the thesis for adjudication and has produced evidence for the same in the form of the reprint in the relevant area of his research:

Athmakur, H., & Kondapi, A. K. (2018). Carmustine loaded lactoferrin nanoparticles demonstrates an enhanced antiproliferative activity against glioblastoma in vitro. International Journal of Applied Pharmaceutics, 10(6), 234-241.

Further, the student has passed the following courses towards the fulfillment of coursework requirement for Ph.D. degree:

S.No.	Course code	Name	Credits	Pass/Fail
1	BT 801	Seminar	1	Pass
2	BT 802	Research ethics and management	2	Pass
3	BT 803	Biostatistics	2	Pass
4	BT 804	Analytical techniques	3	Pass
5	BT 805	Lab work	4	Pass

Supervisor Head of the Department Dean of the School

Department of Biotechnology & Bioinformatics
School of Life Sciences
University of Hyderabad
Hyderabad-500046. Telangana, India.

DECLARATION

I, **Athmakur Hari Kiran Goud**, hereby declare that the work presented in this thesis, entitled as **"Analysis of neuronal survival in the presence of various stress conditions and targeted delivery"** has been carried out by me under the supervision of Prof. Anand K. Kondapi, Department of Biotechnology and Bioinformatics. To the best of my knowledge, thiswork has not been submitted for the award of any degree or diploma at any other University or Institution. I hereby agree that my thesis can be deposited in Shodganga/INFLIBNET.

A report on plagiarism statistics from the University Librarian is enclosed.

Place: Hyderabad — Athmakur Hari Kiran Goud

Date: — 11LTPH05

ACKNOWLEDGEMENTS

This thesis would not have been possible without the care, support, and guidance of many people who contributed directly or indirectly during my entire journey of Ph.D. I shall be highly indebted to all of you, and now it is my opportunity to thank all of you.

First and foremost, I am highly thankful to almighty GOD for rewarding me health and wisdom to accomplish this work.

I express my heartfelt gratitude and utmost respect to my supervisor, Prof. Anand Kumar Kondapi, who has supported me throughout my work with his patience and guidance. His critical inputs and fruitful discussions have always been a great support throughout my research work.

I am thankful to the present Dean, School of Life sciences Prof. S. Dayananda and former Deans Prof. K. V. A Ramaiah, Prof. Reddanna, Prof. R. P Sharma, Prof A. S. Raghavendra, & Prof M. Ramanadham for enabling necessary facilities to carry out my research work.

I am also thankful to the present Head of Department of Biotechnology & Bioinformatics- Prof. K. P. M. S. V. Padmasree, and former Heads Prof. Anand Kumar Kondapi, Prof. Niyaz Ahmed & Prof. P. Prakash Babu for helping me with all the logistics & facilities needed for my research work.

My sincere gratitude to my doctoral committee members, Dr. N. Prakash Prabhu, and Dr. Sunanda Bhattacharyya, for their valuable inputs and constructive comments during my Ph.D. tenure.

I thank all the faculty members of School of Life Sciences for their cooperation and extended support during my research work.

I wish to thank Mrs. Leena Bhashyam, for the assistance in Genomics facility.

I am thankful to Council of Scientific & Industrial Research (CSIR) for the financial support in the form of fellowship during the tenure of my Ph.D., and I am also thankful to funding agencies of Govt. of India (DST, DBT, CSIR, and ICMR) for funding our laboratory and Departments.

I would like to thank my present and past lab mates - Dr. Bhaskar, Dr. Udhay Bhanu, Dr. Priti, Dr. Upendra Dr. Kishore Golla, Dr. Balakrishna, Dr. Sarada, Dr. Farhan,

Dr. Satish, Dr. Pankaj, Dr. Kurumurthy, Dr. Prashant, Dr. Laxmi, Late Srujana, Akhila, Suresh, Jagadeesh, Priya, Chuku, Neha, Satayajit, Kriti, and Reena.

Special thanks to my seniors Dr. Bhaskar, Dr. Farhan, and Dr. Preeti, for helping me in acquiring the technical skills and scientific insights. I want to thank especially Akhila, Suresh, and Dr. Pankaz, who made my work feasible at difficult times.

I want to acknowledge the lab attenders - Chandra, Srinivas, and Srinivas Murthy for the lab maintenance and document processing activities.

I am also thankful to my friends Dr. Pardhu Yella, Dr. Farhan, Deepak, Madhavi, Dr. Surendra Kolli, Dr. Rameshwar Segireddy, Kiranmayi, Sravan, Dr. Sai Krishna, Dr. J. Ravi and Bhavani Shankar for their various kind of support in thick and thin patches of life during my stay in this University.

I am thankful to all the SLS friends for their help and support during my research work.

Deep from my heart I thank to Dr. K. Ramachandra Rao, Warden, J & K hostel, for having an affectionate bonding with me and for his valuable suggestions, help & constant moral support during my stay in the hostel.

I express my sincere gratitude to Ramesh Sharma, Erudite coaching centre for helping me in achieving CSIR and ICMR JRFs.

I want to acknowledge my Class IX Biology Teacher, Intermediate course Teachers, and especially Telugu academy board (for their books) for igniting research passion in me.

I express my heartfelt gratitude to all my teachers from my Schooling to Ph.D., because of whose teaching at different stages of my education, has made it possible for me to reach this stage.

My parents and family members are the greatest sources of inspiration; there unconditional love and care have been a great source of strength and helped me in accomplishing my goals.

It will be an immense pleasure to me to express my love and gratitude to my lovely brother-in-law, Mr. Anil Kumar Gorkal, and my dearest sister Mrs. Sushma Gorkal. They are the truly admirable people, who always help me well before the need arises and

always stands with me in my up & downs. Their unconditional love and affection make me feel fortunate to have them in my life.

Words fall short, to express my sincere thanks to my elder brother, Mr. Sai Prasad, without whose unconditional love, constant encouragement, unwavering confidence, emotional & economical support all through and especially, during the toughest times in my life, I couldn't have achieved this goal.

I express my deepest gratitude and reverence to my Late Father, Sri. Nagarathnam garu, who had this dream and confidence in me. This confidence of his has been a major driving force which kept me focused and determined throughout these years. I wish he could be here today.

-Hari Kiran.

Dedicated

to

My Parents

CONTENTS

ABBREVIATIONS

ASIA	: Autoimmune syndrome induced by adjuvants
AMPK	: Adenosine monophosphate-activated protein kinase
Atg5	: Autophagy-related gene 5
ATP	: Adenosine triphosphate
BBB	: Blood-brain barrier
BCNST	: Brain and other central nervous system tumors
BDNF	: Brain-derived neurotrophic factor
BER	: Base Excision Repair
BSA	: Bovine serum albumin
bp	: Base pairs
CBTRUS	: Central brain tumor registry of the United States
cDNA	: complementary Deoxyribonucleic acid
CLN	: Carmustine loaded lactoferrin nanoparticles
CMF-HBSS	: Calcium, magnesium free Hanks' balanced salt solution
CNS	: Central nervous system
Ca^{2+}	: Calcium
CO_2	: Carbon dioxide
CR	: Calorie Restriction
Da	: Dalton
DAPI	: 4′,6-diamidino-2-phenylindole
DCM	: Dilated cardiomyopathy
DEPC	: Diethyl pyrocarbonate
DIV	: Days *in vitro*
DKC1	: Dyskeratosis congenita 1
DLS	: Dynamic light scattering
DMEM/F12	: Dulbecco's modified eagle medium/Nutrient mixture F-12
DMSO	: Dimethyl sulfoxide
DNA	: Deoxyribonucleic acid
DR	: Dietary restriction
DSBs	: Double-strand breaks

dNTPs	: Deoxy nucleotide triphosphates
EDTA	: Ethylene diamine tetra acetic acid
Em	: Emission wavelength
Ex	: Excitation wavelength
E18	: Embryonic day 18
FBS	: Fetal Bovine Serum
FoxO	: Fork head box O
FESEM	: Field emission scanning electron microscope
GDNF	: Glial cell line-derived neurotrophic factor
GFAP	: Glial cell fibrillary acidic protein
GH	: Growth hormone
GHR-BP	: GH receptor–binding protein
HBSS	: Hanks' balanced salt solution
HCM	: Hypertrophic cardiomyopathy
HPLC	: High-performance liquid chromatography
h	: Hour
IC_{50}	: 50% Inhibitory Concentration
IFNγ	: Interferon gamma
IGF-1	: Insulin-like growth factor 1
IGFBP1	: Insulin-like growth factor-binding protein 1
hTR	: human telomerase RNA
LMNA	: Lamin A/C
MAP2	: Membrane-associated protein 2
MEM	: Minimum essential media
MMP	: Mitochondrial membrane potential
MPTP	: 1-methyl-4-phenyl- 1,2,3,6-tetrahydropyridine
MRI	: Magnetic resonance imaging
MTT	: 3-(4,5-dimethylthiozol-2-yl)-2,5 diphenyl tetrazolium bromide
mA	: Milli Ampere
mg	: Milligram
min	: Minutes

mM	: Millimolar
mm^2	: Square millimetre
mRNA	: Messenger Ribonucleic acid
mTOR	: Mammalian target of Rapamycin,
mV	: Millivolts
NCCS	: National centre for cell science
NLCs	: Nanostructured Lipid Carriers
NPY	: Neuropeptide Y
n	: Sample size
nm	: Nanometer
PACA	: Poly(alkylcyanoacrylates)
PBCA	: Poly(n-butylcyanoacrylate)
PBS	: Phosphate buffer saline
PFA	: Paraformaldehyde
Pdl	: Poly-d-lysine
PDI	: Polydispersity index
PGA	: Poly-glycolic acid
pH	: Potential of Hydrogen
PI3K	: Phosphoinositide 3-kinase
PKA	: Protein kinase A
PLA	: Poly-lactic acid
PLGA	: Poly-(lactic-co-glycolic acid)
PMRS	: Plasma membrane redox system
RNA	: Ribonucleic acid
RT	: Room temperature
SA β-gal	: Senescence-associated beta-galactosidase
SLIT2	: Slit homolog 2 protein
SLNs	: Solid Lipid Nanoparticles
S6K	: Ribosomal S6 protein kinase
TJ	: Tight junctions
Topo II β	: Topoisomerase II β

U	: Enzyme unit
WHO	: World health organization
WRN	: Werner syndrome
X-gal	: 5-Bromo-4-chloro-3-indolyl-β-D-galacto-pyranoside
µg	: Microgram
µL	: Microliter
µM	: Micromolar

LIST OF FIGURES

LIST OF TABLES

CHAPTER 1:

GENERAL INTRODUCTION

BRAIN:

The brain is the principal information processing organ of Human beings and other animals. It acts like the 'command and control system.' It controls the voluntary movements, the functioning of critical involuntary organs (e.g., heart, kidneys, lungs, etc.), balance of the body, hunger and thirst, thermoregulation, circadian rhythms of the body, behavior, activities of various endocrine glands, etc. It is also the location for processing the information relating to vision, speech, hearing, intelligence, memory, emotions, and thoughts.

The brain is very well protected by the skull. Inside the skull, cranial meninges cover the brain. Meninges consist of three-layered membranes viz., dura mater, the outer membrane; pia mater, the inner layer; and arachnoid, the thin middle layer. Brain tissue will be in contact with the pia mater. Between the arachnoid matter and the pia mater is the subarachnoid space, which accommodates the cerebrospinal fluid. Cerebrospinal fluid function as a shock absorber and also circulate chemical substances all over the brain. The brain can be partitioned into three major parts, namely forebrain, midbrain, and hindbrain.

The forebrain comprises of the cerebrum, hypothalamus, and thalamus. Cerebrum constitutes a major portion of the human brain. The cerebrum is longitudinally divided into two halves by a deep cleft. One half of the cerebrum is called the left cerebral hemisphere and the other half as the right cerebral hemisphere. Corpus callosum, a tract of nerve fibers connect the two hemispheres. Each cerebral hemisphere is overlaid by a layer of cells called cerebral cortex, which is organized into prominent folds. Neuron cell bodies are concentrated in the cerebral cortex, which gives the greyish appearance; hence, the cerebral cortex is also called grey matter. Myelinated axons compose the inner portion of the cerebral hemisphere. As myelinated axons give the white appearance to the inner portion, it is called white matter. The cerebral cortex comprises of sensory areas, motor areas, and large areas that are not distinctly motor or sensory in function. These large areas are called association areas and are responsible for performing complex functions such as inter-sensory associations, communication, and memory. The motor areas are concerned with the planning, control, and performance of voluntary movements. The sensory

areas are concern with the auditory, gustatory, olfactory, visual, and somatosensory sensations.

The cerebrum encloses a structure known as the thalamus, which is a leading, coordinating centre for motor and sensory signaling. Underneath thalamus, the hypothalamus is present that comprises numerous centres which regulate hunger, thirst, body temperature, etc. Hypothalamus also contain numerous clusters of neurosecretory cells, which synthesize and secrete certain hormones that regulate the secretion of pituitary hormones. The innermost regions of the cerebrum and its associated structures such as the hippocampus, amygdala, etc., constitute an intricate structure called the limbic system. Limbic system, together with hypothalamus regulate sexual behavior, involve in memory formation, expression of emotions such as fear, rage, pleasure, excitement, etc.

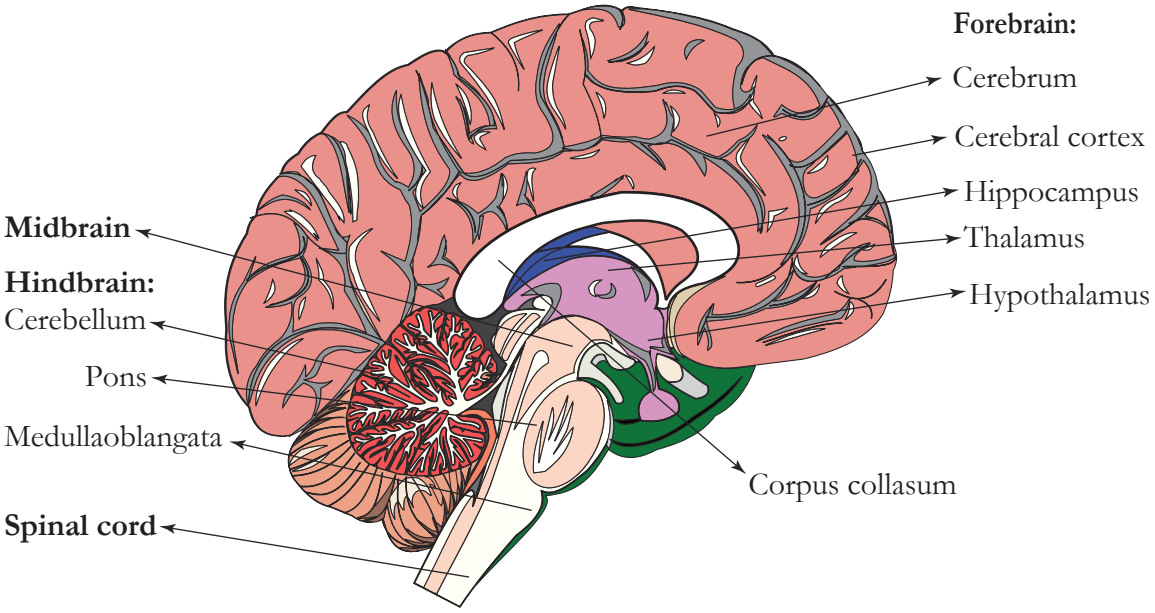

Figure 1: Cross section of the Human brain.

A region between pons of the hindbrain and hypothalamus/thalamus of the forebrain is the midbrain. Tectum, basis pedunculi, tegmentum, and cerebral aqueduct are the parts of the midbrain. It controls movement, attention, behavior, mood, habits, etc. The hindbrain consists of the medulla oblongata, cerebellum, and pons. Pons comprises fibre tracts and neural pathways which make communication between

different regions of the brain. After cerebrum, the cerebellum is the largest structure in the brain, and it contains the highest number of neurons compared to other brain parts. It is structurally separated into three lobes: anterio-posterior lobes, central vermis, and outer floccular lobes. It controls balance, assists in coordinating movement and also assists in learning new motor tasks. Medulla connects the spinal cord to the brain. It contains centres which control cardiovascular reflexes, respiration, and gastric secretions. Medulla, pons, and midbrain together form brain stem (Tortora & Derrickson, 2011).

NEURON:

The neuron is the fundamental functional unit of the brain. Neurons are electrically excitable cells that send and receive information from and to the brain through electrochemical signals. It is estimated that there are 100 billion neurons in the human brain. Neurons vary widely in size, morphology, functions, etc. However, almost all the neurons have three common parts viz., cell body, dendrites, and axon. The cell body is also known as soma comprises nucleus, special granular bodies named Nissl's granules, other typical cell organelles, and cytoplasm. Major protein synthesis and protein sorting occur in the cell body. Cell body also contains a specialized portion called axon hillock, from which axon emerges. Axon hillock is one of the important sites of initiation of the action potential in the neuron. Its plasma membrane contains densely populated voltage-gated ion channels (Tortora & Derrickson, 2011).

Dendrites are short cellular processes projecting from the cell body. They branch profusely and become gradually thinner with each branching. They receive and transmit impulses to the cell body. They contain Nissl's granules. Tiny spines are studded on dendrites, which further increase dendrite's receptive surface area. Spines are morphologically heterogeneous, which categorize them as thin, stubby, mushroom-shaped, filopodia and long spines. Functionally, spine morphology is concerned with synaptic strength. For instance, expression of larger spines, such as mushroom spines, indicate stronger synaptic connections. Further, spines can be morphologically dynamic; they alter their morphology as per the incoming stimuli and thereby contribute to the synaptic plasticity. Synaptic plasticity is one among the crucial neurochemical bases of learning and memory. Abnormalities in spine

morphology and numbers are associated with many psychiatric diseases, depressive disorders, and neurologic diseases like schizophrenia, Alzheimer's disease, etc. (Barha, Nagamatsu, & Liu-Ambrose, 2016).

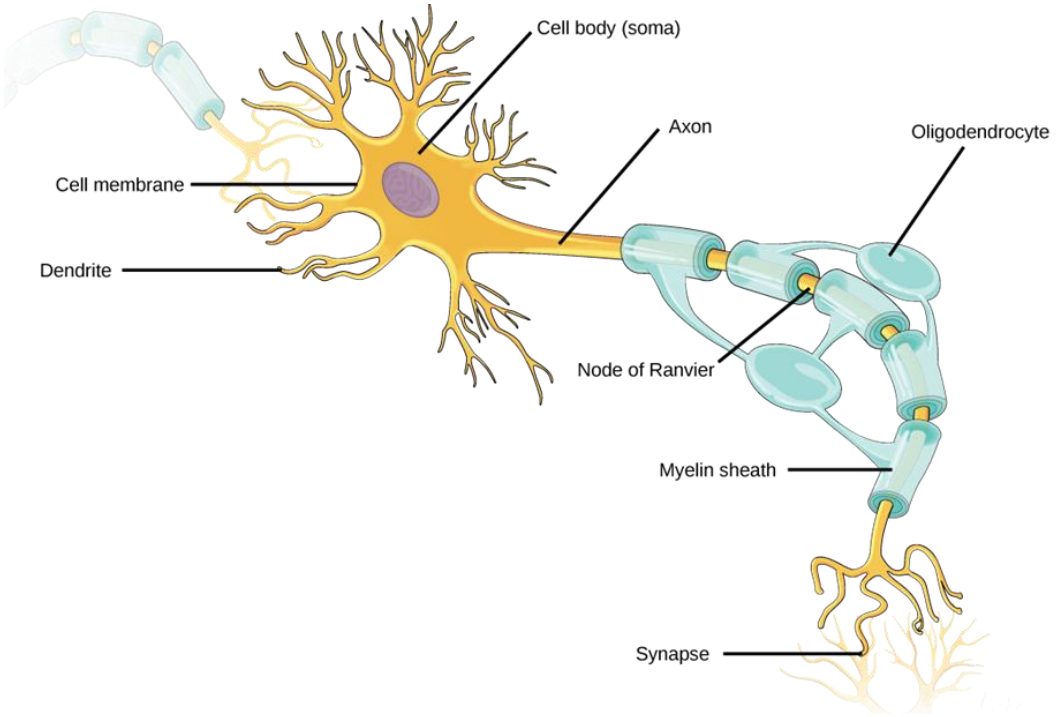

Figure 2: Structure of a typical neuron.

Note. "From 'Neurons and glial cells,' by OpenStax, 2016, http://cnx.org/contents/185cbf87-c72e-48f5-b51e-f14f21b5eabd@10.61. © 2016; used under Creative Commons Attribution License 4.0."

Axon also called nerve fibre is a single, long cellular process that projects from the cell body at a location called axon hillock. An axon can extend to longer distances (in Human, it can extend up to 1 meter) and can branch a number of times before termination; however, it preserves its diameter. Every axon branch ends as a bulb-like formation called synaptic knob, which contains vesicles loaded with neurotransmitters. Axons transfer nerve impulses from the soma to a neuro-muscular junction or a synapse. Most of the axons are wrapped with sheaths of myelin, which escalates the speed of nerve impulse transmission by 10 to 100 folds compared to non-myelinated axons of equivalent diameter while consuming less energy. In the brain, a class of glial cells called oligodendrocytes wrap the axons and synthesize these myelin sheaths. The spaces between two nearby myelin sheaths known as nodes of Ranvier

allow saltatory conduction of nerve impulse. Demyelination of axons results in a neurological disorder called Multiple sclerosis.

Neurons communicate with each other through synapses, where the synaptic knob, the axon terminal of one neuron contacts with another neuron's dendrite, or cell body or rarely axon. The gap between the contacts is called synaptic cleft, where presynaptic neurons release neurotransmitters, which activates receptors and regulate the transmission of nerve impulses in postsynaptic neurons. Neurons also communicate with muscle cells, glands, etc. via synapses. A typical neuron can form 1,000 to 10,000 synapses, and it is estimated that the total number of synapses in an adult human brain would be as many as 10^{14} to 5 x 10^{14} (Tortora & Derrickson, 2011).

TYPES OF NEURONS:

Neurons vary widely in size, morphology, the direction of flow of information, functions, etc. Based on the number of dendrites and axon, they can be classified into

Unipolar: Neurons with single neurite. Ex: Unipolar brush cells of the cerebellum and dorsal cochlear nucleus.

Bipolar: Neurons with single dendrite and single axon on opposite poles of the cell body. Ex: Retina bipolar cells.

Multipolar: Neurons with two or more dendrites and a single axon. Multipolar neurons are further divided into two types

- Golgi type I: multipolar neurons with long axons. Ex: anterior horn cells, Purkinje cells, and pyramidal cells.
- Golgi type II: multipolar neurons with short axons. Ex: granule cell.

Anaxonic: axon and dendrite(s) of the neuron cannot be distinguished.

Pseudounipolar: axon and dendrite develop from the same process. Ex: Neurons present in the dorsal root ganglia and sensory ganglia of cranial nerves.

Based on the location and distinct shape, several peculiar neuronal types can be found in the brain such as Lugaro cells (cerebellum), Medium spiny neurons (corpus striatum), Basket cells (cerebellum and cortex), Purkinje cells (giant neurons in the

cerebellum), Pyramidal cells (cerebral cortex), Unipolar brush cells (cerebellum and dorsal cochlear nucleus) etc.

Based on the function and the direction of flow of information, neurons are categorized as

Sensory neurons: They are also called afferent neurons. They respond to stimulus and carry information from sensory organs to the central nervous system (CNS).

Motor neurons: They are also called efferent neurons. They carry information from CNS to control effector organs such as glands, muscles, etc.

Interneurons: carry information between the neurons and connect them in neural networks.

Based on the type of neurotransmitter released from the neurons, neurons are also classified as cholinergic neurons (neurotransmitter released: acetylcholine), dopaminergic neurons (dopamine), GABAergic neurons (γ-aminobutyric acid), serotonergic neurons (serotonin), glutamatergic neurons (glutamate), etc. (Martini, 2007 ; Tortora & Derrickson, 2011).

GLIAL CELLS:

Glial cells are chief non-neuronal cells present in the brain. They do not conduct nerve impulse but offer supportive functions for the neurons. They constitute approximately 75% of the brain cellular population. They have complex cellular processes emerging from the cell body, but are usually smaller in size compared to neurons and are devoid of dendrites and axons. Major functions of glial cells are: to offer metabolic and physical support for neurons, to maintain the external ionic environment of neurons, to escalate the speed of nerve impulse transmission by myelination, by modulating neurotransmitters uptake regulate synaptic action, aid in neuronal migration during development, are part of blood-brain barrier, secrete trophic factors which support neuronal growth and survival, etc. (Purves et al., 2001).

Mainly three types of glial cells are found in brain namely astrocytes, oligodendrocytes, and microglia. Astrocytes are star-shaped cells that form the major population of glial cells and perform several functions such as maintaining ionic

environment, supplying nutrients for neurons, etc. Oligodendrocytes embrace the neuronal axons and synthesize myelin sheaths which escalate the speed of nerve impulse transmission. Microglia are tiny glial cells, which are specialized macrophages that play a major role in inflammation, tissue scavenging, etc. (Barha et al., 2016; Purves et al., 2001). Glial cells are implicated in a kind of brain tumors

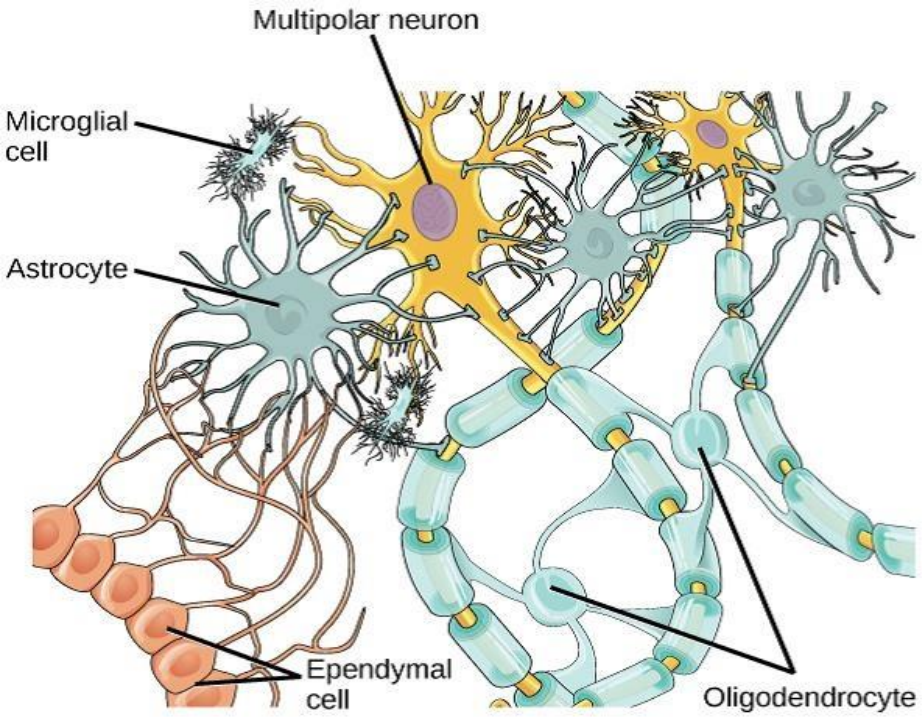

Figure 3: Major types of glial cells found in the brain.

Note. "From 'Neurons and glial cells,' by OpenStax, 2016, http://cnx.org/contents/185cbf87-c72e-48f5-b51e-f14f21b5eabd@10.61. © 2016; used under Creative Commons Attribution License 4.0."

called glioma, which is characterized by uncontrolled proliferation of glial cells (Omuro & DeAngelis, 2013). Malignant gliomas constitute 80% of the malignant CNS tumors. Among malignant gliomas, glioblastoma is the most aggressive and most common malignant tumor with poor prognosis and worst survival rates (Q. T. Ostrom et al., 2017).

AGEING:

"Ageing can be defined as a natural and progressive process occurring in all the living organisms and is characterized by the deterioration of the structure and functional capacities." (Lopez-Lluch & Navas, 2016, p. 2044). Essential features of aging are: alterations in the biochemical compositions in the cells and tissues (loss of the homeostasis) with the increase of age, progressive decline in physiological function with age, decreased ability to react adaptively to environmental incitements with age, increased vulnerability to diseases and increased mortality with the increase of age after maturation (Semsei, 2000; Troen, 2003). The Gompertz law of mortality states that in a protected environment, the age-dependent factor alone exponentially amplifies the mortality rate after sexual maturation (Olshansky & Carnes, 1997).

Ageing is inevitable, progressive, irreversible, a unidirectional process that occurs in all the individuals in almost all the species (Semsei, 2000). It can occur at all the organizational levels of an individual viz., organ, cellular and molecular levels (Mera, 1992). Aging is diverse; it can be diverse in the timing of initiation (heterochrony), diverse in phenotype (heterotroph), diverse in the direction (heterokaften) and diverse in the rate of progression (heterokinetic). Above features are diverse in different species and also in different individuals of the same species. Within the individual, they are diverse in different organs, and tissues, diverse in cells of the same tissue and can be even diverse in different organelles and different macromolecules within the same cell (Rattan, 2000; Semsei, 2000). Along with the genetic factors of an individual, the environmental factors affecting the individual contributes to the diversity of ageing (Carmona & Michan, 2016).

Every day approximately 150,000 people die globally due to various reasons. Among them, nearly 70% of the deaths are due to age-related causes (de Grey Aubrey, 2007). Age-related changes themselves may be a causative or contributory factor for certain diseases which are linked with old age. Hence, ageing is a major risk factor for many human diseases (Mera, 1992). Different aged individuals differently effect by different age-related diseases and even few individuals may not be effected by any of the age-related diseases (Arking, 2006).

Numerous theories were proposed to elucidate the mechanisms of ageing. A short summary of important theories is outlined in table 1. These theories independently only to a certain extent, explained the mechanism of ageing based on the single factorial cause. However, these theories failed to explain the complexity of ageing independently. These failures emphasize that ageing is not a single factorial cause, it is a multifactorial phenomenon and the theories of ageing are not mutually exclusive, but they are complementary to each other in the elucidation of the ageing mechanism. It is possible that various causes simultaneously interact and operate at various levels of a functional organization to induce ageing (Tosato, Zamboni, Ferrini, & Cesari, 2007; Weinert & Timiras, 2003). Therefore, ageing can be defined as an ultimate consequence of the failure of various maintenance mechanisms op at all the organizational levels of an organism (Holliday, 2006).

Table 1: Summary of important theories of ageing (Arking, 2006; Park & Yeo, 2013; Weinert & Timiras, 2003).

BIOLOGICAL LEVEL / THEORY	CAUSE OF AGEING
EVOLUTIONARY	
Antagonistic pleiotropy	Genes advantageous at younger ages become detrimental at older ages, thereby cause ageing.
Disposable soma	Soma is maintained only to assure persistent reproductive success. Soma becomes disposable after reproduction.
Mutation accumulation	Late-acting, detrimental mutations may accumulate in individuals with age and eventually lead to pathology and ageing.
MOLECULAR	
DNA damage and repair	With the increase of age, DNA repair efficiency decreases which leads to increased genetic damage.
Somatic mutation	The accumulation of mutations in the genetic material of somatic cells is the specific cause of ageing.
Error catastrophe	With the increase of age, there will be a decrease in the fidelity of gene expression leading to increased synthesis of abnormal proteins.
Gene regulation	Ageing is caused by fluctuations in gene expressions regulating both development and maturation.

Dysdifferentiation	Damaged gene activation-repression mechanisms cause synthesis of unnecessary proteins resulting in dysregulation of cellular growth and maintenance.
CELLULAR	
Oxidative damage/Free radical	Oxidative metabolism generates ROS which subsequently damages proteins, DNA, and lipids. Damaged macromolecules compromise cellular viability.
Waste accumulation	Waste products of metabolism pile up in the cell and will reduce the cell's efficiency to sub-optimal level.
Cellular senescence-Telomere theory	Phenotypes of aging are induced by an increase in the no. of senescent cells. Senescence possibly develops from telomere loss known as 'replicative senescence' and/or cell stress known as 'cellular senescence.'
Apoptosis	Programmed cell-death from genome crisis or genetic events.
Wear-and-tear	Accumulation of common injuries and insults of daily living compromise organism's efficiency to sub-optimal level.
Post-translational changes	Age-dependent chemical modification of vital macromolecules (e.g., collagen) damages tissue function and reduce the organism's efficiency to sub-optimal level. Protein cross-linking is one subclass of this theory.
SYSTEM	
Immunologic	Deterioration of immune function with aging increase susceptibility to infectious diseases and also escalate the incidence of autoimmunity.
Neuroendocrine	Fluctuations in neuroendocrine control of homeostasis with the age cause aging.
Rate-of-living	Higher the basal metabolic rate of an organism, the shorter its lifespan.

Aging Of the Cerebrum:

One of the important characteristic features of organismal ageing is the deterioration of brain function. Since cerebrum is the largest among the brain parts and involves in numerous motor, sensory and cognitive functions, it has drawn special attention from several researchers to study its age-associated changes. During ageing, cerebrum undergoes various structural, functional and chemical alterations.

The most prominent hallmark of brain ageing is its shrinkage. Shrinkage is also accompanied by the loss of brain weight and enlargement of ventricular volume (Dekaban, 1978; Foundas, Zipin, & Browning, 1998; Ho, Roessmann, Straumfjord, & Monroe, 1980). MRI studies showed shrinkage of the cerebrum in the brain with age (Jernigan et al., 1991; Raz, Briggs, Marks, & Acker, 1999). Age-related cerebral hemispheres atrophy is region specific. For example, extrapyramidal and orbital cortex show more than 15% atrophy, whereas parietal and occipital cortex show negligible atrophy (Haug H et al., 1983; Raz et al., 2005). In age-associated neurodegenerative diseases such as Alzheimer's disease, cerebral atrophy was reported to be much higher than normal ageing, usually around 20-25% (Mouton, Martin, Calhoun, Dal Forno, & Price, 1998). Loss of white matter due to the damage of myelinated fibers with age contributes to the shrinkage of the cerebrum (Feldman & Peters, 1998; Guttmann et al., 1998; Peters, Moss, & Sethares, 2000).

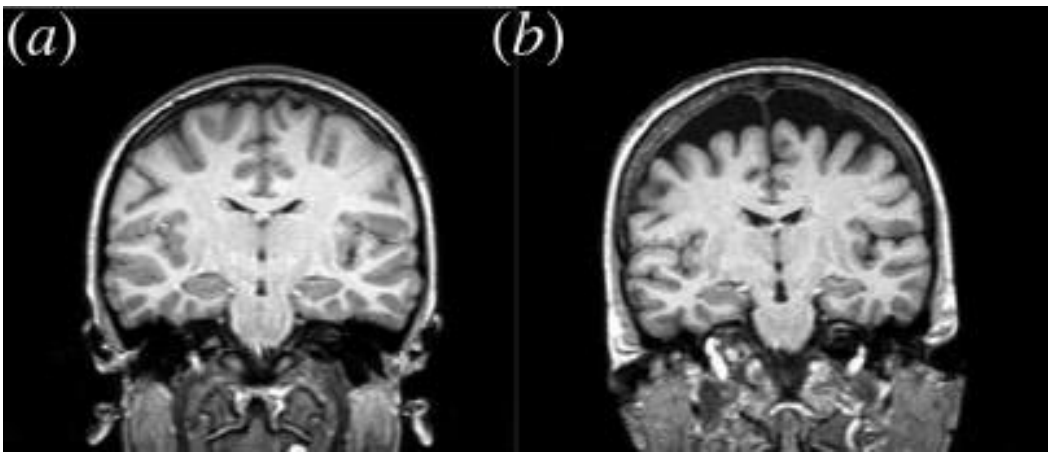

Figure 4: Human brain MRI of (a) young and (b) aged. Cerebral atrophy can be seen in the aged human.

Note. Reprinted with permission of Oxford University Press, from 'Selective atrophy of left hemisphere and frontal lobe of the brain in old men,' by Z. Y. Shan, J. Z. Liu, V. Sahgal, B. Wang, and G. H. Yue, 2005, *J Gerontol A Biol Sci Med Sci, Vol. 60 (2),* p. 168. © 2005; permission conveyed through Copyright Clearance Center, Inc.

Age-related dendritic losses were reported in the cerebral cortex. Dendritic losses are characterized by the decrease in the number and length of dendritic branches. Loss of dendritic spines with age was also consistently observed. Loss of

dendritic structures causes destabilization of synaptic connections between the neurons in aged brains (Jacobs & Scheibel, 1993; Scheibel, Lindsay, Tomiyasu, & Scheibel, 1975; Vaughan, 1977). Age-related synaptic losses, as well as synaptic structure modifications, were also observed in the cerebral cortex (Adams, 1987; Adams & Jones, 1982; Huttenlocher, 1979). Further, age-related synaptic plastic changes were also commonly reported in the cerebral cortex (C. Freitas et al., 2011; Spriggs, Cadwallader, Hamm, Tippett, & Kirk, 2017). Synaptic plasticity is thought to be responsible for memory and learning processes (Fröhlich, 2016). Some reports also displayed that there is an age-related loss of internal structures of cortical neurons such as synaptic vesicles, tubular & vacuolar cisternae, and mitochondria, which compromise synapsis function (Adams & Jones, 1982). The age-associated structural losses in the cerebral cortex cause topographic rearrangement of sensory inputs. This leads to the activation of different cortical areas for performing the same cognitive function in young and aged brains (Grady, 1998).

Ageing differentially affect neurotransmitter systems in the cerebral cortex. The loss of glutamate receptors is the most consistent age-related change, which occurs in the glutamatergic system. Among glutamate receptors, NMDA receptors are more preferentially lost (Carpenter, Parker, & Miledi, 1992; Cohen & Muller, 1992; Kito, Miyoshi, & Nomoto, 1990). In GABAergic system, levels of GABA and its transport decreases remarkably with age (Wheeler, 1982; Wheeler & Ondo, 1986). GABAA receptor's structural properties, rather than its levels, also alter with age (Erdo & Wolff, 1989; Mhatre, Fernandes, & Ticku, 1991). A study in the rats had shown a progressive decrease in the levels of dopamine and norepinephrine with age (Timiras, Hudson, & Oklund, 1973).

The age-related functional decline of cerebral cortex cause decline of memory, vision, audition, cognitive functions, reduction of motor functions, etc. Cortical synaptic structural losses and imbalance between the neurotransmitter systems are regarded as possible causes for the functional decline of the cerebral cortex in aging (Wong, 2002).

Much of the ageing studies of the cerebral cortical neurons were done using Human and animal models. But in these studies, age-associated changes of neurons were under the influence of different glial cells and factors associated with the brain.

It will be interesting to study the ageing of cortical neurons in isolation without the influence of any external factors. This can be achieved by the establishment of *in vitro* ageing model of cortical neurons. *In vitro* ageing model will decrease complexity, the time duration of survival, cost and also avoid confounding interpretations associated with the animal models. They also allow a better understanding of the ageing process at the cellular and molecular levels which may provide interventions of ageing and also allow developing newer strategies for treating age-associated disorders. Hence, part of my Ph.D. work was conceptualized to establish and characterize *in vitro* ageing model of cortical neurons.

INTERVENTIONS OF AGEING:

Since time immemorial, it is a quest of mankind for longevity and superior healthspan. In the last 100 years, there was a significant increase in the life expectancy of humans in developed countries due to medical advances, better nutrition, improved healthcare, etc. With the increase of life expectancy, there is a shift towards an increasing population of ageing people (de Cabo, Carmona-Gutierrez, Bernier, Hall, & Madeo, 2014). Ageing is the primary risk factor for many life-threatening diseases such as neurodegenerative disorders, cardiovascular diseases, cancer, etc., and also a primary cause for the decline of mental and physical capabilities. Interventions that can decelerate the ageing process can prevent or postpone ageing-associated diseases and improve quality of life and performance of the older individual (C. Lee & Longo, 2016). Extensive research using animal models have revealed that currently, there are mainly three ageing interventions that can increase longevity viz., Genetic, Pharmacological and Dietary interventions (Fontana & Partridge, 2015).

Genetic intervention:

In several animal models, it was discovered that there are several single-gene mutations which can delay the ageing process and enhance the lifespan. Mainly, genetic mutations of key players of nutrient-sensing pathways are known to increase longevity and decrease the incidence of age-related pathologies significantly. For instance, it was found that mutations of growth hormone or IGF-1 had substantially increased the lifespan in mice. Mice deficient in GH receptor–binding protein (GHR-BP) showed a 50% increase in the lifespan extension and also lowered disease-related mortality.

Similarly, mutations of S6K1, AKT, type 5 adenylyl cyclase, PKA, TOR, PI3K, etc. were also shown to be associated with the increased lifespan extension (Fontana, Partridge, & Longo, 2010).

Overexpression of autophagy gene Atg5 was found to trigger autophagy and promotes lifespan extension (Pyo et al., 2013). Apart from these genes, there are also few other genes of genetic pathways, whose mutations or epigenetic alterations were reported to trigger accelerated ageing or longevity in animal models. They are DNA repair and nuclear structure regulating genes whose mutation cause progeroid syndromes such as WRN, LMNA; telomere length maintenance genes such as hTR, DKC1; Inflammatory response regulating genes such as genes for Interleukin-6, Toll-like receptors, C-reactive protein, macrophage inhibitory factor, etc. (Browner et al., 2004).

Pharmacological Interventions:

Several natural and synthetic compounds were discovered which have the potential to exhibit senolytic or geroprotective effects, thereby decrease the rate of ageing and increase longevity. Some of such compounds are as follows:

- Glycolytic inhibitors such as glucosamine, mannoheptulose, iodoacetate, etc. These compounds belong to a class of calorie restriction mimetics that directly activates AMPK or indirectly activate sirtuins.
- Sirtuin-activating compounds such as resveratrol. These compounds directly activate sirtuins. Directly or indirectly activated sirtuins promote longevity through the induction of foxo-dependent stress response and by autophagy activation.
- Activators of AMPK such as metformin. AMPK by blocking mTOR pathway induces stress response pathways and activates autophagy which promotes longevity.
- Direct inhibitors of mTOR pathway such as rapamycin.
- Direct autophagy inducers such as spermidine.
- Plasma membrane redox system (PMRS) activators such as epigallocatechin gallate, melatonin, etc., activate multiple oxidoreductase enzymes present in the plasma membrane and regulate cellular redox homeostasis.

- Senolytic drugs such as dasatinib, quercetin, navitoclax, etc. can selectively kill senescent cells and thereby reduce ageing-related diseases (Saraswat & Rizvi, 2017).

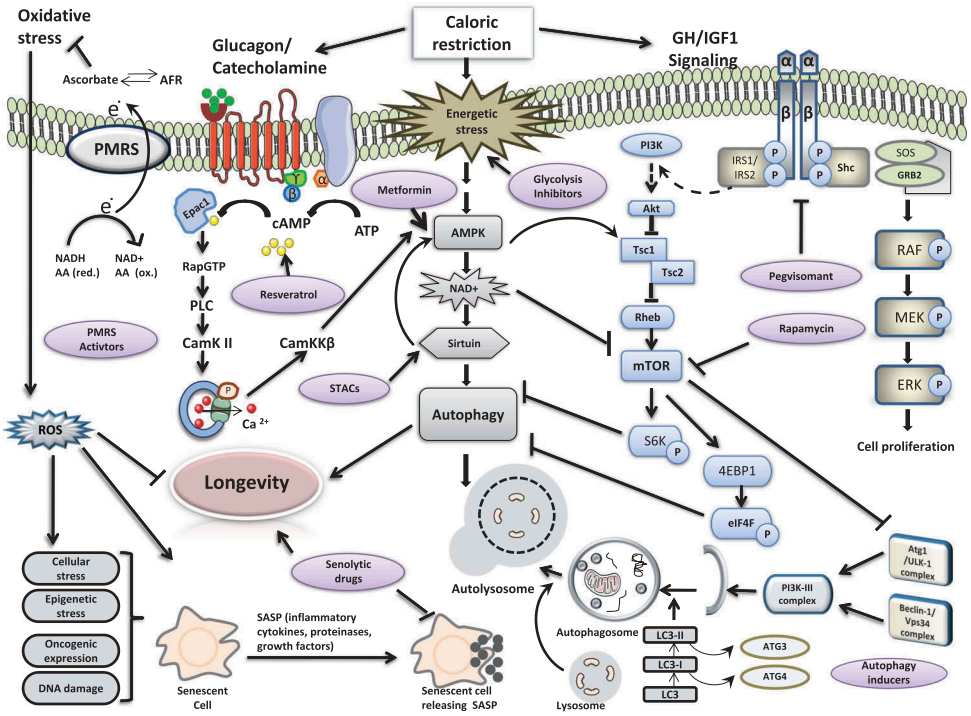

Figure 5: Mode of action of various ageing intervention candidates and approaches.

Abbreviations: ROS: reactive oxygen species, AFR: ascorbate free radical, IGF-1: insulin-like growth factor-1, GH: growth hormone, CamKKβ: Ca(2+)/calmodulin-dependent protein kinase kinase β, AMPK: adenosine monophosphate-activated protein kinase, cAMP: Cyclic adenosine monophosphate, mTOR: mammalian target of Rapamycin, FoxO: forkhead box O, PI3K: Phosphatidylinositol 3-kinase, SASP: senescence-associated secretory phenotype, LC3: light chain 3, PMRS: plasma membrane redox system.

Note. "Reprinted with permission of Taylor & Francis, from 'Novel strategies for anti-aging drug discovery,' by K. Saraswat and S. I. Rizvi, 2017, *Expert Opin Drug Discov, Vol. 12,* p. 962. © 2017; permission conveyed through Copyright Clearance Center, Inc."

DIETARY RESTRICTION:

Dietary restriction is stated as a reduction of intake of either specific nutrient or complete nutrition without causing malnutrition. It is an intervention known to increase longevity and prevent age-related diseases among organisms, from yeast to mammals (Katewa & Kapahi, 2010). Dietary restriction is of various types; they are as follows

Macronutrient restriction: Macronutrient restriction is reduced consumption of particular macronutrients without any calorie restriction. It is one of the promising interventions that promote healthy aging in humans. Among the various kinds of macronutrient restriction, decreased intake of specific amino acids or proteins is the most potent pro-longevity intervention (Mirzaei, Suarez, & Longo, 2014). Reduced protein intake was reported to decrease mortality rates, improve cardio-metabolic health, promote a longer lifespan, etc. despite increased food consumption and increased body fat (Levine et al., 2014; Solon-Biet et al., 2014). Similar observations were also seen with the restricted intake of essential amino acid. Methionine and tryptophan are the vital amino acids whose restriction is most effective in promoting longevity and reducing age-associated diseases (C. Lee & Longo, 2016).

Calorie restriction: Calorie restriction (CR) is a decreased intake of calories, usually 20-40% depletion in total calorie requirement (C. Lee & Longo, 2016). It was most studied and proven dietary restriction which can increase mean and maximum lifespan in organisms such as yeast, flies, worms, rodents, dogs, etc. CR was also reported to be successful in delaying or preventing age-associated diseases. CR decreases the secretion of growth factors such as IGF1, insulin, and growth hormone. These factors are known to accelerate ageing and enhance mortality in many organisms. CR-mediated longevity is governed by conserved nutrient signaling pathways such as the TOR/S6K and insulin pathways. Inhibition of these pathways upon CR, transform the metabolic state of the cells from proliferation and growth to maintenance and survival, which promote longevity (de Cabo et al., 2014; Fontana et al., 2010). Sirtuins were also reported to play a role in the CR-mediated antiaging effects (Haigis & Guarente, 2006). Prolonged CR causes neurologic deficits, wound healing problems, amenorrhea, lowered fertility and libido, osteoporosis, immunosuppression, etc. (de Cabo et al., 2014).

Table 2. Interventions Extending Mean and/or Maximal Lifespan in Wild-Type Mice Fed Normal Chow

	Max Lifespan	Mean Lifespan	Main Mechanism of Action
Dietary Interventions			
Calorie restriction	yes	yes	↓ nutrient-sensing pathways
Intermittent fasting	yes	yes	↓ nutrient-sensing pathways
Protein restriction	no	yes	↓ nutrient-sensing pathways
Methionine restriction	yes	yes	↓ nutrient-sensing pathways
Tryptophan restriction	yes	yes	↓ nutrient -sensing pathways
Physical Exercise Interventions			
Endurance exercise	no	yes	↑ insulin sensitivity; ↑ AMPK ?
Genetic Interventions			
Ames and Snell dwarf	yes	yes	↓ nutrient-sensing pathways
GH receptor KO	yes	yes	↓ nutrient-sensing pathways
IGF-1 R KO	yes (in F)	yes (in F)	↓ nutrient-sensing pathways
Klotho TG	yes (in M)	yes	↓ nutrient-sensing pathways
Fat Insulin Receptor KO	yes	yes	↓ nutrient-sensing pathways
Insulin Receptor Substrate 1 KO	yes (only F)	yes (only F)	↓ nutrient-sensing pathways
Brain IRS-2 KO	yes	yes	↓ nutrient-sensing pathways
PAPP-A KO	yes	yes	↓ nutrient-sensing pathways
Ribosomal S6 protein kinase-1 KO	yes (only F)	yes (only F)	↓ nutrient-sensing pathways
FGF-21TG	yes	yes	↓ nutrient-sensing pathways
miR-17TG	?	yes	↓ nutrient-sensing pathways
DGAT1KO	yes (only F)	yes (only F)	↓ nutrient-sensing pathways
p66shc KO	yes	yes	↓ growth factor-mediated signaling
ATG5 TG	yes	yes	↑ autophagy
Type 5 Adenylyl Cyclase KO	yes	yes	↓ b-adrenergic signaling
Angiotensin II type 1 receptor KO	yes	yes	↓ angiotensin receptor signaling
Catalase targeted to mitochondria TG	yes	yes	↓ oxidative stress (mitochondrial)
Ink4/Arf-TG/TG	no	yes	↓ mitogenic over-stimulation and cell proliferation
C/EBP b/b	yes	yes	↑ mitochondrial biogenesis in white fat cells
Mclk1KO	yes	yes	↓ age-dependent loss of mitochondrial function
Hcrt-UCP2 TG	no	yes	?; ↓ core body temperature
Macrophage migration inhibitory factor KO	yes	yes	↓ inflammation; ↓ insulin pathway
E-DNIkB TG	?	yes	↓ inflammation; ↓ insulin pathway
PKA RIIb KO	yes	yes	↓ IGF signaling?
RasGRF1 KO	yes	yes	↓ nutrient-sensing pathways
Sirt6 TG	yes (only M)	yes (only M)	↓ nutrient-sensing pathways (IGF)
Brain-specific Sirt1 TG	yes (only F)	yes	↑ mitochondrial function via Sirt1/Nkx2-1/Ox2r
TRPV1 pain receptor KO	yes (only F)	yes	modulation of CRTC1/CREB activity
Pharmacological Interventions			
Rapamycin	yes	yes	↓ nutrient-sensing pathways (mTOR)
Acarbose	yes	yes	↓ IGF signaling and [FGF-21
Metformin	no	yes	↓ nutrient-sensing pathways (AMPK)
Aspirin	no	yes (only M)	↓ inflammation
Nordihydroguaiaretic acid	no	yes (only M)	↓ inflammation and oxidative stress
Green tea extract	no	yes (only F)	↓ oxidative stress
17a-Estradiol (non-feminizing estrogen)	no	yes (only M)	? non-genomic actions
Methylene Blue	no	yes (only F)	↑ mitochondrial function
Metoprolol	no	yes (in M)	↓ b-adrenergic receptor signaling
Nebivolol	no	yes (in M)	↓ b-adrenergic receptor signaling

Note. "Reprinted with permission of Elsevier, from 'Promoting health and longevity through diet: from model organisms to humans,' by L. Fontana and L. Partridge, 2015, *Cell, Vol. 161(1),* p. 107. © 2015; permission conveyed through Copyright Clearance Center, Inc."

Fasting regimen:

Fasting is an extreme dietary restriction defined as either a complete deprivation of food or a 60% or higher restriction of food consumption. Fasting regimens are more feasible strategies that can provide beneficial effects of CR with much higher impact and can also overcome the disadvantages of CR (Longo & Mattson, 2014). Fasting is practiced in various ways, some of the important practices are as follows: Intermittent fasting, which is an eating pattern, where individuals go on lengthy periods (usually 16–48 h) without consumption of food and intervening periods of food consumption (without any calorie restriction), regularly. Periodic fasting, where individuals fast regularly for two or more days every week, month, etc. Prolonged fasting, where individuals fast for more than two consecutive days with only water intake. Time-restricted feeding, where individuals are allowed to feed only for a restricted period of time (≤ 8 hours) in a day (C. Lee & Longo, 2016; Longo et al., 2015; Mattson, Longo, & Harvie, 2017).

Studies were reported that fasting regimens could improve the healthspan of individuals by reducing the levels of cholesterol, triglycerides, insulin, leptin, inflammatory markers, oxidative stress markers, etc. Further, by increasing insulin sensitivity, adiponectin, fatty acid mobilization, lipolysis, etc. and also by activating autophagy (Longo & Mattson, 2014; Singh et al., 2009; Wan et al., 2010). In the brain, through above changes and also by stimulating the expression of neurotrophic factors such as BDNF, GDNF, IFN-gamma, etc., fasting increases synaptogenesis, synaptic plasticity, improves cognition, promotes neurogenesis, and promotes neuronal survival by increasing neuronal resistance to excitotoxic stress and injury (Anson et al., 2003; Ghosh, Carnahan, & Greenberg, 1994; J. Lee, Kim, Son, Chan, & Mattson, 2006; Lindsay, 1994; Martin, Mattson, & Maudsley, 2006; Mattson et al., 2017).

In studies using rats and Human, it was reported that fasting promotes lifespan extension (Longo & Mattson, 2014; Mercken, Carboneau, Krzysik-Walker, & de Cabo, 2012). Fasting leads to decrease of circulating insulin and IGF-1 levels, the factors which are associated with accelerated ageing (Fontana et al., 2010). It also increases IGF-1-inhibiting proteins, IGFBP1 (Thissen, Ketelslegers, & Underwood, 1994). These effects downregulate nutrient-sensing pathways such as PI3K–AKT, adenylate cyclase–PKA, and Tor–S6K signaling pathways which promote longevity through the

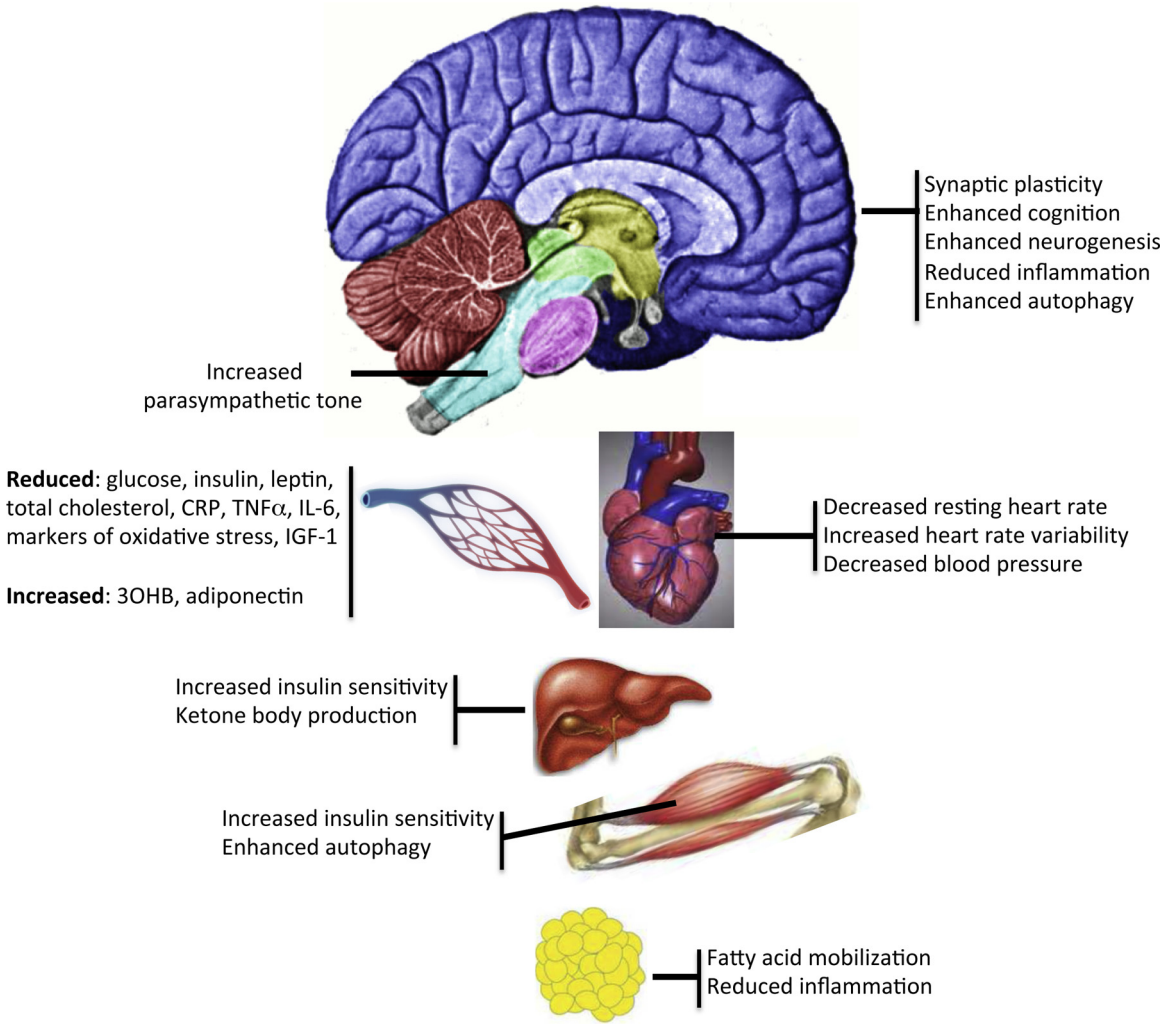

Figure 6: Effects of intermittent fasting on the brain and other organ systems.

Abbreviations: 3OHB: 3-hydroxybutyrate; CRP: C-reactive protein; TNFα: tumor necrosis factor α; IL-6: interleukin-6; IGF-1: insulin-like growth factor-1.

Note. Reprinted with permission of Elsevier, from 'Impact of intermittent fasting on health and disease processes,' by M. P. Mattson, V. D. Longo, & M. Harvie, 2017, *Ageing Res Rev, Vol. 39,* p. 53. © 2017; permission conveyed through Copyright Clearance Center, Inc.

induction of foxo-dependent stress response and by autophagy activation (Cheng et al., 2014). Animal, clinical and epidemiological studies established that fasting regimens can also reduce the risk of developing age associated diseases such as myocardial infarction, stroke, diabetes, neurodegenerative diseases, cancer, etc. in animals as well as in humans (Longo & Mattson, 2014).

Hence, thesis simulated Fasting as a strategy of the intervention of ageing and its effects were evaluated in the developed *in vitro* ageing model.

NEUROTOXICITY:

The global population is living in an environment, which is increasingly exposing to industrial effluents, pesticides, insecticides, plant growth regulators, pollutants and many other hazardous chemicals which became part of day to day human life. Most of these chemicals are adversely affecting human health. Among these chemicals, many are extremely toxic to central and/or peripheral nervous systems, hence are called Neurotoxins (Pogue & Lukiw, 2016). Well-known examples of neurotoxins are lead, arsenic, methylmercury, manganese, organophosphate pesticides, organochlorine pesticides, toluene, polychlorinated biphenyls, environmental tobacco smoke, etc. (Miodovnik, 2011).

Neurotoxins affect the nervous system mainly by causing neuronal cell death, or degeneration of axons or axonal membrane damage or obstruction of neurotransmission or damage to glial cells (Costa, 2017). These damages are manifested in the forms of loss of motor control, dysfunction of autonomic nervous system, cognitive deterioration, behavioral problems, sexual dysfunction, vision disorders, speech disorders, sensation disorders, audition disorder, sleep disorders, paralysis, learning impairment, dementia, etc. (Damstra, 1978; National Institute of Neurological Disorders and Stroke, 2019, March 27).

Neurotoxicity can occur at all the stages of life, from the developmental stage to senescence stage, but the severity of the toxicity may vary with the age of the individual. Chemical-induced neurotoxicity may cause minuscule to life-threatening neurological impairment, and the effects may be reversible or irreversible, temporary or permanent, immediate or delayed. But the prognosis of neurotoxic disorders depends on the degree, length and potential of the chemical exposure and the extent of neurological damage occurred. Neurotoxins causing irreversible, progressive, delayed-onset, residual, or latent effects are of great concern (MacPhail, 1992; National Institute of Neurological Disorders and Stroke, 2019, March 27; Hugh.A. Tilson, 1999).

Importantly, neurotoxins are associated with the etiopathogenesis of neuropsychiatric, neurodevelopmental, and neurodegenerative disorders. Certain

chemicals were identified to cause or replicate symptoms of a variety of neuropsychiatric disorders. Exposure to mercury vapors was found to cause neuropsychiatric problems among the hat makers. Chronic exposure to solvents such as toluene, xylene, turpentine, styrene, and trichloroethylene has been connected with the occurrence of psycho-organic syndrome or chronic painter syndrome (Costa, 2017).

Developing brains is extremely sensitive to neurotoxins even at very low concentrations, compared to adults, due to the immature blood-brain barrier, inability to detoxify exogenous chemicals and higher absorption versus low body weight (Adinolfi, 1985; H. A. Tilson, 2000; Toxicology, 2000). Since developing brain is highly sensitive, exposure to neurotoxins cause permanent damages in the brain and evolve to neurodevelopmental disorders (Grandjean & Landrigan, 2014). According to the National academy of science, toxic environmental exposure directly contributes to 3% and in combination with a genetic predisposition contribute to another 25% of neurodevelopmental disorders (Miodovnik, 2011; Toxicology, 2000). But, this estimation could be an underestimate of the true occurrence of chemically induced neurotoxicity, since the estimation was based on limited information (Grandjean & Landrigan, 2006). Common neurodevelopmental disorders include autism spectrum disorders, cerebral palsy, learning disabilities, sensory deficit, attention deficit & hyperactivity disorder, dyslexia, and mental retardation (Miodovnik, 2011; Smirnova, Hogberg, Leist, & Hartung, 2014). At least one of these disorders affect more than 9.5 million children in the US alone (Miodovnik, 2011). Among these disorders, autism spectrum disorder affects nearly 1.5 % of children aged 8 years (Smirnova et al., 2014), learning disabilities affect 10% of public school going children (Schmid & Rotenberg, 2005), and attention deficit and hyperactivity disorder affect 14 % of newborn children (Landrigan, Lambertini, & Birnbaum, 2012).

In elders, except few familial forms, most of the neurodegenerative disorders are sporadic, which is the consequence of both environmental and genetic factors. Environmental factors were explored for their ability to induce neurodegenerative diseases. Certain chemicals were identified with the capability to predispose the onset or to replicate symptoms or to aggravate pathogenesis of neurodegenerative disorders. Whatever may be the case, studies have shown that chemicals can induce

neurodegeneration through various mechanisms (Zurich & Monnet-Tschudi, 2009). For instance, several pesticides and certain metals such as iron and copper were shown to evoke structural alteration and fibrillation of alpha-synuclein (Uversky, Li, & Fink, 2001a, 2001b). Mercury was shown to induce beta-amyloid secretion and tau hyperphosphorylation (Olivieri et al., 2000). Trimethyltin, ethylene-bis-dithiocarbamate induce neurodegeneration through oxidative stress generation (Domico, Cooper, Bernard, & Zeevalk, 2007; Jenkins & Barone, 2004). Lead induces neurodegeneration through deregulation of protein turnover (Monnet-Tschudi, Zurich, Boschat, Corbaz, & Honegger, 2006).

Until now, as few as 200 chemicals had been identified as potential neurotoxins in Human beings and another 1000 chemicals had been reported to be neurotoxic in laboratorial animal studies (Grandjean & Landrigan, 2014). But in global commerce, there are nearly eighty thousand chemicals are in use and every year around 700 new chemicals are added. Among them, only a small fraction was tested; still, a large fraction has to be tested for their potential to induce neurotoxicity (Grandjean & Landrigan, 2006). Hence, Thesis examines common plant growth regulator such as chlormequat, commonly used pesticide such as paraquat, and a common household metal such as aluminum for their ability to induce neurotoxicity individually or synergistically.

NANOFORMULATIONS IN ENHANCING TARGETED DELIVERY TO BRAIN:

Age-associated neurological disorders are growing world widely resulting in high social impact because of their high morbidity and mortality. They are one of the major causes of mortality, and they alone constitute more than one-tenth of global deaths (Masserini, 2013a). Common age-associated neurological disorders include neurodegenerative diseases such as Parkinson's, Huntington's, and Alzheimer's diseases and certain brain tumors such as glioblastoma, meningioma, etc. Currently, most of these neurological disorders lack effective therapy. The major hurdle for the treatment of these neurological disorders is the presence of blood-brain barrier (BBB), which prevents the entry of the drugs to the brain (Kanwar, Sriramoju, & Kanwar, 2012).

The Blood-Brain Barrier:

The BBB is a structure made by a complex system of astrocytes, pericytes, basement membrane, and vascular endothelial cells. In BBB, vascular endothelial cells are stitched together by tight junctions (TJ) which contributes to the rigidity of the BBB. TJ prevent paracellular transport of ions, molecules, and other compounds and dictate their entry into the brain only through endothelial cells by active transport or diffusion. Further, TJ preserve the basolateral and apical membrane functions of endothelial cells by inhibiting the movement of membrane proteins (Masserini, 2013a). The basement membrane (basal lamina) surrounds the endothelial cell layer. The basement membrane is partially enveloped by pericytes and further ensheathed by astrocyte endfeet. Astrocyte endfeet and pericytes function are to strengthen and maintain the barrier. Astrocytes further supply nutrients to neurons (Abbott, 2013).

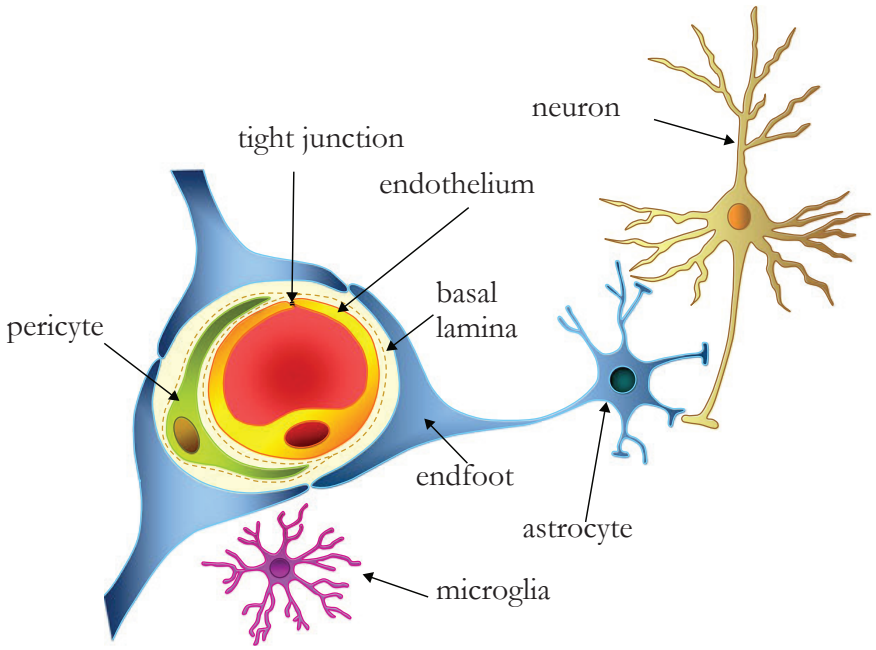

Figure 7: Structure of Blood-brain barrier.

Note. Reprinted with permission of John Wiley and Sons, from 'Blood-brain barrier structure and function and the challenges for CNS drug delivery,' by N. J. Abbott, 2013, *J Inherit Metab Dis, Vol. 36,* p. 441. © 2013; permission conveyed through Copyright Clearance Center, Inc.

Apart from serving as a mechanical fence, the BBB is also a dynamic biological entity, through which carrier-mediated transport occurs. Nutrients such as ketone

bodies, amino acids, and glucose enter the brain through specific transporters present on the BBB, whereas larger molecules such as cytokines and neurotrophins enter the brain through receptor-mediated endocytosis. Except for hydrophilic compounds less than 150 Da and hydrophobic compounds less than 600 Da, uptake of most of the drugs into the brain is prevented by the BBB. Further, the expression of P-glycoprotein pumps on the BBB complicates the uptake of the drugs. P-glycoprotein pumps recognize necessary molecules for the brain and allow only their uptake. It pumps out other molecules including pharmaceuticals from the endothelial cells (Masserini, 2013a).

Overview of drug delivery approaches to the brain:

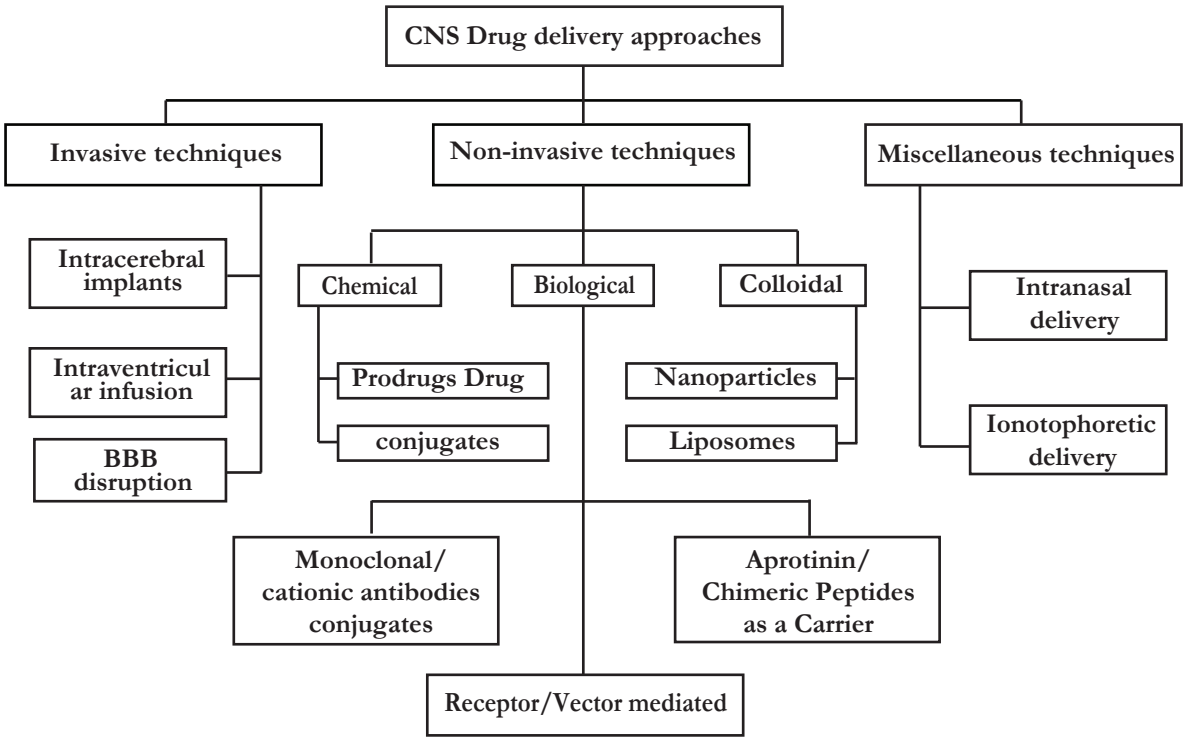

Figure 8: Overview of drug delivery approaches to the brain.

Note. "Reprinted with permission of Bentham Science Publishers Ltd., from 'CNS drug delivery systems: novel approaches,' by S. A. Pathan et al., 2009, *Recent Pat Drug Deliv Formul, Vol. 3,* p. 72. © 2009; permission conveyed through Copyright Clearance Center, Inc."

Nanoparticles-mediated drug delivery to the brain:

The use of nanoparticles for the drug delivery to the brain is the latest and advanced approach which is attracting the attention of researchers globally (Stenehjem, Hartz, Bauer, & Anderson, 2009). The main reasons for the attention are

the multi-functionalization of the nanoparticles and their ability to carry and transport of BBB impermeant drugs to the brain. In the nanoparticle-mediated brain drug delivery, the transport of BBB impermeant drugs to the brain solely depends on the physicochemical and biomimetic characters of the nanoparticles rather than the physicochemical features of the drug (Masserini, 2013a). The word "Nano" is derived from the Latin which literally means "dwarf." The Nanotechnology is concern with the design, preparation, characterization, and application of materials and devices at a nanometer scale. The unique biological, chemical and physical properties of nanoparticles compared to their larger counterparts allow their potential application in the diagnosis and therapy of brain pathologies.

Advantages of using nanoparticles for the drug delivery to the brain:

- Preparation methods are simple, cost-effective and easy to scale-up. The prepared particles are highly stable and can be easily freeze-dried.
- The encapsulated drug is protected from chemical and enzymatic degradation in the systemic circulation, which increases its bioavailability.
- Decreases the systemic toxicity of potential drugs.
- Have comparatively high drug-loading capacity. The encapsulation of the drug doesn't require any chemical modification to the drug, which preserves drug activity.
- Can encapsulate both hydrophobic and hydrophilic drugs.
- Can be administered by various routes viz., oral, intravenous, nasal, etc.
- Disguise the physicochemical features of the encapsulated drug and thereby enhances its ability to transport across BBB.
- Permits controlled and sustained drug release.
- By altering matrix composition, controlled drug release and particle degradation features can be easily dictated.
- Target specificity can be achieved by attaching target-specific ligand or using magnetic guidance.

- High binding affinity can be achieved by multivalent functionalization (Sarkar et al., 2017).

Current Nanoparticle approaches for brain drug delivery

Lipid-Based Nanoparticles:

Solid Lipid Nanoparticles (SLNs): These nanoparticles contain a solid hydrophobic core matrix, surrounded by a phospholipid monolayer. Drug of interest is either dispersed or dissolved in the solid hydrophobic core matrix (Kaur, Bhandari, Bhandari, & Kakkar, 2008). Advantages of SLNs are the smaller size, feasibility to encapsulate both hydrophobic and hydrophilic drugs, greater stability, lower cytotoxicity, etc. (Sarkar et al., 2017). Chances of burst release of drug after administration or drug expulsion during storage and lower drug loading capacity are its drawbacks.

Nanostructured Lipid Carriers (NLCs): They are the advanced version of SLNs. They are developed to solve the drawbacks of SLNs. NLCs possess core matrix made up of both liquid lipids and solid lipids. Different drug release profiles can be obtained by altering the lipid matrix composition (Sarkar et al., 2017).

Metallic nanoparticles:

Metallic nanoparticles have become apparent as a new directional approach in the arena of drug delivery because of their wider applications, which are due to their ease of synthesis, chemical & geometrical tunability, higher surface area to volume proportion, etc. Gold, silver, iron are the most commonly used metallic nanoparticles. Non-biodegradability, systemic toxicities are the serious issues associated with these nanoparticles.

Polymer-Based Nanoparticles:

Polymeric micelles: They are created using amphiphilic block copolymers, which in aqueous solutions spontaneously form nano-sized carriers (Gilmore, Yi, Quan, & Kabanov, 2008). Polymeric micelles have advantages such as smaller size, the capability to encapsulate hydrophobic drugs, etc. Premature discharge of the drug from the nanoparticle before reaching the target site is its main drawback.

Polymeric nanogels: They are cross-linked polymeric networks encompassing non-ionic and ionic polymeric chains. They can encapsulate low molecular weight drugs and charged biomolecules such as oligonucleotides, proteins, etc. (Vinogradov, Batrakova, & Kabanov, 2004).

Dendrimers: Dendrimers are branched polymers, whose structure resembles the structure of a tree. They can be prepared using both natural as well as synthetic monomers. The simplicity of preparation & modification, a void area within the nanocarrier, polyvalency, size control, and uniform particle size are the advantages of these nanoparticles (Khanbabaie & Jahanshahi, 2012; Sarkar et al., 2017).

Polymeric Nanoparticles: These nanoparticles include nanospheres and nanocapsules, which can be prepared using both natural as well as synthetic polymers. In these nanoparticles, the drug of interest can be encapsulated, adsorbed, dissolved, entrapped, or conjugated to the matrix of the nanoparticle (Lockman, Mumper, Khan, & Allen, 2002). Commonly used polymers include polylactic acid (PLA), gelatine, polyglycolic acid (PGA), polycyanoacrylate, polylactic-co-glycolic acid (PLGA) copolymer, Chitosan, and some polysaccharides & proteins. Biodegradability, stability, the presence of surface functional groups, low toxicity, controlled drug release, etc., make polymeric nanoparticles a good choice for brain drug delivery (Olivier, 2005).

Targeted drug delivery:

Most of the nanoparticles lack target specificity. To increase target specificity, nanoparticles are attached with the ligands which are specific for the receptors expressed on the brain capillary endothelial cells. Sugar residues, folic acid, transferrin, lactoferrin are the commonly used ligands for targeting the brain. Engineered monoclonal antibodies are also used as the ligands in some nanoparticles. An efficient, targeted drug delivery system reduce relative drug dosage, minimize systemic toxicity and increase the efficacy of the drug (Tajes et al., 2014).

Protein nanoparticles:

Protein nanoparticles are polymeric nanoparticles made up of natural proteins in which drug of interest is encapsulated. Protein nanoparticles are gaining much interest in the arena of drug delivery since they have numerous advantages.

Some of the advantages of protein nanoparticles are as follows:

- They are highly biodegradable and do not elicit an immune response.
- Protein (drug delivery vehicle) and the drug doesn't require any chemical modifications.
- Any protein-ligand peculiar for the receptor expressed on the diseased cell can be exploited for target-specific delivery, which eliminates the need for conjugating the ligand on the surface of the nanoparticle for targeted delivery.
- Since they don't require any other components (except protein & drug) and also doesn't require any chemical modifications their preparatory methods are very simple and easy.
- Availability of functional groups in the backbone of the protein allows surface modifications if any required (C. Weber, Coester, Kreuter, & Langer, 2000).

In our laboratory, protein nanoparticles such as transferrin nanoparticles and lactoferrin nanoparticles were developed using transferrin and lactoferrin proteins respectively as the single matrix. They were successfully utilized for targeting various cancers such as hepatocellular carcinoma (Golla, Bhaskar, Ahmed, & Kondapi, 2013), retinoblastoma (Ahmed, Ali, & Kondapi, 2014), and colon adenocarcinoma(Ahmed, Kumari, & Kondapi, 2018).

Since glioblastoma is an age-associated neurological disease, it will be a helpful model for developing drug delivery vehicle targeted to the ageing brain. As it was reported that brain capillary endothelial cells and glioblastoma cells express lactoferrin receptors (Carine Fillebeen, 1999; Fang et al., 2014; R. Q. Huang et al., 2007; Ji et al., 2006; Ruirui Qiao, 2012), it will be beneficial to develop carmustine loaded lactoferrin nanoparticles and to evaluate their effectiveness in treating glioblastoma. The developed drug delivery vehicle can also be utilized for other age-associated neurological diseases. Hence, this thesis also focused on developing carmustine loaded lactoferrin nanoparticles and on evaluating their effectiveness in treating glioblastoma.

RATIONALE:

Neurons encounter various stress conditions namely nutrient deprivation, exposure to environmental agents such as pesticides, metals, plant growth regulators, etc. How neurons respond to such conditions is essential information that would help in modeling neuronal survival and ageing. In this thesis, we have simulated various nutritional restriction conditions and monitored the health of the neuron to understand the role of nutrition for healthy aging of neurons. Further, we have put efforts to understand the effect of the environmental pollutants on neuronal survival and its significance in the occupational neurotoxicity. Also, we have put efforts to promote a nanoformulation for targeted delivery in glioma cells, which could be a lead for formulating highly toxic drug carmustine for anti-cancer therapy.

Overall Objectives:

Objective 1: Isolation and culturing of cortical and hippocampal neurons *in vitro.*

Objective 2: Characterization of Ageing of cultured neurons *in vitro.*

Objective 3: Effect of fasting as an intervention of ageing strategy on the longevity of cortical neurons *in vitro*.

Objective 4: Effect of pesticides, plant growth regulators and metals on neuronal survival.

Objective 5: Analysis of the efficacy of carmustine loaded lactoferrin nanoparticles against glioblastoma cell

CHAPTER 2:

ISOLATION AND CULTURING OF CORTICAL AND HIPPOCAMPAL NEURONS *IN VITRO*

INTRODUCTION:

In primary neuronal cultures, neurons are isolated directly from live brain tissues, and they are processed to maintain in culture conditions. The primary neuronal culture had become an essential part of neuroscience since it allows understanding of complex brain functions in much simpler ways (Al-Zabin & Rohleffson, 2017). It presents numerous benefits for studies which are impeded by the complexity of the brain viz. homogenous primary neuronal cultures reduces the uncertainty in unraveling the cellular targets of test substances. It allows electrophysiological recordings and pharmacological agents to be applied directly to the neurons. Conditions that can influence the cell can be defined precisely by the cell culture, which contributes to the higher reproducibility compared to whole animal studies. Primary cultures also allow typical morphological studies of neurons such as plasticity, neuritogenesis, etc. by giving access to continuous visualization (Brewer, 1997). Specific neuronal pathways which are challenging to study in the intact brain can be explored using homogenous neuronal cultures (Al-Zabin & Rohleffson, 2017). It can also be used for ageing studies since the duration of survival of neurons in culture can be related to the developmental age (Aschner & Syversen, 2004). Primary cultures of hippocampal and cortical neurons permit correlation studies between molecular events at the subcellular level and their consequences on the brain's capability to learn and remember (Al-Zabin & Rohleffson, 2017).

Hippocampal and cortical neurons can be cultured *in vitro* in various ways such as organotypic splice culture, co-culture, serum-free culture, etc. Organotypic splice culture maintains neuronal tissue in its three-dimensional structure with the protection of cytoarchitecture and cell populations (Croft & Noble, 2018). But these cultures fail in studying neurons in isolation due to the presence of heterogeneous cell populations (Humpel, 2015). This failure emphasis the need for culturing homogenous neuronal populations. In co-cultures, homogenous population of dissociated primary neurons will be cultured *in vitro* using glial feeder layer. Neurons require glial cells support for humoral factors and contact-dependent interactions. Co-cultures allow the study of neurons at low cell densities (Lesuisse & Martin, 2002). However, co-cultures have many disadvantages viz., to control the proliferation of glial cells in culture, requires regular usage of cytotoxic mitotic inhibitors which damage neurons (Wallace

& Johnson, 1989). Glial conditioned media can influence neuronal gene expression, which can affect innate neuronal activity (Lesuisse, Qiu, Bose, Nakaso, & Rupp, 2000). Further contamination of glial cells will confound neuron-specific studies (Lesuisse & Martin, 2002). These limitations emphasize the need for culturing of pure hippocampal and cortical neurons without the use of glial feeder layer.

Serum-free cultures can overcome the above problems. They allow culturing of a homogenous population of dissociated primary hippocampal and cortical neurons without the use of glial feeder layer (Brewer, 1995; Brewer, Torricelli, Evege, & Price, 1993). They allow the study of pure hippocampal and cortical neurons in isolation, without any confounding interpretations. They also allow the conditions that can influence the neurons in culture to be defined precisely.

Hippocampal and cortical neurons can be isolated and cultured from rat brain at various developmental ages. But isolation from developed brain tissue poses problems such as difficulty in the dissociation of tissue, difficulty in isolating pure neurons, irreversible damage of axons, dendrites, and synaptic connections, etc. (Brewer, 1997). These problems emphasize the need to isolate neurons from early developmental ages. To overcome the above disadvantages, neurons are isolated and cultured from newborn or postnatal day-0 rats. But glial cells contamination is the main problem in this isolation method (Chudotvorova et al., 2005). This problem emphasizes the need to isolate neurons from embryonic stages where the generation of cortical or hippocampal neurons have completed, and the presence of glial cells is limited. Embryonic day-18 embryos can be used for isolation and culturing of neurons to overcome the above problems (Kaech & Banker, 2006).

In the context of the above facts, this objective was conceptualized to isolate cortical and hippocampal neurons from embryonic day 18 embryos and to culture them *in vitro* as the homogenous population without the use of glial feeder layer.

MATERIALS AND METHODS:

Animals:

Wistar rats (Rattus novergicus) used for the study were procured from Sainath Agencies, Hyderabad, India. Rats were maintained until needed at the animal house facility with 12 hours light and 12 hours dark cycle. Rats were given water and food ad libitum. All the guidelines and recommendations of University of Hyderabad animal ethics committee were followed.

Materials:

Calcium, magnesium free HBSS solution (CMF-HBSS), trypsin, DMEM/F12, neurobasal medium, B27 supplement, glutamax, and antimycotic & antibiotic solution were procured from Thermo-Fisher scientific (Waltham, USA); Trypsin inhibitor, Poly-d-lysine from Sigma-Aldrich (St. Louis, USA); DNase from Roche Applied Science (Penzberg, Germany); fetal bovine serum from Lonza (Basel, Switzerland); culture dishes were from Corning (New York, USA) and all other materials were of either analytical or molecular biological grade.

Dissection of Rat Embryonic Hippocampus and Cortex:

Primary rat hippocampal and cortical neuronal cultures were prepared using embryonic day 18 (E18) rat embryos. Dissection of cortex and hippocampus were carried out according to Facci and Skaper (2012). Briefly, E18 pregnant rat was euthanized as per University of Hyderabad guidelines. The rat was placed dorsal side down, and the abdomen was wiped with 70% alcohol. An incision was made across the abdomen to expose uterine horns. Uterine horns were gently excised from the cavity and were placed in cold CMF-HBSS with HEPES buffer, pH-7.4. Embryos were removed from the uterine segment and were decapitated. The scalp was cut along the midbrain line using fine scissors, and the brain was removed from the head. Brainstem, cerebellum, and optic nerve stumps were removed from the brain. Cerebral hemispheres were separated, and the meninges were torn off from the cortex. Using angled forceps white matter and striatum were scooped out of the cortex. Hippocampus, which looks like a banana-shaped area in the cortex was cut apart and transferred to a centrifuge tube containing cold CMF-HBSS with HEPES buffer, pH-7.4

for further processing. The neocortices were minced into small pieces and transferred to another centrifuge tube containing cold CMF-HBSS with HEPES buffer, pH-7.4 for further processing.

Culturing of Cortical Neurons *in vitro*:

The procedure of culturing of Cortical neurons was followed according to Meberg and Miller (2003) with some modifications. The minced cortex tissue was subjected to the enzymatic dissociation using trypsin and DNase for 15 min at 37 ºC. Trypsin inhibitor was added to neutralize trypsin activity. Tissue was triturated 15-20 times through fire-polished Pasteur pipette until most chunks of the tissue disappear. The cell suspension was centrifuged for 5 min at 120 g. The cell pellet was washed twice with media containing DMEM/F12 and serum. After washing, cells were suspended in Neurobasal medium with 0.5mM glutamax, 2% B27, and 1x antimycotic and antibiotic solution. Using hemocytometer cells were counted, and they were plated at a seeding density of 1000-1200 cells/mm^2 in poly-d-lysine (pdl) coated culture dishes. Cortical neuronal cultures were incubated in CO_2 incubators. Neurons were fed weekly once by replacing half of the old medium with fresh cultivating media (Neurobasal medium, 0.5mM glutamax, 2% B27, and 1x antimycotic and antibiotic solution).

Culturing of Hippocampal neurons *in vitro*:

Dissociation steps of Hippocampal neurons from the hippocampus tissue were similar to dissociation steps of cortical neurons. But after washing, cells were resuspended in media containing DMEM/F12 and serum with 1x antimycotic and antibiotic solution. Using hemocytometer cells were counted, and the cells were plated at a seeding density of 160-180 cells/mm^2 in pdl coated culture dishes. At the time of plating, plating media composed of DMEM/F12 and serum. After 24 hours (h), plating media was replaced entirely with cultivating media (Neurobasal medium, 0.5mM glutamax, 2% B27, and 1x antimycotic and antibiotic solution) and were incubated in CO_2 incubators. Neurons were fed once every 2 weeks by replacing two-thirds of the old medium with fresh cultivating media (Bertrand, Aksenova, Aksenov, Mactutus, & Booze, 2011).

RESULTS:

Culturing of Hippocampal neurons *in vitro*:

Hippocampi were dissected out from the cerebral hemispheres of embryos of E18 pregnant rat. Dissected hippocampi are dissociated into single cell suspension. Dissociated single cell suspension of hippocampal neurons were cultured in Neurobasal media with the B27 supplement without using supportive astrocyte feeder layer. Microscopic examination of 7 days old culture (Fig. 9) showed a homogenous population of cells with multipolar dendrites emerging from the soma. Very long axons and dendrites were observed. These dendrites and axons showed profuse branching and formed dendritic trees. Further, an extensive interwoven network of dendrites and axons was predominantly noticed. These suggest the successful growth of homogenous populations of hippocampal neurons with their characteristic morphological features.

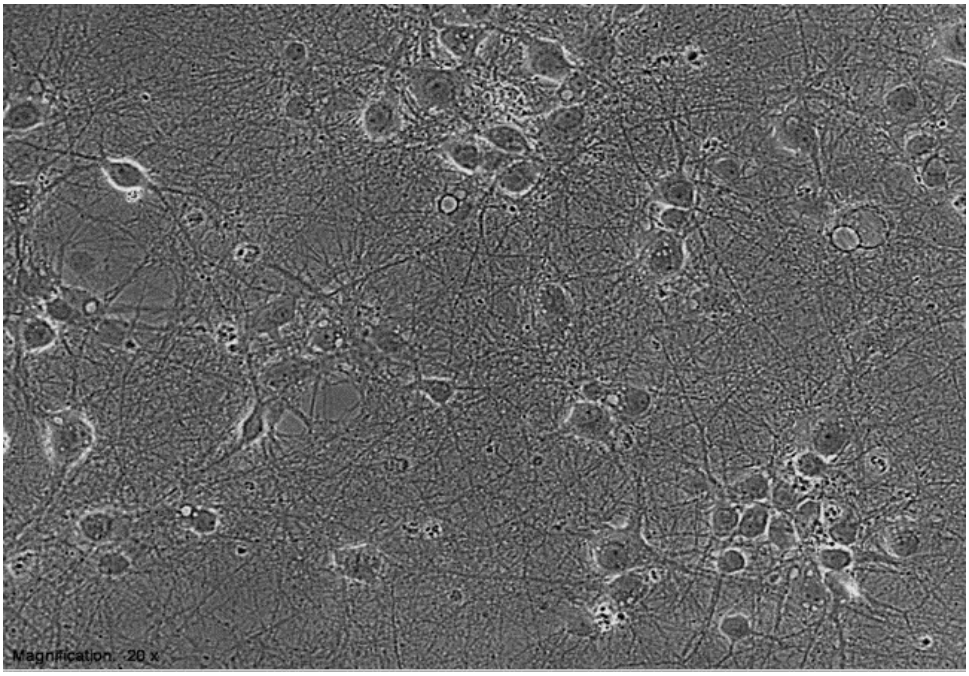

Figure 9: Culturing of Hippocampal neurons *in vitro*. The above figure is a microscopic image of a 7-days old culture of hippocampal neurons. It shows a homogenous population of cells with multipolar dendrites emerging from the soma. Very long axons and dendrites were also observed with profuse branching. Further, an extensive interwoven network of dendrites and axons was predominantly seen. These suggest

the successful growth of a homogenous population of hippocampal neurons in *in vitro* conditions.

Culturing of Cortical neurons *in vitro*:

Neocortices were isolated from embryos of E18 pregnant rat, and the tissue was dissociated into the single cell suspension. The single cell suspension of cortical neurons was cultured successfully without using an astrocyte feeder layer with seeding densities of 1000-1200 cells/mm^2. Microscopic examination of 7 days old cultures (Fig. 10) showed a homogenous population of cells with pyramidal morphology, consisting of a triangular perikaryon with a long axon and tiny basal dendrites. These suggest the successful growth of a homogenous population of cortical neurons with their characteristic morphological features.

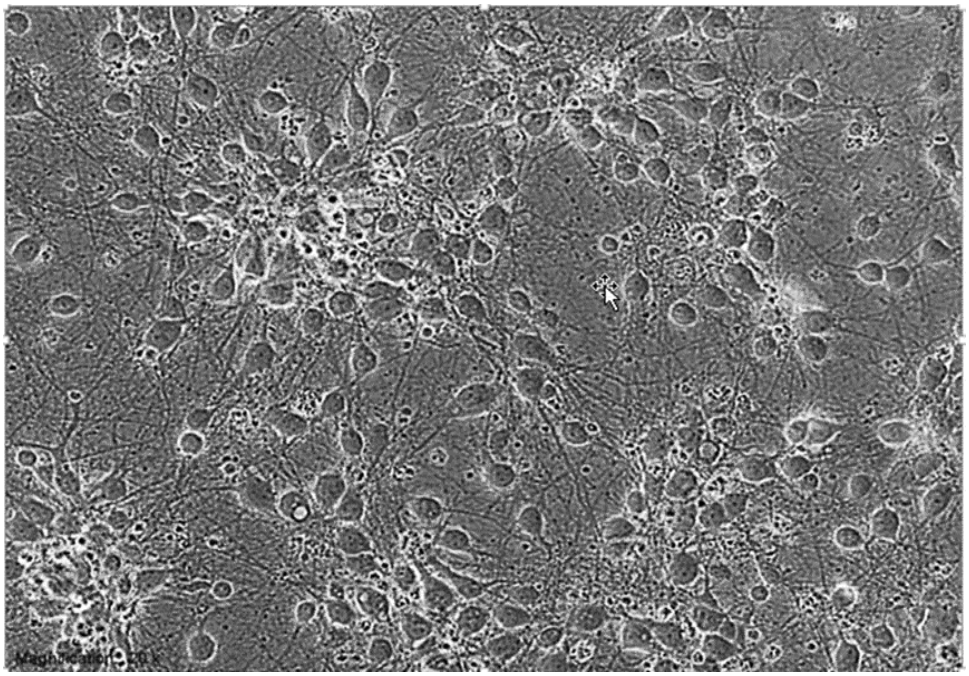

Figure 10: Culturing of Cortical neurons *in vitro*. The above picture is a microscopic image of a 7-days old culture of cortical neurons. It shows a homogenous population of cells with pyramidal morphology, consisting of a triangular perikaryon with a long axon and tiny basal dendrites. These suggest the successful growth of a homogenous population of cortical neurons in *in vitro* conditions.

DISCUSSION:

The primary neuronal culture had become an essential part of neuroscience since it allows understanding of complex brain functions in much simpler ways (Al-Zabin & Rohleffson, 2017). Many primary culturing methods were reported for hippocampal and cortical neurons. But most of these methods either require glial feeder layer or presence of glial cells in the culture (Croft & Noble, 2018; Lesuisse & Martin, 2002). It had also reported that hippocampal and cortical neurons could be isolated from the rat brain at different developmental stages. Except for the embryonic stage, isolation from all other developmental stages give higher glial cells contamination (Brewer, 1997; Chudotvorova et al., 2005; Kaech & Banker, 2006). Hence the purpose of this study was to isolate cortical and hippocampal neurons from embryonic day 18 embryos and to culture them *in vitro* as a homogenous population of dissociated primary neurons, without the use of glial feeder layer.

On the 18th day of pregnancy, hippocampus and neocortices were dissected out from the embryos of the pregnant rat, and the tissues were dissociated into the single cell suspension. The single cell suspensions of hippocampal and cortical neurons were cultured separately without using an astrocyte feeder layer. Microscopic examination of 7 days old primary cultures of hippocampal (Fig. 9) and cortical neurons (Fig. 10) showed successful growth of a homogenous population of neurons with their characteristic morphological features. Successful culturing of a homogenous population of hippocampal and cortical neurons without the usage of glial feeder layer is attributable to the usage of serum-free medium (i.e., Neurobasal media with the B27 supplement), isolation of neurons from embryonic day 18 embryos, and technical expertise. Use of embryonic day 18 embryos increases the efficiency and homogeneity of primary neuronal cultures because of the following reasons: embryonic tissue can be easily dissociated (Al-Zabin & Rohleffson, 2017), contain fewer cell connections which decrease shearing damages (Silva et al., 2006) and by the time, generation of cortical and hippocampal neurons have completed and the presence of glial cells is limited (Kaech & Banker, 2006). The meticulous care taken during the dissection and dissociation steps may also pay to the neuronal viability and minimize the contamination of non-neuronal cells. Neurobasal media with the B27 supplement is a serum-free medium which supports the optimal survival of cortical and hippocampal

neurons in culture. Lower osmolarity, reduced concentration of cysteine and glutamine and exclusion of toxic ferrous sulfate in Neurobasal media compared to DMEM/F12 and DMEM, contributes to the optimal survival of neurons (Brewer et al., 1993). Further, lower concentrations of amino acids in neurobasal medium and serum-free culture conditions significantly reduce glial proliferation in the cultures (Brewer, 1995; Brewer et al., 1993).

Successful culturing of a homogenous population of hippocampal and cortical neurons allow the study of pure hippocampal and cortical neurons in isolation, without any confounding interpretations.

CONCLUSION:

Hippocampal and cortical neurons were isolated from E18 embryos to increase neuronal viability and minimize glial cell contamination in the cultures. The single cell suspensions of hippocampal and cortical neurons were cultured separately using Neurobasal medium with the B27 supplement. Microscopic examination of 7-days old primary cultures of hippocampal and cortical neurons showed successful growth of a homogenous population of neurons with their characteristic morphological features.

CHAPTER 3:

CHARACTERIZATION OF AGEING OF CULTURED NEURONS *IN VITRO*

INTRODUCTION:

"Ageing can be defined as a natural and progressive process occurring in all the living organisms and is characterized by the deterioration of the structure and functional capacities." (Lopez-Lluch & Navas, 2016, p. 2044). This deterioration is the major risk factor for age-associated disorders such as neurodegenerative diseases, diabetes, cancer, cardiovascular disorders, etc. Ageing also increases vulnerability to death (Lopez-Otin, Blasco, Partridge, Serrano, & Kroemer, 2013). Understanding the ageing process at the molecular level allows the intervention of ageing and leads to an extension of lifespan. It also allows in developing newer strategies for treating age-associated disorders. It also allows for the improvement of the quality of life with age (DiLoreto & Murphy, 2015).

Short-lived animals were selected as models for studying the ageing process on the assumption that basic ageing processes are conserved between short-lived animal models and long-lived Humans. But ageing studies in animal models are complicated, necessitating the use of simpler models such as cell culture model. Cell culture models were extensively studied to understand the mechanisms of ageing. Extensive studies in cultured Human T lymphocytes (Pawelec, Rehbein, Haehnel, Merl, & Adibzadeh, 1997), fibroblast cells (Wistrom & Villeponteau, 1990), and other mammalian cells (Augustin-Voss, Voss, & Pauli, 1993) had established that dividing cells have a defined capacity to proliferate in *in vitro*. This phenomenon is called Replicative senescence, and it is considered as ageing at the cellular level (Hayflick, 1998). Replicative senescence is exclusively applicable only to the cells which have a proliferative capacity; it fails to explain the senescence mechanism in non-dividing terminally differentiated cells such as neurons, muscle cells, etc. This failure emphasis the need to study the ageing phenomenon in non-dividing terminally differentiated cells, which can give a generalized concept of ageing.

Above need can be accomplished by the establishment of cellular *in vitro* ageing models using non-dividing terminally differentiated cells. Since the nervous system is the master system which controls the majority of the activities of the animal body, it is rational to use neurons for ageing studies compared to other non-dividing terminally differentiated cells. The increase in the incidence rates of neurodegenerative disorders with age emphasizes the link between ageing and neurodegeneration (Hung, Chen,

Hsieh, Chiou, & Kao, 2010). Additionally, homogenous neuronal populations undergo synchronous changes in the cultures. These further suggest primary neuronal cultures as the best choice to establish *in vitro* ageing model. Since cerebrum constitutes the largest region in the brain, performs numerous motor, sensory and cognitive functions; and many neurodegenerative disorders affect cerebral cortex (Cechetto & Weishaupt, 2017; Robberecht & Philips, 2013; Rosas et al., 2008; Ross & Poirier, 2004), primary rat cortical neurons were chosen to establish *in vitro* ageing model. Primary rat hippocampal neurons were also selected to establish *in vitro* ageing model as they are associated with neurodegenerative disorders such as Alzheimer's disease and Frontotemporal dementia with Parkinsonism (Ross & Poirier, 2004).

Because ageing is a multifactorial process, we hypothesize that if long-term cultures of hippocampal and cortical neurons express multiple characteristic features of physiological ageing, they can serve as an optimal *in vitro* ageing model. In the context of the above facts, this objective was conceptualized to establish and characterize long-term cultures of hippocampal and cortical neurons as an *in vitro* model of ageing.

MATERIALS AND METHODS:

Materials:

Antifade mountant with DAPI, Power SYBR green master mix, TRIzol, X-gal procured from Thermo-Fisher scientific (Waltham, USA); low melting point agarose, Ethidium bromide, Rhodamine123, BSA, Fura-2AM, DEPC, MTT from Sigma-Aldrich (St. Louis, USA); cDNA synthesis kit procured from Takara (Shiga, Japan); Trypan blue from Himedia (Mumbai, India), Primers from Sigma-Aldrich (Bangalore, India); culture dishes were from Corning (New York, USA) and all other materials were of either analytical or molecular biological grade.

Primary antibodies:

Anti-Topoisomerase IIβ antibody (cat. no: 611493) was procured from Becton Dickinson Biosciences, (New Jersey, USA). Anti-MAP-2 antibody (cat. no: ab11267) was from Abcam, (MA, USA); Anti-GFAP antibody (cat. no: G9269) from Sigma-Aldrich, (St. Louis, USA);

Secondary antibodies:

Anti-rabbit Alexa Fluor 594 antibody (cat. no: A11037); Anti-mouse Alexa Fluor 488 antibody (cat. no: A11029) were obtained from Invitrogen, NY, USA.

MTT assay for evaluating neuronal cell viability during long-term culture:

Viability of neurons during long-term culture was assessed at regular time intervals using MTT assay (Mosmann, 1983). Principle of MTT assay is viable cells on exposure to yellow tetrazolium salts (MTT) convert them into purple colored insoluble formazan, which can be dissolved and the intensity of the developed color can be measured spectrophotometrically, which gives the estimation of the percentage of the viable cells. Briefly, cortical and hippocampal neurons were plated at seeding densities of 1200 cells/mm^2 and 180 cells/mm^2 respectively in the pdl coated culture plates. At regular time points, 1.21mM MTT was added to the wells, and the neurons were incubated for 6 h in a CO_2 incubator. After incubation media was discarded, the equivalent amount of DMSO was added and incubated for 5 to 10 min at room temperature (RT). The intensity of the developed color was measured using multiplate

reader-Infinite 200 (Tecan, Mannedorf, Switzerland) at 595 nm. The total number of neurons surviving on 3-days *in vitro* (DIV-3) were considered as control. Percentage of surviving neurons at regular time intervals were calculated using the following formula

$$\mathrm{PS} = \left\{\mathrm{OD}_{\mathrm{Time\ point}}/\mathrm{OD}_{\mathrm{Control}}\right\} \times 100$$

Where, PS = percentage of surviving neurons; $OD_{Control}$ = absorbance at 595 nm for control cells; $OD_{Time\ point}$ = absorbance at 595 nm for time point cells.

Trypan blue exclusion assay for evaluating neuronal cell viability during long-term culture:

Viability of neurons during long-term culture was also assessed at regular time intervals using Trypan blue exclusion assay. Briefly, at regular time intervals, media was discarded from the wells, and neurons were washed twice with HBSS. Trypsin was added to the wells and incubated for 5 min at 37 ℃ to detach the neurons. Trypsinization was then inhibited by adding trypsin inhibitor. Neurons were pelleted by centrifugation. Neurons were washed twice with HBSS and were resuspended in 1 ml of HBSS. 10 µl of 0.5% trypan blue solution was mixed with 10 µl of neuronal suspension and incubated for 10 min at RT. 10 µl of the neuronal suspension-trypan blue mixture was spread on a hemocytometer, and the cells were counted separately in four different squares of hemocytometer using an inverted microscope. Average of the number of cells in each of the four squares were considered, and the total number of cells was calculated by the following formula

$$Total\ number\ of\ cells\ (per\ ml) = Average\ count\ per\ square \times dilution\ factor \times 10^4$$

The total number of cells were counted in a minimum of three independent samples at each time point and presented as mean±SD.

Morphological characterization of hippocampal and cortical neurons during long-term culture:

Hippocampal and cortical neurons were cultured and maintained, as mentioned earlier in this methodological section. At regular time intervals during long-term

culture, images of live hippocampal and cortical neurons were captured using a bright field microscope, and the morphology of neurons was characterized accordingly.

Senescence-associated beta-galactosidase (SA β-gal) assay:

The SA β-gal assay is performed to identify senescence cells in the cultures. The principle behind the assay is the mammalian cells on reaching senescence show increased expression of the beta-galactosidase enzyme. The beta-galactosidase enzyme converts X-gal to a blue colored precipitate. Cells stained with blue color after exposure to X-gal solution indicates their expression of beta-galactosidase and thereby indicates senescence (Dimri et al., 1995). Cortical neurons grown on pdl coated coverslips were washed two times with PBS and were fixed with 4% PFA for 5 min. After fixation coverslips were rewashed three times with PBS and were incubated in X-gal solution pH-6 (100 mM sodium phosphate, 5 mM potassium ferricyanide, 150 mM NaCl, 0.02% NP-40, 2 mM MgCl2, 0.01% sodium deoxycholate, 1 mg/ml X-gal, and 5 mM potassium ferrocyanide) for 10 h in the dark at 37 °C. Coverslips were rewashed three times with PBS and were air dried. Coverslips were observed under a bright field microscope for blue color stained cells. The number of blue color stained cells were counted in four random fields, and percentages were calculated. Minimum 200 cells were counted for drawing the results.

Mitochondrial Membrane Potential:

Mitochondrial-specific fluorescence dye rhodamine123 is used for estimating changes in mitochondrial membrane potential (MMP). Rhodamine123 accumulates electrophoretically in the mitochondria as a function of membrane potential. Changes in the membrane potential lead to differential accumulation of the dye in the mitochondria, which gives differential fluorescence signal. This form the basis for the estimation of MMP (L. B. Chen, 1988; Emaus, Grunwald, & Lemasters, 1986). At regular time points of in vitro aging, cortical neurons were estimated for MMP. Briefly, culture media was aspirated, neurons were washed twice with PBS and were incubated with 1nM rhodamine123 for 15 mins at 37 °C. Cortical neurons were washed thrice with PBS to remove extracellular rhodamine. Fluorescence intensities of rhodamine (Ex = 511 nm and Em = 534 nm) present in the mitochondria were read using fluorimeter (Multilabel Counter Victor 3, Perkin Elmer, Boston, MA). The background fluorescence

signals were also measured in the wells without the cells and were subtracted from fluorescence signals obtained for the cells. The mitochondrial membrane potential was measured as a ratio between fluorescence signals obtained for sample cells and control cells (Alhebshi, Gotoh, & Suzuki, 2013). Cortical neurons at DIV-5 were taken as control.

Immunocytochemistry:

Cortical neurons grown on pdl coated coverslips were washed twice with PBS (comprising 4% sucrose) and were fixed with 4% PFA (made with PBS comprising 4% sucrose) for 10 min at RT. Coverslips were washed again thrice with PBS. Then neurons were permeabilized using 0.3% Triton X-100 (made with PBS comprising 4% sucrose) for 10 min at RT. Coverslips were washed again thrice with PBS. Subsequently, neurons were blocked with 2% BSA (made with PBS comprising 4% sucrose) for 30 min at RT. Coverslips were washed again thrice with PBS. Neurons were stained with primary antibodies for 1 h at 37 ^{0}C. Coverslips were washed again thrice with PBS. Subsequently, neurons were stained with secondary antibodies for 30 min at 37 ^{0}C. Coverslips were washed again thrice with PBS. Antifade mountant with DAPI was added to the coverslips, and the coverslips were fixed to a glass slide. Immunofluorescence images were acquired using a confocal microscope (Leica, Buffalo Grove, USA).

Comet assay:

Comet assay is performed to measure the amount of damaged DNA in the cells. Briefly, cortical neurons were harvested at regular time intervals during long-term culture, and the neurons were mixed with 0.5% low melting point agarose at a final concentration of $1.25x10^{5}$ - $6.25x10^{6}$ cell per ml. Low melting point agarose with cells was layered on frosted glass slides which were precoated with 1% standard agarose. Coverslips were placed on the glass slides, and the glass slides were kept for 5-10 min at 4 ºC to solidify agarose. Coverslips were removed, and another layer of low melting point agarose without cells was layered on the glass slide. Coverslips were placed again on the glass slides, and the glass slides were kept again at 4 ºC for 5-10 min to solidify agarose. Following solidification, coverslips were removed. The glass slides were placed in lysing solution (10 mM Tris (pH-10), 100 mM EDTA, 2.5 M NaCl, and 1%

Triton X-100) for minimum 2 h at 4 ºC in the dark. Glass slides were then placed in electrophoresis buffer (300 mM NaOH and 1 mM EDTA, pH-13) for 30 min at 4 ºC in the dark, followed by electrophoresis (300 mA and 0.75 V/cm) for 30 min at 4 ºC in the dark. Then slides were washed thrice with chilled neutralization buffer (0.4 M of Tris, pH-7.5). Slides were then stained with ethidium bromide (20 µg/ml) for 5 min. After 5 min, slides were washed with chilled water to remove the excess stain (Dhawan, Mathur, & Seth, 2001). Comet images were acquired using a confocal microscope (Leica, Buffalo Grove, USA), and the images were analyzed for comet parameters using Comet Assay IV software (Instem, Staffordshire, UK). A minimum of 50 cells per sample was analyzed and presented as mean±SD.

Intracellular Calcium Levels:

Estimation of intracellular calcium levels in cortical neurons was done as described earlier (Ou et al., 2010) with slight modifications. Briefly, at regular time intervals during *in vitro* ageing of cortical neurons, media was aspirated from the wells and the cortical neurons were washed twice with HBSS buffer (pH-7.4) containing 0.1% BSA and 2.5 mM probenecid. Fura-2AM loading solution (1 µM solution of Fura-2AM in HBSS-BSA-probenecid buffer) was added to the neurons and incubated for 30 min at 37 ºC in the dark. Neurons were washed thrice with HBSS-BSA-probenecid buffer to remove the extracellular dye. Neurons were incubated for another 30 min at 37 ºC in the dark for hydrolysis of AM esters of the dye by non-specific esterases present in the cells. Fluorescence signals were measured in a fluorimeter (Multilabel Counter Victor 3, Perkin Elmer, Boston, MA) using dual excitation at 340 nm and 380 nm wavelengths and emission at 510 nm wavelength. The background fluorescence signals were also measured in the wells without the cells and were subtracted from fluorescence signals obtained for the cells. The intracellular calcium levels were estimated as a ratio obtained from 340/380 fluorescence intensities. Ratioing significantly reduces the effects of dye leakage, uneven dye loading, photobleaching, unequal cell thickness, etc.

Microarray Analysis:

At regular time intervals of *in vitro* ageing, cortical neurons were harvested and processed for microarray analysis using “Whole rat genome microarray Kit,” (Agilent,

Santa Clara, United States) at "Genotypic Technology Pvt Ltd" (Bangalore, India). Briefly, total RNA was isolated from control as well as from aged neurons using TRIzol following manufacturer's instructions. RNA samples were further refined, utilizing RNeasy mini-kit columns. Total RNA purity was evaluated by NanoDrop Spectrophotometer (NanoDrop Technologies, Rockland, USA). cDNA was developed using RNA samples. The cDNA samples were labeled with fluorescent dyes and hybridized to the DNA probes present on the slide. The microarray was scanned for fluorescent signals. Data were interpreted using GeneSpring GX 12.6.1 software and Microsoft Excel. All the samples were analyzed in triplicate. Fold changes used for downregulation and upregulation were ≤ 0.6 and ≥ 0.6 respectively; > 1 in the geometrician mean fold of the replicated samples. $P < 0.05$ was regarded as statistically significant.

Analysis of relative gene expression by quantitative PCR:

RNA isolation:

Total RNA was isolated from cerebral cortices of rat brains of different age groups using TRIzol following manufacturer's instructions. Briefly, 1ml of TRIzol was added per 100 mg of tissue, and the tissue was homogenized. After incubating the homogenate at RT for 5 min, it was centrifuged at 12000 g maintaining 4 °C for 10 min. Pellet was discarded and to the supernatant chloroform (0.2 ml/1 ml of TRIzol) was added, vortexed vigorously and incubated for 2 min at RT. Then the mixture was centrifuged for 15 min at 12000g maintaining 4 °C. Without disturbing interphase, the aqueous phase was transferred into a fresh polypropylene tube, and 2-propanol (0.5 ml/1 ml of TRIzol) was added. After incubating at RT for 10 min, the mixture was centrifuged for 10 min at 12000 g maintaining 4 °C. The supernatant was thrown out, and the pellet was washed 2 times, with 75% alcohol. The suspension was centrifuged for 5 min at 7500 g maintaining 4 °C. The obtained RNA pellet was air-dried, and dissolved in nuclease-free H_2O. Further incubated for 10 min at 55-60 °C for complete solubilization of RNA. Purity and concentration of RNA were checked using NanoDrop Spectrophotometer (NanoDrop Technologies, Rockland, USA).

cDNA synthesis:

Following manufacturer's instructions, cDNA was produced from total RNA using the cDNA synthesis kit. Briefly, in a microtube 0.5 µl (25 pM) of the random hexamer, 5 µg of total RNA, 1 µl of dNTP mixture and RNase free H_2O (to make up to 10 µl) was added. The mixture was incubated for 5 min at 65°C. 4.5 µl of RNase free H_2O, 0.5 µl of RNase Inhibitor, 1 µl of PrimeScript RTase, and 4 µl of PrimeScript buffer was added to the microtube maintaining at 4 ^{0}C. The reaction mixture was adequately mixed and incubated for 45 min at 42 ^{0}C. The enzyme was inactivated, and the synthesized cDNA was preserved at -80 ^{0}C.

Quantitative PCR:

Relative gene expression analysis was performed by utilizing quantitative PCR. Briefly, in each polypropylene tube, 10 µl of 2x SYBR-green PCR master mix, 2 µl containing 50-900 nM reverse primer, 2 µl containing 50-900 nM forward primers, 5 µl containing 1-100 ng cDNA and 1 µl of nuclease-free H_2O was added. Reaction mixtures without template were also made and kept as controls (No template controls) to confirm no cross-contamination of PCR reagents. 18s rRNA was also employed as an internal control. The reaction mixture was gently mixed and briefly centrifuged. qPCR was performed in Real-Time PCR system (Steponeplus, Thermo-Fisher Scientific, Waltham, U.S.) using following thermal cycling conditions. For initial enzyme activation: incubation at 95 ^{0}C for 10 min; for PCR cycles: incubation at 95 ^{0}C for 15 sec for denaturation and 72 ^{0}C for 1 min for annealing and extension. Instrument analyses the fluorescence signals generated from DNA amplifications and quantify the relative fold change employing the $2^{-\Delta\Delta CT}$ method (Schmittgen & Livak, 2008).

Table 3: List of primers used for qPCR.

Oligo Name	Sequence
Topo II beta Forward primer	GACAGAGGAAGGTAGTAGAGCCTG
Topo II beta Reverse primer	CGTTTTCTTCGGTTTCTTGCTGGC
NPY Forward primer	TGCTCGTGTGTTTGGGCATTCTGGCTGA
NPY Reverse primer	ATCAGTGTCTCAGGGCTGGATCTCTTGCCA
SLIT2 Forward primer	AGAACGGCACCAGCTTCCATGGCTGTAT

SLIT2 Reverse primer	TGGGCACACACTTTCTTGTGGCATGGTTCA
18s rRNA Forward primer	GCTACCACATCCAAGGAAGGCAGC
18s rRNA Reverse primer	CGGCTGCTGGCACCAGACTTG

Statistical analysis:

All the experiments were performed in triplicates and repeated a minimum of three times individually. Data were depicted as a mean±SD. Statistical significance between two groups was determined using Student t-test. Statistical significance between multiple groups was determined using one-way ANOVA by Holm-Sidak method. $P < 0.05$ was regarded as statistically significant.

RESULTS:

Morphological characterization of hippocampal neurons during long-term culture:

Pure hippocampal neurons were cultured without using an astrocyte feeder layer and were maintained in culture dishes with optimal conditions and requirements until they underwent natural death. It was observed that pure cultures of hippocampal neurons in the presence of neurobasal media supplemented with the B27 were able to survive for approximately 28 days ± 2 days in *in vitro* conditions (Fig. 11). It was observed that there was an increase in length and thickness of neuronal dendrites, size of the cell bodies, and networks with the increase in days in culture. Oval shaped cell bodies had transformed into pyramidal-shaped cell bodies with the increase in days in culture (Fig. 11). There was a gradual decrease in cell density with the increase in days in culture. Disintegrating neurons were more prominently seen at late stages. These all features indicate ageing pattern in long-term cultures of neurons.

Evaluation of the viability of hippocampal neurons during long-term culture using MTT assay:

MTT assay was performed at regular time intervals to evaluate the viability of hippocampal neurons during long-term culture. The survival percentage derived from the test OD and control OD was utilized to construct the growth curve. In long-term culture, hippocampal neurons were survived approximately for 28 days (± 2 days). It was also observed that there was a gradual reduction in the cell number until DIV-15. After DIV-15, there was a sharp decline in the neuronal survival with the increase in days in vitro. Less than 5% of cells were survived after 28 days (Fig. 12).

Morphological characterization of cortical neurons during long-term culture:

Pure cultures of cortical neurons were maintained under optimal conditions and requirements until they underwent natural death. It was observed that cultures of cortical neurons in the presence of neurobasal media with the B27 supplement were able to survive approximately 50 ± 5 days in *in vitro* conditions (Fig. 13). It was observed that the length of dendrites increased gradually with the increase in time in

culture. After 30 days *in vitro*, neurons become much broader in size (Fig. 13). Increase in the cell volume was reported to be a marker of senescence (Hwang, Yoon, & Kang, 2009). Increased networks were observed with the increase in days. There was a gradual decrease in cell density and an increase in the cell fragments with the increase in days. Disintegrating neurons were more prominently seen at late stages (Fig. 13). These all features indicate ageing phenomena in long-term cultures of neurons.

Immunofluorescent labeling of cortical neurons for showing their purity at different time points:

Immunofluorescence experiment was performed at discrete time points to confirm whether the cells in culture were neurons. Cells were labeled using rat anti-MAP2 (neuronal marker protein) and rat anti-GFAP (glial marker protein). More than 98% of the cells were immunostained with MAP2 which confirms that these cells were purely neurons, and the presence of glial cells was confined to less than 2% (Fig. 14).

Evaluation of the viability of cortical neurons during long-term culture using MTT assay:

MTT assay was performed at regular time intervals to evaluate the viability of cortical neurons during long-term culture. The survival percentage derived from the test OD and control OD was utilized to construct the growth curve. In long-term culture, cortical neurons were able to survive for 50 ± 5 days in *in vitro*. It was also noticed that there was a rapid drop in the cell number until DIV-20. After DIV-20, there was a gradual reduction in the cell number with the increase in days *in vitro* (Fig. 15).

Evaluation of the viability of cortical neurons during long-term culture using trypan blue exclusion assay:

To further scrutinize and evaluate MTT results independently, we have conducted the trypan blue exclusion assay. Similar to MTT assay, trypan blue counting assay also showed that cortical neurons were able to survive for 50 ± 5 days in *in vitro* (Fig. 16). Consistent with the MTT assay results, trypan blue exclusion assay also showed similar cell death pattern during long-term culture.

Senescence-associated beta-galactosidase assay:

SA β-gal assay was performed at regular time intervals on cortical neurons during long-term culture. The activity of beta-galactosidase was evidenced by the appearance of blue color in the cells on X-gal exposure (Fig: 17 A). It was observed that there was a steady increase in the percentage of blue coloured cells with the increase in the number of days of cell survival (Fig: 17 B), which confirms the increased expression of beta-galactosidase in the cortical neurons with the increase in the number of days of survival. As an increased expression of beta-galactosidase is an indicator of senescence (Dimri et al., 1995), these results suggest the progress of ageing in the long-term cultures of cortical neurons.

Mitochondrial Membrane Potential (MMP) during *in vitro* Ageing:

Neurons were exposed to mitochondrial-specific dye rhodamine 123 at specific time points of *in vitro* ageing viz., DIV-5, DIV-15, and DIV-35 to estimate the changes in the MMP of the cortical neurons during *in vitro* ageing. It was observed that there was a decrease in the MMP with the increase of *in vitro* ageing (Fig. 18). There was 33.68% of the decrease in the rhodamine fluorescence intensity percentage in DIV-35 compared to DIV-5.

Estimation of Intracellular Calcium Levels during *in vitro* Ageing:

Neurons were exposed to a Ca^{2+} selective fluorescent indicator, Fura-2AM, at specific time points of *in vitro* ageing viz., DIV-5, DIV-15, and DIV-35 to estimate the changes in the intracellular calcium levels of the cortical neurons during *in vitro* ageing. It was observed that there was a gradual increase in the intracellular calcium levels with the increase of *in vitro* ageing (Fig. 19), these results indicate that there was a dysregulation in the calcium homeostasis with the increase of age.

Estimation of DNA damage during *in vitro* ageing using Comet assay:

Comet assay was performed at specific time points of *in vitro* ageing viz., DIV-5, DIV-15, and DIV-35 to estimate the DNA damage in the cortical neurons during *in vitro* ageing. The intensity of DNA damage is measured through the tail moment in the comet. Tail movement is the product of fraction of DNA and tail length in the comet tail.

It was observed that there was a gradual increase in the tail moment with the increase of the number of *days in vitro* (Fig: 20). These results indicate that there was an increase in the DNA damage accumulation with the increase of *in vitro* ageing.

Levels of Topoisomerase II beta protein during *in vitro* ageing:

Immunocytochemistry experiment was performed at specific time points of *in vitro* ageing of cortical neurons to evaluate the changes in the expression levels of Topo IIβ protein. It was observed that cortical neurons at 5 days *in vitro* (DIV-5) had higher levels of Topo IIβ protein, which was reduced moderately by 15 days *in vitro* (DIV-15). Further Topo IIβ protein levels had decreased drastically by 35 days *in vitro* (DIV-35) (Fig. 21). It demonstrated that there was an age-dependent reduction in the levels of Topo IIβ protein during the *in vitro* ageing of cortical neurons.

Analysis of relative gene expression by quantitative PCR in different age groups of the rat:

Further Topo IIβ gene expression levels were evaluated in the cerebral cortex of rat brains at different age groups by quantitative PCR. Gene expression results have demonstrated that there was a decrease in the expression levels of Topo IIβ in adults and old age groups compared to the new-born age group. There was an increase in the expression levels of Topo IIβ in the old age group compared to the adult age group (Fig: 22 A). This increase could be due to age-associated inflammation in the brain that promotes the proliferation of glial cells, which contributes towards the increase of Topo IIβ (R. K. Mandraju & Kondapi, 2007; Sanada et al., 2018); otherwise, it has been shown from the above results as well as literature reports that Topo IIβ levels decrease in neurons with age. In our laboratory, previously it was reported that Slit2 and NPY genes were upregulated in the *in vitro* ageing of cerebral granule neurons (Gupta, Dholaniya, Chekuri, & Kondapi, 2015). So, Slit2 and NPY genes expression levels were evaluated in the cerebral cortex of rat brains at different age groups. It was observed that Slit2 gene expression levels had increased steadily with the ageing in rat cerebral cortex (Fig: 22 B), similar to that found in granule neurons (Gupta et al., 2015). It was noticed that there was no significant fold difference in the expression levels of NPY gene with ageing in rat cerebral cortex (Fig: 22 C), which show differential regulation of NPY in the cortical region.

Gene expression analysis of *in vitro* ageing of cortical neurons using Microarray:

At regular time intervals of *in vitro* ageing, cortical neurons were harvested and processed for microarray analysis. For filtering differentially expressed genes, we considered fold change ≤ -0.6 and ≥ 0.6 with P-value < 0.05 in the aged sample. Differentially expressed genes were subjected to pathway analysis using Biointerpreter software. A total of 2700 genes were identified as differentially upregulated (Fold change ≥ 0.6), reported being involved in 198 different pathways. On the other hand, 2339 genes were identified as differentially downregulated (Fold change ≤ -0.6), which were found to be involved in 195 different pathways. All the pathways in both categories were ranked based on the number of differentially expressed genes involved. The pathways having a higher number of genes were termed as most active pathways. 20 most active pathways from both differentially upregulated and downregulated genes were shown in figure 23. The list of individual genes is provided in table 4 & table 5.

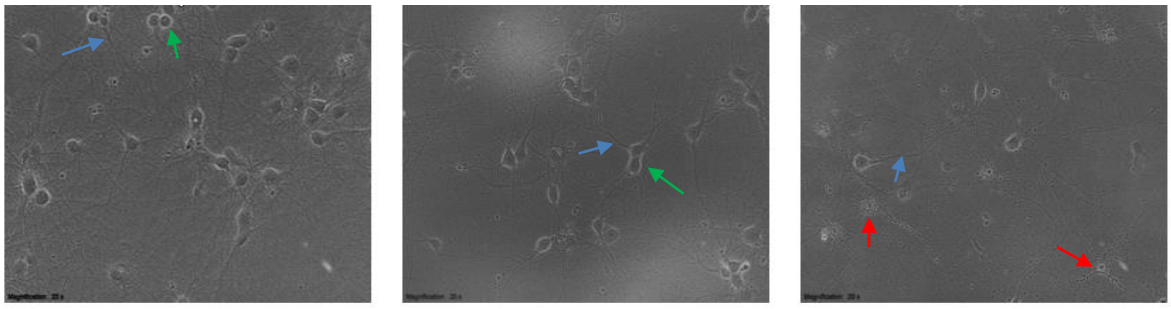

(A) **(B)** **(C)**

Figure 11: Establishment of Hippocampal neurons as *in vitro* Ageing model. Above figures show cultures of Hippocampal neurons at different time points of long-term culture (A) DIV-7, (B) DIV-14, (C) DIV-21. It was observed that there was an increase in length and thickness of neuronal dendrites (Blue colour arrow), size of the cell bodies (Green colour arrow) with the increase in days in culture. Oval shaped cell bodies had transformed into pyramidal-shaped cell bodies with the increase in days in culture (Green colour arrow). There was a gradual decrease in cell density with the increase in days in culture. Disintegrating neurons were more prominently seen at late stages (Red colour arrow). These all features indicate an ageing pattern in long-term cultures of neurons.

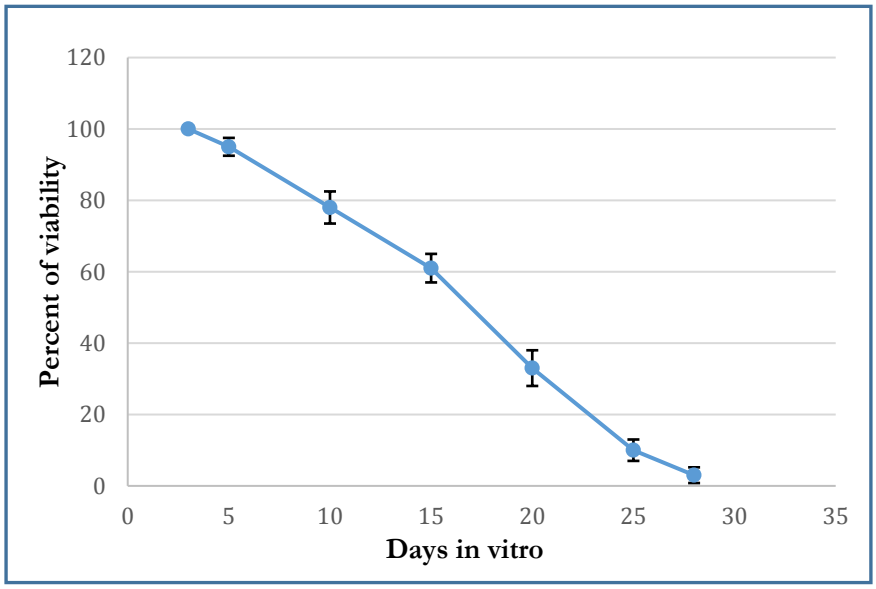

Figure 12: Evaluation of the viability of hippocampal neurons during long-term culture using MTT assay. It was observed that there was a gradual reduction in the cell number until DIV-15. After DIV 15, there was a sharp decline in the neuronal survival with the increase in days *in vitro*. Data were depicted as mean±SD, n=3.

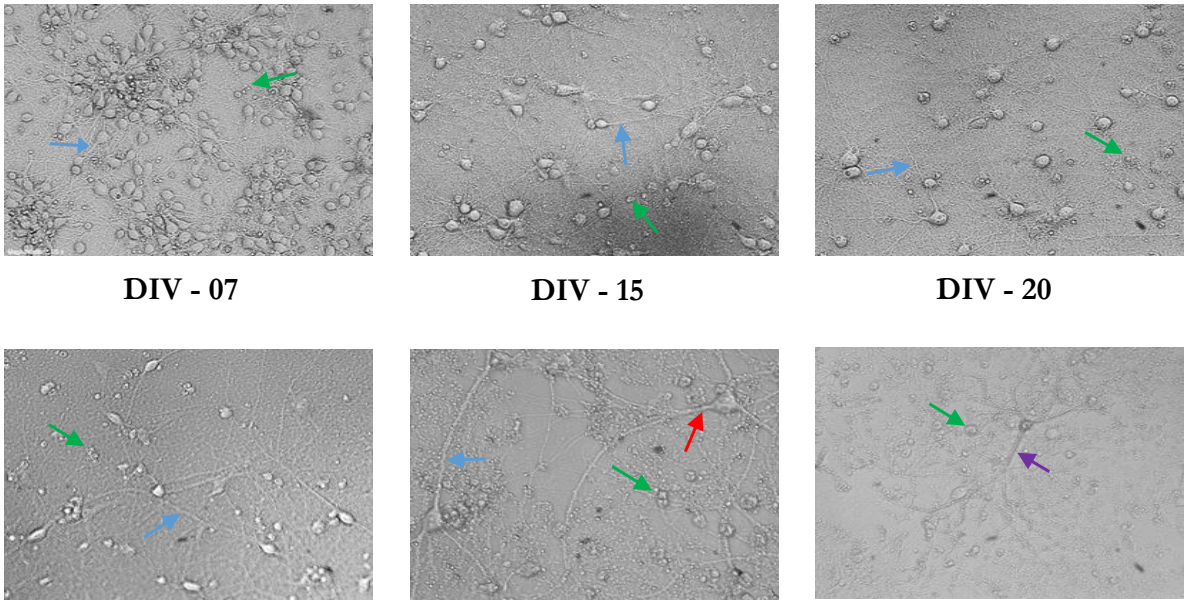

Figure 13: Morphological characterization of cortical neurons during long-term culture. Above images show cultures of cortical neurons at different time intervals of long-term culture. It was observed that the length of neuronal dendrites got gradual increased as the culture becomes older (Blue colour arrow in the image). After 30 days *in vitro* (DIV) neurons become much broader in size (Red colour arrow in the image). There was a gradual decrease in cell density and an increase in the cell fragments with the increase in time (Green colour arrow in the image). Disintegrating neurons were more prominently seen at late stages of *in vitro* aging (Purple colour arrow in the image). These all features indicate an ageing pattern in long-term cultures of neurons.

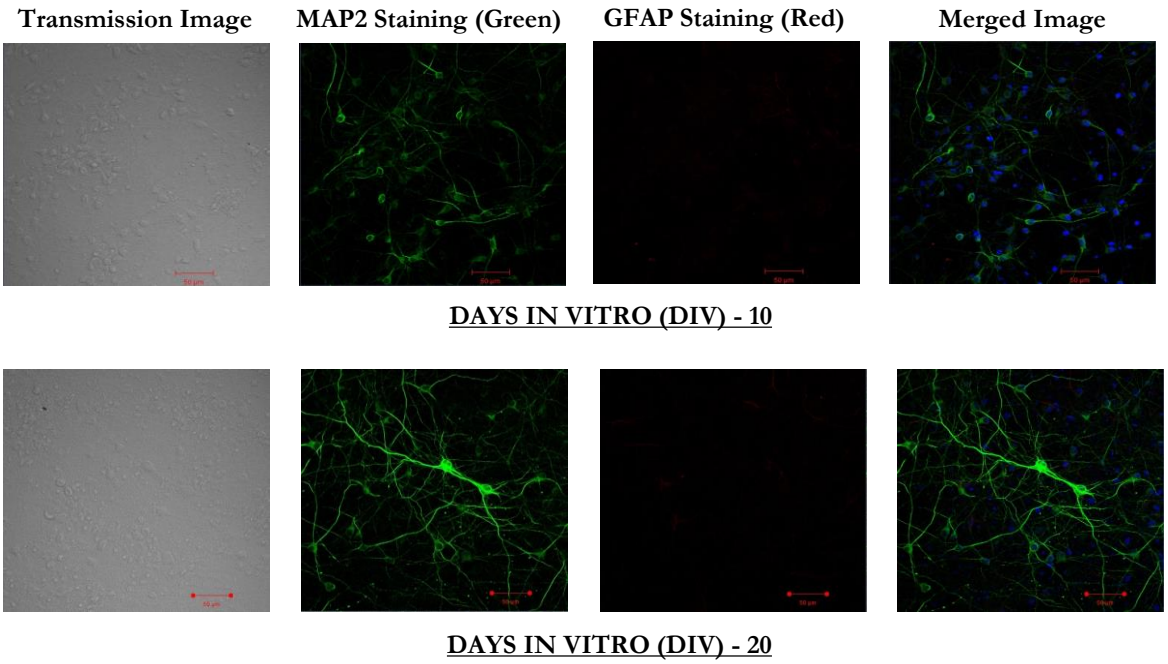

Figure 14: Immunofluorescent labeling of cortical neurons during long-term culture for showing their purity at different time points. Green colour: MAP2 (neuronal marker protein) red colour: GFAP (glial marker protein) and blue colour: DAPI (nucleus-specific stain). More than 98% of the cells were immunostained with MAP2, which confirms that these cells were purely neurons, and the presence of glial cells was negligible. The experiment was performed three times independently (n=3).

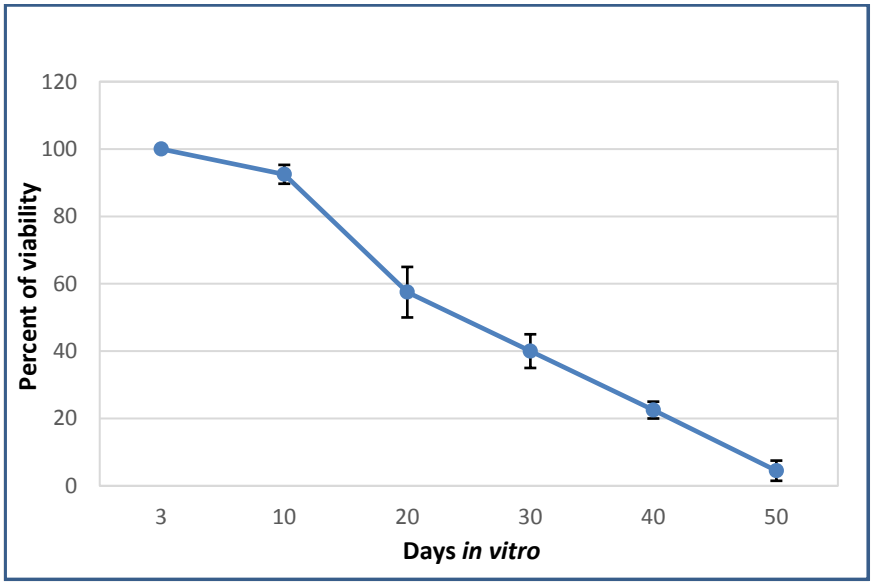

Figure 15: Evaluation of the viability of cortical neurons during long-term culture using MTT assay. It was observed that there was a rapid drop in the cell number until DIV-20. After DIV-20, there was a gradual reduction in the cell number with the increase in days *in vitro*. Data were depicted as mean±SD; n=3.

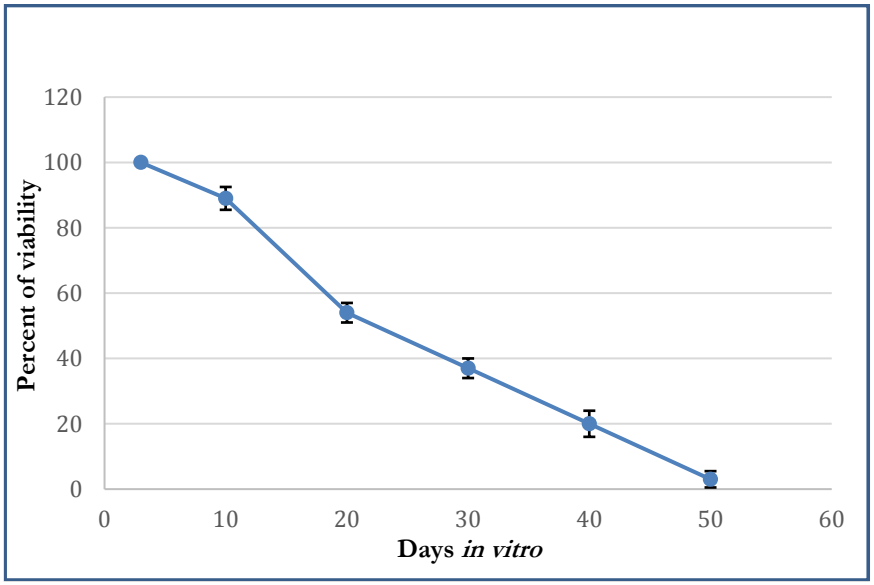

Figure 16: Evaluation of the viability of cortical neurons during long-term culture using trypan blue exclusion assay. It was observed that there was a rapid drop in the cell number until DIV-20, followed by a gradual reduction in the cell number with the increase in days *in vitro*. Data were depicted as mean±SD; n=3.

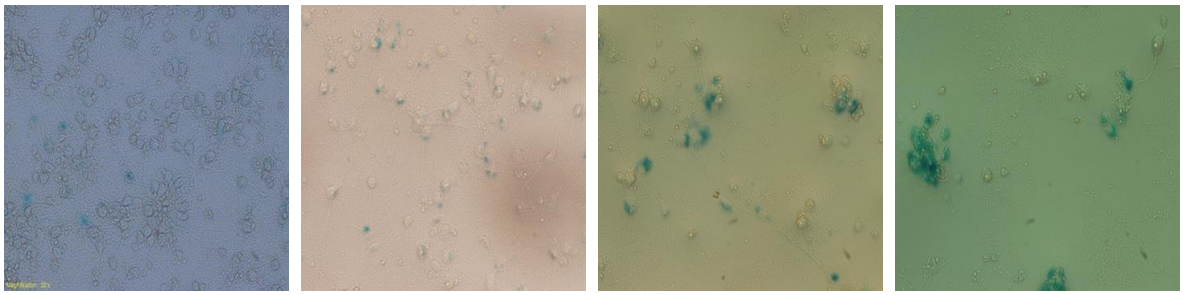

DIV – 10 DIV – 20 DIV – 30 DIV – 40

(A)

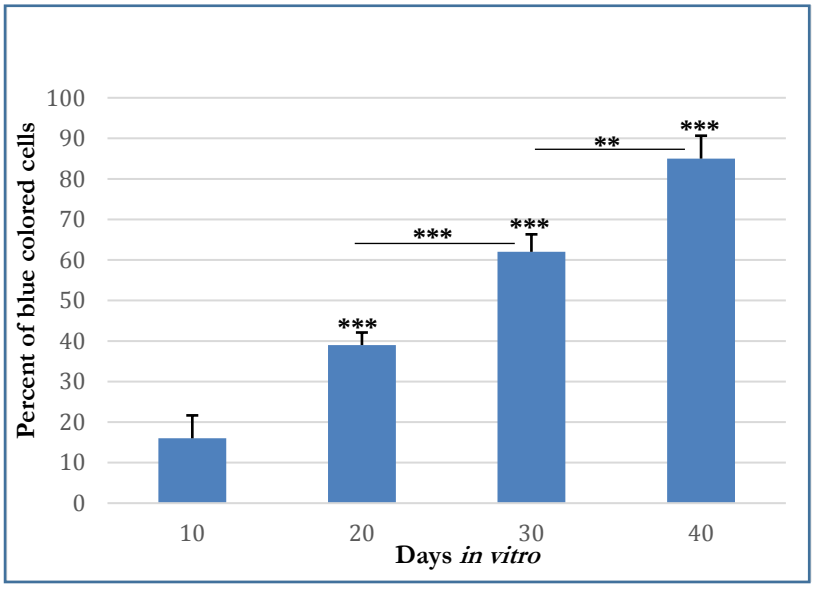

(B)

Figure 17: Senescence-associated beta-galactosidase assay: (A) Bright-field microscopic images of activity of SA β-gal in cortical neurons during long-term culture. (B) Bar diagram represents the percent of blue color stained cells at regular time intervals during the long-term. The activity of SA β-gal was evidenced by the appearance of blue colour in the cells on x-gal exposure. There was an increase in the activity and expression of SA β-gal with the increase in the number of days of neuronal survival. Data were depicted as mean±SD; n = 3. ***P < 0.001, **P < 0.01 by one-way ANOVA using the Holm-Sidak method.

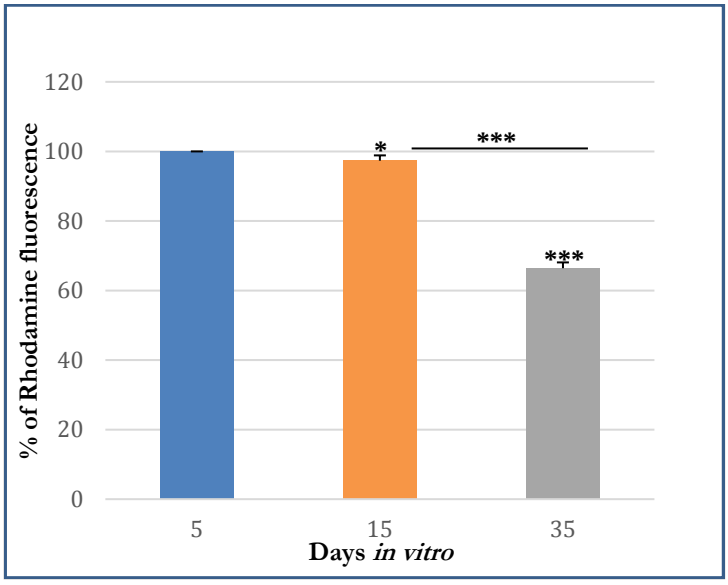

Figure 18: Mitochondrial Membrane Potential during *in vitro* Ageing. There was a decrease in mitochondrial membrane potential with the increase of *in vitro* ageing of cortical neurons. Data were depicted as mean±SD; n = 3. ***P < 0.001, **P < 0.01, *P < 0.05 by one-way ANOVA using the Holm-Sidak method.

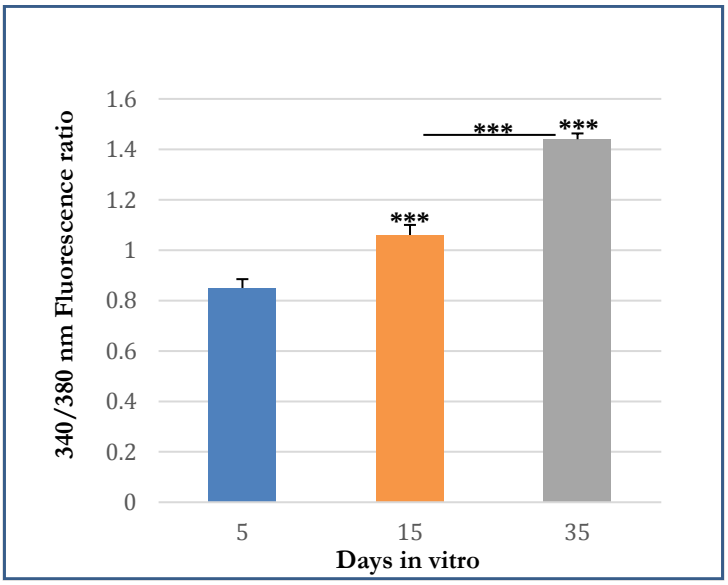

Figure 19: Estimation of Intracellular Calcium Levels during *in vitro* Ageing. There was a gradual increase in the intracellular calcium levels with the increase of *in vitro* ageing of cortical neurons. These results indicate that there was a dysregulation in the calcium homeostasis with the increase of age *in vitro*. Data were depicted as mean±SD; n = 3. ***P < 0.001 by one-way ANOVA using the Holm-Sidak method.

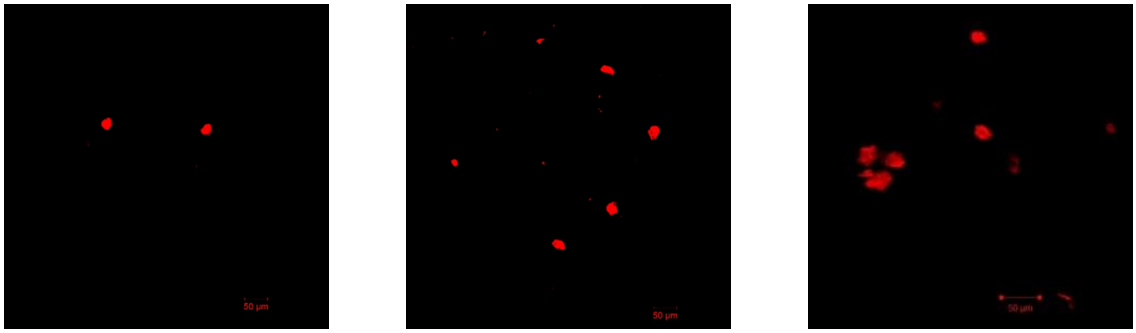

DIV-5 DIV-15 DIV-35

(A)

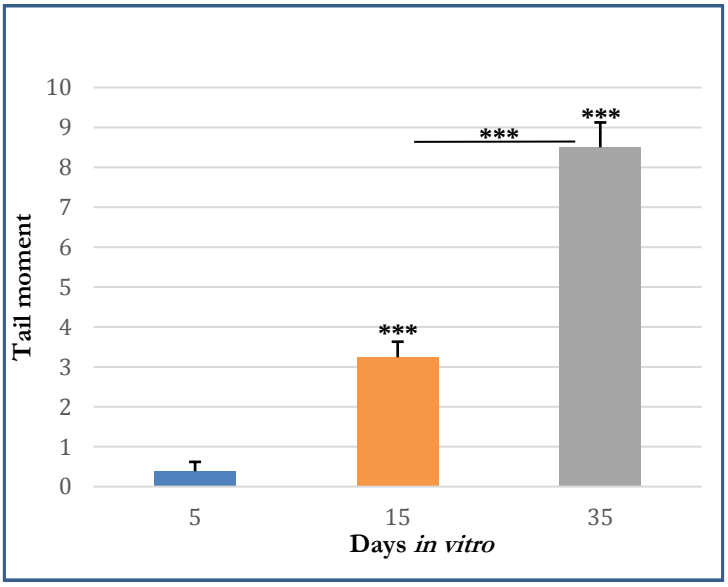

(B)

Figure 20: Comet assay. (A) Confocal images of comets at regular time points of *in vitro* ageing of cortical neurons. (B) Measurements of tail moments of comets at regular time points of *in vitro* ageing of cortical neurons using "Comet assay-IV software." The intensity of DNA damage is measured through the tail moment in the comet. Tail movement is the product of fraction of DNA and tail length in the comet tail. It was observed that there was a gradual increase in the tail moment with the increase of the number of *days in vitro*, which indicate that there was an increase in the DNA damage with the increase of *in vitro* ageing. Data were depicted as mean±SD; n = 3. ***P < 0.001 by one-way ANOVA using the Holm-Sidak method.

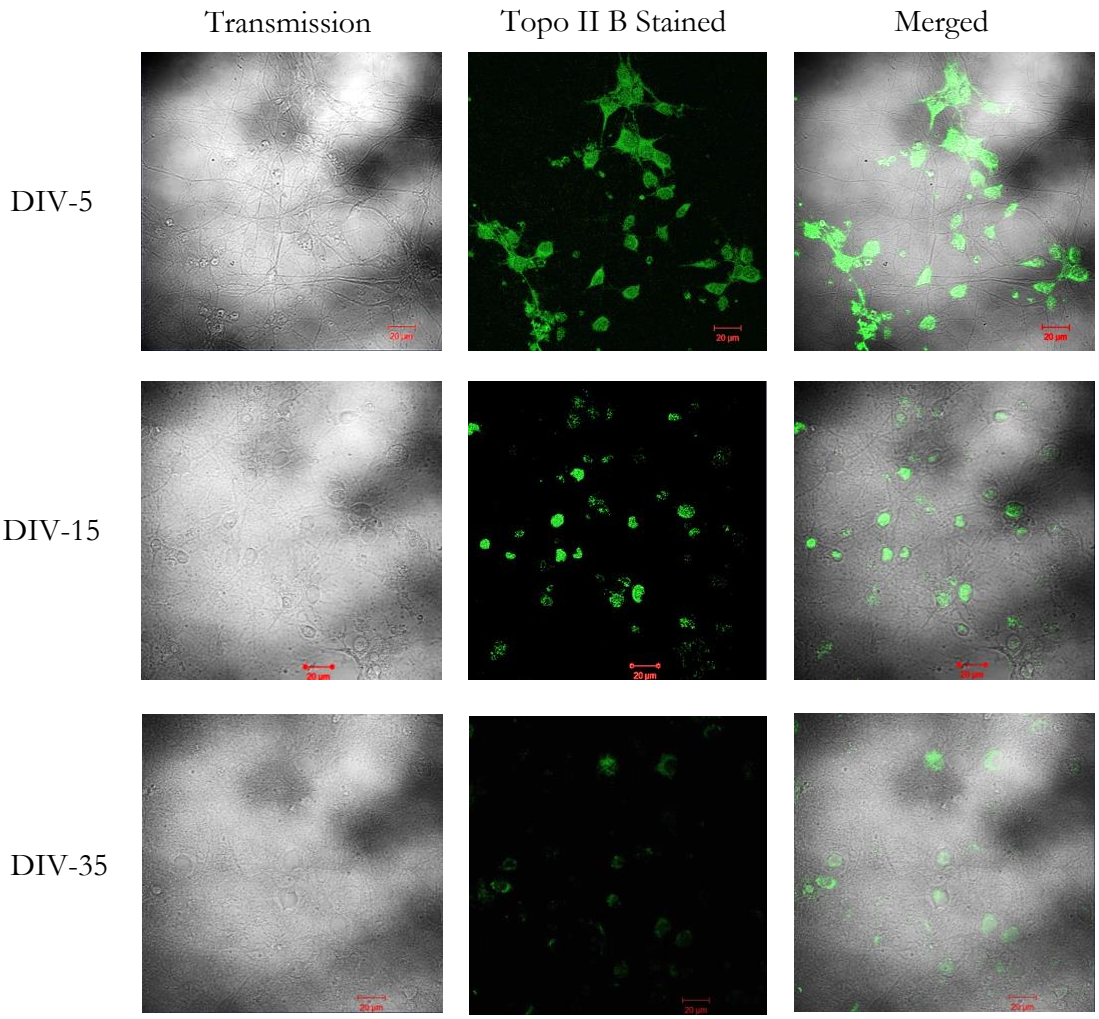

Figure 21: Immunocytochemistry of Topoisomerase II beta (Topo IIβ) during *in vitro* ageing. Cortical neurons at DIV-5 showed higher expression of Topo IIβ protein, which was reduced moderately by DIV-15. By DIV-35 Topo IIβ protein expression had drastically declined. These suggest an age-dependent reduction in the expression levels of Topo IIβ protein. The experiment was performed three times independently (n=3).

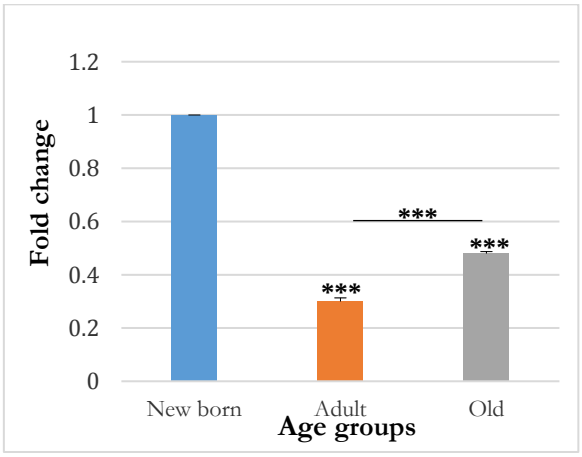

(A)

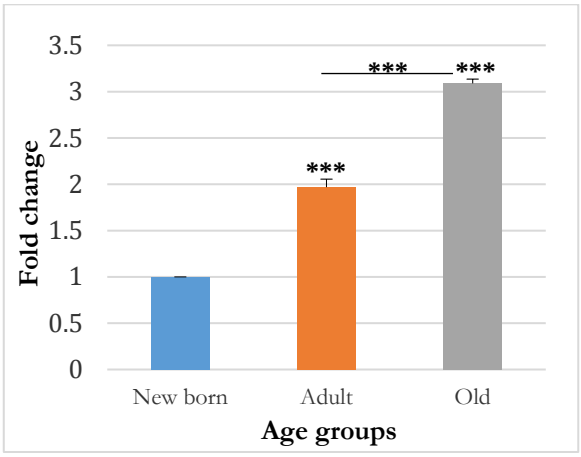

(B)

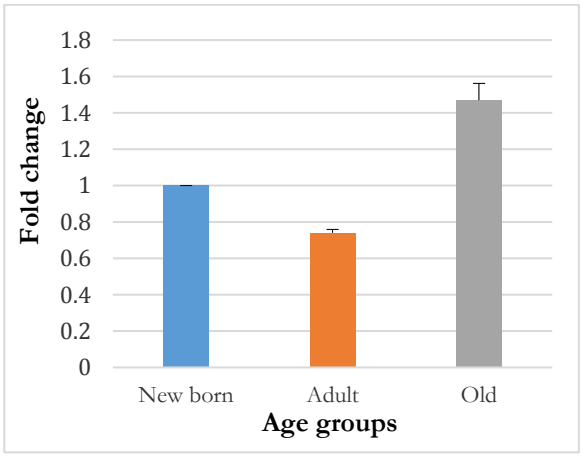

(C)

Figure 22: Analysis of relative gene expression by quantitative PCR in different age groups of the rat for (A) Topoisomerase II beta gene, (B) Slit2 gene, (C) NPY gene. Topoisomerase II beta gene expression had decreased by four-fold in adults, followed by an increase of two folds in old. Slit2 gene expression had increased steadily with the ageing. There was no significant fold difference in the expression levels of NPY gene over ageing. Data were represented as mean±SD; n = 3. ***P < 0.001 by one-way ANOVA using the Holm-Sidak method.

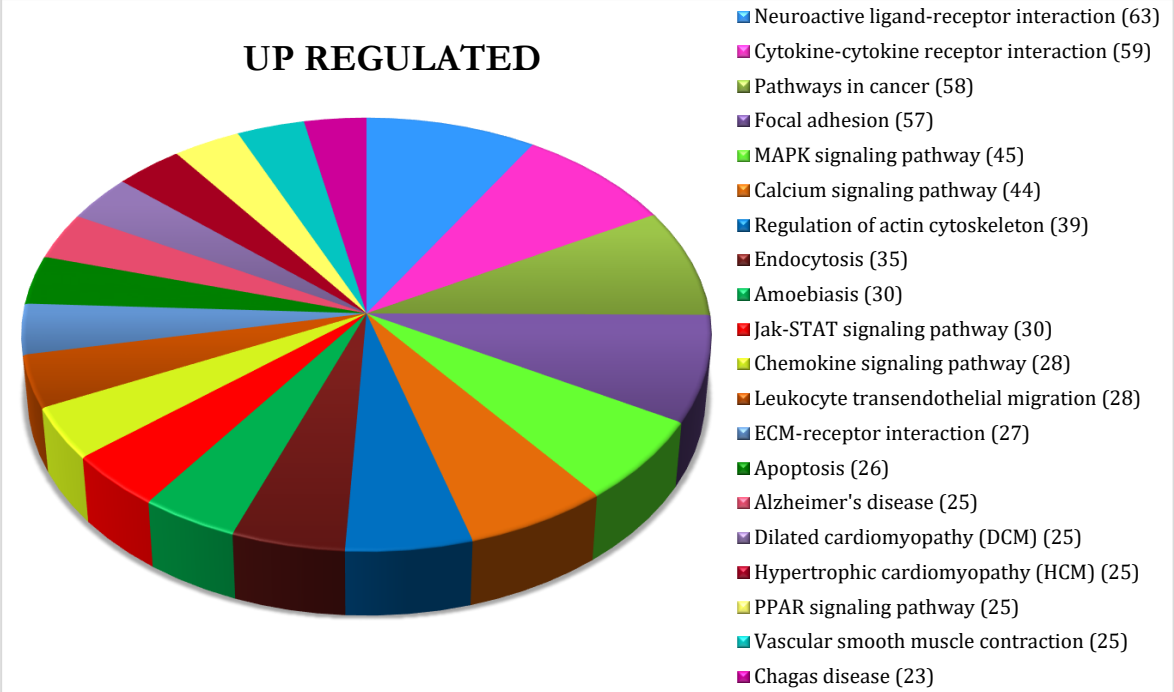

(A)

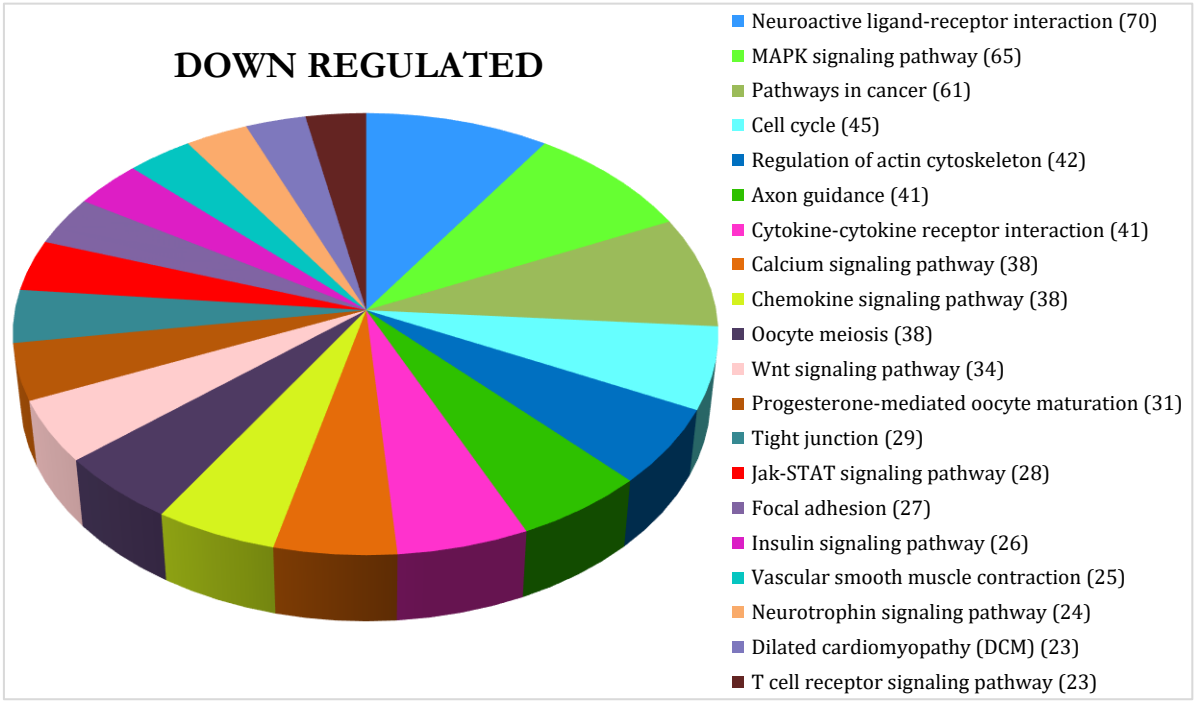

(B)

Figure 23: Microarray analysis of *in vitro* ageing of cortical neurons. (A) 20 most active pathways among differentially upregulated genes and (B) 20 most active pathways among differentially downregulated genes (in the bracket is the number of genes

appeared in that pathway). Differentially expressed genes were subjected to pathway analysis using Biointerpreter software. A total of 2700 genes were identified as differentially upregulated and reported to be involved in 198 different pathways. On the other hand, 2339 genes were identified as differentially downregulated, which were found to be involved in 195 different pathways. All the pathways in both categories were ranked based on the number of differentially expressed genes involved. The pathways having a higher number of genes were termed as most active pathways.

Table: 4. Details of 20 most active pathways among differentially upregulated genes

Pathway name	Kegg ID	Genes	No. of genes
Neuroactive ligand-receptor interaction	mmu04080	GRM8,NMUR1,AGTR1B,HTR2B,HTR2C,HTR2A,POMC,GAL,GRPR,GRIN2C,DRD4,PLG,EDNRB,TACR2,OPRM1,OPRL1,TRPV1,PPY,OPRD1,LPAR1,PTH2R,PTH1R,P2RX4,P2RX6,P2RX2,P2RX3,P2RY1,P2RY2,TAAR4,GRIN1,GABBR1,CHRNB1,ADRA1D,CHRNA9,ADRA2A,THRB,GABRG1,APLN,HRH1,HRH4,HRH3,GABRB1,AGRP,ADORA2B,S1PR3,S1PR1,S1PR5,CHRNA10,GLRB,NTSR2,LGR4,FSHB,MC4R,PRLR,TSHR,ADCYAP1R1,CYSLTR1,LHB,HTR6,HTR4,LEPR,TSPO,F2R	63
Cytokine-cytokine receptor interaction	mmu04060	IL7R,TNFRSF11A,FAS,IL1A,IL24,IL13RA1,FLT3,FLT4,TNFRSF12A,CSF2RB,BMP6,BMP4,CNTFR,IL6ST,ACVR1B,LTBR,IL12A,IL12B,PGF,BMPR1B,CXCL14,CXCL16,CXCL12,CXCL10,CLCF1,IL5,CCL11,TNFRSF8,CSF1,TNFRSF25,TNFRSF1A,TNFRSF1A,CX3CL1,PDGFRB,CCL2,CCL7,CTF1,KDR,IL2RA,IFNG,CCR3,PRLR,PDGFC,PDGFD,IL17RA,IL22RA1,IL3RA,CXCR4,CSF1R,TGFB3,TGFB2,TGFB1,EGF,TNFSF12,TNFSF10,LEPR,IL11RA1,TNF,IL12RB1	59

Pathways in cancer	mmu05200	ITGA2,TCF7L2,AKT2,FAS,FLT3,DAPK2,PIK3R5,PIK3R3,RARB,BMP4,BIRC3,LAMA5,CDKN1A,CDKN1A,LAMB2,LAMC1,CDKN2B,ABL1,FN1,SLC2A1,PGF,RXRA,SIRT2,STAT1,ARAF,BCL2L1,PRKCA,FGFR2,FGFR1,TRAF3,PDGFRB,WNT7B,WNT9B,FZD8,FZD6,SMO,WNT6,RET,STAT5A,EPAS1,FGF2,GLI3,FGF7,DCC,CTNNA3,VHL,ERBB2,ITGA2B,CSF1R,TGFB3,TGFB2,TGFB1,MITF,MITF,WNT5A,EGF,PPARG,XIAP	58
Focal adhesion	mmu04510	ITGA7,ITGA2,ITGA1,IBSP,ITGB6,ITGB5,ITGB3,AKT2,FLT4,FLNC,FLNA,PIK3R5,PIK3R3,COL6A1,COL6A2,BIRC3,LAMA5,LAMB2,LAMC1,MYLK3,MYLK2,FN1,VAV3,PGF,COL1A1,COL1A2,PXN,ILK,CAV2,CAV3,CAV1,PRKCA,PDGFRB,MYL9,MYLK,THBS2,SHC1,SHC4,COL3A1,KDR,SPP1,COL11A1,COL11A2,PDGFC,PDGFD,VCL,ERBB2,ITGA2B,ARHGAP5,EGF,BCAR1,CCND3,COL5A2,TNR,TNR,PARVB,XIAP	57
MAPK signaling pathway	mmu04010	MAPK4,AKT2,FAS,IL1A,PLA2G5,FLNC,FLNA,DUSP16,DUSP14,RASGRP3,HSPB1,HSPA2,MAPK12,ECSIT,PLA2G2C,PLA2G10,NTRK2,PLA2G4E,PLA2G4A,PTPN7,DUSP3,PPP3R2,CACNB4,CACNB4,PRKCA,TAB2,TNFRSF1A,TNFRSF1A,CACNG8,FGFR2,FGFR1,NFATC4,PDGFRB,CD14,MAPKAPK3,MAP4K4,FGF2,FGF7,DDIT3,RPS6KA5,TGFB3,TGFB2,TGFB1,EGF,TNF	45
Calcium signaling pathway	mmu04020	VDAC2,PHKG1,PHKG2,AGTR1B,HTR2B,HTR2C,HTR2A,GRPR,MYLK3,MYLK2,GRIN2C,PHKB,EDNRB,TACR2,SLC25A4,PDE1B,P2RX4,P2RX6,P2RX2,P2RX3,GRIN1,PPP3R2,PRKCA,ADRA1D,PLCE1,PLCD1,PLCD4,PLCD3,PDGFRB,HRH1,MYLK,ADORA2B,CD38,CYSLTR1,TNNC2,ERBB3,ERBB2,GNA14,ADCY2,ADCY7,HTR6,HTR4,SPHK1,F2R	44
Regulation of actin cytoskeleton	mmu04810	ITGA7,ITGA2,ITGA1,ITGB6,ITGB5,ITGB3,EZR,NCKAP1,PIK3IP1,PIK3R5,PIK3R3,MYLK3,MYLK2,FN1,ARPC5L,VAV3,WASF2,PXN,GSN,SSH3,ARAF,FGFR2,FGF	39

		R1,PDGFRB,MYL9,MYLK,CD14,IQGAP1,FGF2,FGF7,PDGFC,PDGFD,VCL,ITGA2B,LIMK2,EGF,BCAR1,F2R,MSN	
Endocytosis	mmu04144	TSG101,HSPA2,PLD2,RAB31,TFRC,VPS37C,LDLRAP1,CAV2,ASAP2,CAV3,CAV1,ZFYVE16,SMURF2,FGFR2,CHMP1B,FOLR1,RET,KDR,IL2RA,PSD2,SH3GLB2,DNM2,ERBB3,ARAP2,ARAP1,CXCR4,CSF1R,TGFB3,TGFB2,TGFB1,EHD2,EGF,EPN3,EPS15,F2R	35
Amoebiasis	mmu05146	TLR2,TLR4,PIK3R5,PIK3R3,MUC2,MUC2,LAMA5,CD1D1,LAMB2,LAMC1,HSPB1,FN1,IL12A,IL12B,COL1A1,COL1A2,PRKCA,CD14,COL3A1,SERPINB9,COL11A1,COL11A2,IFNG,VCL,GNA14,TGFB3,TGFB2,TGFB1,COL5A2,TNF	30
Jak-STAT signaling pathway	mmu04630	IL7R,AKT2,IL24,IL13RA1,PIK3R5,PIK3R3,CSF2RB,SPRY3,SPRY4,CNTFR,IL6ST,IL12A,IL12B,JAK3,CLCF1,IL5,STAT1,STAT4,BCL2L1,CTF1,STAT5A,IL2RA,IFNG,PRLR,IL22RA1,IL3RA,LEPR,CCND3,IL11RA1,IL12RB1	30
Chemokine signaling pathway	mmu04062	AKT2,PIK3R5,PIK3R3,VAV3,JAK3,PXN,CXCL14,CXCL16,CXCL12,CXCL10,CCL11,STAT1,DOCK2,PRKCD,GNB3,GNG5,GNG5,CX3CL1,CCL2,CCL7,SHC1,SHC4,CCR3,CXCR4,ADCY2,ADCY6,ADCY7,BCAR1	28
Leukocyte transendothelial migration	mmu04670	EZR,CYBA,PIK3R5,PIK3R3,VCAM1,MAPK12,VAV3,JAM2,PXN,RAPGEF3,CXCL12,PRKCA,CD99,MYL9,CLDN19,CLDN11,CLDN2,CLDN9,CLDN5,CLDN6,VCL,CTNNA3,F11R,CXCR4,ARHGAP5,BCAR1,ICAM1,MSN	28
ECM-receptor interaction	mmu04512	ITGA7,ITGA2,ITGA1,IBSP,ITGB6,ITGB5,ITGB3,SDC2,COL6A1,COL6A2,LAMA5,LAMB2,LAMC1,FN1,COL1A1,COL1A2,GP1BB,CD44,THBS2,COL3A1,SPP1,COL11A1,COL11A2,ITGA2B,COL5A2,TNR,TNR	27
Apoptosis	mmu04210	MYD88,AKT2,FAS,IL1A,PIK3R5,PIK3R3,CSF2RB,BIRC3,ENDOG,CASP6,CAPN1,BCL2L1,PPP3R2,TNFRSF1A,	26

		TNFRSF1A,CASP12,TRADD,IRAK3,IRAK2,CFLAR,RIPK1,IL3RA,ENDOD1,TNFSF10,TNF,XIAP	
Alzheimer's disease	mmu05010	GAPDH,GAPDH,GAPDH,GAPDH,GAPDH,GAPDH,FAS,PSEN2,GRIN2C,ATF6,PSENEN,UQCRB,NDUFV3,CAPN1,CAR14,GRIN1,PPP3R2,TNFRSF1A,TNFRSF1A,CASP12,ATP5G1,COX7C,COX8B,BACE2,TNF	25
Dilated cardiomyopathy (DCM)	mmu05414	ITGA7,ITGA2,ITGA1,ITGB6,ITGB5,ITGB3,MYBPC3,CACNB4,CACNB4,CACNG8,SGCG,SGCB,SGCA,LMNA,ITGA2B,TNNT2,TGFB3,TGFB2,TGFB1,ADCY2,ADCY6,ADCY7,DMD,TNF,TTN	25
Hypertrophic cardiomyopathy (HCM)	mmu05410	ITGA7,ITGA2,ITGA1,ITGB6,ITGB5,ITGB3,MYBPC3,PRKAG3,CACNB4,CACNB4,CACNG8,SGCG,SGCB,SGCA,ACE,AGT,LMNA,ITGA2B,TNNT2,TGFB3,TGFB2,TGFB1,DMD,TNF,TTN	25
PPAR signaling pathway	mmu03320	NR1H3,ACSL6,HMGCS2,CPT2,CYP7A1,RXRA,PCK2,ILK,ACADL,ACADM,CYP8B1,PLTP,CPT1C,CPT1A,SLC27A5,SORBS1,ACOX1,ACOX2,SLC27A1,CYP27A1,ANGPTL4,PPARG,PPARA,ME1,ME1	25
Vascular smooth muscle contraction	mmu04270	PLA2G5,AGTR1B,MYLK3,MYLK2,PLA2G2C,PLA2G10,PLA2G4E,PLA2G4A,PPP1R14A,ARAF,PRKCA,PRKCD,ADRA1D,ADM,MYL9,MYLK,AGT,ADORA2B,GUCY1B2,ADCY2,ADCY6,ADCY7,CALD1,NPR1,NPR2	25
Chagas disease	mmu05142	MYD88,AKT2,FAS,TLR2,TLR4,TLR6,PIK3R5,PIK3R3,MAPK12,IL12A,IL12B,TNFRSF1A,TNFRSF1A,ACE,CCL2,IFNG,CD247,CFLAR,GNA14,TGFB3,TGFB2,TGFB1,TNF	23

Table: 5. Details of 20 most active pathways among differentially downregulated genes

Pathway name	Kegg ID	Genes	No. of genes
Neuroactive ligand-receptor interaction	mmu04080	GNRH1,GRM6,GRM4,GRM1,NTS,RXFP1,GIPR,CORT,LTB4R2,AGTR1A,GHR,GRIN3B,GRIN3A,DRD3,F2,BDKRB2,CHRNE,PYY,CCKBR,CHRM5,CHRM3,GRP,PPY,GRIA2,GRIK2,GRIK1,TAAR7B,GRIN1,ADRB3,TRHR2,TAC1,GABBR1,AVP,AVPR2,UTS2,ADRA1B,CHRNA3,CHRNA6,CHRNA4,CHRNA5,ADRA2C,PTGER3,ADCYAP1,GABRG2,GABRA3,GABRA5,HRH3,SCT,GABRB2,GABRB3,GABRD,SST,S1PR4,HCRTR1,CCK,NTSR1,LGR5,CTSG,MC2R,VIPR1,MAS1,VIP,GZMA,CRH,SSTR4,SSTR1,CNR1,HTR7,NPY1R,NPY1R	70
MAPK signaling pathway	mmu04010	STK4,RRAS2,PRKACB,MAPK8,MYC,AKT3,PAK1,NLK,DUSP10,RASGRF1,CDC42,MAPK13,FOS,PLA2G2F,NR4A1,NTRK2,NTRK1,CDC25B,PTPN5,DUSP1,DUSP2,DUSP5,DUSP4,DUSP8,PPP3CC,PPP3CB,NTF3,CACNB3,PRKCB,CACNG1,CACNG3,CACNG2,MAPKAPK5,CACNA1B,CACNA1G,CACNA1H,CACNA1E,MEF2C,MAP4K1,MAP4K3,MAP3K13,MAP3K10,KRAS,MAPT,FGF8,FGF9,CACNA2D3,CACNA2D1,STMN1,FGF20,FGF21,MAP3K1,FGF12,FGF13,MAP3K9,FGF14,FGF18,MAP3K6,RPS6KA2,RPS6KA1,RPS6KA6,TAOK3,JUND,RAC2,MOS	65
Pathways in cancer	mmu05200	STK4,PIK3CD,PIK3CB,MAPK8,MYC,AKT3,RAD51,PIK3R1,SKP2,EGLN1,BIRC5,E2F1,BRCA2,CDC42,FN1,FOS,RXRG,NTRK1,CTBP2,CTBP1,ARNT,CREBBP,PRKCB,CKS1B,TRAF4,TPM3,TPM3,IGF1,CBLB,WNT8A,FZD9,APC,JUP,WNT2,WNT3,KRAS,KIT,CEBPA,GLI2,GLI1,FGF8,FGF9,LEF1,CDK6,CDK6,CDK2,FGF20,FGF21,FGF12,FGF13,FGF14,FGF18,CTNNA2,CTNNA3,RAC2,COL4A1,PTCH1,CCNE1,CCNE2,CCND1,RUNX1T1	61

Cell cycle	mmu04110	RBL1,DBF4,MYC,BUB1,MAD2L1,MCM7,MCM2,MCM3,MCM4,MCM5,MCM6,SKP2,YWHAH,CDC20,CDC23,CDKN2D,E2F1,CHEK2,CHEK1,CDC45,ESPL1,PLK1,SMC1A,CDC25C,CDC25B,ANAPC1,CREBBP,ATM,BUB1B,SFN,PTTG1,CDK1,CDK6,CDK6,CDK2,CDC7,CDC6,CCNE1,CCNE2,CCND1,CCNA2,CCNB1,CCNB1,CCNB2,TTK	45
Regulation of actin cytoskeleton	mmu04810	ITGA4,RRAS2,ITGAD,ARPC5,PIK3CD,PIK3CB,PAK7,PAK3,PAK1,PIK3R1,MYLK2,CDC42,FN1,CYFIP2,VAV2,F2,BDKRB2,CHRM5,CHRM3,ROCK2,TIAM1,ARHGEF7,MYH10,INS2,PIP4K2B,MYL2,APC,KRAS,RDX,IQGAP3,FGF8,FGF9,FGF20,FGF21,FGF12,FGF13,FGF14,FGF18,RAC2,PFN3,PFN3,MOS	42
Axon guidance	mmu04360	FES,L1CAM,PAK7,PAK3,PAK1,CDC42,PLXNC1,SLIT2,SLIT3,ROCK2,ROBO3,ROBO2,ROBO1,PPP3CC,PPP3CB,SRGAP2,NCK2,NCK2,GNAI1,DPYSL5,DPYSL2,ABLIM3,KRAS,EPHA5,EPHA7,EPHA8,EPHA2,EPHA3,RAC2,NGEF,EFNA2,EFNB3,EFNB1,SEMA7A,SEMA6A,SEMA6C,SEMA6B,SEMA4F,SEMA4C,SEMA3F,SEMA3A	41
Cytokine-cytokine receptor interaction	mmu04060	TNFRSF11B,IL11,IL10,IL20,IL21,EPO,BMP7,GHR,ACVR2B,BMP8A,OSM,C3,PF4,IL4,IL3,IL7,CCL20,TNFRSF9,BMPR2,TNFSF9,TNFRSF21,TNFRSF1B,CX3CR1,CCL3,CCL6,INHBA,OSMR,KIT,GDF7,CCR8,CCR2,CXCL2,CXCL9,IL22RA2,CXCR5,CXCR5,LTB,TNFSF11,TSLP,EPOR,IL12RB2	41
Calcium signaling pathway	mmu04020	PRKACB,GRM1,ITPR1,LTB4R2,AGTR1A,MYLK2,BDKRB2,CCKBR,ATP2B1,ATP2B3,CHRM5,CHRM3,CAMK2B,PDE1A,GRIN1,ADRB3,PPP3CC,PPP3CB,TRHR2,PRKCB,GNAL,GNAS,PLCB4,ADRA1B,PTGER3,CACNA1B,CACNA1G,CACNA1H,CACNA1E,SLC8A3,NTSR1,NOS1,ERBB4,CALM1,ADCY1,ADCY9,HTR7,CAMK4	38
Chemokine signaling pathway	mmu04062	PIK3CD,PIK3CB,PRKACB,AKT3,PAK1,PIK3R1,CDC42,VAV2,PF4,HCK,GNGT2,ROCK2,TIAM1,CCL20,PRKCB,GNB4,GNG3,GNG7,PLCB4,CX3CR1,NCF1,GNG13,GNAI	38

		1,CCL3,CCL6,SHC1,SHC2,KRAS,CCR8,CCR2,CXCL2,CXCL9,RAC2,CXCR5,CXCR5,ADCY1,ADCY5,ADCY9	
Oocyte meiosis	mmu04114	PRKACB,BUB1,ITPR1,MAD2L1,YWHAH,AURKA,CDC20,CDC23,ESPL1,CAMK2B,PLK1,SMC1A,CDC25C,ANAPC1,PPP3CC,PPP3CB,INS2,FBXO5,PPP2R5C,PPP2R5C,IGF1,SGOL1,PTTG1,CDK1,CDK2,RPS6KA2,RPS6KA1,RPS6KA6,CALM1,ADCY1,ADCY5,ADCY9,CCNE1,CCNE2,MOS,CCNB1,CCNB1,CCNB2	38
Wnt signaling pathway	mmu04310	WIF1,PRKACB,MAPK8,MYC,NLK,CXXC4,SFRP1,SFRP2,SFRP5,CAMK2B,ROCK2,NKD2,NKD1,CTBP2,CTBP1,PPP3CC,PPP3CB,CREBBP,PRKCB,CSNK1E,PLCB4,PPP2R5C,PPP2R5C,WNT8A,FZD9,APC,WNT2,WNT3,CSNK2A1,CTNNBIP1,LEF1,DAAM1,RAC2,CCND1	34
Progesterone-mediated oocyte maturation	mmu04914	PIK3CD,PIK3CB,PRKACB,MAPK8,AKT3,BUB1,MAD2L1,PIK3R1,CDC23,MAPK13,PLK1,CDC25C,CDC25B,ANAPC1,INS2,IGF1,GNAI1,KRAS,CDK1,CDK2,RPS6KA2,RPS6KA1,RPS6KA6,ADCY1,ADCY5,ADCY9,MOS,CCNA2,CCNB1,CCNB1,CCNB2	31
Tight junction	mmu04530	RRAS2,AKT3,MAGI1,MAGI2,CDC42,MYH13,MYH10,PRKCH,PRKCB,PRKCE,CSDA,YES1,PPP2R2C,PPP2R2B,MYL2,CLDN23,GNAI1,MYH3,MYH7,MYH6,KRAS,CLDN3,CSNK2A1,CTNNA2,CTNNA3,EPB4.1,CGN,TJP1,TJP3	29
Jak-STAT signaling pathway	mmu04630	PIK3CD,PIK3CB,MYC,AKT3,IL11,IL10,IL20,IL21,EPO,PIK3R1,SPRY1,SPRY4,PIM1,GHR,OSM,IL4,IL3,IL7,CISH,CREBBP,SOCS1,CBLB,OSMR,IL22RA2,CCND1,TSLP,EPOR,IL12RB2	28
Focal adhesion	mmu04510	ITGA4,PIK3CD,PIK3CB,MAPK8,AKT3,PAK7,PAK3,PAK1,PIK3R1,RASGRF1,MYLK2,CDC42,FN1,VAV2,TNXB,ROCK2,RELN,PRKCB,MYL2,IGF1,THBS4,SHC1,SHC2,RAC2,COL4A1,CCND1,COL5A1	27

Insulin signaling pathway	mmu04910	PRKAA2,PIK3CD,PIK3CB,PRKACB,PRKAB2,MAPK8,AKT3,PRKAG3,PIK3R1,ACACA,G6PC,SOCS1,INS2,CBLB,SHC1,SHC2,KRAS,FASN,TSC2,RPS6,RPS6,CALM1,FBP2,SH2B2,PYGL,PRKAR1B	26
Vascular smooth muscle contraction	mmu04270	PRKACB,ITPR1,AGTR1A,MYLK2,ACTG2,PLA2G2F,ROCK2,PRKCH,PRKCB,PRKCE,GNAS,AVP,PLCB4,ADRA1B,KCNMB2,KCNMB3,GUCY1A2,GUCY1A3,GUCY1B3,CALM1,ADCY1,ADCY5,ADCY9,NPPC,RAMP1	25
Neurotrophin signaling pathway	mmu04722	ARHGDIB,PIK3CD,PIK3CB,MAPK8,AKT3,PIK3R1,YWHAH,CDC42,MAPK13,CAMK2B,NTRK2,NTRK1,NTRK3,NTF3,SHC1,SHC2,KRAS,MAP3K1,RPS6KA2,RPS6KA1,RPS6KA6,CALM1,SH2B2,CAMK4	24
Dilated cardiomyopathy (DCM)	mmu05414	ITGA4,PRKACB,CACNB3,GNAS,CACNG1,CACNG3,CACNG2,TPM1,TPM4,TPM3,TPM3,MYL2,IGF1,MYH7,MYH6,CACNA2D3,CACNA2D1,DES,TNNT2,ADCY1,ADCY5,ADCY9,DMD	23
T cell receptor signaling pathway	mmu04660	PIK3CD,PIK3CB,AKT3,IL10,PAK7,PAK3,PAK1,PIK3R1,CDC42,MAPK13,FOS,VAV2,IL4,PPP3CC,PPP3CB,TEC,NCK2,NCK2,CBLB,ZAP70,KRAS,LCK,CTLA4	23

DISCUSSION:

A deeper insight into the ageing process at the molecular and cellular level allows the intervention of ageing, development of newer strategies for treating age-associated disorders and improves quality of life with age (DiLoreto & Murphy, 2015). Since ageing studies in animal models are complicated to study and replicative senescence concept of dividing cells in cell culture models had failed to explain senescence mechanism in non-dividing terminally differentiated cells, there is a need to study the ageing phenomenon in non-dividing terminally differentiated cells. Hence the purpose of this objective was to establish and characterize long-term cultures of hippocampal and cortical neurons as an *in vitro* model of ageing.

Efforts were made to establish *in vitro* ageing model using primary rat hippocampal neurons but were abandoned due to lower yields of hippocampal neurons from the embryos and higher neuronal deaths during long-term cultures. These make primary hippocampal neuronal cultures unfeasible to perform extensive ageing related experiments. Primary rat cortical neurons can overcome the above problems; hence, primary rat cortical neurons were preferred for establishing *in vitro* ageing model.

Pure cultures of cortical neurons were maintained under optimal conditions and requirements until they underwent natural death. The purity of the cultures was validated by immunofluorescence studies using MAP2 and GFAP antibodies, which confirmed that the majority of the cells were neurons, and glial cells were negligible in the cultures. Long-term cultures of cortical neurons showed typical morphological features of ageing such as an increase in growth of neurons in terms of size and thickness, increased network, increased neuronal degeneration, etc., with the increase in time. There was a periodic decline in the viability of neurons with the progress of time during long-term culture. There was an upsurge in the number of cortical neurons expressing beta-galactosidase in the culture with the increase of days *in vitro*. Indeed, Dimri et al. (1995) had reported that the mammalian cells on reaching senescence show increased expression of the beta-galactosidase enzyme and also showed that the SA β-gal positive cells increase with age in the skin tissue sections and cell cultures of Humans. Similarly, it was reported that in rat's hippocampus and also in *in vitro* cultures, there was an increase in SA β-gal positive cells with the increase in the age

(Geng, Guan, Xu, & Fu, 2010). Thus, suggesting the progress of ageing in the long-term cultures of cortical neurons, which is similar to physiological ageing.

Mitochondrial membrane potential (MMP) is an essential mitochondrial parameter which gives information regarding ATP generation potential of the cells (Perry, Norman, Barbieri, Brown, & Gelbard, 2011). Reduced MMP decreases ATP generation in the mitochondria, which compromise vital cellular functions (Nicholls, 2004; Zorova et al., 2018). Ageing is defined as a progressive decline of cellular functions (Troen, 2003); hence, MMP is an important parameter to investigate cellular ageing. In our study, there was a decrease in the MMP with the increase of *in vitro* ageing of cortical neurons. These results were strengthened by earlier reports, which showed that brain, liver, heart, and kidneys in the aged rats display decreased MMP compared to younger rats (Duicu et al., 2013; Sastre et al., 1998; Serviddio et al., 2007). Also in Humans, a decrease of MMP with age were reported in leukocytes and mural granulosa cells (Liu et al., 2017; K. Tsai et al., 2001).

According to "Calcium theory of brain ageing" ageing causes disturbance of calcium homeostasis in neurons, which cause dysfunction of neurons by activating calcium-dependent pathways and eventually leads to neuronal death or neurodegenerative diseases (Disterhoft, Moyer, & Thompson, 1994; Ottavio Arancio et al., 2017). Several *in vivo* findings had implicated increased intracellular calcium levels in the decline of neuronal function and neuronal death in ageing and age-associated disorders (Disterhoft et al., 1994; Nikoletopoulou & Tavernarakis, 2012). Hence it is important to study intracellular calcium levels to establish *in vitro* ageing in the long-term cultures of cortical neurons. In our study, it was observed that there was a gradual increase in the intracellular calcium levels with the progress of time, which indicates a dysregulation in the calcium homeostasis in the cortical neurons with the increase of days *in vitro*. These results are in accordance with "Calcium theory of brain ageing," and this establishes long-term cultures of cortical neurons as a useful *in vitro* ageing model.

According to the "DNA damage hypothesis of ageing," with the progress of time DNA repair capabilities of the cells deteriorate, which increase DNA damage in the cells that lead to the ageing (Best, 2009; A. A. Freitas & de Magalhaes, 2011). So, we have performed comet assay to quantify the DNA damage in cortical neurons during long-

term culture. In our study, we had noticed an increase in the DNA damage in the cortical neurons with the increase of days *in vitro*. These results corroborated with earlier finding, which showed that DNA damage increases in the rat brain cortex with the increase of age (Swain & Subba Rao, 2011). And also similar observation was seen in cultured cerebellar granule neurons (Bhanu, Mandraju, Bhaskar, & Kondapi, 2010).

Since Topoisomerase IIβ plays a role in Double-strand break repair (R. Mandraju et al., 2011; R. K. Mandraju, Kannapiran, & Kondapi, 2008) and Base excision repair (Gupta, Swain, Rao, & Kondapi, 2012) and as it was reported its levels decrease with the brain ageing (Kondapi, Mulpuri, Mandraju, Sasikaran, & Subba Rao, 2004) and *in vitro* ageing of cerebellar granule neurons (Bhanu et al., 2010), Topoisomerase IIβ levels were investigated in long-term cultures of cortical neurons as an additional marker of ageing. Our study showed that Topoisomerase IIβ levels were decreased gradually with the progress of time in long-term cultures of cortical neurons. These findings were further substantiated by Topoisomerase IIβ gene expression analysis in the ageing rat brain cortex. These results suggest *in vitro* ageing in long-term cultures of cortical neurons.

Thus, the profile of the above ageing markers demonstrates that long-term cultures of cortical neurons can serve as an effective *in vitro* ageing model. Further, microarray analysis performed showed some potential pathways associated with *in vitro* ageing of cortical neurons. The similarity of *in vitro* aging with physiological ageing will provide a better understanding of the ageing process in Human beings. Understanding the molecular basis of the cellular aging process in neurons should also provide cues to gain insights into age-associated neurological disorders.

CONCLUSION:

In this chapter, hippocampal and cortical neurons were isolated to homogeneity, their ageing phenomena *in vitro* was established based on the senescence markers, wherein hippocampal neurons survived for 28 days, while cortical neurons survived for 50 days. Furthermore, topoisomerase II beta levels decreased with ageing, and Slit2 levels increased with the ageing of cortical neurons, similar lines of observations were seen in granule neurons, while NPY levels show differential expression in cortical neurons compared to granule neurons.

CHAPTER 4:

EFFECT OF STARVATION ON THE LONGEVITY OF CORTICAL NEURONS *IN VITRO*

INTRODUCTION:

Dietary restriction is stated as a reduction of intake of either specific nutrient or complete nutrition without causing malnutrition. It is a non-pharmacological and non-genetic intervention known to increase longevity among organisms, from yeast to mammals (Katewa & Kapahi, 2010). Apart from increasing longevity, dietary restriction presents numerous benefits. It increases insulin and leptin sensitivity in animals. It protects from metabolic disorders such as diabetes, cardiovascular diseases, stroke, etc. (Mattson et al., 2017). It reduces the risk of cancer development (de Cabo et al., 2014). It enhances the endurance of neurons to excitotoxic stress (Anson et al., 2003). It confers cellular protection by decreasing oxidative stress (Pani, 2015). It delays the inception and progression of allergic dermatitis (Fan, Kouda, Nakamura, & Takeuchi, 2001; Nakamura, Kouda, Tokunaga, & Takeuchi, 2004). It prevents or delays age-dependent physiological changes such as muscle impairment (Katewa & Kapahi, 2010), immune dysfunction (Choi, Lee, & Longo, 2017), T-cell senescence (Messaoudi et al., 2006), dementia (Marti-Nicolovius & Arevalo-Garcia, 2018), etc. In mice, it was showed that dietary restriction prevents autoimmune disease development (Kouda & Iki, 2010). In animal models of Huntington's, Parkinson's and Alzheimer's diseases, it delayed the onset and advancement of neurodegeneration (Mattson et al., 2017). In monkeys, dietary restriction showed a decrease in the age-dependent brain atrophy (Pani, 2015).

Dietary restriction comprises various types of interventions viz., calorie restriction, restriction of specific macronutrient, short term starvation, intermittent fasting, periodic fasting, prolonged fasting, time-restricted feeding, etc. Calorie restriction is a decreased intake of calories, usually 20-40% depletion in total calorie requirement. In macronutrient restriction, intake of proteins or amino-acids is reduced. Time-restricted feeding is a dietary restriction where animals were allowed to feed only for a restricted period of time in a day. Short term starvation, intermittent fasting, periodic fasting, and prolonged fasting are the different methods of starvations which differ in the duration and frequency (Choi et al., 2017; C. Lee & Longo, 2016).

Since dietary restriction is the only natural intervention of ageing progression in mammals, most of the active gerontological research is focused on unwinding the mechanisms by which dietary restriction enhances longevity in mammals. But, dietary

restriction induces enormous biological changes in mammals, making it very complicated in identifying the contributory changes which retard ageing (Weindruch, Kayo, Lee, & Prolla, 2001). This complication emphasis the need for a simpler dietary restriction model which is highly relevant to mammals and it can induce limited, but significant biological changes. Research in the dietary restriction is lagging due to the longer duration of the studies. This retardation emphasis the need for models which decrease the length of the study. Since the available models are expensive, there is also a need for cost-effective models.

Above problems can be overcome by using primary rat cortical neuronal cultures as they decrease complexity, the time duration of survival and cost compared to the animal models. Additionally, as neurons are non-dividing, terminally differentiated, and highly metabolically active cells, they are highly reliable and very helpful in ageing and ageing retardation studies. Homogenous neuronal cultures allow for the study of pathways which are difficult to study in the animal models. Further, conditions that can influence the cell can be defined precisely by the cell culture, which contributes to the higher reproducibility compared to whole animal studies.

We hypothesize that if regular starvation periods can induce longevity in the cultured cortical neurons, they can serve as an *in vitro* dietary restriction model. In the context of above facts, this objective was conceptualized to study the effect of starvation durations on the longevity of cortical neurons *in vitro* and also to study the factors which can influence the longevity of cortical neurons *in vitro.*

MATERIALS AND METHODS:

Effect of seeding density on the survival of cortical neurons at different nutrition supply time points:

Cortical neurons were isolated from E18 rat embryos and were dissociated into single cell suspension. Cell number was counted thrice using trypan blue exclusion method and cells were plated at a seeding density of 100-1200 cells/mm^2 in triplicates in two sets of cultures and were cultivated using neurobasal media with the B27 supplement. In one set of culture, media replacement was done at every 3 days, while in other culture media replacement was done at every 7 days. At regular time intervals, the percentage of surviving neurons at each seeding density was estimated using MTT method (Mosmann, 1983). The total number of neurons surviving on DIV-3 were considered as control for respective seeding densities. Percentage of surviving neurons at different time points were calculated using the formula mentioned in the method, MTT assay for assaying neuronal cell viability during long-term culture.

Effect of starvation on the longevity of cortical neurons:

Cortical neurons were plated at a seeding density of 800 cells/mm^2 in triplicates in different sets of cultures and were grown in Neurobasal media supplemented with the B27. In every set of culture, different durations of starvation viz., 3-days, 7-days, 14-days, 21-days, 30-days, 60-days, etc., were maintained by delaying media replacement for specified time periods. At regular time intervals, the percentage of surviving neurons under these starvation conditions were estimated using MTT method (Mosmann, 1983). The total number of neurons surviving on DIV-3 were considered as control for respective starvation durations, and accordingly percentage of surviving neurons were calculated for other time points using the formula mentioned in the method, MTT assay for assaying neuronal cell viability during long-term culture.

Effect of starvation on the maximum lifespan of neurons at different maturational stages:

Cortical neurons were plated at a seeding density of 800 cells/mm^2 in triplicates in two sets of cultures and were grown in Neurobasal media supplemented

with the B27. In one set of culture, there was no media replacement after DIV-1, which was considered as immature neuronal culture. In the second set of culture, media was replaced only once at DIV-14, and after that there was no further media replacement, which was considered as mature neuronal culture. Both the cultures were incubated in a CO_2 incubator until they undergo natural death. At regular time intervals, the survival of neurons was monitored using an inverted microscope, and the total number of days they survive were manually counted.

RESULTS:

Effect of seeding density on the survival of cortical neurons at different nutrition supply time points:

To see the effect of seeding densities on the survival of neurons, cortical neurons were cultured at varying seeding densities (100 cells/mm^2 to 1200 cells/mm^2) and verified at different time periods of media replacement viz., every 3-days (Fig. 24A) and every 7-days (Fig. 24B). At both the time periods of media replacements, at all the seeding densities, neurons were able to survive during initial days. However, neurons at seeding densities of 100 cells/mm^2 to 600 cells/mm^2 were unable to survive for a longer duration. But, neurons at seeding densities of 800 cells/mm^2 to 1200 cells/mm^2 showed significant survival for a longer duration. It was observed that the percentage of survival of neurons had increased with the increase of seeding densities. Further, it was also observed that there was an increase in the longevity of neurons with the increase of seeding densities.

Effect of starvation on the longevity of cortical neurons:

To find the effect of starvation on the survival of neurons, cortical neurons were cultured at constant seeding density (800 cells/mm^2), but the timing of media change was altered viz., after every 3-days, 7-days, 14-days, and 21-days. It had been observed that there was an increase in the percent of survival of neurons with the increase of starvation duration. And also there was an increase in the longevity of neurons with the increase of starvation duration (Fig. 25). Cultures with 21-days media change shown higher longevity and cultures with 3 days media change shown lower longevity compare to others.

More than 21-day starvation limits the longevity of cortical neurons:

To check whether a further increase of starvation duration beyond 21-days will increase the longevity of neurons, cortical neurons were cultured at constant seeding density (800 cells/mm^2), but the timing of media change was at 30-days and 60-days. Extending starvation duration beyond 21-days didn't increase the longevity of neurons. And also there was a decrease in the percent of survival of neurons with the

increase of starvation duration (Fig. 26). Cultures with 21-days of media change shown higher longevity compared to others.

21-day starvation is optimal for maintenance of longevity of cortical neurons:

A comparison of all the timings of media change demonstrated that longevity of neurons followed a sigmoidal curve pattern (Fig. 27). There was a gradual increase in the longevity of neurons from 3-days starvation to 21-days starvation, followed by a small reduction in the longevity between 21-days starvation and 30-days starvation. There was no significant change in the longevity of neurons with the increase of starvation after 30-days starvation. Among cultures with varying timing of media change, cultures with 21-days starvation shown higher longevity and cultures with 3-days starvation shown lower longevity.

Effect of starvation on the maximum lifespan of neurons at different maturational stages:

It was tested whether starvation initiated at different maturational stages, does increase the longevity of cortical neurons. Starvation was initiated at DIV-1 for immature neurons, and starvation was initiated at DIV-14 for mature neurons. There was a significant increase in the maximum lifespan of neurons when starvation was initiated after the maturation of neurons compared to starvation initiated in immature neurons (Fig. 28).

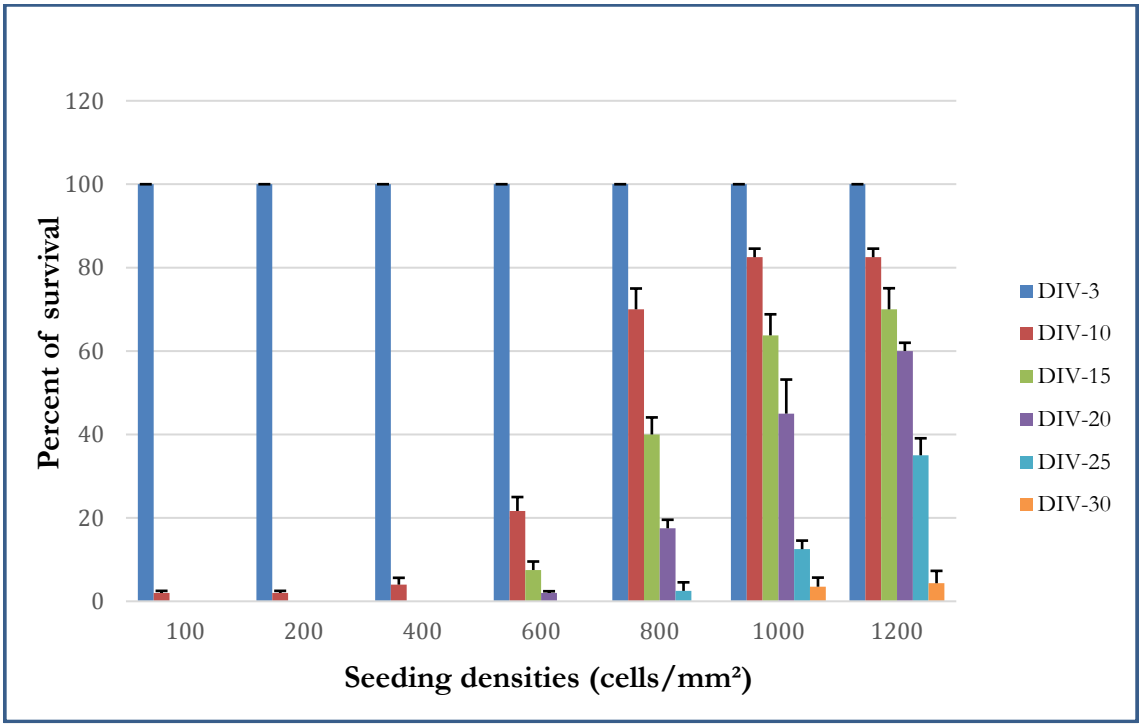

(A)

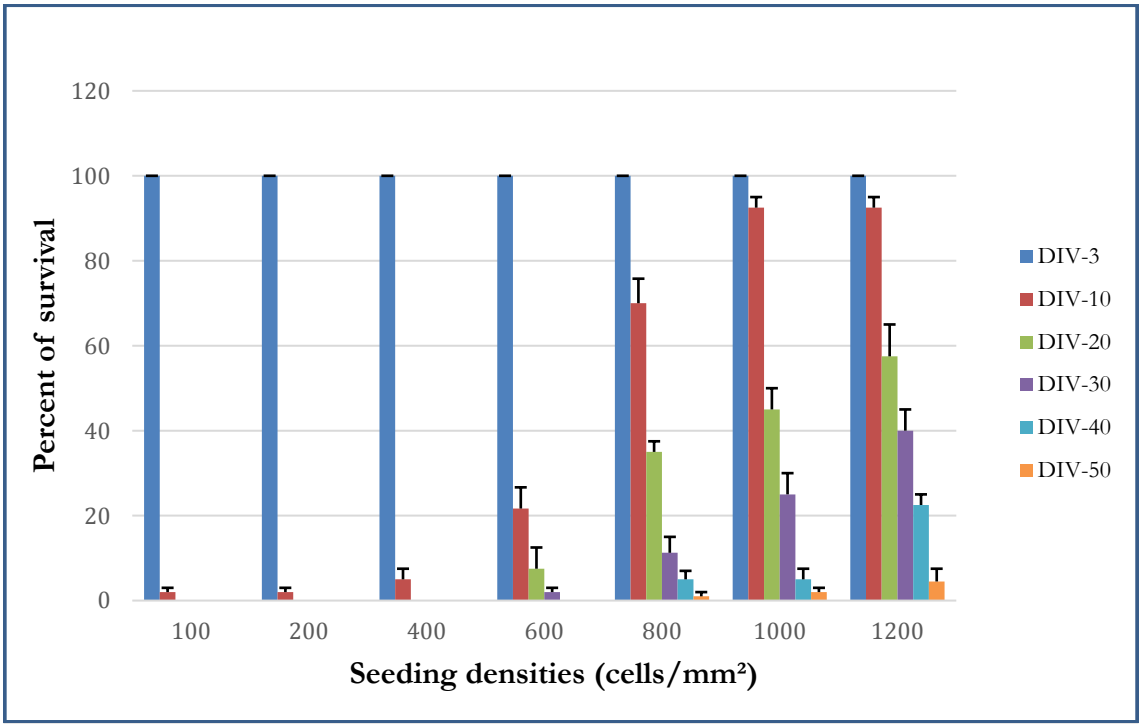

(B)

Figure 24: Effect of seeding density on the survival of cortical neurons. (A) Culturing of cortical neurons at seeding densities of 100 cells/mm^2 to 1200 cells/mm^2 and media replacement after every 3-days. (B) Culturing of cortical neurons at seeding densities

of 100 cells/mm^2 to 1200 cells/mm^2 and media replacement after every 7-days. At DIV-3, the total number of neurons surviving was considered as 100%. At regular time intervals, the percentage of surviving neurons was calculated with reference to DIV-3. At both the time periods of media change, at seeding densities of 800 cells/mm^2, 1000 cells/mm^2, and 1200 cells/mm^2 neurons showed significant survival. It was observed that the percentage of survival of neurons had increased with the increase of seeding densities. Further, it was also observed that there was an increase in the longevity of neurons with the increase of seeding densities. Data were represented as mean±SD (n = 4). DIV: Days *in vitro*.

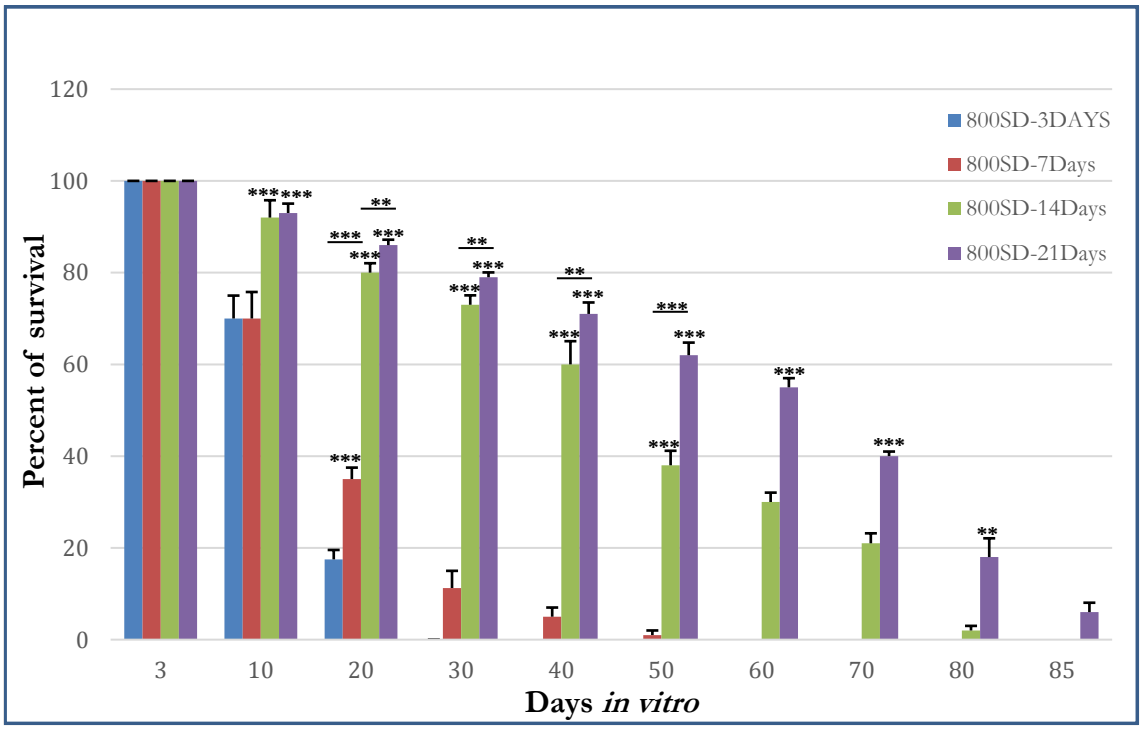

Figure 25: Effect of duration of starvation on the longevity of cortical neurons. Seeding density was constant (800 cells/mm^2), but the timing of media change was different (after every 3-days, 7-days, 14-days, and 21-days). There was an increase in the percent of survival of neurons with the increase of timing of media change. And also there was an increase in the longevity of neurons with the increase of timing of media change. SD represents the seeding density of neurons (neurons/mm^2). Data were depicted as mean±SD; n = 4. ***P < 0.001, **P < 0.01 by one-way ANOVA using Holm-Sidak method.

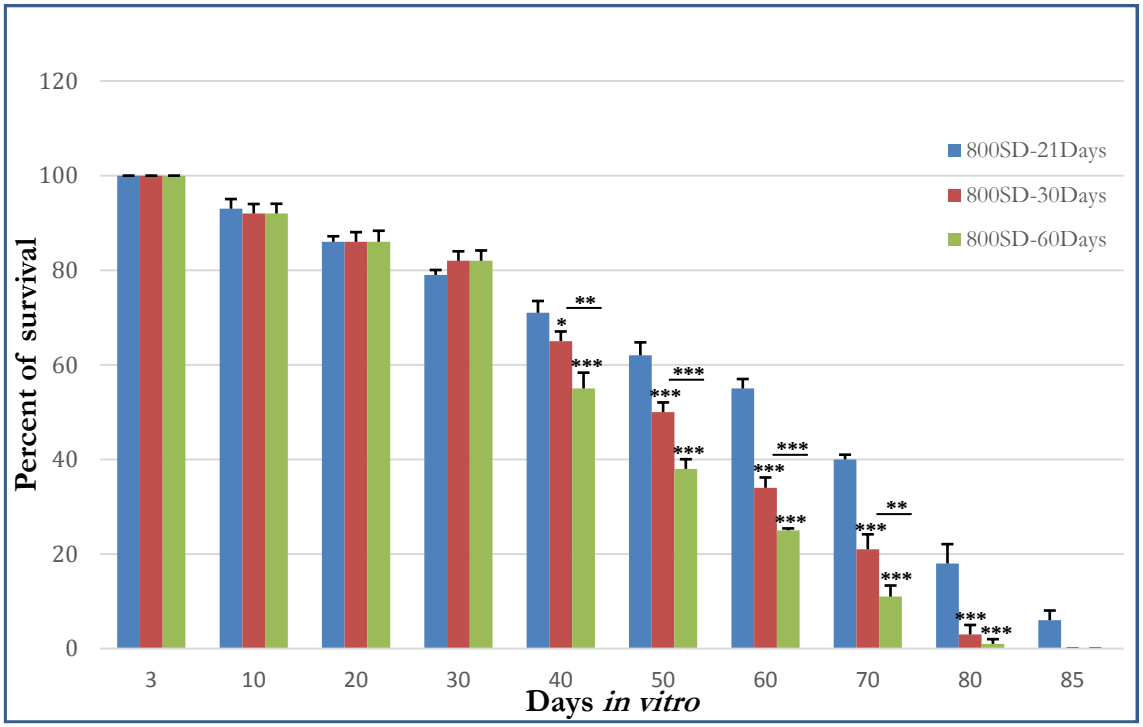

Figure 26: More than 21-day starvation limits the longevity of cortical neurons. Seeding Density was constant (800 cells/mm^2), but the timing of media change was different (after every 21-days, 30-days, and 60-days). Extending the timing of Media change beyond 21-days didn't increase the longevity of neurons. And also there was a decrease in the percent of survival of neurons with the increase of timing of media change. SD represents the seeding density of neurons (neurons/mm^2). Data were depicted as mean±SD; n = 4. ***P < 0.001, **P < 0.01, *P < 0.05 by one-way ANOVA using Holm-Sidak method.

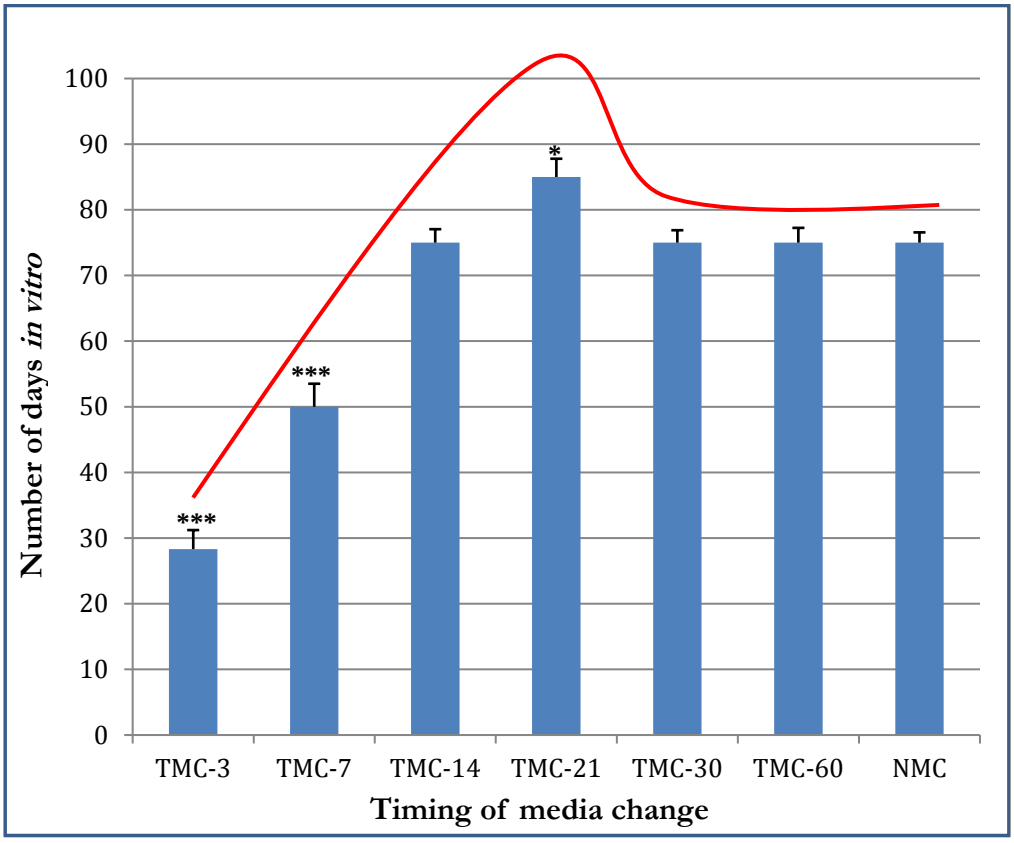

Figure 27: Comparison of timing of media change and the number of days of survival of neurons *in vitro*. A comparison of all the timings of media change showed that the longevity of neurons followed a sigmoidal curve pattern. Among all, cultures with 21-days media change shown higher longevity and cultures with 3-days media change shown lower longevity. TMC represents the timing of media change; NMC represents no media change. Data were depicted as mean±SD; n = 4. ***P < 0.001, *P < 0.05 by one-way ANOVA using Holm-Sidak method.

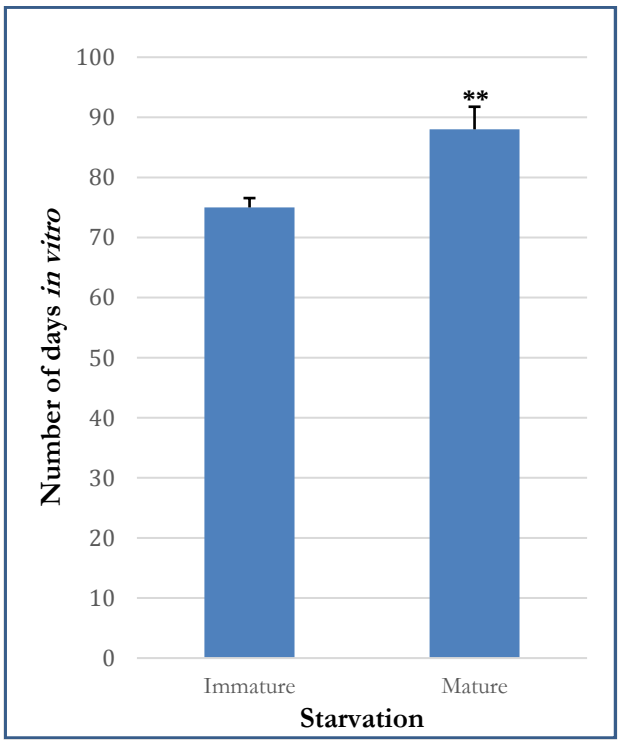

Figure 28: Effect of starvation on the maximum lifespan of neurons at different maturational stages. There was an increase in the maximum lifespan of neurons when starvation was initiated after the maturation of neurons compared to starvation initiated in immature neurons. Data were represented as mean±SD (n = 3), **P < 0.01 by Student's t-test.

DISCUSSION:

Dietary restriction is a non-pharmacological and non-genetic intervention known to increase longevity and prevent age-related diseases among organisms, from yeast to mammals (Katewa & Kapahi, 2010). Since dietary restriction studies in animal models are complicated, more time consuming, and expensive; there is a need to search for alternatives. The purpose of the objective was to evaluate whether starvation as a dietary restriction approach can induce longevity in the cultured primary cortical neurons *in vitro*. And also to analyze the effect of factors such as seeding density and neuronal maturation on the longevity of cortical neurons *in vitro*.

Cortical neurons cultured at varying seeding densities with every 3-days and every 7-days of media replacement time periods had demonstrated that at lower seeding densities (100 cells/mm^2 to 600 cells/mm^2), neurons failed to survive for longer duration whereas at higher seeding densities (800 cells/mm^2 to 1200 cells/mm^2) neurons were able to survive for longer duration. These results infer that optimal seeding densities for cortical neuronal culture are in the range of 800 cells/mm^2 to 1200 cells/mm^2. Failure in the proper formation of synapses, decreased contacts between the neurons, and lack of optimal concentrations of secreted autocrine trophic factors might be the reasons for the poor survival of neurons at lower seeding densities (Brewer, 1995; Brewer et al., 1993). It was also demonstrated that with the increase of seeding density, there was an increase in both the percentage of survival and longevity of neurons. With the increase of seeding density, there might be an increase in the concentration of autocrine trophic factors and also an increase in the connectivity among neurons, which might have contributed to the increase in both the percentage of survival and longevity of neurons.

Since seeding density independently can influence the longevity in neuronal cultures *in vitro*, seeding density was kept constant to study the effect of duration of starvation on cultured cortical neurons. A comparison of timings of media change of every 3-days, every 7-days, every 14-days, and every 21-days had shown that with the increase in the starvation duration there was an increase in the longevity of neurons and also in the percent of survival of neurons. With the increase of duration of starvation, there will be an increase in the nutrition depletion in the cultures. It was reported that increased nutrition depletion activates certain molecular and cellular

adaptive stress responses in the cells which not only allow cells to cope up with the nutritional stress conditions but also enhances the longevity of the cells (Fontana & Partridge, 2015). Nutrition depletion (particularly carbohydrates and amino acids) also partially or completely inhibits nutrient-sensing pathways which change the metabolic state of the cells from growth to maintenance & repair and maximise the utilization of available energy for cellular survival. Inhibition of these signalling pathways also cause expression of transcription factors that induce autophagy, anti-oxidant enzymes, activate DNA repair pathways, etc., which decrease oxidative stress and increase the repair of damaged macromolecules, thereby contributes to the longevity (Eskelinen & Saftig, 2009; Fontana et al., 2010). Starvation-induced longevity is mainly attributable to autophagy (Klionsky & Emr, 2000). Autophagy allows degradation of harmful protein aggregates, damaged proteins, organelles, and other cellular constituents whose build-up induce ageing and neuronal death (Bagherniya, Butler, Barreto, & Sahebkar, 2018; Cuervo et al., 2005). Further autophagy provides energy, generated in the above breakdowns, for the cellular survival during starvation and also supply the amino acids generated for the synthesis of essential proteins, which are required for survival under starvation. (Vellai & Takacs-Vellai, 2010). Nutrition deprivation also stimulates the expression of BDNF in the neurons, which plays a significant role in stress response (Duan et al., 2003; Mattson, 2005). It promotes synaptogenesis, synaptic plasticity, and neuronal survival (Ghosh et al., 1994; Lindsay, 1994; Russo-Neustadt, 2003).

Further extending the duration of starvation beyond 21-days had decreased the longevity and percent of survival of neurons. This could be due to an extreme increase in nutrition demand, which leads to increased cell death due to severe insufficiency of nutrition for minimal maintenance and survival of cells.

A comparison of longevities of all the durations of starvation had demonstrated that longevity of neurons followed a sigmoidal curve pattern, where 21-days starvation duration was the saturation point for the increase of longevity, beyond which there was no further increase. A similar trend was also observed in flies, worms, and rodents, which were exposed to increased magnitude of dietary restriction (Fontana et al., 2010; Mattson, 2005).

It was tested whether starvation initiated after neuronal maturity *in vitro*, do increase longevity compared to starvation initiated in immature neurons. In *in vitro* conditions maturation of cortical neurons complete by 14 days *in vitro* (DIV-14) (de Lima, Merten, & Voigt, 1997; Falace et al., 2014), hence we have initiated starvation after DIV-14 for mature neurons. It was observed that there was an increase in the maximum lifespan of neurons when starvation was initiated after the maturation of neurons. The increase in the maximum lifespan of neurons when starvation was initiated after the maturation could be due to the differences in the maturation stages of the neurons.

To conclude, these results demonstrate that both the seeding density and starvation can induce longevity in the cultured rat primary cortical neurons *in vitro*. And neuronal maturation plays an additive role in starvation-induced longevity extension of cortical neurons.

CONCLUSION:

Culturing of cortical neurons at varying seeding densities had demonstrated that there was an increase in both the percentage of survival and longevity of cortical neurons with the increase of seeding densities. Culturing of cortical neurons at constant seeding densities with the exposure to different durations of starvation had demonstrated that there was an increase in both the percentage of survival and longevity of cortical neurons with the increase of duration of starvation from 3-days to 21-days. There was a decrease in both the percentage of survival and longevity of cortical neurons with a further increase of duration of starvation from 21-days to 60-days. Comparison of longevities of all the durations of starvation had demonstrated that longevity of neurons followed a sigmoidal curve pattern, where 21-days starvation duration was the saturation point for the increase of longevity. There was an increase in the maximum lifespan of neurons when starvation was initiated after the maturation of neurons compared to starvation initiation in immature neurons. These findings suggest that both the seeding density and starvation can induce longevity in the cultured rat primary cortical neurons *in vitro*. And neuronal maturation plays an additive role in starvation-induced longevity extension of cortical neurons.

CHAPTER 5:

EFFECT OF PESTICIDES, PLANT GROWTH REGULATORS, AND METALS ON NEURONAL SURVIVAL.

INTRODUCTION:

Until recent times, toxicological studies had majorly focused on testing chemicals for their lethal effect or their carcinogenic effect. Very limited research had done in neurotoxicology; whatsoever was done; it was only after poisoning incidents or suicide attempts or after acute occupational exposures. But early precautionary testing to identify potential neurotoxins were completely lacking. Since neurodevelopmental and neurodegenerative disorders will be detected long after individual's exposure, chemicals inducing these disorders were unrecognizable due to longer duration of diagnosis. Until now, as few as 200 chemicals had been identified as potential neurotoxins in Human beings and another 1000 chemicals had been reported to be neurotoxic in laboratorial animal studies (Grandjean & Landrigan, 2014). But in global commerce, there are nearly eighty thousand chemicals in use, and every year around 700 new chemicals are added. Among them, only a small fraction was tested; still, a large fraction has to be tested for their potential to induce neurotoxicity (Grandjean & Landrigan, 2006). Further, in nature combinatorial effects are more predominant than individual effect, but till now there are no such reports on screening of chemicals in combinations for identifying their synergistic neurotoxicity or compounding effects.

Chlormequat is a common plant growth regulator, used to prevent lodging and for the sturdier growth of cereal crops (Xiagedeer, Wu, Liu, & Hao, 2016). Its mechanism of action is by inhibiting gibberellin biosynthesis, which results in the inhibition of cell elongation and promotion of thicker stalks, which make plants sturdier and avoids lodging (Rademacher & Brahm, 2010). Human beings and other animals commonly expose to chlormequat due to its wide usage. In plants and animals, it remains metabolically unaltered (Blinn, 1967; Lindh, Littorin, Johannesson, & Jonsson, 2011). It was reported that animals fed with crops, treated with chlormequat showed impaired reproduction. In pigs, it causes impaired estrous; in mice, it jeopardizes *in vitro* fertilizing ability of epididymal spermatozoa (Sorensen & Danielsen, 2006). Further, it also affects embryo growth and development in rats (Xiagedeer et al., 2016). It also causes skeletal development damage in pubertal rats (D. Huang et al., 2017). Although chlormequat induced reproductive and developmental damage was well studied, its neurotoxicological studies were

completely lacking, which emphasizes the need to study chlormequat induced neurotoxicity.

Paraquat is a commonly used, fast acting herbicide. It non-specifically kills broad-leaved weeds, annual grasses, and other general weeds upon contact (Sagar, 1987). Since paraquat is a redox-active heterocycle, it produces reactive oxygen species, which cause toxic effects in human beings (Dinis-Oliveira et al., 2008). By the oral route, it induces category II toxicity, and by the dermal route, it induces category III toxicity (W.-T. Tsai, 2013). Paraquat is structurally similar to MPTP, a well-known chemical which induces Parkinson's disease (Broussolle & Thobois, 2002; Smeyne & Jackson-Lewis, 2005). Furthermore, many studies have linked the onset of Parkinson's disease with chronic exposure to paraquat (Dinis-Oliveira et al., 2006). In spite of its known toxicities, many nations have approved its wide usage. There is a need to understand better the potential of paraquat in inducing neurotoxicity since its wide usage will contribute to its higher bioaccumulation and can damage both developing and adult brain.

Aluminum is one of the common most elements widespread (Domingo, 2003). It has numerous applications in the fields of food, food technology, medicine, cosmetics, etc. It is commonly used as kitchen utensils and cooking vessels (Inan-Eroglu & Ayaz, 2018). In the form of alum, aluminum is used for water purification (Swaminathan, 2013). In cosmetics, aluminum hydroxide is used as a buffering agent, pH adjuster, corrosion inhibitor, etc. Aluminum salts are used in antiperspirants. In the field of medicine, aluminum hydroxide is used as antacids and also to control hyperphosphatemia in patients suffering from renal failure (Becker et al., 2016; Willhite, Ball, & McLellan, 2012). Aluminum salts and aluminum hydroxide are commonly used as adjuvants in vaccines (A. R. Shaw & Feinberg, 2008; Vera-Lastra, Medina, Cruz-Dominguez Mdel, Jara, & Shoenfeld, 2013).

Human exposure to aluminum occurs mainly through occupation, environment, medical, and dietary factors (Inan-Eroglu & Ayaz, 2018). The aluminum present in the form of adjuvants induces an autoimmune disorder called ASIA (autoimmune syndrome induced by adjuvants) (Vera-Lastra et al., 2013). Aluminum toxicity is implicated in diseases such as dialysis dementia (Swaminathan, 2013), dialysis encephalopathy (King, Savory, & Wills, 1981), non-iron responsible anemia

(McGonigle & Parsons, 1985), osteomalacia (Gura, 2010), etc. It was observed that aluminum ammonium sulfate administration through drinking water to the mice caused altered dopamine turnover in the hypothalamus and increased TNF alpha expression in the cerebrum (Tsunoda & Sharma, 1999a, 1999b). Injection of aluminum hydroxide to the mice induced dementia and anxiety increment (P. Chen, Miah, & Aschner, 2016). In many epidemiological studies, human exposure to aluminum has been associated with many neurodegenerative diseases (Tsunoda & Sharma, 1999b). In children, a significant correlation exists between Autism spectrum disorder rate and aluminum-adjuvanted vaccine exposure (C. A. Shaw & Tomljenovic, 2013). Aluminum-related toxicological studies are at their infancy stage; still, a lot of studies has to be done to decipher absolute aluminum toxicity. Aluminum-related neurotoxicity studies have yet to be elucidated, which draw the attention to study aluminum-induced neurotoxicity.

We hypothesize that pesticides, plant growth regulators, and metals can be neurotoxic if they inhibit *in vitro* proliferation of neurons upon exposures. In the context of above facts, this objective was conceptualized to study commonly used pesticide (paraquat), common plant growth regulator (chlormequat) and a common metal (ammonium aluminum sulphate and aluminum hydroxide) for their ability to induce neurotoxicity individually or synergistically.

MATERIALS AND METHODS:

Materials:

Non-essential amino acids, sodium pyruvate, MEM were procured from Thermo-Fisher scientific (Waltham, USA). DAPI, MTT were procured from Sigma–Aldrich (St. Louis, USA); Fetal bovine serum from Lonza (Basel, Switzerland); SK-N-SH cell lines were acquired NCCS (Pune, India). Rest of the materials were of either analytical or molecular biological grade.

Estimation of toxicity of independent and combined exposure of chemicals on neurons for 24 hours:

MTT assay was performed to estimate the toxicity of exposure of pesticide, plant growth regulator, and various forms of aluminum on neurons using increasing concentrations of individual compounds. Briefly, 50000 SK-N-SH cells were seeded in every well of the 96-wellplate and were incubated in a CO_2 incubator for 12 h. After incubation, media was substituted with fresh media containing increasing concentrations of paraquat, chlormequat, aluminum hydroxide, ammonium aluminum sulphate. Control cells were also kept, without the addition of any chemicals. Cells were incubated in a CO_2 incubator for 24 h. After 24 h, media was aspirated, and cells were washed twice. Fresh media containing 10%, 1.21mM MTT, was added to the cells and they were incubated in a CO_2 incubator for 8 h. During incubation, cells that survived after the treatment convert yellow tetrazolium salt into insoluble formazan crystals. MTT containing media was discarded, and insoluble formazan crystals were dissolved by the addition of DMSO. The intensity of the developed color was measured using multiplate reader-Infinite 200 (Tecan, Mannedorf, Switzerland) at 595 nm. Percentage of cell death (PCD) was calculated according to the following formula.

$$\mathrm{PCD} = \{(\mathrm{OD}_{\mathrm{Control}} - \mathrm{OD}_{\mathrm{Treated}})/\mathrm{OD}_{\mathrm{Control}}\} \times 100$$

Where, PCD = percentage of cell death; $\mathrm{OD}_{\mathrm{Control}}$ = absorbance at 595 nm for control cells; $\mathrm{OD}_{\mathrm{Treated}}$ = absorbance at 595 nm for treated cells.

After plotting the graph, 50 % of cell death was calculated from it. Toxicity of combinatorial exposure of paraquat, chlormequat, aluminum hydroxide, ammonium aluminum sulphate was also estimated similarly, but using combinations of chemicals.

Confocal microscopy of neurons treated with chemicals independently and combinatorially for 120 hours:

SK-N-SH cells were cultured on treated glass coverslips for 24 h. After 24 h, cells were treated independently with paraquat, chlormequat, aluminum hydroxide, and ammonium aluminum sulphate, at their 50 % cell death concentrations and were incubated for 120 h in the carbon dioxide incubator. After incubation, media was discarded, and cells were washed thrice with PBS (pH-7.4). Cells were fixed with 4% PFA for 10 mins. Cells were washed again thrice with PBS and they were permeabilized using 0.3% of Triton-X 100 for 10 mins, which was followed by thrice washing with PBS. Subsequently, cells were treated with DAPI, and coverslips containing cells were mounted on glass slides. Cells were examined for their morphological changes using the confocal microscope (Leica, Buffalo Grove, USA), utilizing the intrinsic fluorescence of DAPI (excitation and emission maxima are 350 nm and 470 nm respectively). Toxic effects of combinatorial exposure of paraquat, chlormequat, aluminum hydroxide, ammonium aluminum sulphate on SK-N-SH cells were also studied similarly, but cells were treated with various combinations.

RESULTS:

Estimation of toxicity of independent exposure of chemicals on neurons for 24 hours:

SK-N-SH cells were treated independently with increasing concentrations of paraquat, chlormequat, aluminum hydroxide, and ammonium aluminum sulphate for 24 hours. MTT assay was performed to estimate the toxicity of acute exposure. 50% of cell death was observed at 192 µM, 219 µM, 21 µM and 107 µM for ammonium aluminum sulphate (Fig. 29 A), aluminum hydroxide (Fig. 29 B), paraquat (Fig. 29 C), chlormequat (Fig. 29 D) respectively.

Estimation of toxicity of combinatorial exposure of chemicals on neurons for 24 hours:

Since in nature, multifactorial effects are more prone than individual effects, combinatorial neurotoxic effects of different aluminum metal forms, pesticide, and plant growth regulator were also assayed. Combination of aluminum hydroxide and ammonium aluminum sulphate showed 50% of cell death at 207 µM concentration of both aluminum hydroxide and ammonium aluminum sulphate (Fig. 30 A). Combination of paraquat and chlormequat showed 50% of cell death at 23 µM concentration of paraquat and 79 µM concentration of chlormequat (Fig. 30 B). Combination of aluminum hydroxide, ammonium aluminum sulphate, paraquat, and chlormequat (Fig. 31) showed 50% of cell death at 86 µM concentration of aluminum hydroxide, 86 µM concentration of ammonium aluminum sulphate, 8 µM concentration of paraquat, and 28 µM concentration of chlormequat.

These results infer that the combination of aluminum hydroxide, ammonium aluminum sulphate, paraquat, and chlormequat showed the highest synergy, whereas the combination of paraquat and chlormequat and the combination of aluminum metal two forms show no synergy.

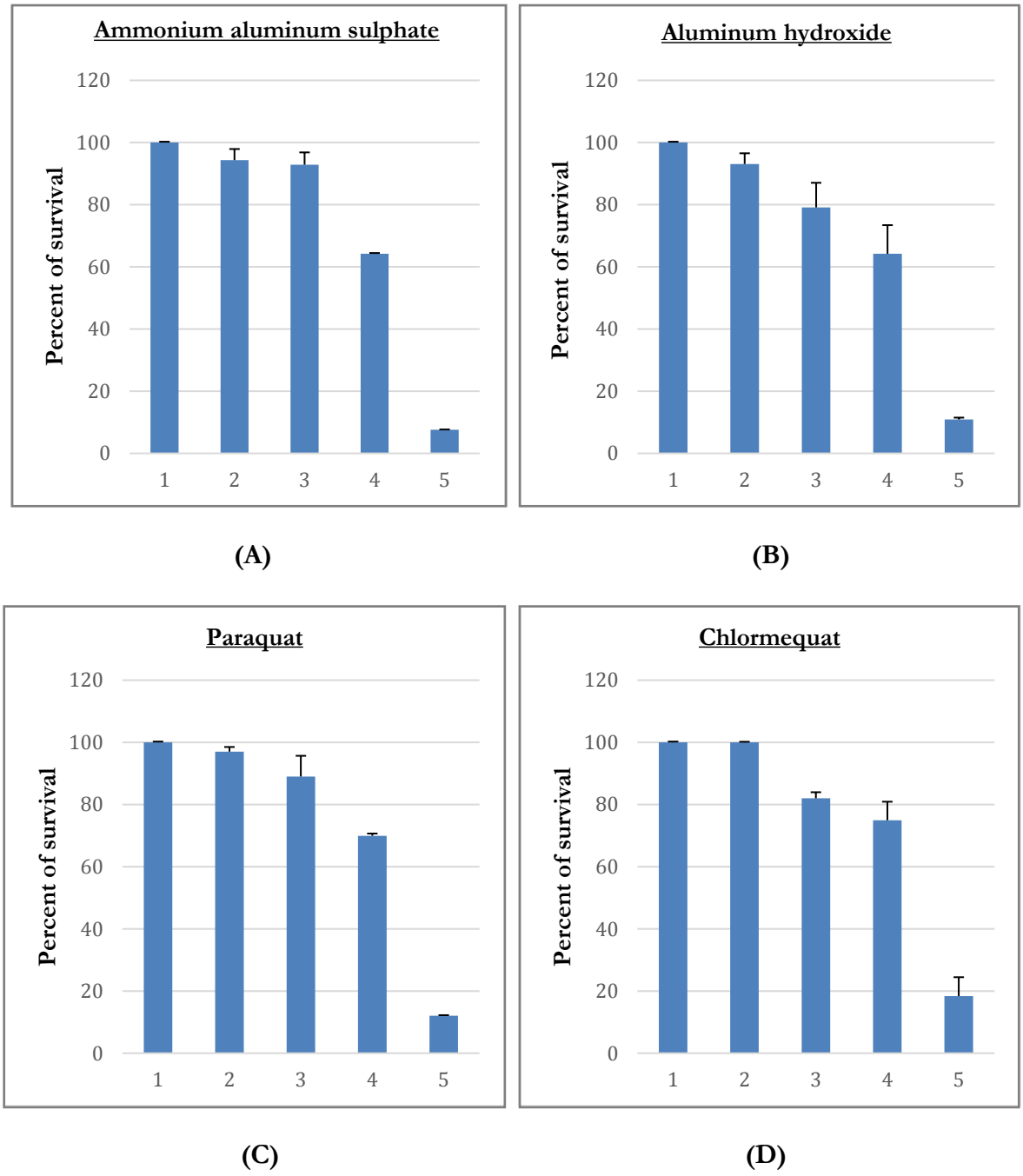

Figure 29: Estimation of dose dependent toxicity of independent exposure of chemicals on neurons for 24 hours. (A) Ammonium aluminum sulphate; #1: nil concentration, #2: 10 nM concentration, #3: 1 µM concentration, #4: 100 µM concentration, #5: 10 mM concentration. (B) Aluminium hydroxide; #1: nil concentration, #2: 10 nM concentration, #3: 1 µM concentration, #4: 100 µM concentration, #5: 10 mM concentration. (C) Paraquat; #1: nil concentration, #2: 933 pM concentration, #3: 93.3 nM concentration, #4: 9.33 µM concentration, #5: 933 µM concentration. (D) Chloromequat; #1: nil concentration, #2: 3.26 nM concentration, #3: 326 nM concentration, #4: 32.6 µM concentration, #5: 3.26 mM concentration. Data were depicted as mean±SD; n = 3.

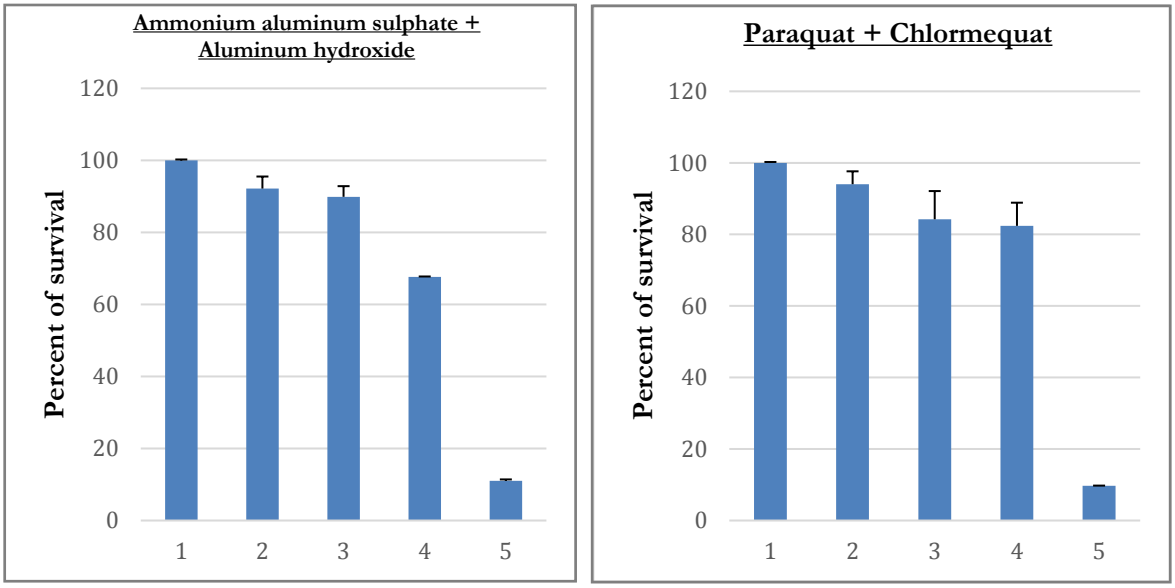

(A) **(B)**

Figure 30: Estimation of dose dependent toxicity of combinatorial exposure of chemicals on neurons for 24 hours. (A) Ammonium aluminum sulphate + Aluminum hydroxide; #1: nil concentration of ammonium aluminum sulphate and aluminum hydroxide, #2: 10 nM ammonium aluminum sulphate and 10 nM aluminum hydroxide, #3: 1 µM ammonium aluminum sulphate and 1 µM aluminum hydroxide, #4: 100 µM ammonium aluminum sulphate and 100 µM aluminum hydroxide, #5: 10 mM ammonium aluminum sulphate and 10 mM aluminum hydroxide. (B) Paraquat + Chlormequat; #1: nil concentration of paraquat and chlormequat, #2: 933 pM paraquat and 3.26 nM chlormequat, #3: 93.3 nM paraquat and 326 nM chlormequat, #4: 9.33 µM paraquat and 32.6 µM chlormequat, #5: 933 µM paraquat and 3.26 mM chlormequat. Data were depicted as mean±SD; n = 3.

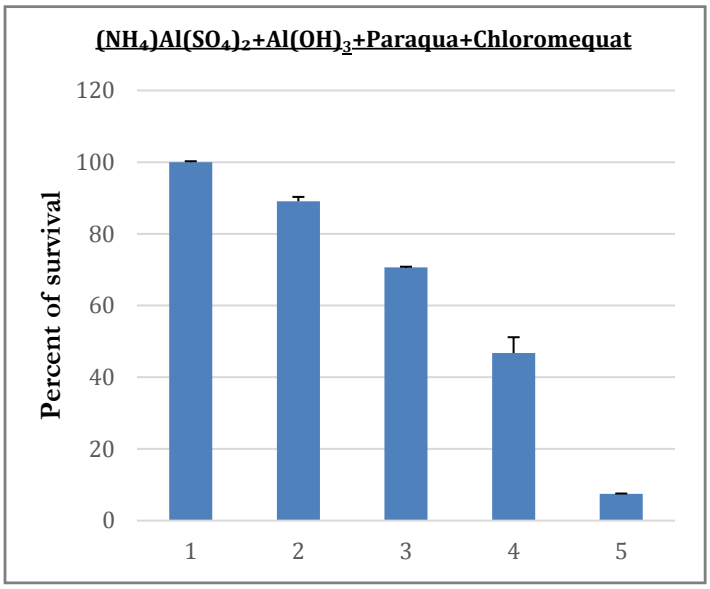

Figure 31: Estimation of dose dependent toxicity of combinatorial exposure of Ammonium aluminum sulphate + Aluminum hydroxide + Paraquat + Chlormequat; #1: nil concentration of ammonium aluminum sulphate, aluminum hydroxide, paraquat and chlormequat; #2: 10 nM ammonium aluminum sulphate, 10 nM aluminum hydroxide, 933 pM paraquat and 3.26 nM chlormequat; #3: 1 µM ammonium aluminum sulphate, 1 µM aluminum hydroxide, 93.3 nM paraquat and 326 nM chlormequat; #4: 100 µM ammonium aluminum sulphate, 100 µM aluminum hydroxide, 9.33 µM paraquat and 32.6 µM chlormequat; #5: 10 mM ammonium aluminum sulphate, 10 mM aluminum hydroxide, 933 µM paraquat and 3.26 mM chlormequat. Data were depicted as mean±SD; n = 3.

Confocal microscopy of neurons treated with chemicals independently for 120 hours:

SK-n-SH cells were treated with various aluminum metal forms, plant growth regulator, and pesticide individually for 120 hours at their 50% cell death concentrations. Confocal microscopy was performed after 120 hours, to assess individual toxic effects of exposures of metals, plant growth regulator, and pesticide on neurons. On microscopic examination, cells treated with aluminum hydroxide (Fig. 32C) exhibited morphological features of healthy cells, which are similar to untreated cells (Fig. 32A). Cells treated with paraquat (Fig. 32D) and chlormequat (Fig. 32E) exhibited typical morphological features of dead cells and apoptosis.

Further, it was observed that chlormequat was highly toxic than paraquat at long time exposure. Cells treated with ammonium aluminum sulphate (Fig. 32B) exhibited morphological features of both apoptotic and healthy cells. Comparatively the toxicity of ammonium aluminum sulphate was very low compared to the paraquat and chlormequat.

Confocal microscopy of neurons treated with chemicals combinatorially for 120 hours:

SK-n-SH cells were treated with the combination of ammonium aluminum sulphate and aluminum hydroxide, the combination of paraquat and chlormequat, and the combination of aluminum metal forms, paraquat, and chlormequat for 120 hours at their 50% cell death concentrations. Confocal microscopy was performed after 120 hours, to assess combined toxic effects of exposures of aluminum metals, pesticide, and plant growth regulator on neurons. On microscopic examination, cells treated with the combination of paraquat and chlormequat (Fig. 33B), the combination of aluminum metal forms, paraquat and chlormequat (Fig. 34B) exhibited typical morphological features of apoptosis. Exposure of the combination of ammonium aluminum sulphate and aluminum hydroxide (Fig. 33C) to the cells did not show any significant toxicity.

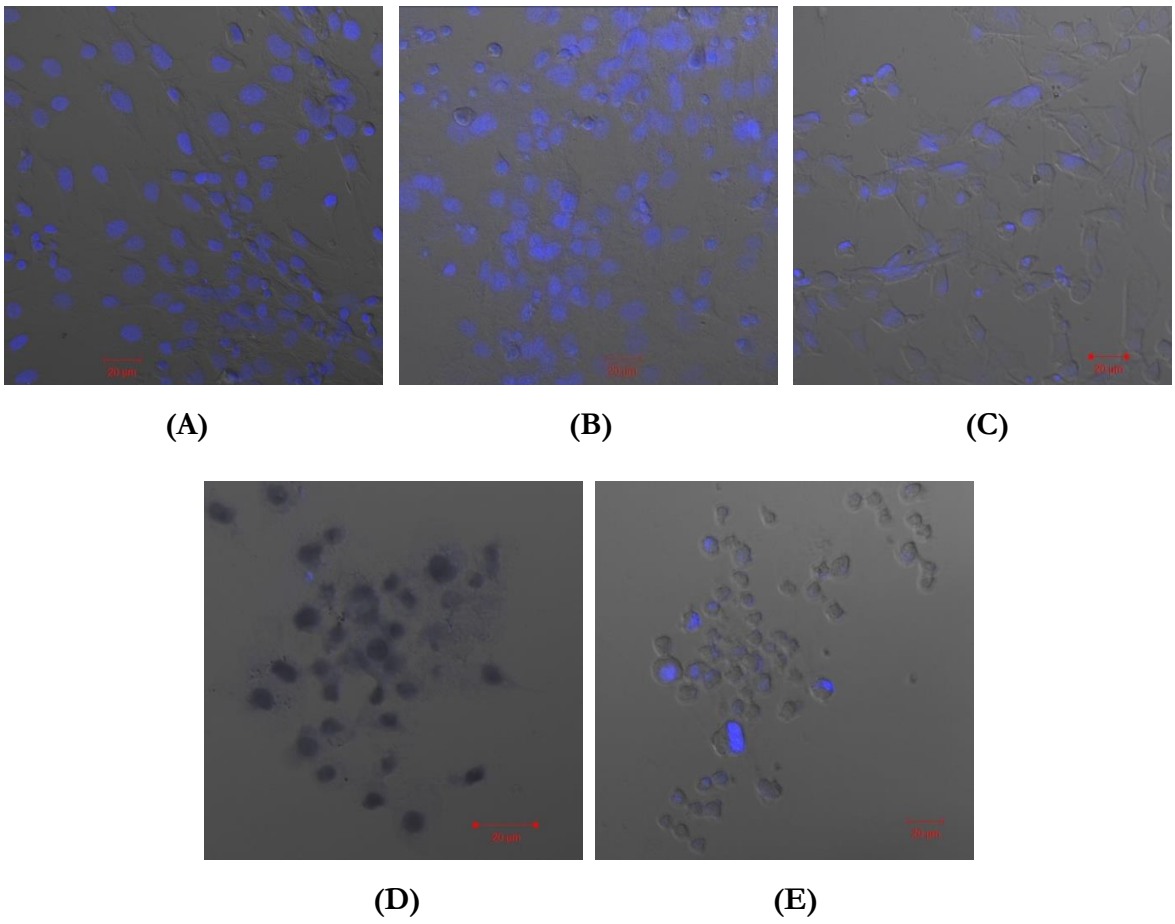

(A) **(B)** **(C)**

(D) **(E)**

Figure 32: Confocal microscopy of SK-n-SH cells treated with chemicals independently for 120 hours. (A) Control, (B) Ammonium aluminum sulphate, (C) Aluminum Hydroxide, (D) Paraquat, (E) Chlormequat.

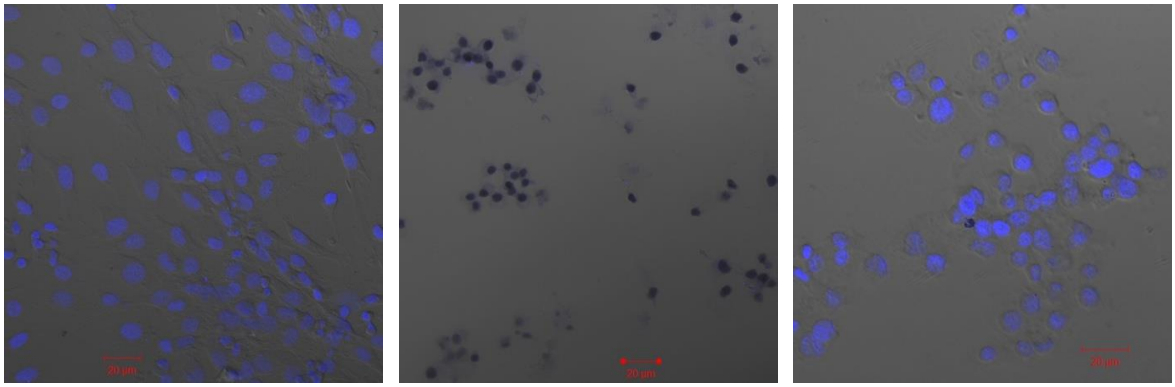

(A) **(B)** **(C)**

Figure 33: Confocal microscopy of SK-n-SH cells treated with chemicals combinatorially for 120 hours. (A) Control, (B) Paraquat + Chlormequat, (C) Aluminium hydroxide + Ammonium aluminum sulphate.

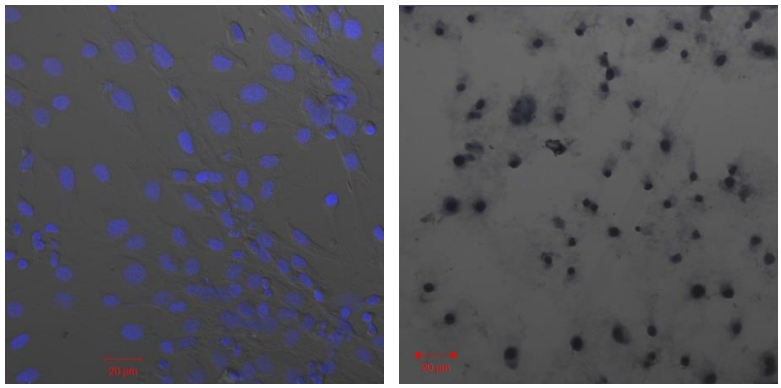

(A) **(B)**

Figure 34: Confocal microscopy of SK-n-SH cells treated for 120 hours of combinatorial exposure of (A) Control, (B) Aluminium hydroxide + Ammonium aluminum sulphate + Aluminium oxide + Paraquat + Chlormequat.

DISCUSSION:

Neurotoxins are chemicals, which are highly toxic to central and/or peripheral nervous systems. Early precautionary testings are required to identify potential neurotoxins to overcome neurodevelopmental disorders in infants and neurodegenerative diseases in elders. Among eighty thousand chemicals present in global commerce, only a small fraction was tested; still, a large fraction has to be tested for their potency in inducing neurotoxicity (Grandjean & Landrigan, 2006). In nature, combinatorial effects are more predominant than individual effect, but till now there are no such reports on screening of chemicals in combinations for identifying their synergistic neurotoxicity or compounding effects. Hence, the purpose of this study was to identify commonly used pesticides, plant growth regulators, and metals for their ability to induce neurotoxicity individually or synergistically.

Since paraquat, chlormequat and aluminum are commonly used pesticide, plant growth regulator, and metal respectively, their effects have been studied. As aluminum exists in many forms, commonly available aluminum forms such as aluminum hydroxide and ammonium aluminum sulphate were selected for the study. Because chemicals can induce toxicity individually or synergistically, both the ways are employed. As the duration of the exposure can also affect toxicity, 24 hours and 120 hours of exposure to chemicals were also studied.

Exposure of individual chemicals to neurons for 24 hours showed that paraquat, chlormequat, ammonium aluminum sulphate, aluminum hydroxide were neurotoxic. Order of neurotoxicity was paraquat > chlormequat > ammonium aluminum sulphate > aluminum hydroxide. Among all individual compounds, paraquat showed the highest neurotoxicity, whereas aluminum hydroxide showed the least neurotoxicity. Higher toxicity of paraquat is mainly due to its capability of redox cycling and the generation of intracellular oxidative stress (Dinis-Oliveira et al., 2008).

Among combinatorial treatments, the combination of aluminum hydroxide, ammonium aluminum sulphate, paraquat, and chlormequat showed synergistic toxicity. The combination of paraquat & chlormequat, the combination of aluminum hydroxide & ammonium aluminum sulphate didn't show any statistically significant synergistic toxicity. Synergistic toxicity of the combination of aluminum hydroxide,

ammonium aluminum sulphate, paraquat, and chlormequat could be due to the combined effect of aluminum and paraquat on neurons. Toxicity of paraquat is mainly due to its redox cycling capability and generation of intracellular oxidative stress (Dinis-Oliveira et al., 2008) and toxicity of aluminum is due to its mitochondrial dysfunction capability and induction of oxidative stress (P. Chen et al., 2016).

Treatment of neurons with aluminum metal forms, plant growth regulator and pesticide individually for 120 hours at their IC_{50} values showed that, cells treated with aluminum hydroxide displayed morphological features of healthy cells, which may be probably due to neutralization of aluminum hydroxide and recovery of proliferating neurons from the initial toxicity over the period of exposure. Cells treated with paraquat and chlormequat displayed cell death and apoptosis, which indicates that paraquat and chlormequat were highly lethal at 120 hours of exposures. Cells treated with ammonium aluminum sulphate displayed both apoptotic and healthy cells, which indicates 120 hours of exposure of ammonium aluminum sulphate was moderately toxic to the cells. These results emphasize that paraquat and chlormequat were highly neurotoxic even at their IC_{50} values when exposed for 120 hours and also demonstrate that pesticides and plant growth regulators can pose a severe threat to the neurons even at lower dosages.

Treatment of neurons with various aluminum metal forms, plant growth regulator and pesticide combinatorially for 120 hours at their IC_{50} values showed that, cells treated with the combination of ammonium aluminum sulphate and aluminum hydroxide did not show any significant toxicity which indicates that the combination of ammonium aluminum sulphate and aluminum hydroxide was non-toxic at 120 hours of exposure. Treatment of cells with the combination of paraquat and chlormequat, the combination of aluminum metal forms, paraquat, and chlormequat, displayed extreme apoptosis, which indicates that combination of paraquat and chlormequat, the combination of aluminum metal forms, paraquat and chlormequat were highly lethal at their IC_{50} values for 120 hours of exposures. Synergistic effect of paraquat and chlormequat might have contributed to their higher lethality. These results emphasize that exposures of the combination of paraquat and chlormequat were extremely neurotoxic even at their IC_{50} values when exposed for 120 hours and

also demonstrate that combination of pesticides and plant growth regulators can pose an extremely severe threat to the neurons even at lower dosages.

To conclude, paraquat, chlormequat, ammonium aluminum sulphate, and aluminum hydroxide exhibit potential neurotoxicity independently and also synergistically. Further, these results alarm the common usage of paraquat, chlormequat, ammonium aluminum sulphate, and aluminum hydroxide.

CONCLUSION:

Neurons were treated with a commonly used pesticide (paraquat), a common plant growth regulator (chlormequat) and a common household metal (ammonium aluminum sulphate and aluminum hydroxide) for 24 hours and 120 hours, individually and combinatorially to study for their ability to induce neurotoxicity independently or synergistically. 24 hours of exposure of individual chemicals on neurons had shown that paraquat, chlormequat, ammonium aluminum sulphate, aluminum hydroxide were neurotoxic. Order of neurotoxicity was paraquat > chlormequat > ammonium aluminum sulphate > aluminum hydroxide. Among 24 hours of combinatorial treatments, the combination of aluminum metal forms, paraquat and chlormequat showed synergistic neurotoxicity. Treatment of neurons with individual chemicals at their IC50 values for 120 hours showed that paraquat and chlormequat were highly neurotoxic even at lower dosages. Combinatorial treatments at their IC50 values for 120 hours showed that the combination of paraquat and chlormequat, the combination of aluminum metal forms, paraquat and chlormequat had synergistic neurotoxicity even at lower dosages. These findings suggest that certain pesticides, plant growth regulators, and metals can induce neurotoxicity independently and also synergistically.

CHAPTER 6:

ANALYSIS OF THE EFFICACY OF CARMUSTINE LOADED LACTOFERRIN NANOPARTICLES AGAINST GLIOBLASTOMA CELLS.

INTRODUCTION:

"Brain and other central nervous system tumors" (BCNST), are known to be one of the leading causes of cancerous deaths. According to the "Central brain tumor registry of the United States" (CBTRUS), in the US alone, every year on an average 15 000 deaths occur due to BCNST, and approximately 80 000 new cases are diagnosing yearly (Q. T. Ostrom et al., 2017). No known environmental risk factors other than ionizing radiation had identified for such higher incidence rates (Johnson, 2014; Quinn T. Ostrom et al., 2014; Wiemels, Wrensch, & Claus, 2010). Amongst all the BCNST, glioblastoma is the most aggressive and most common malignant tumor with 5 y post-diagnosis survival rates of less than 6 % (Q. T. Ostrom et al., 2017). World health organization (WHO) grade IV classified, glioblastoma arises from malignantly transformed glial cells, and it diffusely invades other regions of the brain, making it highly lethal (Louis DN, 2007; Omuro & DeAngelis, 2013; Quirk et al., 2015). Its higher reoccurrence even after surgical resection adds to the complexity (Demuth & Berens, 2004).

Current preferred treatment for glioblastoma is surgical resection of tumors, followed by radiotherapy with concurrent chemotherapy (Brem et al., 1995; Patel, Kim, Ruzevick, Li, & Lim, 2014; Stupp et al., 2005; Westphal et al., 2003; Woodworth, Dunn, Nance, Hanes, & Brem, 2014). Despite these advanced treatments, there is no significant improvement reported in the overall survival rates of patients (Demuth & Berens, 2004). These failures are mainly due to (a) reoccurrence of tumors that arise from surgically inaccessible infiltrating malignant cells (Demuth & Berens, 2004); (b) emergence of resistance to radiotherapy and chemotherapy due to suboptimal dosage exposure for prolonged periods as a result of inefficient dosage delivery (Bao et al., 2006; Beier, Schulz, & Beier, 2011; Sarkaria et al., 2008; J. Zhang, Stevens, Laughton, Madhusudan, & Bradshaw, 2010); (c) higher systemic toxicity as a consequence of nonspecific localization of drugs (Blakeley & Grossman, 2012; Chamberlain, 2010; Lin & Kleinberg, 2008). These failures emphasize the need for the development of efficient drug delivery vehicles with significant drug localization in glioma cells.

In recent years, numerous efforts have been made to develop different drug delivery vehicles to overcome the above problems. Some of these are namely liposomes, nanoshells, dendrimers, solid lipid nanoparticles, polymeric micelles,

carbon nanotubes, polyglycolic acid (PGA) nanoparticles, polylactic acid (PLA) nanoparticles, polylactic-co-glycolic acid (PLGA) nanoparticles, polyanhydride nanoparticles, polyorthoesters nanoparticles, polycyanoacrylate nanoparticles, polycaprolactone nanoparticles, chitosan nanoparticles, albumin nanoparticles, etc. (Invernici et al., 2011; Krupa, Rehak, Diaz-Garcia, & Filip, 2014). But, many of these drug delivery vehicles lack target specificity, making their scope limited. Further, the poor ability of these vehicles in the transport of drugs across the BBB significantly limits their application for delivery of drugs to the brain. Many strategies have developed to overcome the above limitations (Invernici et al., 2011; Rempe, Cramer, Qiao, & Galla, 2014). Among them, exploiting one of the brain's natural transport systems, the receptor-mediated endocytosis, is gaining much interest in delivering therapeutic drugs to the brain. Ligands commonly used for this purpose are folate, transferrin, lactoferrin, etc. These ligands are either coated or conjugated to the nanoparticles, to facilitate nanoparticles entry into the brain via receptor-mediated endocytosis (J. Chang et al., 2012; Rempe et al., 2014).

Lactoferrin is an 80 kDa protein, which is mainly found in milk and other secretory body fluids. It has numerous clinically significant physiological functions viz., anti-inflammation, host defense against infections, maintenance of iron homeostasis, etc. (Jan H. Nuijens, 1996; Jayasinghe, Siriwardhana, & Karunaratne, 2015; Moreno-Exposito et al., 2018; Ward, Paz, & Conneely, 2005). Since brain endothelial cells, and glioblastoma cells (Carine Fillebeen, 1999; Fang et al., 2014; R. Q. Huang et al., 2007; Ji et al., 2006; Ruirui Qiao, 2012) express lactoferrin receptors and also its low endogenous levels in serum (Sánchez, Calvo, & Brock, 1992; Talukder, Takeuchi, & Harada, 2003), make lactoferrin more advantageous in using it for targeting to the brain as it avoids competition with endogenous ligands and also increases target specificity. Drug-loaded nanoparticles were reported to possess a significant advantage over drug conjugated nanoparticles regarding efficacy and drug release in the targeted cells (Krishna, Mandraju, Kishore, & Kondapi, 2009).

In the context of these facts, biodegradable protein nanoparticles were developed using lactoferrin itself as a matrix, into which chemotherapeutic drug, carmustine was loaded, and these nanoparticles were used for targeting brain tumors *in vitro*. The objective was to exploit lactoferrin nanoparticles for a dual purpose, as a

drug carrier, as well as a targeting ligand. Cell culture models were used to evaluate the efficiency of carmustine loaded lactoferrin nanoparticles in drug localization and cytotoxicity.

We hypothesize that carmustine loaded lactoferrin nanoparticles will be an effective treatment strategy for targeting brain tumors if it increases target specificity, enhance therapeutic efficacy, bioavailability, and stability, and also minimizes the systemic toxicity of the drug. This paper discusses the preparation of carmustine loaded lactoferrin nanoparticles, their optimal characteristic features which make them better drug delivery vehicles and further about their efficacy in treating brain tumors in general and more particularly glioblastoma *in vitro.*

MATERIALS AND METHODS:

Materials:

MTT, DAPI, rhodamine 123 were procured from Sigma–Aldrich (St. Louis, USA), lactoferrin from Naturade LLC (Irvine, USA), and olive oil from Nicola Pantaleo (Fasano, Italy). Non-essential amino acids, MEM, DMEM, sodium pyruvate procured from Thermo-Fisher scientific (Waltham, USA). Carmustine was of pharmaceutical grade (Emcure pharmaceuticals, Pune, India). Fetal bovine serum from Lonza (Basel, Switzerland); C_6 glioma, SK-N-SH cell lines were acquired from NCCS (Pune, India). Rest of the materials were of either analytical or molecular biological grade.

Preparation of carmustine loaded lactoferrin, blank lactoferrin and rhodamine loaded lactoferrin nanoparticles:

Nanoparticles were prepared as described by Krishna AD et al. (2009) (Krishna et al., 2009). Briefly, 1 ml of cold phosphate-buffered saline (PBS) pH-7.4 containing 50 mg of dissolved lactoferrin was mixed with 20 mg of carmustine dissolved in dimethyl sulfoxide (DMSO). The mixture was incubated at 4 ºC for 30 min. After incubation, the mixture was slowly added to 30 ml of cold olive oil and was gently dispersed by vortexing. The mixture was subjected to sonication at 4 ºC. Immediately the processed mixture was snap-frozen by keeping it in the liquid nitrogen for 10 min. After thawing the mixture on ice, it was centrifuged at 8000 g maintaining 4 ºC for 15 min. The supernatant was thrown out, and the pellet was washed 3 times with diethyl ether. Following air drying, the pellet was dispersed in cold PBS by sonication and was stored in 4 ºC freezer until use. For fluorescent studies, rhodamine loaded lactoferrin nanoparticles were prepared similarly, but instead of carmustine, rhodamine was used. Similarly, blank lactoferrin nanoparticles were also prepared, but without the use of drug or dye.

Characterization of nanoparticles by FESEM:

Size and shape of lactoferrin nanoparticles were characterized by FESEM (Field electron and ion, Hillsboro, USA). Freshly prepared lactoferrin nanoparticles were coated on a glass slide and were dried overnight in a dust-free chamber. Subsequently, samples were coated with gold and were viewed under the electron microscope. For

image capturing and data analysis, the manufacturer's standard operative procedures were followed.

Characterization of nanoparticles by DLS:

Zeta potential, hydrodynamic diameter, and polydispersity index (PDI) of lactoferrin nanoparticles in suspension form were analyzed by dynamic light scattering method using nanoparticle analyzer (Horiba scientific, Irvine, USA). Particle analysis and data acquisition were carried out according to the manufacturer's instructions.

Estimation of drug loading efficiency of carmustine loaded lactoferrin nanoparticles:

Carmustine loaded lactoferrin nanoparticles (CLN) were suspended in 1 ml of PBS of pH-5 and were kept under gentle rocking for 30 min at 4 ^{0}C for the release of the drug from the nanoparticles (n = 3). 30% $AgNO_3$ was added to the suspension to precipitate protein out of the solution. The resulting solution was centrifuged for 15 min at 15000 g maintaining 4 °C. The obtained supernatant was filtered and used for the drug estimation by HPLC (Waters, Milford, USA) (Lakshmi, Kumar, Kishore, Bhaskar, & Kondapi, 2016). The supernatant was analyzed in triplicate. Different concentrations of carmustine solutions were also prepared and estimated by HPLC to construct a standard curve. Amount of carmustine loaded in the lactoferrin nanoparticles was determined using the constructed standard curve.

Drug loading efficiency was calculated employing the following formula.

$$\text{Loading efficiency } \% = (D_{Loaded}/D_{Total}) \times 100$$

$$D_{Loaded} = D_{Total} - D_{Lost}$$

Where D_{Loaded} = amount of loaded drug; D_{Total} = amount of total drug used; D_{Lost} = amount of drug lost during preparation.

in vitro pH-dependent drug release assay:

pH-dependent drug release assay was performed by quantifying drug released under different pH conditions (Kumari & Kondapi, 2017). Pelleted nanoparticles equivalent to 200 µg of carmustine were suspended in PBS solutions of varying pH ranges (1-9) and were kept under gentle rocking for 4 h at 4 ^{0}C. 30% $AgNO_3$ was added to the suspension to precipitate protein out of the solution. The mobile phase was also added to extract the drug, followed by centrifugation for 15 min at 15000 g maintaining 4 ^{0}C. The obtained supernatant was filtered, and the amount of drug present in the supernatant was estimated using HPLC at 230 nm wavelength for carmustine. For quantification of unknown amounts of the drug in the samples, a standard curve was developed using known concentrations of the drug in the same incubation media and quantified by HPLC. Each sample was quantified in triplicate (n = 3).

Cellular uptake assay by confocal microscopy:

SK-N-SH cells were grown on treated glass coverslips in 12-wellplates. Equivalent amounts of rhodamine loaded lactoferrin nanoparticles were added to the wells and were incubated for different time points (0.5 h, 1 h, 2 h, 4 h, and 8 h). Untreated cells were kept as control. After specified time points, cells were washed thrice with PBS buffer and were fixed with 4% PFA for 10 min. After subsequent washings with PBS buffer, cells were counterstained with DAPI, and the coverslips were mounted on a glass slide. Cells were viewed under the confocal microscope (Leica, Buffalo Grove, USA) for analyzing the amount of uptake of nanoparticles, by utilizing the intrinsic fluorescence of rhodamine 123 (excitation and emission maxima are 511 nm and 534 nm respectively) (Ahmed et al., 2014).

Evaluation of the antiproliferative activity of carmustine loaded lactoferrin nanoparticles:

The antiproliferative assay was performed using the MTT method (Mosmann, 1983). Briefly, 50000 C_6 glioma cells were seeded in every well of the 96-wellplate and were incubated for 12 h in a CO_2 incubator. After incubation, media was substituted with fresh media containing increasing concentrations of either soluble carmustine or its equivalent carmustine loaded nanoparticles. Similar treatment was given with

blank lactoferrin nanoparticles. Control cells were also kept, without the addition of neither soluble drug nor the nanoparticles. Cells were incubated in a CO_2 incubator for 24 h. After incubation, media was aspirated, and cells were washed twice. Fresh media containing 10%, 1.21mM MTT, was added to the cells and they were incubated for 8 h in a CO_2 incubator. During incubation, cells that survived after the treatment convert yellow tetrazolium salt into insoluble formazan crystals. MTT containing media was discarded, and insoluble formazan crystals were dissolved by the addition of DMSO. The intensity of the developed color was measured using multiplate reader-Infinite 200 (Tecan, Mannedorf, Switzerland) at 595 nm. Percentage of inhibition (PI) was calculated according to the following formula.

$$PI = \{(OD_{Control} - OD_{Treated})/OD_{Control}\} \times 100$$

Where, PI = percentage of inhibition; $OD_{Control}$ = absorbance at 595 nm for control cells; $OD_{Treated}$ = absorbance at 595 nm for treated cells.

After plotting the graph, half maximal inhibitory concentration (IC_{50} value) was calculated from it.

RESULTS:

Characterization of nanoparticles by FESEM:

Blank lactoferrin nanoparticles and carmustine loaded lactoferrin nanoparticles were prepared as described in materials and methods. The prepared nanoparticles were characterized by FESEM to obtain information relating to their size and morphology. The FESEM analysis revealed that their sizes were in the range of 13-22 nm, with a mean size of 17.5±3.06 nm for blank lactoferrin nanoparticles (Fig. 35A) and in the range of 32-41 nm, with a mean size of 36.5±3.90 nm for carmustine loaded lactoferrin nanoparticles (Fig. 35B). It is apparent that lactoferrin nanoparticles become more than double in their average size after loading of the drug. Further, FESEM analysis revealed that the nanoparticles were homogenous in their sizes and were spherical in their shapes.

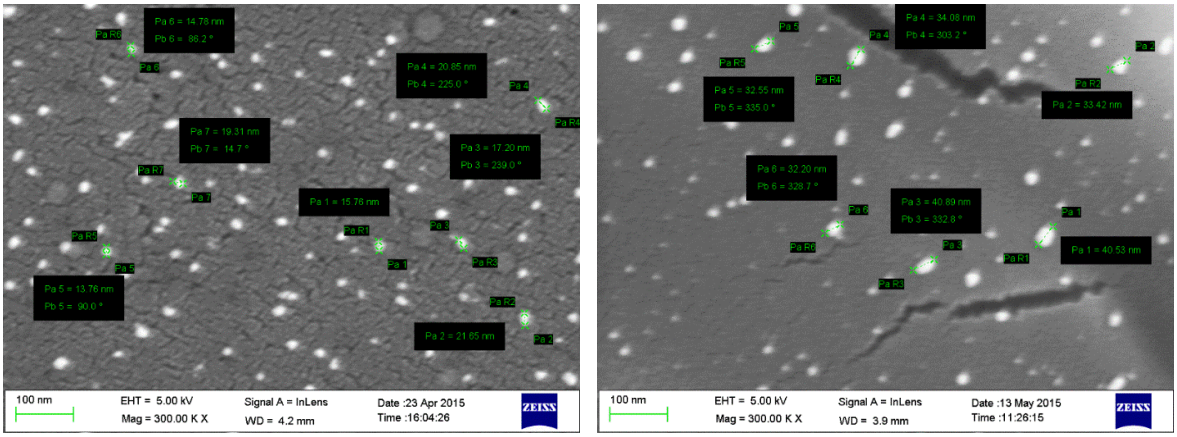

(A) **(B)**

Figure 35: FESEM analysis of (A) Blank lactoferrin nanoparticles, (B) Carmustine loaded lactoferrin nanoparticles. Above image was representative of a quadruplicate experiment (n = 4).

Characterization of nanoparticles by DLS:

Zeta potential values of blank lactoferrin nanoparticles and carmustine loaded lactoferrin nanoparticles were -14.9±3.87 mV (mean±SD) (Fig. 36A) and -24.6±5.94 mV (mean±SD) (Fig. 36B) respectively. These zeta potential values indicate that carmustine loaded lactoferrin nanoparticles were under colloidal stability in nature, and blank lactoferrin nanoparticles were under moderately colloidal stability in

nature. Hydrodynamic sizes of nanoparticles were also investigated using DLS analysis (Fig. 36C and Fig. 36D). Since DLS measures the hydrodynamic diameter of the particles, whereas FESEM measures size in the dry state, nanoparticles sizes were little larger in DLS compared to the FESEM analysis. PDI for blank lactoferrin nanoparticles was 0.264±0.03 and for carmustine loaded lactoferrin nanoparticles was 0.338±0.05. These PDI values confirm that these nanoparticles had a homogeneously dispersed size distribution.

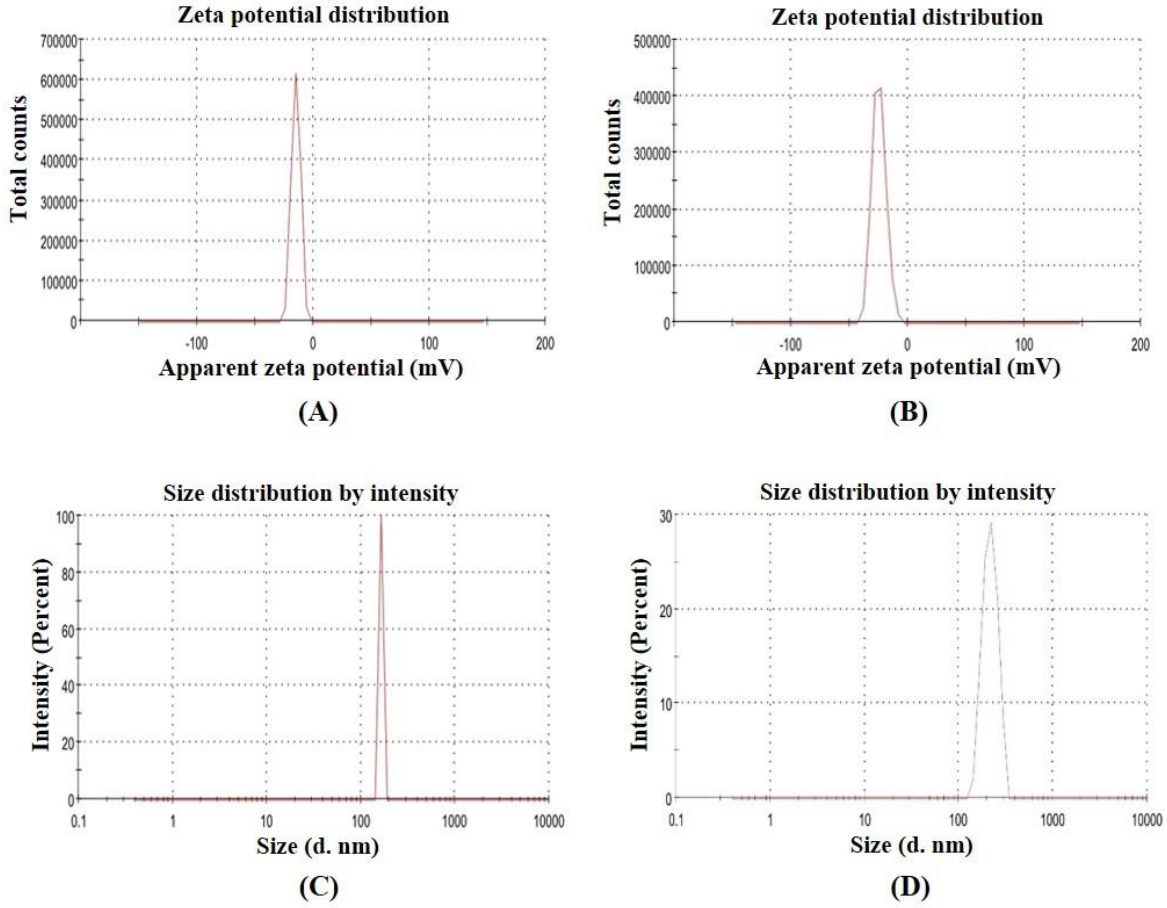

Figure 36: DLS analysis: Zeta potential measurements of (A) blank lactoferrin nanoparticles, (B) carmustine loaded lactoferrin nanoparticles. Hydrodynamic diameter measurements of (C) blank lactoferrin nanoparticles, (D) carmustine loaded lactoferrin nanoparticles. The experiment was conducted in triplicates (n = 3).

Estimation of drug loading efficiency of carmustine loaded lactoferrin nanoparticles:

Significantly higher drug loading efficiency was achieved in the nanoparticles by using the Sol-oil method. Different concentrations of carmustine solutions were prepared, estimated by HPLC, and the standard graph was developed for calculating the amount of encapsulated carmustine present in the lactoferrin nanoparticles (Fig. 37B). Carmustine loaded lactoferrin nanoformulations were treated as described in the materials and methods, the released drug was estimated by HPLC (Fig. 37A) and correlated with the standard graph. Then the loading efficiencies were calculated using the formula mentioned in the materials and methods. Loading efficiency of carmustine in the carmustine loaded lactoferrin nanoparticles was found to be 43±3.7 % (n = 3).

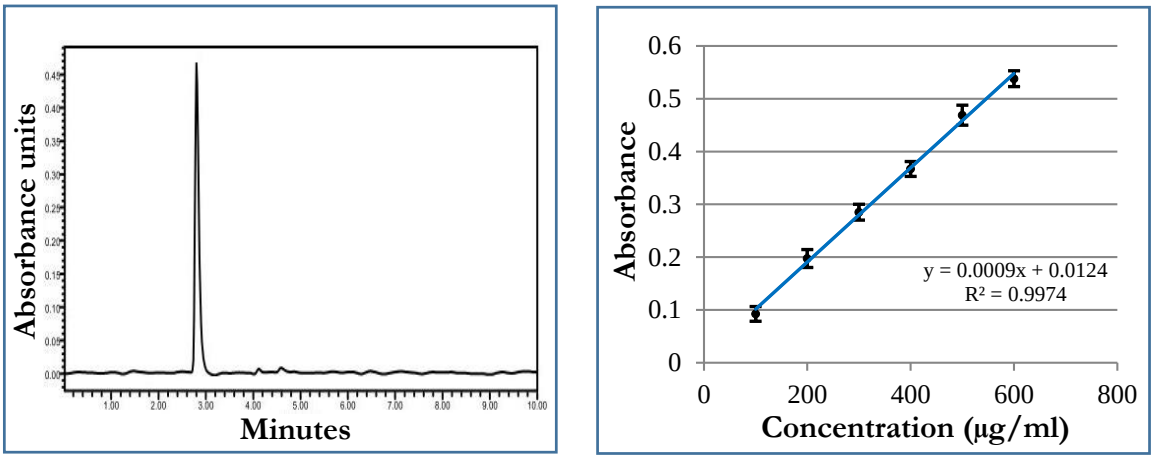

(A) (B)

Figure 37: (A) HPLC analysis of carmustine at 230 nm wavelength. (B) Quantification of carmustine by HPLC; data were depicted as mean±SD, n = 3.

in vitro pH-dependent drug release assay:

pH-dependent drug release assay of CLN was performed at varying pH ranges (1–9) (Fig. 38). The maximum amount of drug release was observed at pH 5, which was followed by pH 6. At all other pH conditions, the release was comparatively low. At physiological pH (pH 7.2 to 7.4) and gastric pH (pH 1 to 2.5), drug release was less than 20 % and whereas maximum release was observed at endocytotic vesicular pH (pH 5) and around tumor extracellular pH (pH 5.85-7.35) (Wike-Hooley, Haveman, & Reinhold, 1984), from the nanoparticles.

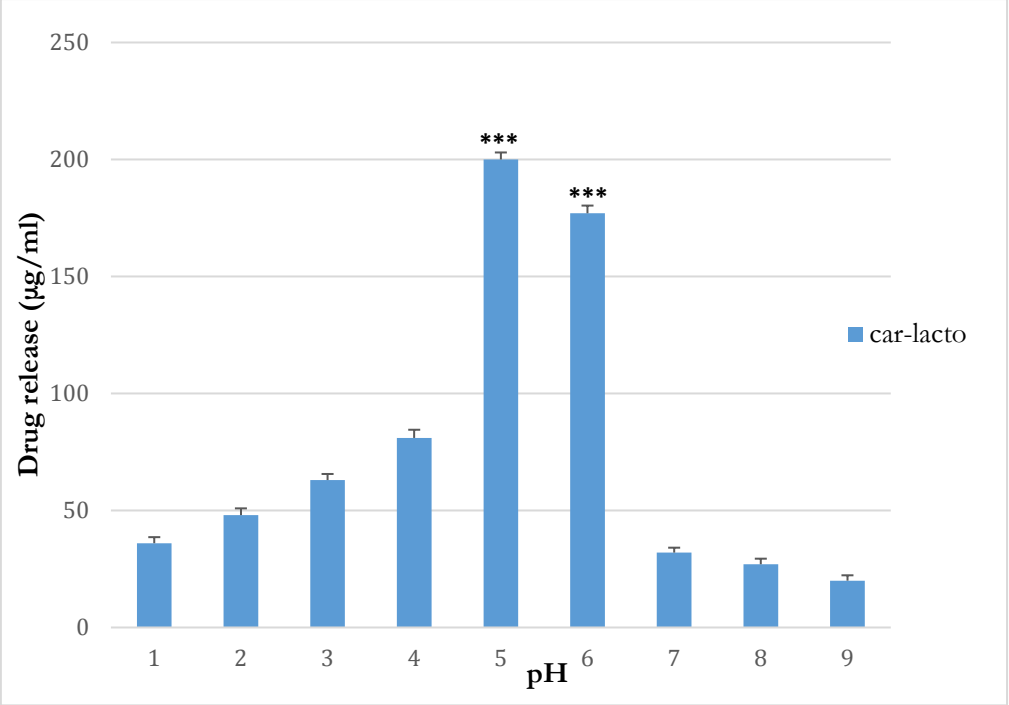

Figure 38: pH-dependent release assay of carmustine loaded lactoferrin nanoparticles. Car-lacto represents carmustine loaded lactoferrin nanoparticle. Averages and standard deviations from three experiments (n = 3) were shown as mean±SD. ***P < 0.001 by one-way ANOVA using Holm-Sidak method.

Cellular uptake assay by confocal microscopy:

Rhodamine 123 loaded lactoferrin nanoparticles were incubated with the cells for different time points to confirm the cellular uptake of nanoparticles. Up to 1 h of incubation, rhodamine was not visible, but after 2 h, it was noticed that its level had increased with the increment of time. By the end of 8 h, cells were localized entirely with rhodamine 123. Cells, which were not exposed to rhodamine 123 loaded nanoparticles, were taken as the control (Fig. 39). Time course experiment showed that there was a gradual increase of rhodamine in the cells with the time, which confirmed the cellular uptake of nanoparticles and their rise was gradual and proportional to the time. This result also confirmed the longer retention of lactoferrin nanoparticles within the cells, which provides a longer resident time for chemotherapeutic drugs to confer the antiproliferative effect.

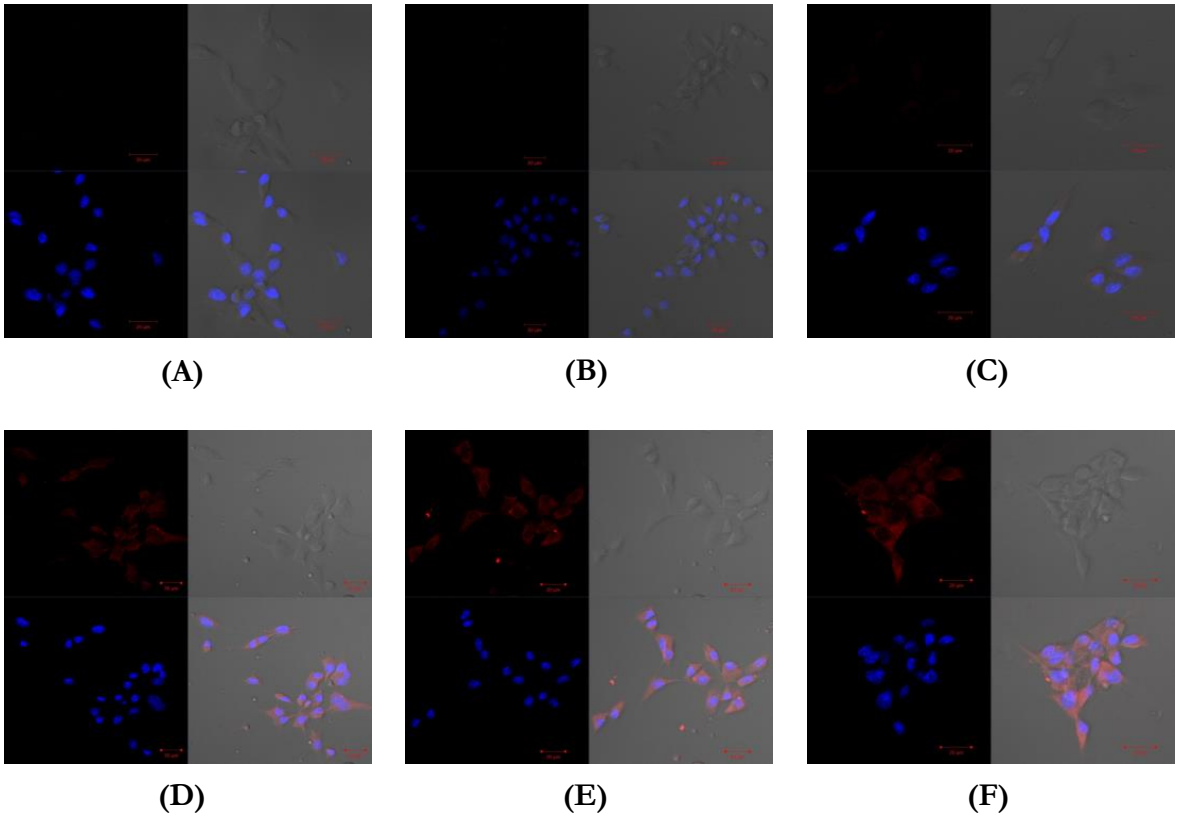

Figure 39: Cellular uptake of rhodamine 123 loaded lactoferrin nanoparticles. Time course experiment showed the uptake of nanoparticles into the cells, and there was a gradual increase in the uptake of nanoparticles with the increment of time. A, B, C, D, E, F represent control, 0.5 h, 1h, 2h, 4h, and 8h time points respectively. In each big square, the upper left square represents the rhodamine 123 (red), the upper right square represents transmission image, the lower left square represents DAPI (blue), and the lower right square represents merger image. Total number of independent experimentation, n = 3.

Evaluation of the antiproliferative activity of carmustine loaded lactoferrin nanoparticles:

Antiproliferative activity of carmustine loaded lactoferrin nanoparticles were compared with the antiproliferative activity of the free drug (carmustine) after 24 h of treatment with the free drug and drug-loaded nanoparticles. The results clearly showed that carmustine loaded lactoferrin nanoparticles had a higher antiproliferative effect compared to free carmustine at all the concentrations (Fig. 40A). And there was

a reduction of 3.29 times in the IC_{50} value with the treatment of carmustine loaded lactoferrin nanoparticles compared to free carmustine treatment. IC_{50} values of free carmustine and carmustine loaded lactoferrin nanoparticles were 43.22 µg/ml and 12.76 µg/ml respectively. Blank lactoferrin nanoparticles (delivery vehicle) didn't show any significant antiproliferative activity at all the concentrations (Fig. 40B).

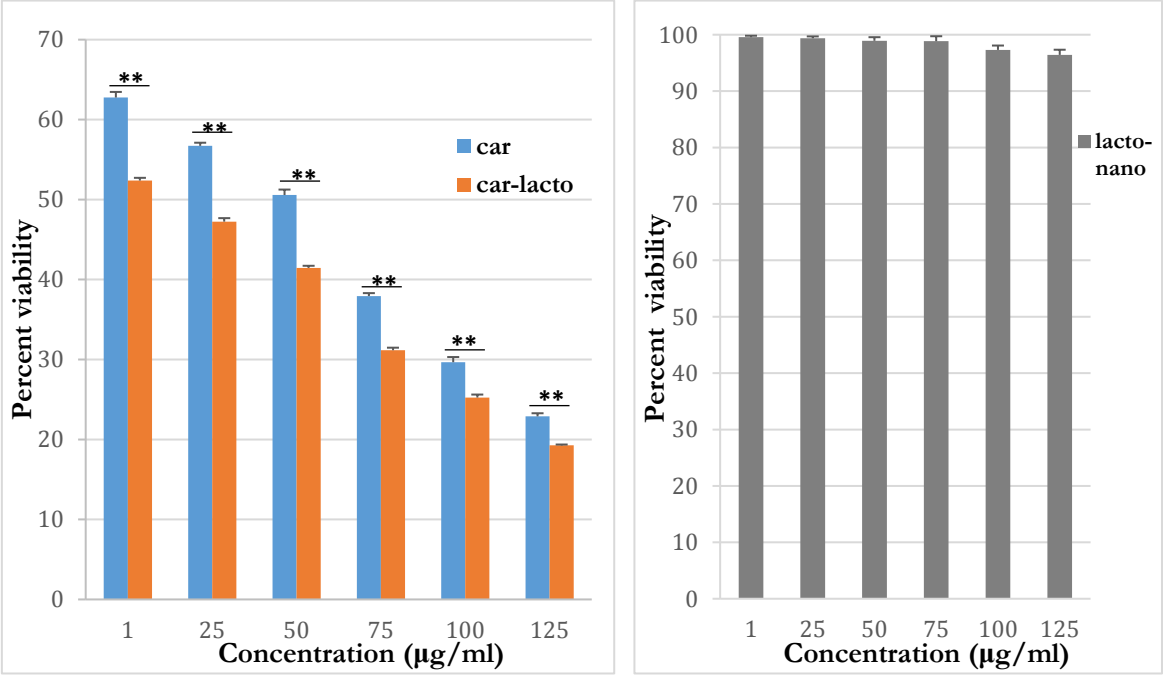

(A) **(B)**

Figure 40: Dose-dependent antiproliferative activities of (A) free carmustine & carmustine loaded lactoferrin nanoparticles and (B) free lactoferrin nanoparticles after 24 h of treatment. Car, car-lacto, and lacto-nano represent the treatment of carmustine drug, carmustine loaded lactoferrin nanoparticles and blank lactoferrin nanoparticles respectively. Data were depicted as mean±SD (n = 3), **P < 0.01 by Student's t-test.

DISCUSSION:

Current advanced treatments for glioblastoma remain not so effective since there is no significant improvement in the survival of the patients. The purpose of this objective was to develop an effective target-specific drug delivery vehicle with reduced systemic toxicity and increased therapeutic efficacy against glioblastoma. As it is known, lactoferrin receptors are expressed on brain endothelial cells, and glioblastoma cells, a target-specific drug delivery vehicle was developed, using lactoferrin itself as a matrix, into which chemotherapeutic drug carmustine was loaded. In the present study, carmustine loaded lactoferrin nanoparticles (CLN) were prepared and characterized their features such as size, shape, polydispersity, stability, drug loading efficiency, drug releasing efficiency, cellular uptake ability, etc., and further evaluated their efficacy in treating glioblastoma.

For decades, carmustine was a drug of choice for treating glioblastoma (C. H. Chang et al., 1983; Selker et al., 2002; Weiss & Issell, 1982). Due to its side effects viz. pulmonary fibrosis, bone marrow suppression, etc. (De Vita et al., 1965; O'Driscoll, Kalra, Gattamaneni, & Woodcock, 1995), its usage was limited. To reduce systemic toxicity, intracranial polymer implants (gliadel wafers) impregnated with carmustine, have been using clinically since 1996 (Lin & Kleinberg, 2008). But these gliadel wafers were found to be not successful as they do not show effective therapeutic efficacy due to many limitations such as lower penetration, inability in preventing short distant tumor recurrence, lack of synergetic action in combination with radiotherapy and other chemotherapeutic drugs, practical difficulties in prescribing regular dosage schedules as it requires regular intracranial surgeries (Bota, Desjardins, Quinn, Affronti, & Friedman, 2007; Lin & Kleinberg, 2008). Further, complications are reported in the use of gliadel wafers due to severe adverse effects such as healing abnormalities (Subach et al., 1999), craniotomy infections (McGovern, Lautenbach, Brennan, Lustig, & Fishman, 2003), seizures (Brem et al., 1995), oedema (Brem et al., 1995; E. L. Weber & Goebel, 2005), neurological decline (E. L. Weber & Goebel, 2005), intracranial hypertension (Westphal et al., 2003), cerebrospinal fluid leaks (Westphal et al., 2003), tumor bed cyst formation (Engelhard, 2000), pericavity necrosis (Kleinberg et al., 2004), etc. These limitations and adverse effects emphasize the need for a better drug delivery vehicle for the efficient treatment of glioblastoma.

In the present study, CLN were prepared using the Sol-oil method. This method is simple, less time consuming and doesn't involve any chemical modifications either to the drug or protein unlike other methods such as protein coacervation method (Shome et al., 2009). Further, lactoferrin conformation remains in the native state. As the nanoparticles are prepared using lactoferrin, a natural protein present abundantly in milk and other secretory body fluids, these nanoparticles are safer to use even at high dosages. Besides, significantly higher drug loading efficiency was also achieved in the nanoparticles by using this method. Drug loading was indeed higher compared to commercially available carmustine implants, which have only 3.85 % drug loading capacity (Brem et al., 1995). The reported maximum drug loading capacity that can be achieved in the biodegradable polymers was 28 % (Olivi et al., 2003), which was less than that observed in carmustine loaded lactoferrin nanoparticles (43±3.7 %). The drug loading efficiency of a drug delivery vehicle can influence its therapeutic index. Higher the achieved drug loading efficiency, higher will be the therapeutic index. With the increased therapeutic index, there will be an enhanced antitumor effect and reduced toxicity (Sharma & Sharma, 1997).

Using Sol-oil method, nanoparticles of sizes ≤ 41 nm were successfully developed, which was confirmed by FESEM analysis. FESEM studies also showed that blank lactoferrin nanoparticles of 13-22 nm size became enlarged to 32-41 nm size after successful loading of carmustine drug. It is an advantage to have smaller sized nanoparticles because several studies had consistently shown that smaller sized nanoparticles were capable of escaping from the reticuloendothelial system, thereby evaded rapid clearance from systemic circulation and had longer circulation time & stability in the blood (Alexis, Pridgen, Molnar, & Farokhzad, 2008; Ferroni et al., 2015; Hemant, Raizaday, Sivadasu, Uniyal, & Kumar, 2015; Masserini, 2013b). Several other studies also had shown, an inverse correlation between nanoparticle size's and blood-brain barrier penetration (Etame, Smith, Chan, & Rutka, 2011; Hanada et al., 2014; Sonavane, Tomoda, & Makino, 2008). It indicates that particles, which are smaller in size can cross the blood-brain barrier more efficiently than particles which are larger. Thus, the smaller size of these nanoparticles can increase their circulatory half-life and also make them more efficient in crossing the blood-brain barrier.

The measured zeta potential values indicate that these nanoparticles were stable. Carmustine loaded lactoferrin nanoparticles were under colloidal stability range, whereas blank lactoferrin nanoparticles were under moderately colloidal stability range. Measured nanoparticle sizes were found to be little larger in DLS compared to FESEM analysis. Since, DLS measures the hydrodynamic diameter of the particle, which includes not only the particle but also the ionic and solvent layers associated with the particle in the solution, the particle sizes will be larger in DLS compared to FESEM, which measures the size in the dry state (Uskoković, 2012; Williams, Oatley-Radcliffe, & Hilal, 2017). The polydispersity index values of 0.264±0.03 and 0.338±0.05 for blank lactoferrin nanoparticles and carmustine loaded lactoferrin nanoparticles respectively indicate that these nanoparticles possess a homogenous population with narrow size distribution.

The release of the drug from the nanoparticles was found to be pH dependent. It was observed that at physiological and gastric pH, drug release from the nanoparticles was very minimum, whereas maximum drug release was observed at the endocytotic vesicular pH (pH 5) and around tumor extracellular pH (pH 5.85-7.35) (Wike-Hooley et al., 1984), which indicates that these nanoparticles can have low loss of the drug during systemic circulation, thereby exhibit reduced systemic toxicity. And they also show more specificity in the drug release, mainly in the endocytotic vesicles, which are involved in receptor-mediated endocytosis and around tumor environment, which have reduced pH as a consequence of higher anaerobic respiration of cancerous cells (Gatenby & Gillies, 2004; Webb, Chimenti, Jacobson, & Barber, 2011). pH-dependent drug release is an added advantage, which makes these nanoparticles optimal drug delivery vehicles with reduced systemic toxicity and increases tumor specificity.

As carmustine drug was nonfluorescent, cellular uptake of nanoparticles was tested by loading fluorescent dye, rhodamine 123 into the lactoferrin nanoparticles. Time course study using confocal microscopy had shown that there was a gradual increase of rhodamine in the cells with the increment of time, which confirmed the active cellular uptake of lactoferrin nanoparticles. Earlier it was reported that the mechanism of lactoferrin nanoparticles uptake into the cells was through receptor-mediated endocytosis (Ahmed et al., 2014; Krishna et al., 2009). As the brain

endothelial cells and glioblastoma cells express lactoferrin receptors (Carine Fillebeen, 1999; Fang et al., 2014; R. Q. Huang et al., 2007; Ji et al., 2006; Ruirui Qiao, 2012), a similar mechanism could be operative, during the transport of CLN across the BBB and also at the entry into the tumor cells.

Comparative study of the antiproliferative effect of free carmustine and carmustine loaded lactoferrin nanoparticles, had validated that carmustine loaded lactoferrin nanoparticles had higher therapeutic efficacy than free carmustine. Previously, carmustine encapsulated liposomes, and carmustine-magnetic nanoparticles showed 50 % inhibition at around 467 μM and 100 μM concentrations of carmustine respectively (P. Y. Chen et al., 2010; Kitamura et al., 1996), whereas carmustine loaded lactoferrin nanoparticles showed 50 % inhibition at 59.6 μM of carmustine, which was significantly lower and further substantiates the higher therapeutic efficacy of carmustine loaded lactoferrin nanoparticles. These results were also consistent with the earlier reports (Ahmed et al., 2014; Kumari & Kondapi, 2017), where lactoferrin nanoparticles had used as drug delivery vehicles. Higher uptake of nanoparticles, sustained drug release from the nanoparticles and the longer retention of the drug inside the cells might have contributed to the increased therapeutic efficacy of carmustine loaded lactoferrin nanoparticles against C_6 glioma cells compared to the free carmustine.

Current state of the art, drug delivery vehicles for the treatment of glioblastoma includes solid lipid nanoparticles, polymeric nanoparticles, micelles, magnetic nanoparticles, liposomes, gold nanoshells, nanostructured lipid carriers, carbon nanotubes, etc. These drug delivery vehicles are failing to be an effective therapeutics due to one or more of the crucial issues viz., lower encapsulation efficiency, higher toxicity, lower stability, rapid clearance from the blood, lower biodegradability, lack of specificity, lower therapeutic indices, higher manufacturing costs, etc. (Bhujbal, de Vos, & Niclou, 2014; Krupa et al., 2014; Tapeinos, Battaglini, & Ciofani, 2017; F. Zhang, Xu, & Liu, 2015). But, as may be seen from the results of the present study, carmustine loaded lactoferrin nanoparticles are showing promising results, which may overcome these challenges.

Thus, carmustine loaded lactoferrin nanoparticles serve as potential drug delivery vehicles in treating glioblastoma effectively *in vitro*. Further studies are required to establish *in vivo* efficacy.

CONCLUSION:

Carmustine loaded lactoferrin nanoparticles, with ≤ 41 nm size were successfully developed, using lactoferrin as a single matrix. These nanoparticles were spherical with homogeneous distribution, enhanced stability, and higher drug loading efficiency. The release of the drug from nanoparticles was pH dependent, which adds additional advantage to this target specific drug delivery vehicle. Further, active cellular uptake of nanoparticles with a significant antiproliferative effect in cell culture models substantiated carmustine loaded nanoparticles as an efficient drug delivery vehicle in treating glioblastoma.

Further *in vivo* efficacy and toxicological studies using carmustine loaded lactoferrin nanoparticles would provide an opportunity for the development of an effective treatment strategy against glioblastoma without any systemic toxicity.

OVERALL CONCLUSIONS

- ✓ Hippocampal and cortical neurons were isolated from E18 rat embryos and were cultured separately without the use of glial feeder layer. Microscopic examination of 7-days old primary cultures of hippocampal and cortical neurons showed successful growth of a homogenous population of neurons with their characteristic morphological features.
- ✓ Ageing phenomena of cortical neurons *in vitro* was established based on the senescence markers, wherein cortical neurons survived for 50 days.
- ✓ Topoisomerase II beta levels decreased with ageing, and Slit2 levels increased with the ageing of cortical neurons, similar lines of observations were seen in granule neurons. While NPY levels shown differential expression in cortical neurons compared to granule neurons.
- ✓ Both the seeding density and starvation can induce longevity in the cultured rat primary cortical neurons *in vitro*. And neuronal maturation plays an additive role in starvation-induced longevity extension of cortical neurons.
- ✓ Chlormequat, paraquat, ammonium aluminum sulphate, aluminum hydroxide were found to be neurotoxic individually and also showed synergistic neurotoxicity when treated combinatorially. These findings suggest that certain commonly used pesticides, plant growth regulators, and metals can induce neurotoxicity independently and also synergistically.
- ✓ Carmustine loaded lactoferrin nanoparticles serve as potential drug delivery vehicles in treating glioblastoma effectively *in vitro*.

REFERENCES

Abbott, N. J. (2013). Blood-brain barrier structure and function and the challenges for CNS drug delivery. *J Inherit Metab Dis, 36*(3), 437-449. doi:10.1007/s10545-013-9608-0

Adams, I. (1987). Comparison of synaptic changes in the precentral and postcentral cerebral cortex of aging humans: a quantitative ultrastructural study. *Neurobiol Aging, 8*(3), 203-212.

Adams, I., & Jones, D. G. (1982). Quantitative ultrastructural changes in rat cortical synapses during early-, mid- and late-adulthood. *Brain Res, 239*(2), 349-363.

Adinolfi, M. (1985). The development of the human blood-CSF-brain barrier. *Dev Med Child Neurol, 27*(4), 532-537.

Ahmed, F., Ali, M. J., & Kondapi, A. K. (2014). Carboplatin loaded protein nanoparticles exhibit improve anti-proliferative activity in retinoblastoma cells. *Int J Biol Macromol, 70*, 572-582. doi:10.1016/j.ijbiomac.2014.07.041

Ahmed, F., Kumari, S., & Kondapi, A. K. (2018). Evaluation of Antiproliferative Activity, Safety and Biodistribution of Oxaliplatin and 5-Fluorouracil Loaded Lactoferrin Nanoparticles for the Management of Colon Adenocarcinoma: an In Vitro and an In Vivo Study. *Pharm Res, 35*(9), 178. doi:10.1007/s11095-018-2457-7

Al-Zabin, M., & Rohleffson, J. (2017). Isolation, Culture, and Characterization of Cortical and Hippocampal Neurons from Prenatal Mice: Evaluation Study of Technique and Applications. *International Journal of Novel Research in Life Sciences, 4*(2), 54-73.

Alexis, F., Pridgen, E., Molnar, L. K., & Farokhzad, O. C. (2008). Factors affecting the clearance and biodistribution of polymeric nanoparticles. *Mol Pharm, 5*(4), 505-515. doi:10.1021/mp800051m

Alhebshi, A. H., Gotoh, M., & Suzuki, I. (2013). Thymoquinone protects cultured rat primary neurons against amyloid beta-induced neurotoxicity. *Biochem Biophys Res Commun, 433*(4), 362-367. doi:10.1016/j.bbrc.2012.11.139

Anson, R. M., Guo, Z., de Cabo, R., Iyun, T., Rios, M., Hagepanos, A., . . . Mattson, M. P. (2003). Intermittent fasting dissociates beneficial effects of dietary restriction

on glucose metabolism and neuronal resistance to injury from calorie intake. *Proc Natl Acad Sci U S A, 100*(10), 6216-6220. doi:10.1073/pnas.1035720100

Arking, R. (2006). *Biology of Aging: Observations and Principles*. New York (NY): Oxford University Press.

Aschner, M., & Syversen, T. (2004). Neurotoxicology: principles and considerations of in vitro assessment. *Altern Lab Anim, 32*(4), 323-327.

Augustin-Voss, H. G., Voss, A. K., & Pauli, B. U. (1993). Senescence of aortic endothelial cells in culture: effects of basic fibroblast growth factor expression on cell phenotype, migration, and proliferation. *J Cell Physiol, 157*(2), 279-288. doi:10.1002/jcp.1041570210

Bagherniya, M., Butler, A. E., Barreto, G. E., & Sahebkar, A. (2018). The effect of fasting or calorie restriction on autophagy induction: A review of the literature. *Ageing Res Rev, 47*, 183-197. doi:10.1016/j.arr.2018.08.004

Bao, S., Wu, Q., McLendon, R. E., Hao, Y., Shi, Q., Hjelmeland, A. B., . . . Rich, J. N. (2006). Glioma stem cells promote radioresistance by preferential activation of the DNA damage response. *Nature, 444*, 756-760. doi:10.1038/nature05236

Barha, C. K., Nagamatsu, L. S., & Liu-Ambrose, T. (2016). Basics of neuroanatomy and neurophysiology. *Handb Clin Neurol, 138*, 53-68. doi:10.1016/b978-0-12-802973-2.00004-5

Becker, L. C., Boyer, I., Bergfeld, W. F., Belsito, D. V., Hill, R. A., Klaassen, C. D., . . . Andersen, F. A. (2016). Safety Assessment of Alumina and Aluminum Hydroxide as Used in Cosmetics. *Int J Toxicol, 35*(3 suppl), 16s-33s. doi:10.1177/1091581816677948

Beier, D., Schulz, J. B., & Beier, C. P. (2011). Chemoresistance of glioblastoma cancer stem cells - much more complex than expected. *Molecular Cancer, 10*(128), 1-11. doi:10.1186/1476-4598-10-128

Bertrand, S. J., Aksenova, M. V., Aksenov, M. Y., Mactutus, C. F., & Booze, R. M. (2011). Endogenous amyloidogenesis in long-term rat hippocampal cell cultures. *BMC Neurosci, 12*, 38. doi:10.1186/1471-2202-12-38

Best, B. P. (2009). Nuclear DNA damage as a direct cause of aging. *Rejuvenation Res, 12*(3), 199-208. doi:10.1089/rej.2009.0847

Bhanu, M. U., Mandraju, R. K., Bhaskar, C., & Kondapi, A. K. (2010). Cultured cerebellar granule neurons as an in vitro aging model: topoisomerase IIbeta as an additional biomarker in DNA repair and aging. *Toxicol In Vitro, 24*(7), 1935-1945. doi:10.1016/j.tiv.2010.08.003

Bhujbal, S. V., de Vos, P., & Niclou, S. P. (2014). Drug and cell encapsulation: alternative delivery options for the treatment of malignant brain tumors. *Adv Drug Deliv Rev, 67-68*, 142-153. doi:10.1016/j.addr.2014.01.010

Blakeley, J., & Grossman, S. A. (2012). Chapter 17 - Chemotherapy with cytotoxic and cytostatic agents in brain cancer. In M. J. Aminoff, F. Boller, & D. F. Swaab (Eds.), *Handbook of Clinical Neurology* (Vol. 104, pp. 229-254): Elsevier.

Blinn, R. C. (1967). Plant-growth regulant. Biochemical behavior of 2-chloroethyl trimethylammonium chloride in wheat and in rats. *Journal of Agricultural and Food Chemistry, 15*(6), 984-988. doi:10.1021/jf60154a003

Bota, D. A., Desjardins, A., Quinn, J. A., Affronti, M. L., & Friedman, H. S. (2007). Interstitial chemotherapy with biodegradable BCNU (Gliadel) wafers in the treatment of malignant gliomas. *Ther Clin Risk Manag, 3*(5), 707-715.

Brem, H., Piantadosi, S., Burger, P. C., Walker, M., Selker, R., Vick, N. A., . . . Schold, S. C. (1995). Placebo-controlled trial of safety and efficacy of intraoperative controlled delivery by biodegradable polymers of chemotherapy for recurrent gliomas. *The Lancet, 345*(8956), 1008-1012.

Brewer, G. J. (1995). Serum-free B27/neurobasal medium supports differentiated growth of neurons from the striatum, substantia nigra, septum, cerebral cortex, cerebellum, and dentate gyrus. *J Neurosci Res, 42*(5), 674-683. doi:10.1002/jnr.490420510

Brewer, G. J. (1997). Isolation and culture of adult rat hippocampal neurons. *J Neurosci Methods, 71*(2), 143-155.

Brewer, G. J., Torricelli, J. R., Evege, E. K., & Price, P. J. (1993). Optimized survival of hippocampal neurons in B27-supplemented Neurobasal, a new serum-free

medium combination. *J Neurosci Res, 35*(5), 567-576. doi:10.1002/jnr.490350513

Broussolle, E., & Thobois, S. (2002). [Genetics and environmental factors of Parkinson disease]. *Rev Neurol (Paris), 158 Spec no 1*, S11-23.

Browner, W. S., Kahn, A. J., Ziv, E., Reiner, A. P., Oshima, J., Cawthon, R. M., . . . Cummings, S. R. (2004). The genetics of human longevity. *Am J Med, 117*(11), 851-860. doi:10.1016/j.amjmed.2004.06.033

Carine Fillebeen, L. D., Marie-Pierre Dehouck, Laurence Fenart, Monique Benaıssa, Genevie`ve Spik, Rome´o Cecchelli, and Annick Pierce. (1999). Receptor-mediated Transcytosis of Lactoferrin through the Blood-Brain Barrier. *J Biol Chem., 274* (11), 7011–7017.

Carmona, J. J., & Michan, S. (2016). Biology of Healthy Aging and Longevity. *Rev Invest Clin, 68*(1), 7-16.

Carpenter, M. K., Parker, I., & Miledi, R. (1992). Messenger RNAs coding for receptors and channels in the cerebral cortex of adult and aged rats. *Brain Res Mol Brain Res, 13*(1-2), 1-5.

Cechetto, D., & Weishaupt, N. (2017). *The cerebral cortex in neurodegenerative and neuropsychiatric disorders: Experimental approaches to clinical issues*. London, UK: Academic Press.

Chamberlain, M. C. (2010). Temozolomide: therapeutic limitations in the treatment of adult high-grade gliomas. *Expert Review of Neurotherapeutics, 10*(10), 1537-1544. doi:10.1586/ern.10.32

Chang, C. H., Horton, J., Schoenfeld, D., Salazer, O., Perez-Tamayo, R., Kramer, S., . . . Tsukada, Y. (1983). Comparison of postoperative radiotherapy and combined postoperative radiotherapy and chemotherapy in the multidisciplinary management of malignant gliomas. A joint Radiation Therapy Oncology Group and Eastern Cooperative Oncology Group study. *Cancer, 52*(6), 997-1007.

Chang, J., Paillard, A., Passirani, C., Morille, M., Benoit, J. P., Betbeder, D., & Garcion, E. (2012). Transferrin adsorption onto PLGA nanoparticles governs their

interaction with biological systems from blood circulation to brain cancer cells. *Pharm Res, 29*(6), 1495-1505. doi:10.1007/s11095-011-0624-1

Chen, L. B. (1988). Mitochondrial membrane potential in living cells. *Annu Rev Cell Biol, 4*, 155-181. doi:10.1146/annurev.cb.04.110188.001103

Chen, P., Miah, M. R., & Aschner, M. (2016). Metals and Neurodegeneration. *F1000Res, 5*. doi:10.12688/f1000research.7431.1

Chen, P. Y., Liu, H. L., Hua, M. Y., Yang, H. W., Huang, C. Y., Chu, P. C., . . . Wei, K. C. (2010). Novel magnetic/ultrasound focusing system enhances nanoparticle drug delivery for glioma treatment. *Neuro Oncol, 12*(10), 1050-1060. doi:10.1093/neuonc/noq054

Cheng, C. W., Adams, G. B., Perin, L., Wei, M., Zhou, X., Lam, B. S., . . . Longo, V. D. (2014). Prolonged fasting reduces IGF-1/PKA to promote hematopoietic-stem-cell-based regeneration and reverse immunosuppression. *Cell Stem Cell, 14*(6), 810-823. doi:10.1016/j.stem.2014.04.014

Choi, I. Y., Lee, C., & Longo, V. D. (2017). Nutrition and fasting mimicking diets in the prevention and treatment of autoimmune diseases and immunosenescence. *Mol Cell Endocrinol, 455*, 4-12. doi:10.1016/j.mce.2017.01.042

Chudotvorova, I., Ivanov, A., Rama, S., Hubner, C. A., Pellegrino, C., Ben-Ari, Y., & Medina, I. (2005). Early expression of KCC2 in rat hippocampal cultures augments expression of functional GABA synapses. *J Physiol, 566*(Pt 3), 671-679. doi:10.1113/jphysiol.2005.089821

Cohen, S. A., & Muller, W. E. (1992). Age-related alterations of NMDA-receptor properties in the mouse forebrain: partial restoration by chronic phosphatidylserine treatment. *Brain Res, 584*(1-2), 174-180.

Costa, L. G. (2017). Overview of Neurotoxicology. *Curr Protoc Toxicol, 74*, 11.11.11-11.11.11. doi:10.1002/cptx.36

Croft, C. L., & Noble, W. (2018). Preparation of organotypic brain slice cultures for the study of Alzheimer's disease. *F1000Res, 7*, 592. doi:10.12688/f1000research.14500.2

Cuervo, A. M., Bergamini, E., Brunk, U. T., Droge, W., Ffrench, M., & Terman, A. (2005). Autophagy and aging: the importance of maintaining "clean" cells. *Autophagy, 1*(3), 131-140.

Damstra, T. (1978). Environmental chemicals and nervous system dysfunction. *Yale J Biol Med, 51*(4), 457-468.

de Cabo, R., Carmona-Gutierrez, D., Bernier, M., Hall, M. N., & Madeo, F. (2014). The search for antiaging interventions: from elixirs to fasting regimens. *Cell, 157*(7), 1515-1526. doi:10.1016/j.cell.2014.05.031

de Grey Aubrey, D. N. J. (2007). Life Span Extension Research and Public Debate: Societal Considerations. *Studies in Ethics, Law, and Technology, 1*(1), 1-13. doi:10.2202/1941-6008.1011

de Lima, A. D., Merten, M. D., & Voigt, T. (1997). Neuritic differentiation and synaptogenesis in serum-free neuronal cultures of the rat cerebral cortex. *J Comp Neurol, 382*(2), 230-246.

De Vita, V. T., Carbone, P. P., Owens, A. H., Gold, G. L., Krant, M. J., & Edmonson, J. (1965). Clinical Trials with 1, 3-Bis(2-chloroethyl)-1-nitrosourea, NSC-409962. *Cancer Research, 25*(11 Part 1), 1876-1881.

Dekaban, A. S. (1978). Changes in brain weights during the span of human life: relation of brain weights to body heights and body weights. *Ann Neurol, 4*(4), 345-356. doi:10.1002/ana.410040410

Demuth, T., & Berens, M. E. (2004). Molecular mechanisms of glioma cell migration and invasion. *J Neurooncol, 70*(2), 217-228.

Dhawan, A., Mathur, N., & Seth, P. K. (2001). The effect of smoking and eating habits on DNA damage in Indian population as measured in the Comet assay. *Mutat Res, 474*(1-2), 121-128.

DiLoreto, R., & Murphy, C. T. (2015). The cell biology of aging. *Mol Biol Cell, 26*(25), 4524-4531. doi:10.1091/mbc.E14-06-1084

Dimri, G. P., Lee, X., Basile, G., Acosta, M., Scott, G., Roskelley, C., . . . et al. (1995). A biomarker that identifies senescent human cells in culture and in aging skin in vivo. *Proc Natl Acad Sci U S A, 92*(20), 9363-9367.

Dinis-Oliveira, R. J., Duarte, J. A., Sanchez-Navarro, A., Remiao, F., Bastos, M. L., & Carvalho, F. (2008). Paraquat poisonings: mechanisms of lung toxicity, clinical features, and treatment. *Crit Rev Toxicol, 38*(1), 13-71. doi:10.1080/10408440701669959

Dinis-Oliveira, R. J., Remiao, F., Carmo, H., Duarte, J. A., Navarro, A. S., Bastos, M. L., & Carvalho, F. (2006). Paraquat exposure as an etiological factor of Parkinson's disease. *Neurotoxicology, 27*(6), 1110-1122. doi:10.1016/j.neuro.2006.05.012

Disterhoft, J. F., Moyer, J. R., Jr., & Thompson, L. T. (1994). The calcium rationale in aging and Alzheimer's disease. Evidence from an animal model of normal aging. *Ann N Y Acad Sci, 747*, 382-406.

Domico, L. M., Cooper, K. R., Bernard, L. P., & Zeevalk, G. D. (2007). Reactive oxygen species generation by the ethylene-bis-dithiocarbamate (EBDC) fungicide mancozeb and its contribution to neuronal toxicity in mesencephalic cells. *Neurotoxicology, 28*(6), 1079-1091. doi:10.1016/j.neuro.2007.04.008

Domingo, J. L. (2003). ALUMINUM (ALUMINIUM) | Toxicology. In B. Caballero (Ed.), *Encyclopedia of Food Sciences and Nutrition (Second Edition)* (pp. 160-166). Oxford: Academic Press.

Duan, W., Guo, Z., Jiang, H., Ware, M., Li, X. J., & Mattson, M. P. (2003). Dietary restriction normalizes glucose metabolism and BDNF levels, slows disease progression, and increases survival in huntingtin mutant mice. *Proc Natl Acad Sci U S A, 100*(5), 2911-2916. doi:10.1073/pnas.0536856100

Duicu, O. M., Mirica, S. N., Gheorgheosu, D. E., Privistirescu, A. I., Fira-Mladinescu, O., & Muntean, D. M. (2013). Ageing-induced decrease in cardiac mitochondrial function in healthy rats. *Can J Physiol Pharmacol, 91*(8), 593-600. doi:10.1139/cjpp-2012-0422

Emaus, R. K., Grunwald, R., & Lemasters, J. J. (1986). Rhodamine 123 as a probe of transmembrane potential in isolated rat-liver mitochondria: spectral and metabolic properties. *Biochim Biophys Acta, 850*(3), 436-448.

Engelhard, H. H. (2000). Tumor bed cyst formation after BCNU wafer implantation: report of two cases. *Surg Neurol, 53*(3), 220-224.

Erdo, S. L., & Wolff, J. R. (1989). Age-related loss of t-[35S]butylbicyclophosphorothionate binding to the gamma-aminobutyric acidA receptor-coupled chloride ionophore in rat cerebral cortex. *J Neurochem, 53*(2), 648-651.

Eskelinen, E. L., & Saftig, P. (2009). Autophagy: a lysosomal degradation pathway with a central role in health and disease. *Biochim Biophys Acta, 1793*(4), 664-673. doi:10.1016/j.bbamcr.2008.07.014

Etame, A. B., Smith, C. A., Chan, W. C., & Rutka, J. T. (2011). Design and potential application of PEGylated gold nanoparticles with size-dependent permeation through brain microvasculature. *Nanomedicine, 7*(6), 992-1000. doi:10.1016/j.nano.2011.04.004

Facci, L., & Skaper, S. D. (2012). Culture of Rodent Cortical and Hippocampal Neurons. In S. D. Skaper (Ed.), *Neurotrophic Factors: Methods and Protocols* (pp. 49-56). Totowa, NJ: Humana Press.

Falace, A., Buhler, E., Fadda, M., Watrin, F., Lippiello, P., Pallesi-Pocachard, E., . . . Cardoso, C. (2014). TBC1D24 regulates neuronal migration and maturation through modulation of the ARF6-dependent pathway. *Proc Natl Acad Sci U S A, 111*(6), 2337-2342. doi:10.1073/pnas.1316294111

Fan, W., Kouda, K., Nakamura, H., & Takeuchi, H. (2001). Effects of dietary restriction on spontaneous dermatitis in NC/Nga mice. *Exp Biol Med (Maywood), 226*(11), 1045-1050.

Fang, J. H., Lai, Y. H., Chiu, T. L., Chen, Y. Y., Hu, S. H., & Chen, S. Y. (2014). Magnetic core-shell nanocapsules with dual-targeting capabilities and co-delivery of multiple drugs to treat brain gliomas. *Adv Healthc Mater, 3*(8), 1250-1260. doi:10.1002/adhm.201300598

Feldman, M. L., & Peters, A. (1998). Ballooning of myelin sheaths in normally aged macaques. *J Neurocytol, 27*(8), 605-614.

Ferroni, L., Gardin, C., Della Puppa, A., Sivolella, S., Brunello, G., Scienza, R., . . . Zavan, B. (2015). Novel Nanotechnologies for Brain Cancer Therapeutics and Imaging. *J Biomed Nanotechnol, 11*(11), 1899-1912.

Fontana, L., & Partridge, L. (2015). Promoting health and longevity through diet: from model organisms to humans. *Cell, 161*(1), 106-118. doi:10.1016/j.cell.2015.02.020

Fontana, L., Partridge, L., & Longo, V. D. (2010). Extending healthy life span--from yeast to humans. *Science, 328*(5976), 321-326. doi:10.1126/science.1172539

Foundas, A. L., Zipin, D., & Browning, C. A. (1998). Age-related changes of the insular cortex and lateral ventricles: conventional MRI volumetric measures. *J Neuroimaging, 8*(4), 216-221.

Freitas, A. A., & de Magalhaes, J. P. (2011). A review and appraisal of the DNA damage theory of ageing. *Mutat Res, 728*(1-2), 12-22. doi:10.1016/j.mrrev.2011.05.001

Freitas, C., Perez, J., Knobel, M., Tormos, J. M., Oberman, L., Eldaief, M., . . . Pascual-Leone, A. (2011). Changes in cortical plasticity across the lifespan. *Frontiers in aging neuroscience, 3*, 5-5. doi:10.3389/fnagi.2011.00005

Fröhlich, F. (2016). Chapter 4 - Synaptic Plasticity. In F. Fröhlich (Ed.), *Network Neuroscience* (pp. 47-58). San Diego: Academic Press.

Gatenby, R. A., & Gillies, R. J. (2004). Why do cancers have high aerobic glycolysis? *Nat Rev Cancer, 4*(11), 891-899. doi:10.1038/nrc1478

Geng, Y. Q., Guan, J. T., Xu, X. H., & Fu, Y. C. (2010). Senescence-associated beta-galactosidase activity expression in aging hippocampal neurons. *Biochem Biophys Res Commun, 396*(4), 866-869. doi:10.1016/j.bbrc.2010.05.011

Ghosh, A., Carnahan, J., & Greenberg, M. E. (1994). Requirement for BDNF in activity-dependent survival of cortical neurons. *Science, 263*(5153), 1618-1623.

Gilmore, J. L., Yi, X., Quan, L., & Kabanov, A. V. (2008). Novel nanomaterials for clinical neuroscience. *Journal of neuroimmune pharmacology : the official journal of the Society on NeuroImmune Pharmacology, 3*(2), 83-94. doi:10.1007/s11481-007-9099-6

Golla, K., Bhaskar, C., Ahmed, F., & Kondapi, A. K. (2013). A target-specific oral formulation of Doxorubicin-protein nanoparticles: efficacy and safety in hepatocellular cancer. *J Cancer, 4*(8), 644-652. doi:10.7150/jca.7093

Grady, C. L. (1998). Brain imaging and age-related changes in cognition. *Exp Gerontol, 33*(7-8), 661-673.

Grandjean, P., & Landrigan, P. J. (2006). Developmental neurotoxicity of industrial chemicals. *Lancet, 368*(9553), 2167-2178. doi:10.1016/s0140-6736(06)69665-7

Grandjean, P., & Landrigan, P. J. (2014). Neurobehavioural effects of developmental toxicity. *Lancet Neurol, 13*(3), 330-338. doi:10.1016/s1474-4422(13)70278-3

Gupta, K. P., Dholaniya, P. S., Chekuri, A., & Kondapi, A. K. (2015). Analysis of gene expression during aging of CGNs in culture: implication of SLIT2 and NPY in senescence. *Age (Dordr), 37*(3), 62. doi:10.1007/s11357-015-9789-6

Gupta, K. P., Swain, U., Rao, K. S., & Kondapi, A. K. (2012). Topoisomerase IIbeta regulates base excision repair capacity of neurons. *Mech Ageing Dev, 133*(4), 203-213. doi:10.1016/j.mad.2012.03.010

Gura, K. M. (2010). Aluminum contamination in products used in parenteral nutrition: has anything changed? *Nutrition, 26*(6), 585-594. doi:10.1016/j.nut.2009.10.015

Guttmann, C. R., Jolesz, F. A., Kikinis, R., Killiany, R. J., Moss, M. B., Sandor, T., & Albert, M. S. (1998). White matter changes with normal aging. *Neurology, 50*(4), 972-978.

Haigis, M. C., & Guarente, L. P. (2006). Mammalian sirtuins--emerging roles in physiology, aging, and calorie restriction. *Genes Dev, 20*(21), 2913-2921. doi:10.1101/gad.1467506

Hanada, S., Fujioka, K., Inoue, Y., Kanaya, F., Manome, Y., & Yamamoto, K. (2014). Cell-based in vitro blood-brain barrier model can rapidly evaluate nanoparticles' brain permeability in association with particle size and surface modification. *Int J Mol Sci, 15*(2), 1812-1825. doi:10.3390/ijms15021812

Haug H, Barmwater U, Eggers R, Fischer D, Kuhel S, & Sass NL. (1983). Anatomical changes in aging brain: morphometric analysis of

the human presencephalon. In Cervos-Navarro J & Sarkander HI (Eds.), *Aging.* (pp. 1-12). New York: Raven Press.

Hayflick, L. (1998). A brief history of the mortality and immortality of cultured cells. *Keio J Med, 47*(3), 174-182.

Hemant, K., Raizaday, A., Sivadasu, P., Uniyal, S., & Kumar, S. H. (2015). Cancer nanotechnology: nanoparticulate drug delivery for the treatment of cancer. *Int J Pharm Pharm Sci, 7*, 40-46.

Ho, K. C., Roessmann, U., Straumfjord, J. V., & Monroe, G. (1980). Analysis of brain weight. I. Adult brain weight in relation to sex, race, and age. *Arch Pathol Lab Med, 104*(12), 635-639.

Holliday, R. (2006). Aging is no longer an unsolved problem in biology. *Ann N Y Acad Sci, 1067*, 1-9. doi:10.1196/annals.1354.002

Huang, D., Wu, S., Hou, X., Jia, L., Meng, Q., Chu, H., . . . Hao, W. (2017). The skeletal developmental toxicity of chlormequat chloride and its underlying mechanisms. *Toxicology, 381*, 1-9. doi:10.1016/j.tox.2017.02.003

Huang, R. Q., Ke, W. L., Qu, Y. H., Zhu, J. H., Pei, Y. Y., & Jiang, C. (2007). Characterization of lactoferrin receptor in brain endothelial capillary cells and mouse brain. *J Biomed Sci, 14*(1), 121-128. doi:10.1007/s11373-006-9121-7

Humpel, C. (2015). Organotypic brain slice cultures: A review. *Neuroscience, 305*, 86-98. doi:10.1016/j.neuroscience.2015.07.086

Hung, C. W., Chen, Y. C., Hsieh, W. L., Chiou, S. H., & Kao, C. L. (2010). Ageing and neurodegenerative diseases. *Ageing Res Rev, 9 Suppl 1*, S36-46. doi:10.1016/j.arr.2010.08.006

Huttenlocher, P. R. (1979). Synaptic density in human frontal cortex - developmental changes and effects of aging. *Brain Res, 163*(2), 195-205.

Hwang, E. S., Yoon, G., & Kang, H. T. (2009). A comparative analysis of the cell biology of senescence and aging. *Cell Mol Life Sci, 66*(15), 2503-2524. doi:10.1007/s00018-009-0034-2

Inan-Eroglu, E., & Ayaz, A. (2018). Is aluminum exposure a risk factor for neurological disorders? *J Res Med Sci, 23*, 51. doi:10.4103/jrms.JRMS_921_17

Invernici, G., Cristini, S., Alessandri, G., Navone, S. E., Canzi, L., Tavian, D., . . . Parati, E. A. (2011). Nanotechnology advances in brain tumors: the state of the art. *Recent Pat Anticancer Drug Discov, 6*(1), 58-69.

Jacobs, B., & Scheibel, A. B. (1993). A quantitative dendritic analysis of Wernicke's area in humans. I. Lifespan changes. *J Comp Neurol, 327*(1), 83-96. doi:10.1002/cne.903270107

Jan H. Nuijens, P. H. C. v. B., and Floyd L. Schanbacher. (1996). Structure and Biological Actions of Lactoferrin. *Journal of Mammary Gland Biology and Neoplasia, 1*(3), 285-295.

Jayasinghe, S., Siriwardhana, A., & Karunaratne, V. (2015). Natural iron sequestering agents: their roles in nature and therapeutic potential. *Int J Pharm Pharm Sci, 7*, 8-12.

Jenkins, S. M., & Barone, S. (2004). The neurotoxicant trimethyltin induces apoptosis via caspase activation, p38 protein kinase, and oxidative stress in PC12 cells. *Toxicol Lett, 147*(1), 63-72.

Jernigan, T. L., Archibald, S. L., Berhow, M. T., Sowell, E. R., Foster, D. S., & Hesselink, J. R. (1991). Cerebral structure on MRI, Part I: Localization of age-related changes. *Biol Psychiatry, 29*(1), 55-67.

Ji, B., Maeda, J., Higuchi, M., Inoue, K., Akita, H., Harashima, H., & Suhara, T. (2006). Pharmacokinetics and brain uptake of lactoferrin in rats. *Life Sci, 78*(8), 851-855. doi:10.1016/j.lfs.2005.05.085

Johnson, K. J. C., Jennifer. Barnholtz-Sloan, Jill S. Ostrom, Quinn T. Langer, Chelsea E. Turner, Michelle C. McKean-Cowdin, Roberta Fisher, James L. Lupo, Philip J. Partap, Sonia Schwartzbaum, Judith A. Scheurer, Michael E. (2014). Childhood Brain Tumor Epidemiology: A Brain Tumor Epidemiology Consortium Review. *Cancer epidemiology, biomarkers & prevention : a publication of the American Association for Cancer Research, cosponsored by the American Society of Preventive Oncology, 23*(12), 2716-2736. doi:10.1158/1055-9965.EPI-14-0207

Kaech, S., & Banker, G. (2006). Culturing hippocampal neurons. *Nat Protoc, 1*(5), 2406-2415. doi:10.1038/nprot.2006.356

Kanwar, J. R., Sriramoju, B., & Kanwar, R. K. (2012). Neurological disorders and therapeutics targeted to surmount the blood-brain barrier. *Int J Nanomedicine, 7*, 3259-3278. doi:10.2147/ijn.s30919

Katewa, S. D., & Kapahi, P. (2010). Dietary restriction and aging, 2009. *Aging Cell, 9*(2), 105-112. doi:10.1111/j.1474-9726.2010.00552.x

Kaur, I. P., Bhandari, R., Bhandari, S., & Kakkar, V. (2008). Potential of solid lipid nanoparticles in brain targeting. *J Control Release, 127*(2), 97-109. doi:10.1016/j.jconrel.2007.12.018

Khanbabaie, R., & Jahanshahi, M. (2012). Revolutionary impact of nanodrug delivery on neuroscience. *Curr Neuropharmacol, 10*(4), 370-392. doi:10.2174/157015912804143513

King, S. W., Savory, J., & Wills, M. R. (1981). Aluminum toxicity in relation to kidney disorders. *Ann Clin Lab Sci, 11*(4), 337-342.

Kitamura, I., Kochi, M., Matsumoto, Y., Ueoka, R., Kuratsu, J., & Ushio, Y. (1996). Intrathecal chemotherapy with 1,3-bis(2-chloroethyl)-1-nitrosourea encapsulated into hybrid liposomes for meningeal gliomatosis: an experimental study. *Cancer Res, 56*(17), 3986-3992.

Kito, S., Miyoshi, R., & Nomoto, T. (1990). Influence of age on NMDA receptor complex in rat brain studied by in vitro autoradiography. *J Histochem Cytochem, 38*(12), 1725-1731. doi:10.1177/38.12.2147708

Kleinberg, L. R., Weingart, J., Burger, P., Carson, K., Grossman, S. A., Li, K., . . . Brem, H. (2004). Clinical course and pathologic findings after Gliadel and radiotherapy for newly diagnosed malignant glioma: implications for patient management. *Cancer Invest, 22*(1), 1-9.

Klionsky, D. J., & Emr, S. D. (2000). Autophagy as a regulated pathway of cellular degradation. *Science, 290*(5497), 1717-1721.

Kondapi, A. K., Mulpuri, N., Mandraju, R. K., Sasikaran, B., & Subba Rao, K. (2004). Analysis of age dependent changes of Topoisomerase II alpha and beta in rat brain. *Int J Dev Neurosci, 22*(1), 19-30. doi:10.1016/j.ijdevneu.2003.10.006

Kouda, K., & Iki, M. (2010). Beneficial effects of mild stress (hormetic effects): dietary restriction and health. *J Physiol Anthropol, 29*(4), 127-132.

Krishna, A. D., Mandraju, R. K., Kishore, G., & Kondapi, A. K. (2009). An efficient targeted drug delivery through apotransferrin loaded nanoparticles. *PLoS One, 4*(10), e7240. doi:10.1371/journal.pone.0007240

Krupa, P., Rehak, S., Diaz-Garcia, D., & Filip, S. (2014). NANOTECHNOLOGY - NEW TRENDS IN THE TREATMENT OF BRAIN TUMOURS. *Acta Medica (Hradec Kralove), 57*(4), 142-150. doi:10.14712/18059694.2015.79

Kumari, S., & Kondapi, A. K. (2017). Lactoferrin nanoparticle mediated targeted delivery of 5-fluorouracil for enhanced therapeutic efficacy. *Int J Biol Macromol, 95*, 232-237. doi:10.1016/j.ijbiomac.2016.10.110

Lakshmi, Y. S., Kumar, P., Kishore, G., Bhaskar, C., & Kondapi, A. K. (2016). Triple combination MPT vaginal microbicide using curcumin and efavirenz loaded lactoferrin nanoparticles. *Scientific Reports, 6*, 25479. doi:10.1038/srep25479

Landrigan, P. J., Lambertini, L., & Birnbaum, L. S. (2012). A research strategy to discover the environmental causes of autism and neurodevelopmental disabilities. *Environ Health Perspect, 120*(7), a258-260. doi:10.1289/ehp.1104285

Lee, C., & Longo, V. (2016). Dietary restriction with and without caloric restriction for healthy aging. *F1000Res, 5*. doi:10.12688/f1000research.7136.1

Lee, J., Kim, S. J., Son, T. G., Chan, S. L., & Mattson, M. P. (2006). Interferon-gamma is up-regulated in the hippocampus in response to intermittent fasting and protects hippocampal neurons against excitotoxicity. *J Neurosci Res, 83*(8), 1552-1557. doi:10.1002/jnr.20831

Lesuisse, C., & Martin, L. J. (2002). Long-term culture of mouse cortical neurons as a model for neuronal development, aging, and death. *J Neurobiol, 51*(1), 9-23.

Lesuisse, C., Qiu, D., Bose, C. M., Nakaso, K., & Rupp, F. (2000). Regulation of agrin expression in hippocampal neurons by cell contact and electrical activity. *Brain Res Mol Brain Res, 81*(1-2), 92-100.

Levine, M. E., Suarez, J. A., Brandhorst, S., Balasubramanian, P., Cheng, C. W., Madia, F., . . . Longo, V. D. (2014). Low protein intake is associated with a major reduction

in IGF-1, cancer, and overall mortality in the 65 and younger but not older population. *Cell Metab, 19*(3), 407-417. doi:10.1016/j.cmet.2014.02.006

Lin, S. H., & Kleinberg, L. R. (2008). Carmustine wafers: localized delivery of chemotherapeutic agents in CNS malignancies. *Expert Rev Anticancer Ther, 8*(3), 343-359. doi:10.1586/14737140.8.3.343

Lindh, C. H., Littorin, M., Johannesson, G., & Jonsson, B. A. (2011). Analysis of chlormequat in human urine as a biomarker of exposure using liquid chromatography triple quadrupole mass spectrometry. *J Chromatogr B Analyt Technol Biomed Life Sci, 879*(19), 1551-1556. doi:10.1016/j.jchromb.2011.03.046

Lindsay, R. M. (1994). Neurotrophins and receptors. *Prog Brain Res, 103*, 3-14.

Liu, Y., Han, M., Li, X., Wang, H., Ma, M., Zhang, S., . . . Yao, Y. (2017). Age-related changes in the mitochondria of human mural granulosa cells. *Hum Reprod, 32*(12), 2465-2473. doi:10.1093/humrep/dex309

Lockman, P. R., Mumper, R. J., Khan, M. A., & Allen, D. D. (2002). Nanoparticle technology for drug delivery across the blood-brain barrier. *Drug Dev Ind Pharm, 28*(1), 1-13. doi:10.1081/ddc-120001481

Longo, V. D., Antebi, A., Bartke, A., Barzilai, N., Brown-Borg, H. M., Caruso, C., . . . Fontana, L. (2015). Interventions to Slow Aging in Humans: Are We Ready? *Aging Cell, 14*(4), 497-510. doi:10.1111/acel.12338

Longo, V. D., & Mattson, M. P. (2014). Fasting: molecular mechanisms and clinical applications. *Cell Metab, 19*(2), 181-192. doi:10.1016/j.cmet.2013.12.008

Lopez-Lluch, G., & Navas, P. (2016). Calorie restriction as an intervention in ageing. *J Physiol, 594*(8), 2043-2060. doi:10.1113/jp270543

Lopez-Otin, C., Blasco, M. A., Partridge, L., Serrano, M., & Kroemer, G. (2013). The hallmarks of aging. *Cell, 153*(6), 1194-1217. doi:10.1016/j.cell.2013.05.039

Louis DN, O. H., Wiestler OD, Cavenee WK, Burger PC, Jouvet A, Scheithauer BW, Kleihues P. (2007). The 2007 WHO classification of tumours of the central nervous system. *Acta Neuropathol, 114*, 97–109.

MacPhail, R. C. (1992). Principles of identifying and characterizing neurotoxicity. *Toxicol Lett, 64-65 Spec No*, 209-215.

Mandraju, R., Chekuri, A., Bhaskar, C., Duning, K., Kremerskothen, J., & Kondapi, A. K. (2011). Topoisomerase IIbeta associates with Ku70 and PARP-1 during double strand break repair of DNA in neurons. *Arch Biochem Biophys, 516*(2), 128-137. doi:10.1016/j.abb.2011.10.001

Mandraju, R. K., Kannapiran, P., & Kondapi, A. K. (2008). Distinct roles of Topoisomerase II isoforms: DNA damage accelerating alpha, double strand break repair promoting beta. *Arch Biochem Biophys, 470*(1), 27-34. doi:10.1016/j.abb.2007.10.017

Mandraju, R. K., & Kondapi, A. K. (2007). Regulation of topoisomerase II alpha and beta in HIV-1 infected and uninfected neuroblastoma and astrocytoma cells: involvement of distinct nordihydroguaretic acid sensitive inflammatory pathways. *Arch Biochem Biophys, 461*(1), 40-49. doi:10.1016/j.abb.2007.01.026

Marti-Nicolovius, M., & Arevalo-Garcia, R. (2018). [Caloric restriction and memory during aging]. *Rev Neurol, 66*(12), 415-422.

Martin, B., Mattson, M. P., & Maudsley, S. (2006). Caloric restriction and intermittent fasting: two potential diets for successful brain aging. *Ageing Res Rev, 5*(3), 332-353. doi:10.1016/j.arr.2006.04.002

Martini, F. H. (2007). *Anatomy and Physiology*. Quezon (PH): Rex Bookstore, Inc.

Masserini, M. (2013a). Nanoparticles for brain drug delivery. *ISRN Biochem, 2013*, 238428. doi:10.1155/2013/238428

Masserini, M. (2013b). Nanoparticles for brain drug delivery. *ISRN Biochem, 2013*, 1-18. doi:10.1155/2013/238428

Mattson, M. P. (2005). Energy intake, meal frequency, and health: a neurobiological perspective. *Annu Rev Nutr, 25*, 237-260. doi:10.1146/annurev.nutr.25.050304.092526

Mattson, M. P., Longo, V. D., & Harvie, M. (2017). Impact of intermittent fasting on health and disease processes. *Ageing Res Rev, 39*, 46-58. doi:10.1016/j.arr.2016.10.005

McGonigle, R. J., & Parsons, V. (1985). Aluminium-induced anaemia in haemodialysis patients. *Nephron, 39*(1), 1-9. doi:10.1159/000183328

McGovern, P. C., Lautenbach, E., Brennan, P. J., Lustig, R. A., & Fishman, N. O. (2003). Risk factors for postcraniotomy surgical site infection after 1,3-bis (2-chloroethyl)-1-nitrosourea (Gliadel) wafer placement. *Clin Infect Dis, 36*(6), 759-765. doi:10.1086/368082

Meberg, P. J., & Miller, M. W. (2003). *Culturing Hippocampal and Cortical Neurons.* Vol. 71. *Methods Cell Biol* (pp. 111-127). Retrieved from http://www.sciencedirect.com/science/article/pii/S0091679X03010070 doi:https://doi.org/10.1016/S0091-679X(03)01007-0

Mera, S. L. (1992). Senescence and pathology in ageing. *Med Lab Sci, 49*(4), 271-282.

Mercken, E. M., Carboneau, B. A., Krzysik-Walker, S. M., & de Cabo, R. (2012). Of mice and men: the benefits of caloric restriction, exercise, and mimetics. *Ageing Res Rev, 11*(3), 390-398. doi:10.1016/j.arr.2011.11.005

Messaoudi, I., Warner, J., Fischer, M., Park, B., Hill, B., Mattison, J., . . . Nikolich-Zugich, J. (2006). Delay of T cell senescence by caloric restriction in aged long-lived nonhuman primates. *Proc Natl Acad Sci U S A, 103*(51), 19448-19453. doi:10.1073/pnas.0606661103

Mhatre, M. C., Fernandes, G., & Ticku, M. K. (1991). Aging reduces the mRNA of alpha 1 GABAA receptor subunit in rat cerebral cortex. *Eur J Pharmacol, 208*(2), 171-174.

Miodovnik, A. (2011). Environmental neurotoxicants and developing brain. *Mt Sinai J Med, 78*(1), 58-77. doi:10.1002/msj.20237

Mirzaei, H., Suarez, J. A., & Longo, V. D. (2014). Protein and amino acid restriction, aging and disease: from yeast to humans. *Trends Endocrinol Metab, 25*(11), 558-566. doi:10.1016/j.tem.2014.07.002

Monnet-Tschudi, F., Zurich, M. G., Boschat, C., Corbaz, A., & Honegger, P. (2006). Involvement of environmental mercury and lead in the etiology of neurodegenerative diseases. *Rev Environ Health, 21*(2), 105-117.

Moreno-Exposito, L., Illescas-Montes, R., Melguizo-Rodriguez, L., Ruiz, C., Ramos-Torrecillas, J., & de Luna-Bertos, E. (2018). Multifunctional capacity and therapeutic potential of lactoferrin. *Life Sci, 195*, 61-64. doi:10.1016/j.lfs.2018.01.002

Mosmann, T. (1983). Rapid colorimetric assay for cellular growth and survival: application to proliferation and cytotoxicity assays. *J Immunol Methods, 65*(1-2), 55-63.

Mouton, P. R., Martin, L. J., Calhoun, M. E., Dal Forno, G., & Price, D. L. (1998). Cognitive decline strongly correlates with cortical atrophy in Alzheimer's dementia. *Neurobiol Aging, 19*(5), 371-377.

Nakamura, H., Kouda, K., Tokunaga, R., & Takeuchi, H. (2004). Suppressive effects on delayed type hypersensitivity by fasting and dietary restriction in ICR mice. *Toxicol Lett, 146*(3), 259-267.

National Institute of Neurological Disorders and Stroke. (2019, March 27). Neurotoxicity information page. Retrieved from https://www.ninds.nih.gov/Disorders/All-Disorders/Neurotoxicity-Information-Page

Nicholls, D. G. (2004). Mitochondrial membrane potential and aging. *Aging Cell, 3*(1), 35-40. doi:10.1111/j.1474-9728.2003.00079.x

Nikoletopoulou, V., & Tavernarakis, N. (2012). Calcium homeostasis in aging neurons. *Front Genet, 3*, 200. doi:10.3389/fgene.2012.00200

O'Driscoll, B. R., Kalra, S., Gattamaneni, H. R., & Woodcock, A. A. (1995). Late Carmustine Lung Fibrosis. *CHEST, 107*(5), 1355-1357. doi:10.1378/chest.107.5.1355

Olivi, A., Grossman, S. A., Tatter, S., Barker, F., Judy, K., Olsen, J., . . . Piantadosi, S. (2003). Dose escalation of carmustine in surgically implanted polymers in patients with recurrent malignant glioma: a New Approaches to Brain Tumor Therapy CNS Consortium trial. *J Clin Oncol, 21*(9), 1845-1849. doi:10.1200/jco.2003.09.041

Olivier, J. C. (2005). Drug transport to brain with targeted nanoparticles. *NeuroRx, 2*(1), 108-119. doi:10.1602/neurorx.2.1.108

Olivieri, G., Brack, C., Muller-Spahn, F., Stahelin, H. B., Herrmann, M., Renard, P., . . . Hock, C. (2000). Mercury induces cell cytotoxicity and oxidative stress and increases beta-amyloid secretion and tau phosphorylation in SHSY5Y neuroblastoma cells. *J Neurochem, 74*(1), 231-236.

Olshansky, S. J., & Carnes, B. A. (1997). Ever since Gompertz. *Demography, 34*(1), 1-15.

Omuro, A., & DeAngelis, L. M. (2013). Glioblastoma and other malignant gliomas: A clinical review. *JAMA, 310*(17), 1842-1850. doi:10.1001/jama.2013.280319

OpenStax. (2016, May 27). Neurons and glial cells [Online image]. Retrieved from http://cnx.org/contents/185cbf87-c72e-48f5-b51e-f14f21b5eabd@10.61.

Ostrom, Q. T., Bauchet, L., Davis, F. G., Deltour, I., Fisher, J. L., Langer, C. E., . . . Barnholtz-Sloan, J. S. (2014). The epidemiology of glioma in adults: a "state of the science" review. *Neuro-Oncology, 16*(7), 896-913. doi:10.1093/neuonc/nou087

Ostrom, Q. T., Gittleman, H., Liao, P., Vecchione-Koval, T., Wolinsky, Y., Kruchko, C., & Barnholtz-Sloan, J. S. (2017). CBTRUS Statistical Report: Primary brain and other central nervous system tumors diagnosed in the United States in 2010-2014. *Neuro Oncol, 19*(suppl_5), v1-v88. doi:10.1093/neuonc/nox158

Ottavio Arancio, Bezprozvanny, Ilya, Theodore Berger, Jean-Marie Bouteiller, Maria Carrillo, . . . Khachaturian., Z. (2017). Calcium Hypothesis of Alzheimer's disease and brain aging: A framework for integrating new evidence into a comprehensive theory of pathogenesis. *Alzheimers Dement, 13*(2), 178-182.e117. doi:10.1016/j.jalz.2016.12.006

Ou, Y., Dong, X., Liu, X. Y., Cheng, X. C., Cheng, Y. N., Yu, L. G., & Guo, X. L. (2010). Mechanism of tetramethylpyrazine analogue CXC195 inhibition of hydrogen peroxide-induced apoptosis in human endothelial cells. *Biol Pharm Bull, 33*(3), 432-438.

Pani, G. (2015). Neuroprotective effects of dietary restriction: Evidence and mechanisms. *Semin Cell Dev Biol, 40*, 106-114. doi:10.1016/j.semcdb.2015.03.004

Park, D. C., & Yeo, S. G. (2013). Aging. *Korean journal of audiology, 17*(2), 39-44. doi:10.7874/kja.2013.17.2.39

Patel, M. A., Kim, J. E., Ruzevick, J., Li, G., & Lim, M. (2014). The Future of Glioblastoma Therapy: Synergism of Standard of Care and Immunotherapy. *Cancers, 6*(4), 1953-1985. doi:10.3390/cancers6041953

Pathan, S. A., Iqbal, Z., Zaidi, S. M., Talegaonkar, S., Vohra, D., Jain, G. K., . . . Ahmad, F. J. (2009). CNS drug delivery systems: novel approaches. *Recent Pat Drug Deliv Formul, 3*(1), 71-89.

Pawelec, G., Rehbein, A., Haehnel, K., Merl, A., & Adibzadeh, M. (1997). Human T-cell clones in long-term culture as a model of immunosenescence. *Immunol Rev, 160*, 31-42.

Perry, S. W., Norman, J. P., Barbieri, J., Brown, E. B., & Gelbard, H. A. (2011). Mitochondrial membrane potential probes and the proton gradient: a practical usage guide. *Biotechniques, 50*(2), 98-115. doi:10.2144/000113610

Peters, A., Moss, M. B., & Sethares, C. (2000). Effects of aging on myelinated nerve fibers in monkey primary visual cortex. *J Comp Neurol, 419*(3), 364-376.

Pogue, A. I., & Lukiw, W. J. (2016). Natural and Synthetic Neurotoxins in Our Environment: From Alzheimer's Disease (AD) to Autism Spectrum Disorder (ASD). *J Alzheimers Dis Parkinsonism, 6*(4). doi:10.4172/2161-0460.1000249

Purves, D., Augustine, G. J., Fitzpatrick, D., Katz, L. C., LaMantia, A.-S., McNamara, J. O., & Williams, S. M. (2001). *Neuroscience*. Sunderland (MA): Sinauer Associates.

Pyo, J. O., Yoo, S. M., Ahn, H. H., Nah, J., Hong, S. H., Kam, T. I., . . . Jung, Y. K. (2013). Overexpression of Atg5 in mice activates autophagy and extends lifespan. *Nat Commun, 4*, 2300. doi:10.1038/ncomms3300

Quirk, B. J., Brandal, G., Donlon, S., Vera, J. C., Mang, T. S., Foy, A. B., . . . Whelan, H. T. (2015). Photodynamic therapy (PDT) for malignant brain tumors – Where do we stand? *Photodiagnosis and Photodynamic Therapy, 12*(3), 530-544. doi:https://doi.org/10.1016/j.pdpdt.2015.04.009

Rademacher, W., & Brahm, L. (2010). Plant Growth Regulators. *In Ullmann's Encyclopedia of Industrial Chemistry, (Ed.).*

Rattan, S. I. (2000). Biogerontology: the next step. *Ann N Y Acad Sci, 908*, 282-290.

Raz, N., Briggs, S. D., Marks, W., & Acker, J. D. (1999). Age-related deficits in generation and manipulation of mental images: II. The role of dorsolateral prefrontal cortex. *Psychol Aging, 14*(3), 436-444. doi:10.1037/0882-7974.14.3.436

Raz, N., Lindenberger, U., Rodrigue, K. M., Kennedy, K. M., Head, D., Williamson, A., . . . Acker, J. D. (2005). Regional brain changes in aging healthy adults: general trends, individual differences and modifiers. *Cereb Cortex, 15*(11), 1676-1689. doi:10.1093/cercor/bhi044

Rempe, R., Cramer, S., Qiao, R., & Galla, H.-J. (2014). Strategies to overcome the barrier: use of nanoparticles as carriers and modulators of barrier properties. *Cell and Tissue Research, 355*(3), 717-726. doi:10.1007/s00441-014-1819-7

Robberecht, W., & Philips, T. (2013). The changing scene of amyotrophic lateral sclerosis. *Nat Rev Neurosci, 14*(4), 248-264. doi:10.1038/nrn3430

Rosas, H. D., Salat, D. H., Lee, S. Y., Zaleta, A. K., Pappu, V., Fischl, B., . . . Hersch, S. M. (2008). Cerebral cortex and the clinical expression of Huntington's disease: complexity and heterogeneity. *Brain, 131*(Pt 4), 1057-1068. doi:10.1093/brain/awn025

Ross, C. A., & Poirier, M. A. (2004). Protein aggregation and neurodegenerative disease. *Nat Med, 10 Suppl*, S10-17. doi:10.1038/nm1066

Ruirui Qiao, Q. J., Sabine Huwel, Rui Xia, Ting Liu, Fabao Gao, Hans-Joachim Galla, and Mingyuan Gao. (2012). Receptor-Mediated Delivery of Magnetic Nanoparticles across the Blood Brain Barrier. *ACS Nano, 6* (4), 3304-3310. doi:10.1021/nn300240p

Russo-Neustadt, A. (2003). Brain-derived neurotrophic factor, behavior, and new directions for the treatment of mental disorders. *Semin Clin Neuropsychiatry, 8*(2), 109-118. doi:10.1053/scnp.2003.50014

Sagar, G. R. (1987). Uses and usefulness of paraquat. *Hum Toxicol, 6*(1), 7-11.

Sanada, F., Taniyama, Y., Muratsu, J., Otsu, R., Shimizu, H., Rakugi, H., & Morishita, R. (2018). Source of Chronic Inflammation in Aging. *Front Cardiovasc Med, 5*, 12. doi:10.3389/fcvm.2018.00012

Sánchez, L., Calvo, M., & Brock, J. H. (1992). Biological role of lactoferrin. *Archives of Disease in Childhood, 67*(5), 657-661.

Saraswat, K., & Rizvi, S. I. (2017). Novel strategies for anti-aging drug discovery. *Expert Opin Drug Discov, 12*(9), 955-966. doi:10.1080/17460441.2017.1349750

Sarkar, A., Fatima, I., Jamal, Q. M. S., Sayeed, U., Khan, M. K. A., Akhtar, S., . . . Siddiqui, M. H. (2017). Nanoparticles as a Carrier System for Drug Delivery Across Blood Brain Barrier. *Curr Drug Metab, 18*(2), 129-137. doi:10.2174/1389200218666170113125132

Sarkaria, J. N., Kitange, G. J., James, C. D., Plummer, R., Calvert, H., Weller, M., & Wick, W. (2008). Mechanisms of Chemoresistance in Malignant Glioma. *Clinical cancer research : an official journal of the American Association for Cancer Research, 14*(10), 2900-2908. doi:10.1158/1078-0432.CCR-07-1719

Sastre, J., Millan, A., Garcia de la Asuncion, J., Pla, R., Juan, G., Pallardo, . . . Vina, J. (1998). A Ginkgo biloba extract (EGb 761) prevents mitochondrial aging by protecting against oxidative stress. *Free Radic Biol Med, 24*(2), 298-304.

Scheibel, M. E., Lindsay, R. D., Tomiyasu, U., & Scheibel, A. B. (1975). Progressive dendritic changes in aging human cortex. *Exp Neurol, 47*(3), 392-403.

Schmid, C., & Rotenberg, J. S. (2005). Neurodevelopmental toxicology. *Neurol Clin, 23*(2), 321-336. doi:10.1016/j.ncl.2004.12.010

Schmittgen, T. D., & Livak, K. J. (2008). Analyzing real-time PCR data by the comparative C(T) method. *Nat Protoc, 3*(6), 1101-1108.

Selker, R. G., Shapiro, W. R., Burger, P., Blackwood, M. S., Arena, V. C., Gilder, J. C., . . . Green, S. (2002). The Brain Tumor Cooperative Group NIH Trial 87-01: a randomized comparison of surgery, external radiotherapy, and carmustine versus surgery, interstitial radiotherapy boost, external radiation therapy, and carmustine. *Neurosurgery, 51*(2), 343-355; discussion 355-347.

Semsei, I. (2000). On the nature of aging. *Mech Ageing Dev, 117*(1-3), 93-108.

Serviddio, G., Bellanti, F., Romano, A. D., Tamborra, R., Rollo, T., Altomare, E., & Vendemiale, G. (2007). Bioenergetics in aging: mitochondrial proton leak in

aging rat liver, kidney and heart. *Redox Rep, 12*(1), 91-95. doi:10.1179/135100007x162112

Shan, Z. Y., Liu, J. Z., Sahgal, V., Wang, B., & Yue, G. H. (2005). Selective atrophy of left hemisphere and frontal lobe of the brain in old men [Image]. *J Gerontol A Biol Sci Med Sci, 60*(2), 165-174.

Sharma, A., & Sharma, U. S. (1997). Liposomes in drug delivery: Progress and limitations. *International Journal of Pharmaceutics, 154*(2), 123-140. doi:https://doi.org/10.1016/S0378-5173(97)00135-X

Shaw, A. R., & Feinberg, M. B. (2008). 92 - Vaccines. In R. R. Rich, T. A. Fleisher, W. T. Shearer, H. W. Schroeder, A. J. Frew, & C. M. Weyand (Eds.), *Clinical Immunology (Third Edition)* (pp. 1353-1382). Edinburgh: Mosby.

Shaw, C. A., & Tomljenovic, L. (2013). Aluminum in the central nervous system (CNS): toxicity in humans and animals, vaccine adjuvants, and autoimmunity. *Immunol Res, 56*(2-3), 304-316. doi:10.1007/s12026-013-8403-1

Shome, D., Poddar, N., Sharma, V., Sheorey, U., Maru, G. B., Ingle, A., . . . Bellare, J. (2009). Does a Nanomolecule of Carboplatin Injected Periocularly Help in Attaining Higher Intravitreal Concentrations? *Investigative Ophthalmology & Visual Science, 50*(12), 5896-5900. doi:10.1167/iovs.09-3914

Silva, R. F., Falcao, A. S., Fernandes, A., Gordo, A. C., Brito, M. A., & Brites, D. (2006). Dissociated primary nerve cell cultures as models for assessment of neurotoxicity. *Toxicol Lett, 163*(1), 1-9. doi:10.1016/j.toxlet.2005.09.033

Singh, R., Kaushik, S., Wang, Y., Xiang, Y., Novak, I., Komatsu, M., . . . Czaja, M. J. (2009). Autophagy regulates lipid metabolism. *Nature, 458*(7242), 1131-1135. doi:10.1038/nature07976

Smeyne, R. J., & Jackson-Lewis, V. (2005). The MPTP model of Parkinson's disease. *Brain Res Mol Brain Res, 134*(1), 57-66. doi:10.1016/j.molbrainres.2004.09.017

Smirnova, L., Hogberg, H. T., Leist, M., & Hartung, T. (2014). Developmental neurotoxicity - challenges in the 21st century and in vitro opportunities. *Altex, 31*(2), 129-156. doi:10.14573/altex.1403271

Solon-Biet, S. M., McMahon, A. C., Ballard, J. W., Ruohonen, K., Wu, L. E., Cogger, V. C., . . . Simpson, S. J. (2014). The ratio of macronutrients, not caloric intake, dictates cardiometabolic health, aging, and longevity in ad libitum-fed mice. *Cell Metab, 19*(3), 418-430. doi:10.1016/j.cmet.2014.02.009

Sonavane, G., Tomoda, K., & Makino, K. (2008). Biodistribution of colloidal gold nanoparticles after intravenous administration: effect of particle size. *Colloids Surf B Biointerfaces, 66*(2), 274-280. doi:10.1016/j.colsurfb.2008.07.004

Sorensen, M. T., & Danielsen, V. (2006). Effects of the plant growth regulator, chlormequat, on mammalian fertility. *Int J Androl, 29*(1), 129-133. doi:10.1111/j.1365-2605.2005.00629.x

Spriggs, M. J., Cadwallader, C. J., Hamm, J. P., Tippett, L. J., & Kirk, I. J. (2017). Age-related alterations in human neocortical plasticity. *Brain Res Bull, 130*, 53-59. doi:10.1016/j.brainresbull.2016.12.015

Stenehjem, D. D., Hartz, A. M., Bauer, B., & Anderson, G. W. (2009). Novel and emerging strategies in drug delivery for overcoming the blood-brain barrier. *Future Med Chem, 1*(9), 1623-1641. doi:10.4155/fmc.09.137

Stupp, R., Mason, W. P., van den Bent, M. J., Weller, M., Fisher, B., Taphoorn, M. J., . . . Mirimanoff, R. O. (2005). Radiotherapy plus concomitant and adjuvant temozolomide for glioblastoma. *N Engl J Med, 352*(10), 987-996. doi:10.1056/NEJMoa043330

Subach, B. R., Witham, T. F., Kondziolka, D., Lunsford, L. D., Bozik, M., & Schiff, D. (1999). Morbidity and survival after 1,3-bis(2-chloroethyl)-1-nitrosourea wafer implantation for recurrent glioblastoma: a retrospective case-matched cohort series. *Neurosurgery, 45*(1), 17-22; discussion 22-13.

Swain, U., & Subba Rao, K. (2011). Study of DNA damage via the comet assay and base excision repair activities in rat brain neurons and astrocytes during aging. *Mech Ageing Dev, 132*(8-9), 374-381. doi:10.1016/j.mad.2011.04.012

Swaminathan, S. (2013). Chapter 23 - Trace Elements, Toxic Metals, and Metalloids in Kidney Disease. In J. D. Kopple, S. G. Massry, & K. Kalantar-Zadeh (Eds.), *Nutritional Management of Renal Disease* (pp. 339-349): Academic Press.

Tajes, M., Ramos-Fernandez, E., Weng-Jiang, X., Bosch-Morato, M., Guivernau, B., Eraso-Pichot, A., . . . Munoz, F. J. (2014). The blood-brain barrier: structure, function and therapeutic approaches to cross it. *Mol Membr Biol, 31*(5), 152-167. doi:10.3109/09687688.2014.937468

Talukder, M. J., Takeuchi, T., & Harada, E. (2003). Characteristics of lactoferrin receptor in bovine intestine: higher binding activity to the epithelium overlying Peyer's patches. *J Vet Med A Physiol Pathol Clin Med, 50*(3), 123-131.

Tapeinos, C., Battaglini, M., & Ciofani, G. (2017). Advances in the design of solid lipid nanoparticles and nanostructured lipid carriers for targeting brain diseases. *J Control Release, 264*, 306-332. doi:10.1016/j.jconrel.2017.08.033

Thissen, J. P., Ketelslegers, J. M., & Underwood, L. E. (1994). Nutritional regulation of the insulin-like growth factors. *Endocr Rev, 15*(1), 80-101. doi:10.1210/edrv-15-1-80

Tilson, H. A. (1999). Overview of Neurotoxicology. *Curr Protoc Toxicol, 00*(1), 11.11.11-11.11.18. doi:10.1002/0471140856.tx1101s06

Tilson, H. A. (2000). Neurotoxicology risk assessment guidelines: developmental neurotoxicology. *Neurotoxicology, 21*(1-2), 189-194.

Timiras, P. S., Hudson, D. B., & Oklund, S. (1973). Changes in Central Nervous System Free Amino Acids with Development and Aging. In D. H. Ford (Ed.), *Prog Brain Res* (Vol. 40, pp. 267-275): Elsevier.

Tortora, G. J., & Derrickson, B. (2011). *Principles of anatomy & physiology* (Vol. 1). Hoboken (NJ): John Wiley & Sons, Inc

Tosato, M., Zamboni, V., Ferrini, A., & Cesari, M. (2007). The aging process and potential interventions to extend life expectancy. *Clin Interv Aging, 2*(3), 401-412.

Toxicology, N. R. C. C. o. D. (2000) *Scientific Frontiers in Developmental Toxicology and Risk Assessment*. Washington, DC, US: National Academies Press.

Troen, B. R. (2003). The biology of aging. *Mt Sinai J Med, 70*(1), 3-22.

Tsai, K., Hsu, T. G., Lu, F. J., Hsu, C. F., Liu, T. Y., & Kong, C. W. (2001). Age-related changes in the mitochondrial depolarization induced by oxidative injury in human peripheral blood leukocytes. *Free Radic Res, 35*(4), 395-403.

Tsai, W.-T. (2013). A review on environmental exposure and health risks of herbicide paraquat. *Toxicological & Environmental Chemistry, 95*(2), 197-206. doi:10.1080/02772248.2012.761999

Tsunoda, M., & Sharma, R. P. (1999a). Altered dopamine turnover in murine hypothalamus after low-dose continuous oral administration of aluminum. *J Trace Elem Med Biol, 13*(4), 224-231. doi:10.1016/s0946-672x(99)80040-6

Tsunoda, M., & Sharma, R. P. (1999b). Modulation of tumor necrosis factor alpha expression in mouse brain after exposure to aluminum in drinking water. *Arch Toxicol, 73*(8-9), 419-426.

Uskoković, V. (2012). Dynamic Light Scattering Based Microelectrophoresis: Main Prospects and Limitations. *Journal of dispersion science and technology, 33*(12), 1762-1786. doi:10.1080/01932691.2011.625523

Uversky, V. N., Li, J., & Fink, A. L. (2001a). Metal-triggered structural transformations, aggregation, and fibrillation of human alpha-synuclein. A possible molecular NK between Parkinson's disease and heavy metal exposure. *J Biol Chem, 276*(47), 44284-44296. doi:10.1074/jbc.M105343200

Uversky, V. N., Li, J., & Fink, A. L. (2001b). Pesticides directly accelerate the rate of alpha-synuclein fibril formation: a possible factor in Parkinson's disease. *FEBS Lett, 500*(3), 105-108.

Vaughan, D. W. (1977). Age-related deterioration of pyramidal cell basal dendrites in rat auditory cortex. *J Comp Neurol, 171*(4), 501-515. doi:10.1002/cne.901710406

Vellai, T., & Takacs-Vellai, K. (2010). Regulation of protein turnover by longevity pathways. *Adv Exp Med Biol, 694*, 69-80.

Vera-Lastra, O., Medina, G., Cruz-Dominguez Mdel, P., Jara, L. J., & Shoenfeld, Y. (2013). Autoimmune/inflammatory syndrome induced by adjuvants (Shoenfeld's syndrome): clinical and immunological spectrum. *Expert Rev Clin Immunol, 9*(4), 361-373. doi:10.1586/eci.13.2

Vinogradov, S. V., Batrakova, E. V., & Kabanov, A. V. (2004). Nanogels for oligonucleotide delivery to the brain. *Bioconjug Chem, 15*(1), 50-60. doi:10.1021/bc034164r

Wallace, T. L., & Johnson, E. M., Jr. (1989). Cytosine arabinoside kills postmitotic neurons: evidence that deoxycytidine may have a role in neuronal survival that is independent of DNA synthesis. *J Neurosci, 9*(1), 115-124.

Wan, R., Ahmet, I., Brown, M., Cheng, A., Kamimura, N., Talan, M., & Mattson, M. P. (2010). Cardioprotective effect of intermittent fasting is associated with an elevation of adiponectin levels in rats. *J Nutr Biochem, 21*(5), 413-417. doi:10.1016/j.jnutbio.2009.01.020

Ward, P. P., Paz, E., & Conneely, O. M. (2005). Multifunctional roles of lactoferrin: a critical overview. *Cell Mol Life Sci, 62*(22), 2540-2548. doi:10.1007/s00018-005-5369-8

Webb, B. A., Chimenti, M., Jacobson, M. P., & Barber, D. L. (2011). Dysregulated pH: a perfect storm for cancer progression. *Nat Rev Cancer, 11*(9), 671-677. doi:10.1038/nrc3110

Weber, C., Coester, C., Kreuter, J., & Langer, K. (2000). Desolvation process and surface characterisation of protein nanoparticles. *Int J Pharm, 194*(1), 91-102.

Weber, E. L., & Goebel, E. A. (2005). Cerebral edema associated with Gliadel wafers: two case studies. *Neuro Oncol, 7*(1), 84-89. doi:10.1215/s1152851704000614

Weindruch, R., Kayo, T., Lee, C. K., & Prolla, T. A. (2001). Microarray profiling of gene expression in aging and its alteration by caloric restriction in mice. *J Nutr, 131*(3), 918s-923s. doi:10.1093/jn/131.3.918S

Weinert, B. T., & Timiras, P. S. (2003). Invited review: Theories of aging. *J Appl Physiol (1985), 95*(4), 1706-1716. doi:10.1152/japplphysiol.00288.2003

Weiss, R. B., & Issell, B. F. (1982). The nitrosoureas: carmustine (BCNU) and lomustine (CCNU). *Cancer Treatment Reviews, 9*(4), 313-330. doi:https://doi.org/10.1016/S0305-7372(82)80043-1

Westphal, M., Hilt, D. C., Bortey, E., Delavault, P., Olivares, R., Warnke, P. C., . . . Ram, Z. (2003). A phase 3 trial of local chemotherapy with biodegradable carmustine

(BCNU) wafers (Gliadel wafers) in patients with primary malignant glioma. *Neuro Oncol, 5*(2), 79-88. doi:10.1093/neuonc/5.2.79

Wheeler, D. D. (1982). Aging of membrane transport mechanisms in the central nervous system. GABA transport in rat cortical synaptosomes. *Exp Gerontol, 17*(1), 71-85.

Wheeler, D. D., & Ondo, J. G. (1986). Endogenous GABA concentration in cortical synaptosomes from young and aged rats. *Exp Gerontol, 21*(2), 79-85.

Wiemels, J., Wrensch, M., & Claus, E. B. (2010). Epidemiology and etiology of meningioma. *Journal of Neuro-Oncology, 99*(3), 307-314. doi:10.1007/s11060-010-0386-3

Wike-Hooley, J. L., Haveman, J., & Reinhold, H. S. (1984). The relevance of tumour pH to the treatment of malignant disease. *Radiotherapy and Oncology, 2*(4), 343-366. doi:https://doi.org/10.1016/S0167-8140(84)80077-8

Willhite, C. C., Ball, G. L., & McLellan, C. J. (2012). Total allowable concentrations of monomeric inorganic aluminum and hydrated aluminum silicates in drinking water. *Crit Rev Toxicol, 42*(5), 358-442. doi:10.3109/10408444.2012.674101

Williams, P. M., Oatley-Radcliffe, D. L., & Hilal, N. (2017). Chapter 17 - Feed Solution Characterization. In A. F. I. Nidal Hilal, Takeshi Matsuura, Darren Oatley-Radcliffe (Ed.), *Membrane Characterization* (pp. 379-404): Elsevier.

Wistrom, C., & Villeponteau, B. (1990). Long-term growth of diploid human fibroblasts in low serum media. *Exp Gerontol, 25*(2), 97-105.

Wong, T. (2002). Aging of the Cerebral Cortex. *Mcgill J. Med, 6*, 104-113.

Woodworth, G. F., Dunn, G. P., Nance, E. A., Hanes, J., & Brem, H. (2014). Emerging Insights into Barriers to Effective Brain Tumor Therapeutics. *Frontiers in Oncology, 4*(126), 1-14. doi:10.3389/fonc.2014.00126

Xiagedeer, B., Wu, S., Liu, Y., & Hao, W. (2016). Chlormequat chloride retards rat embryo growth in vitro. *Toxicol In Vitro, 34*, 274-282. doi:10.1016/j.tiv.2016.05.001

Zhang, F., Xu, C. L., & Liu, C. M. (2015). Drug delivery strategies to enhance the permeability of the blood-brain barrier for treatment of glioma. *Drug Des Devel Ther, 9*, 2089-2100. doi:10.2147/dddt.s79592

Zhang, J., Stevens, M. F., Laughton, C. A., Madhusudan, S., & Bradshaw, T. D. (2010). Acquired resistance to temozolomide in glioma cell lines: molecular mechanisms and potential translational applications. *Oncology, 78*(2), 103-114. doi:10.1159/000306139

Zorova, L. D., Popkov, V. A., Plotnikov, E. Y., Silachev, D. N., Pevzner, I. B., Jankauskas, S. S., . . . Zorov, D. B. (2018). Mitochondrial membrane potential. *Anal Biochem, 552*, 50-59. doi:10.1016/j.ab.2017.07.009

Zurich, M. G., & Monnet-Tschudi, F. (2009). Contribution of in vitro neurotoxicology studies to the elucidation of neurodegenerative processes. *Brain Res Bull, 80*(4-5), 211-216.

PUBLICATIONS

- Athmakur, H., & Kondapi, A. K. (2018). Carmustine loaded lactoferrin nanoparticles demonstrates an enhanced antiproliferative activity against glioblastoma in vitro. *International Journal of Applied Pharmaceutics*, *10*(6), 234-241. https://doi.org/10.22159/ijap.2018v10i6.28004

- Harikiran A, Kondapi AK. "Characterization of ageing cortical neurons *in vitro*: Role of nutrition." (Manuscript under communication)

- Harikiran A, Kondapi AK. "Effect of pesticides, plant growth regulators and metals on neuronal survival." (Manuscript under preparation)

International Journal of Applied Pharmaceutics

ISSN- 0975-7058 Vol 10, Issue 6, 2018

Original Article

CARMUSTINE LOADED LACTOFERRIN NANOPARTICLES DEMONSTRATES AN ENHANCED ANTIPROLIFERATIVE ACTIVITY AGAINST GLIOBLASTOMA *IN VITRO*

HARIKIRAN ATHMAKUR, ANAND KUMAR KONDAPI*

Department of Biotechnology and Bioinformatics, School of Life Sciences, University of Hyderabad, India
Email: akondapi@gmail.com

Received: 18 Jun 2018, Revised and Accepted: 04 Oct 2018

ABSTRACT

Objective: Despite sophisticated treatment regimens, there is no significant improvement in the mortality rates of glioblastoma due to insufficient dosage delivery, reoccurrence of tumors, higher systemic toxicity, etc. Since brain endothelial cells and glioblastoma cells express lactoferrin receptors, a target-specific drug delivery vehicle was developed using lactoferrin itself as a matrix, into which carmustine was loaded. The objective was to use carmustine loaded lactoferrin nanoparticles (CLN) to achieve higher therapeutic efficacy and target specificity compared to free carmustine.

Methods: CLN were prepared using the Sol-oil method. The nanoparticles prepared were characterized for their size, shape, polydispersity, and stability using FESEM and DLS methods. Drug loading and drug releasing efficiencies were also estimated. Further, cellular uptake of nanoparticles and their antiproliferative efficacy against glioblastoma cells were evaluated.

Results: Characterization of CLN showed that they were spherical with ≤ 41 nm diameter and exhibited homogeneously dispersed stable distribution. Loading efficiency of carmustine in CLN was estimated to be 43±3.7 %. Drug release from the nanoparticles was pH dependent with the maximum observed at pH 5. At physiological and gastric pH, drug release was lower, whereas maximum release was observed at endocytotic vesicular and around tumor extracellular pH. Confocal microscopic studies showed an active cellular uptake of nanoparticles. Results of antiproliferative analysis substantiated a higher antiproliferative effect for CLN compared to free carmustine.

Conclusion: The results of the study demonstrated that CLN serves as a vital tool, in designing an effective treatment strategy for targeted drug delivery to glioblastoma.

Keywords: Lactoferrin nanoparticles, Carmustine, Glioblastoma, Drug delivery vehicle

DOI: http://dx.doi.org/10.22159/ijap.2018v10i6.28004

INTRODUCTION

Brain and other central nervous system tumors (BCNST), are known to be one of the leading causes of cancerous deaths. According to the central brain tumor registry of the United States (CBTRUS), in the US alone, every year on an average 15 000 deaths occur due to BCNST, and approximately 80 000 new cases are diagnosing yearly [1]. No known environmental risk factors other than ionizing radiation had identified for such higher incidence rates [2-4]. Amongst all the BCNST, glioblastoma is the most common and most aggressive malignant tumor with 5 y post-diagnosis survival rates of less than 6 % [1]. World health organization (WHO) grade IV classified, glioblastoma arises from malignantly transformed glial cells, and it diffusely invades other regions of the brain, making it highly lethal [5-7]. Its higher reoccurrence even after surgical resection adds to the complexity [8].

Current preferred treatment for glioblastoma is surgical resection of tumors, followed by radiotherapy with concurrent chemotherapy [9-13]. Despite these advanced treatments, there is no significant improvement reported in the overall survival rates of patients [8]. These failures are mainly due to (a) reoccurrence of tumors that arise from surgically inaccessible infiltrating malignant cells [8]; (b) emergence of resistance to radiotherapy and chemotherapy due to suboptimal dosage exposure for prolonged periods as a result of inefficient dosage delivery [14-17]; (c) higher systemic toxicity as a consequence of nonspecific localization of drugs [18-20]. These failures emphasize the need for the development of efficient drug delivery vehicles with significant drug localization in glioma cells.

In recent years, numerous efforts have been made to develop different drug delivery vehicles to overcome the above problems. Some of these are namely liposomes, nanoshells, dendrimers, solid lipid nanoparticles, polymeric micelles, carbon nanotubes, polyglycolic acid (PGA) nanoparticles, polylactic acid (PLA) nanoparticles, poly(D,L-lactic-co-glycolides) acid (PLGA) nanoparticles, polyanhydride nanoparticles, polyorthoesters nanoparticles, polycyanoacrylate nanoparticles, polycaprolactone nanoparticles, chitosan nanoparticles, albumin nanoparticles, etc. [21, 22]. But, many of these drug delivery vehicles lack target specificity, making their scope limited. Further, the poor ability of these vehicles in the transport of drugs across the blood-brain barrier significantly limits their application for delivery of drugs to the brain. Many strategies have developed to overcome the above limitations [22, 23]. Among them, exploiting one of the brain's natural transport systems, the receptor-mediated endocytosis, is gaining much interest in delivering therapeutic drugs to the brain. Ligands commonly used for this purpose are folate, transferrin, lactoferrin, etc. These ligands are either coated or conjugated to the nanoparticles, to facilitate nanoparticles entry into the brain via receptor-mediated endocytosis [23, 24].

Lactoferrin is an 80 kDa protein, which is mainly found in milk and other secretory body fluids. It has numerous clinically significant physiological functions viz., anti-inflammation, host defense against infections, maintenance of iron homeostasis, etc. [25-28]. Since brain endothelial cells, and glioblastoma cells [29-33] express lactoferrin receptors and also its low endogenous levels in serum [34, 35], make lactoferrin more advantageous in using it for targeting to the brain as it avoids competition with endogenous ligands and also increases target specificity. Drug-loaded nanoparticles were reported to possess a significant advantage over drug conjugated nanoparticles regarding efficacy and drug release in the targeted cells [36].

In the context of these facts, biodegradable protein nanoparticles were developed using lactoferrin itself as a matrix, into which chemotherapeutic drug, carmustine was loaded, and these nanoparticles were used for targeting brain tumors *in vitro*. The objective was to exploit lactoferrin nanoparticles for a dual purpose, as a drug carrier, as well as a targeting ligand. Cell culture models were used to evaluate the efficiency of carmustine loaded lactoferrin nanoparticles in drug localization and cytotoxicity.

We hypothesize that carmustine loaded lactoferrin nanoparticles will be an effective treatment strategy for targeting brain tumors if it increases target specificity, enhance therapeutic efficacy,

bioavailability, and stability, and also minimizes the systemic toxicity of the drug. This paper discusses the preparation of carmustine loaded lactoferrin nanoparticles, their optimal characteristic features which make them better drug delivery vehicles and further about their efficacy in treating brain tumors in general and more particularly glioblastoma *in vitro.*

MATERIALS AND METHODS

Materials

3-(4,5-dimethylthiazol-2-yl)-2,5-diphenyltetrazolium bromide (MTT), 4′,6-diamidino-2-phenylindole (DAPI), rhodamine 123 were procured from Sigma–Aldrich (St. Louis, USA), lactoferrin was obtained from Naturade LLC (Irvine, USA), and olive oil from Nicola pantaleo (Fasano, Italy). Carmustine was of pharmaceutical grade (Emcure pharmaceuticals, Pune, India). Minimum essential media, non-essential amino acids, sodium pyruvate, Dulbecco's modified eagle medium, fetal bovine serum were bought from Thermo fisher scientific (Waltham, USA). C_6 glioma, SK-N-SH cell lines were acquired from National centre for cell science (Pune, India). Rest of the materials were of either analytical or molecular biological grade.

Preparation of carmustine loaded lactoferrin, blank lactoferrin and rhodamine loaded lactoferrin nanoparticles

Nanoparticles were prepared as described by Krishna AD *et al.* (2009) [36]. Briefly, 1 ml of cold phosphate-buffered saline (PBS) pH-7.4 containing 50 mg of dissolved lactoferrin was gently mixed with 20 mg of carmustine dissolved in dimethyl sulfoxide (DMSO). The mixture was incubated at 4 °C for 30 min. After incubation, the mixture was slowly added to 30 ml of cold olive oil and was gently dispersed by vortexing, followed by sonication using ultrasonic homogenizer at 4 °C. Immediately the resulting mixture was snap frozen by keeping it in the liquid nitrogen for 10 min. After thawing the mixture at 4 °C, it was centrifuged at 8000 g for 15 min at 4 °C. The supernatant was discarded, and the pellet was washed thrice with diethyl ether. Following air drying, the pellet was dispersed in cold PBS (pH-7.4) by sonication and was stored at 4 °C until use. For fluorescent studies, rhodamine loaded lactoferrin nanoparticles were prepared similarly, but instead of carmustine, rhodamine was used. Similarly, blank lactoferrin nanoparticles were also prepared, but without the use of drug or dye.

Characterization of nanoparticles by field emission scanning electron microscope (FE-SEM)

Size and morphology of lactoferrin nanoparticles were characterized by FE-SEM (Field electron and ion, Hillsboro, USA). Freshly prepared lactoferrin nanoparticles were coated on a clean glass slide and were dried overnight in a dust-free chamber. Samples were then coated with gold and were viewed under the electron microscope. For image capturing and data analysis, the manufacturer's standard operative procedures were followed.

Characterization of nanoparticles by dynamic light scattering (DLS)

Zeta potential, hydrodynamic diameter, and polydispersity index (PDI) of lactoferrin nanoparticles in suspension form were analyzed by dynamic light scattering method using SZ-100 Nanopartica analyzer system equipped with a diode-pumped solid-state laser having a wavelength of 532 nm (Horiba scientific, Irvine, USA). Particle analysis and data acquisition were carried out according to the manufacturer's instructions.

Evaluation of loading efficiency

Carmustine loaded lactoferrin nanoparticles were suspended in 1 ml of PBS of pH-5 and were kept under gentle rocking at 4 °C for 30 min for the release of the drug from the nanoparticles (n = 3). 30 % silver nitrate was added to precipitate the protein out of the solution. The resulting solution was centrifuged at 15 000 g for 15 min at 4 °C. The obtained supernatant was filtered and used for the drug estimation by high-performance liquid chromatography (HPLC) (Waters, Milford, USA) [37]. The supernatant was analyzed in triplicate. Different concentrations of carmustine solutions were also prepared and estimated by HPLC to develop a standard curve. Amount of carmustine loaded in the lactoferrin nanoparticles was determined using the developed standard curve.

Drug loading efficiency was calculated using the following formula.

$$\text{Loading efficiency } \% = (D_{Loaded}/D_{Total}) \times 100$$

$$D_{Loaded} = D_{Total} - D_{Lost}$$

where D_{Loaded} = amount of loaded drug; D_{Total} = amount of total drug used; D_{Lost} = amount of drug lost during preparation.

In vitro pH-dependent drug release assay

pH-dependent drug release assay was performed by quantifying drug released under different pH conditions [38]. Pelleted nanoparticles equivalent to 200 µg of carmustine were suspended in PBS solutions of varying pH ranges (1-9) and were incubated for 4 h at 4 °C on a rocker with moderate speed. After incubation, 30 % silver nitrate was added to the PBS solutions to precipitate protein. The mobile phase was also added to extract the drug, followed by centrifugation at 15000 g for 15 min at 4 °C. The obtained supernatant was filtered using a 0.2-micron filter, and the amount of drug present in the supernatant was estimated using HPLC at 230 nm wavelength for carmustine. For quantification of unknown amounts of the drug in the samples, a standard curve was developed using known concentrations of the drug in the same incubation media and quantified by HPLC. Each sample was quantified in triplicate (n = 3).

Cellular uptake assay by confocal microscopy

SK-N-SH cells (seeding density of 2×10^5 cells) were grown on glass coverslips in 12 well plates. Equivalent amounts of rhodamine loaded lactoferrin nanoparticles were added to the wells and were incubated for different time points (0.5 h, 1 h, 2 h, 4 h, and 8 h). Untreated cells were kept as control. After specified time points, cells were washed thrice with PBS buffer (pH-7.4) and were fixed with 4 % paraformaldehyde for 10 min. After subsequent washings with PBS buffer, cells were counterstained with DAPI, and the coverslips were mounted on a glass slide. Cells were viewed under the confocal microscope (Leica, Buffalo grove, USA) for analyzing the amount of uptake of nanoparticles, by utilizing the intrinsic fluorescence of rhodamine 123 (excitation and emission maxima are 511 nm and 534 nm respectively) [39].

Evaluation of the antiproliferative activity of carmustine loaded lactoferrin nanoparticles

The antiproliferative assay was performed using the MTT method [40]. Briefly, 50 000 C6 glioma cells were seeded in every well of the 96 well plate and were incubated in the carbon dioxide incubator at 37 °C for 12 h. After incubation, media was replaced with fresh media containing increasing concentrations of either soluble carmustine or its equivalent carmustine loaded nanoparticles. Similar treatment was given with blank lactoferrin nanoparticles. Control cells were also kept, without the addition of neither soluble drug nor the nanoparticles. Cells were incubated in the 37 °C carbon dioxide incubator for 24 h. After incubation, media was discarded, and cells were washed twice. Fresh media containing 10 %, 5 mg/ml MTT, was added to the cells followed by incubation for 8 h in a carbon dioxide incubator at 37 °C. During incubation, cells that survived after the treatment convert yellow tetrazolium salt into insoluble formazan crystals. MTT containing media was discarded, and insoluble formazan crystals were dissolved by the addition of DMSO. The intensity of the developed color was measured using multiplate reader-Infinite 200 (Tecan, Mannedorf, Switzerland) at 595 nm. Percentage of inhibition (PI) was calculated according to the following formula.

$$PI = \{(OD_{Control} - OD_{Treated})/OD_{Control}\} \times 100$$

where, PI = percentage of inhibition; $OD_{Control}$ = absorbance at 595 nm for control cells; $OD_{Treated}$ = absorbance at 595 nm for treated cells.

After plotting the graph, half maximal inhibitory concentration (IC_{50} value) was calculated from it.

Statistics

All the experiments were performed a minimum of three times individually. Data were presented as mean±standard deviation. Amounts of drug released at various pH conditions were statistically analyzed by one-way ANOVA using the Student-Newman-Keuls

method. Antiproliferative activities of free carmustine and carmustine loaded lactoferrin nanoparticles were statistically compared by Student t-test. P<0.05 was regarded as statistically significant.

RESULTS

Characterization of nanoparticles by FESEM

Blank lactoferrin nanoparticles and carmustine loaded lactoferrin nanoparticles were prepared as described in materials and methods. The prepared nanoparticles were characterized by FESEM to obtain information relating to their size and morphology. The FESEM analysis revealed that their sizes were in the range of 13-22 nm, with an average size of 17.5±3.06 nm (mean±SD) for blank lactoferrin nanoparticles (fig. 1a) and in the range of 32-41 nm, with an average size of 36.5±3.90 nm (mean±SD) for carmustine loaded lactoferrin nanoparticles (fig. 1b). It is apparent that lactoferrin nanoparticles become more than double in their average size after loading of the drug. Further, FESEM analysis revealed that the nanoparticles were homogenous in their sizes and were spherical in their shapes.

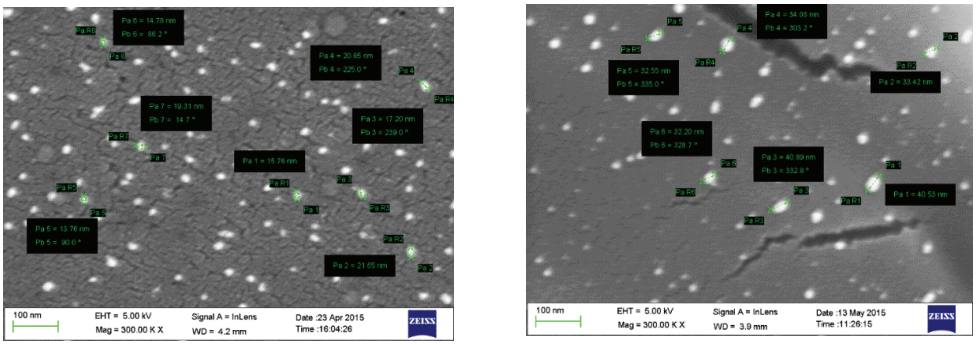

(A) **(B)**

Fig. 1: FESEM analysis of (A) blank lactoferrin nanoparticles, (B) carmustine loaded lactoferrin nanoparticles. Above image was representative of a quadruplicate experiment (n = 4)

Characterization of nanoparticles by DLS

Zeta potential values of blank lactoferrin nanoparticles and carmustine loaded lactoferrin nanoparticles were -14.9±3.87 mV (mean±SD) (fig. 2a) and -24.6±5.94 mV (mean±SD) (fig. 2b) respectively. These zeta potential values indicate that carmustine loaded lactoferrin nanoparticles were under colloidal stability in nature, and blank lactoferrin nanoparticles were under moderately colloidal stability in nature. Hydrodynamic sizes of nanoparticles were also investigated using DLS analysis (fig. 2c and fig. 2d). Since DLS measures the hydrodynamic diameter of the particles, whereas FESEM measures size in the dry state, nanoparticles sizes were little larger in DLS compared to FESEM analysis. PDI for blank lactoferrin nanoparticles was 0.264±0.03 and for carmustine loaded lactoferrin nanoparticles was 0.338±0.05. These PDI values confirm that these nanoparticles had a homogeneously dispersed size distribution.

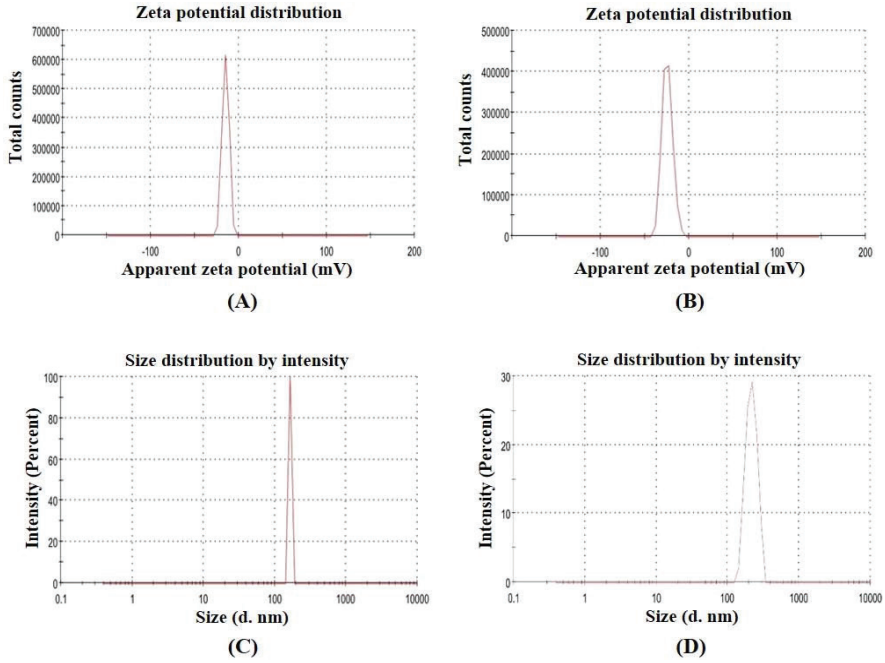

Fig. 2: DLS analysis: Zeta potential measurements of (A) blank lactoferrin nanoparticles, (B) carmustine loaded lactoferrin nanoparticles. Hydrodynamic diameter measurements of (C) blank lactoferrin nanoparticles, (D) carmustine loaded lactoferrin nanoparticles. The experiment was conducted in triplicates (n = 3)

Estimation of drug loading efficiency of carmustine loaded lactoferrin nanoparticles

Significantly higher drug loading efficiency was achieved in the nanoparticles by using the Sol-oil method. Carmustine solutions of different concentrations were prepared and estimated by HPLC, and the standard graph was developed for calculating the amount of encapsulated carmustine present in the lactoferrin nanoparticles (fig. 3b). Carmustine loaded lactoferrin nanoformulations were treated as described in the materials and methods, the released drug was estimated by HPLC (fig. 3a) and correlated with the standard graph. Then the loading efficiencies were calculated using the formula mentioned in the materials and methods. Loading efficiency of carmustine in the carmustine loaded lactoferrin nanoparticles was found to be 43±3.7 % (n = 3).

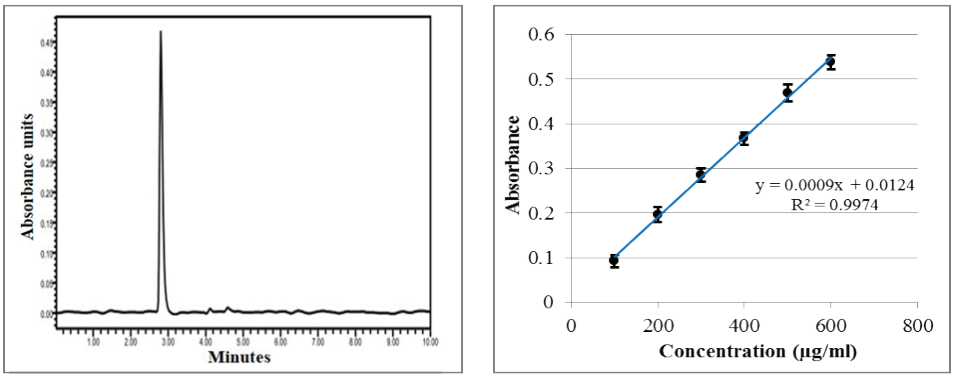

Fig. 3: (A) HPLC analysis of carmustine at 230 nm wavelength. (B) Quantification of carmustine by HPLC; data were represented as mean±SD (n = 3)

***In vitro* pH-dependent drug release assay**

pH-dependent release assay of carmustine loaded lactoferrin nanoparticles were carried out at various pH ranges (1–9) (fig. 4). The maximum amount of drug was released at pH 5, which was followed by pH 6. At all other pH conditions, the release was comparatively low. At physiological pH (pH 7.2 to 7.4) and gastric pH (pH 1 to 2.5), drug release was less than 20 % and whereas maximum release was observed at endocytotic vesicular pH (pH 5) and around tumor extracellular pH (pH 5.85-7.35) [41], from the nanoparticles.

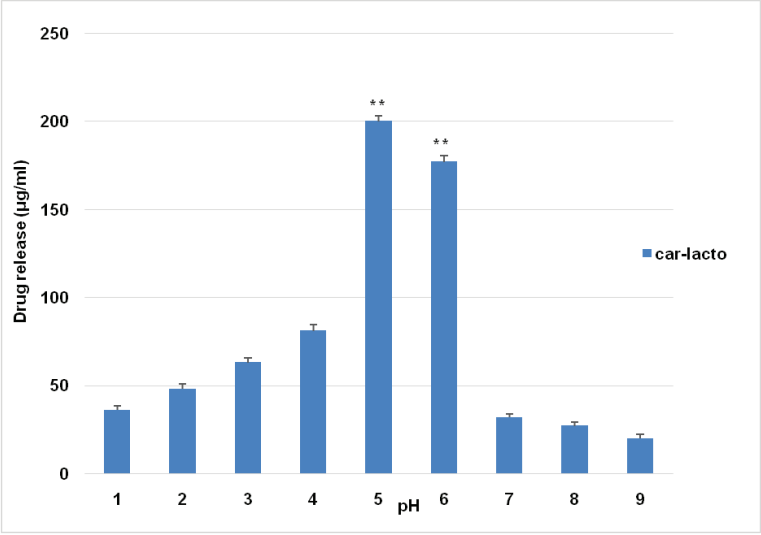

Fig. 4: pH-dependent release assay of carmustine loaded lactoferrin nanoparticles. Car-lacto represents carmustine loaded lactoferrin nanoparticle. Averages and standard deviations from three experiments (n = 3) were shown as mean±SD. **P<0.01 by one-way ANOVA using Student-Newman-Keuls method

Cellular uptake assay by confocal microscopy

Rhodamine 123 loaded lactoferrin nanoparticles were incubated with the cells for different time points to confirm the cellular uptake of nanoparticles. Up to 1 h of incubation, rhodamine was not visible, but after 2 h, it was noticed that its level had increased with the increment of time. By the end of 8 h, cells were localized entirely with rhodamine 123. Cells, which were not exposed to rhodamine 123 loaded nanoparticles, were taken as the control (fig. 5). Time

course experiment showed that there was a gradual increase of rhodamine in the cells with the time, which confirmed the cellular uptake of nanoparticles and their rise was gradual and proportional to the time. This result also confirmed the longer retention of lactoferrin nanoparticles within the cells, which provides a longer time for chemotherapeutic drugs to confer the antiproliferative effect.

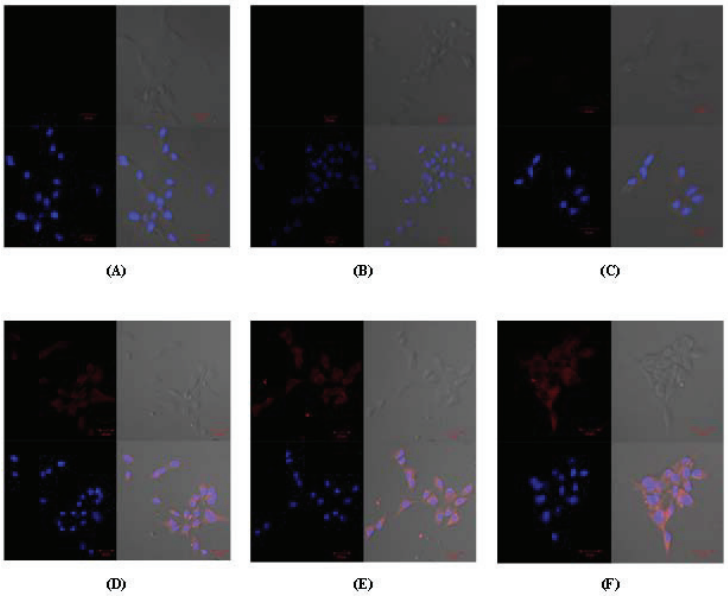

Fig. 5: Cellular uptake of rhodamine 123 loaded lactoferrin nanoparticles. Time course experiment showed the uptake of nanoparticles into the cells, and there was a gradual increase in the uptake of nanoparticles with the increment of time. A, B, C, D, E, F represent control, 0.5 h, 1h, 2h, 4h, and 8h time points respectively. In each big square, the upper left square represents the rhodamine 123 (red), the upper right square represents transmission image, the lower left square represents DAPI (blue), and the lower right square represents merger image. Total number of independent experimentation, n = 3

Evaluation of the antiproliferative activity of carmustine loaded lactoferrin nanoparticles

Antiproliferative activity of carmustine loaded lactoferrin nanoparticles were compared with the antiproliferative activity of the free drug (carmustine) after 24 h of treatment with free drug and drug-loaded nanoparticles. The results clearly showed that carmustine loaded lactoferrin nanoparticles had a higher antiproliferative effect compared to free carmustine at all the experimental concentrations (fig. 6a). And there was a reduction of 3.29 times in the IC_{50} value with the treatment of carmustine loaded lactoferrin nanoparticles compared to free carmustine treatment. IC_{50} values of free carmustine and carmustine loaded lactoferrin nanoparticles were 43.22 µg/ml and 12.76 µg/ml respectively. Blank lactoferrin nanoparticles (delivery vehicle) didn't show any significant antiproliferative activity at all the experimental concentrations (fig. 6b).

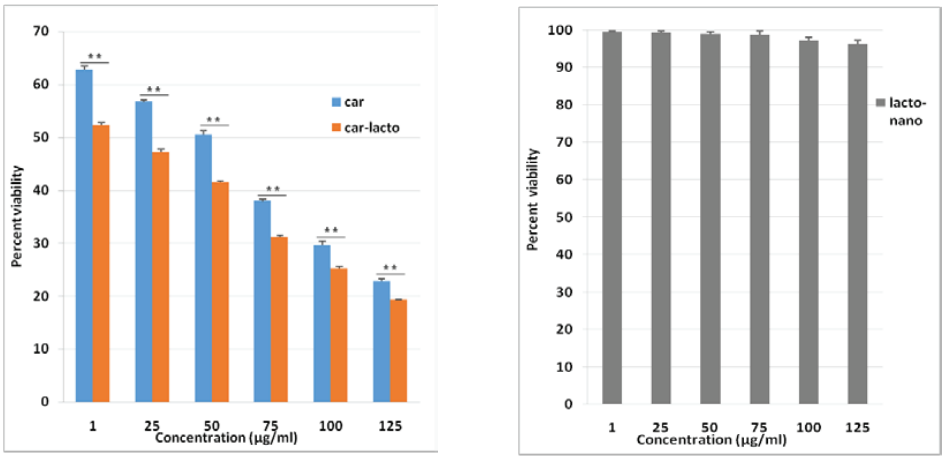

Fig. 6: Dose-dependent antiproliferative activities of (A) free carmustine and carmustine loaded lactoferrin nanoparticles and (B) free lactoferrin nanoparticles after 24 h of treatment. Car, car-lacto, and lacto-nano represent the treatment of carmustine drug, carmustine

loaded lactoferrin nanoparticles and blank lactoferrin nanoparticles respectively. Data were represented as mean±SD (n = 3), **P<0.01 by student t-test

DISCUSSION

Current advanced treatments for glioblastoma remain not so effective since there is no significant improvement in the survival of the patients. The purpose of this study was to develop an effective target-specific drug delivery vehicle with reduced systemic toxicity and increased therapeutic efficacy against glioblastoma. As it is known, lactoferrin receptors are expressed on brain endothelial cells, and glioblastoma cells, a target-specific drug delivery vehicle was developed, using lactoferrin itself as a matrix, into which chemotherapeutic drug, carmustine was loaded. In the present study, carmustine loaded lactoferrin nanoparticles were prepared and characterized their features such as size, shape, polydispersity, stability, drug loading efficiency, drug releasing efficiency, cellular uptake ability, etc., and further evaluated their efficacy in treating glioblastoma.

For decades, carmustine was a drug of choice for treating glioblastoma [42-44]. Due to its dose-limiting side effects such as bone marrow suppression [45] and non-dose dependent pulmonary fibrosis [46], its usage was limited. To reduce systemic toxicity, intracranial polymer implants (gliadel wafers) impregnated with carmustine, have been using clinically since 1996 [19]. But these gliadel wafers were found to be not successful as they do not show effective therapeutic efficacy due to many limitations such as lower penetration, inability in preventing short distant tumor recurrence, lack of synergetic action in combination with radiotherapy and other chemotherapeutic drugs, practical difficulties in prescribing regular dosage schedules as it requires regular intracranial surgeries [47, 19]. Further, complications are reported in the use of gliadel wafers due to severe adverse effects such as healing abnormalities [48], craniotomy infections [49], seizures [11], oedema [11, 50], neurological decline [50], intracranial hypertension [10], cerebrospinal fluid leaks [10], tumor bed cyst formation [51], pericavity necrosis [52] etc. These limitations and adverse effects emphasize the need for a better drug delivery vehicle for efficient treatment of glioblastoma.

In the present study, carmustine loaded lactoferrin nanoparticles were prepared using the Sol-oil method. This method is simple, less time consuming and doesn't involve any chemical modifications either to the drug or protein unlike other methods such as protein coacervation method [53]. Further, lactoferrin conformation remains in the native state. As the nanoparticles are prepared using lactoferrin, a natural protein present abundantly in milk and other secretory body fluids, these nanoparticles are safer to use even at high dosages. Besides, significantly higher drug loading efficiency was also achieved in the nanoparticles by using this method. Drug loading was indeed higher compared to commercially available carmustine implants, which have only 3.85 % drug loading capacity [11]. The reported maximum drug loading capacity that can be achieved in the biodegradable polymers was 28 % [54], which was less than that observed in carmustine loaded lactoferrin nanoparticles (43±3.7 %). Drug loading efficiency of a drug delivery vehicle can influence its therapeutic index. Higher the achieved drug loading efficiency, higher will be the therapeutic index. With the increased therapeutic index there will be an enhanced antitumor effect and reduced toxicity [55].

Using Sol-oil method, nanoparticles of sizes ≤ 41 nm were successfully developed, which was confirmed by FESEM analysis. FESEM studies also showed that blank lactoferrin nanoparticles of 13-22 nm size became enlarged to 32-41 nm size after successful loading of carmustine drug. It is an advantage to have smaller sized nanoparticles because several studies had consistently shown that smaller sized nanoparticles were capable of escaping from the reticuloendothelial system, thereby evaded rapid clearance from systemic circulation and had longer circulation time and stability in the blood [56-59]. Several other studies also had shown, an inverse correlation between nanoparticle size's and blood-brain barrier penetration [60-62]. It indicates that particles, which are smaller in size can cross the blood-brain barrier more efficiently than particles which are larger. Thus, the smaller size of these nanoparticles can increase their circulatory half-life and also make them more efficient in crossing the blood-brain barrier.

The measured zeta potential values indicate that these nanoparticles were stable. Carmustine loaded lactoferrin nanoparticles were under colloidal stability range, whereas blank lactoferrin nanoparticles were under moderately colloidal stability range. Measured nanoparticle sizes were found to be little larger in DLS compared to FESEM analysis. Since, DLS measures the hydrodynamic diameter of the particle, which includes not only the particle but also the ionic and solvent layers associated with the particle in the solution, the particle sizes will be larger in DLS compared to FESEM, which measures size in the dry state [63, 64]. Polydispersity index values of 0.264±0.03 and 0.338±0.05 for blank lactoferrin nanoparticles and carmustine loaded lactoferrin nanoparticles respectively indicate that these nanoparticles possess a homogenous population with narrow size distribution.

The release of the drug from the nanoparticles was found to be pH dependent. It was observed that at physiological and gastric pH, drug release from the nanoparticles was very minimum, whereas maximum drug release was observed at the endocytotic vesicular pH (pH 5) and around tumor extracellular pH (pH 5.85-7.35) [41], which indicates that these nanoparticles can have low loss of the drug during systemic circulation, thereby exhibit reduced systemic toxicity. And they also show more specificity in the drug release, mainly in the endocytotic vesicles, which are involved in receptor-mediated endocytosis and around tumor environment, which have reduced pH as a consequence of higher anaerobic respiration of cancerous cells [65, 66]. pH-dependent drug release is an added advantage, which makes these nanoparticles optimal drug delivery vehicles with reduced systemic toxicity and increased tumor specificity.

As carmustine drug was nonfluorescent, cellular uptake of nanoparticles was tested by loading fluorescent dye, rhodamine 123 into the lactoferrin nanoparticles. Time course study using confocal microscopy had shown that there was a gradual increase of rhodamine in the cells with the increment of time, which confirmed the active cellular uptake of lactoferrin nanoparticles. Earlier it was reported that the mechanism of uptake of lactoferrin nanoparticles into the cells was through receptor-mediated endocytosis [36, 39]. As the brain endothelial cells and glioblastoma cells express lactoferrin receptors [29-33], a similar mechanism could be operative, during the transport of carmustine loaded lactoferrin nanoparticles across the blood-brain barrier and also at the entry into the tumor cells.

Comparative study of the antiproliferative effect of free carmustine and carmustine loaded lactoferrin nanoparticles, had validated that carmustine loaded lactoferrin nanoparticles had a higher therapeutic efficacy than free carmustine. Previously, carmustine encapsulated liposomes, and carmustine-magnetic nanoparticles showed 50 % inhibition at around 467 μM and 100 μM concentrations of carmustine respectively [67, 68], whereas carmustine loaded lactoferrin nanoparticles showed 50 % inhibition at 59.6 μM of carmustine, which was significantly lower and further substantiates the higher therapeutic efficacy of carmustine loaded lactoferrin nanoparticles. These results were also consistent with the earlier reports [39, 38], where lactoferrin nanoparticles had used as drug delivery vehicles. Higher uptake of nanoparticles, sustained drug release from the nanoparticles and the longer retention of the drug inside the cells might have contributed to the increased therapeutic efficacy of carmustine loaded lactoferrin nanoparticles against C6 glioma cells compared to the free carmustine.

Current state of the art, drug delivery vehicles for the treatment of glioblastoma includes solid lipid nanoparticles, nanostructured lipid carriers, liposomes, polymeric nanoparticles, micelles, magnetic nanoparticles, gold nanoshells, carbon nanotubes, etc. These drug delivery vehicles are failing to be an effective therapeutics due to one or more of the crucial issues viz., lower encapsulation efficiency, higher toxicity, lower stability, rapid clearance from the blood, lower biodegradability, lack of specificity, lower therapeutic indices, higher manufacturing costs, etc. [69-71, 21]. But, as may be seen from the results of the present study, carmustine loaded lactoferrin

nanoparticles are showing promising results, which may overcome these challenges.

Thus, carmustine loaded lactoferrin nanoparticles serve as potential drug delivery vehicles in treating glioblastoma effectively *in vitro*. Further studies are required to establish *in vivo* efficacy.

CONCLUSION

Carmustine loaded lactoferrin nanoparticles, with ≤ 41 nm size were successfully developed, using lactoferrin as a single matrix. These nanoparticles were spherical with homogeneous distribution, enhanced stability, and higher drug loading efficiency. The release of the drug from nanoparticles was pH dependent, which adds additional advantage to this target specific drug delivery vehicle. Further, active cellular uptake of nanoparticles with a significant antiproliferative effect in cell culture models substantiated carmustine loaded nanoparticles as an effective drug delivery vehicle in treating glioblastoma.

Further *in vivo* efficacy and toxicological studies using carmustine loaded lactoferrin nanoparticles would provide an opportunity for the development of an effective treatment strategy against glioblastoma without any systemic toxicity.

ACKNOWLEDGEMENT

Authors are thankful to the Indian Council of Medical Research and Department of Science and Technology, India for providing the grant for this work. Authors are grateful to the University Grants Commission, India and the Department of Biotechnology-Centre for Research and Education in Biology and Biotechnology program of the University of Hyderabad, India for providing the infrastructure for this work. Authors are also thankful to the Council of Scientific and Industrial Research, India for providing doctoral fellowship to Harikiran.

AUTHORS CONTRIBUTIONS

Harikiran performed all experiments, compiled data, and drafted manuscript. Anand Kumar planned experiments, analyzed results and edited manuscript. All the authors have approved the final article.

CONFLICT OF INTERESTS

Declared none

REFERENCES

1. Ostrom QT, Gittleman H, Liao P, Vecchione-Koval T, Wolinsky Y, Kruchko C, *et al.* CBTRUS statistical report: primary brain and other central nervous system tumors diagnosed in the united states in 2010-2014. Neurol Oncol 2017;19 Suppl 5:1-88.
2. Johnson KJC, Cullen J, Barnholtz Sloan JS, Ostrom QT, Langer CE, Turner MC, *et al.* Childhood brain tumor epidemiology: a brain tumor epidemiology consortium review. Cancer Epidemiol Biomarkers Prev 2014;23:2716-36.
3. Ostrom QT, Bauchet L, Davis FG, Deltour I, Fisher JL, Langer CE, *et al.* The epidemiology of glioma in adults: a state of the science review. Neurol Oncol 2014;16:896-913.
4. Wiemels J, Wrensch M, Claus EB. Epidemiology and etiology of meningioma. J Neurooncol 2010;99:307-14.
5. Louis DN, Ohgaki H, Wiestler OD, Cavenee WK, Burger PC, Jouvet A, *et al.* The 2007 WHO classification of tumours of the central nervous system. Acta Neuropathol 2007;114:97–109.
6. Quirk BJ, Brandal G, Donlon S, Vera JC, Mang TS, Foy AB, *et al.* Photodynamic therapy (PDT) for malignant brain tumors–where do we stand? Photodiagnosis Photodyn Ther 2015;12:530-44.
7. Omuro A, DeAngelis LM. Glioblastoma and other malignant gliomas: a clinical review. JAMA 2013;310:1842-50.
8. Demuth T, Berens ME. Molecular mechanisms of glioma cell migration and invasion. J Neurooncol 2004;70:217-28.
9. Stupp R, Mason WP, Van den Bent MJ, Weller M, Fisher B, Taphoorn MJ, *et al.* Radiotherapy plus concomitant and adjuvant temozolomide for glioblastoma. N Engl J Med 2005;352:987-96.
10. Westphal M, Hilt DC, Bortey E, Delavault P, Olivares R, Warnke PC, *et al.* A phase 3 trial of local chemotherapy with biodegradable carmustine (BCNU) wafers (gliadel wafers) in patients with primary malignant glioma. Neurol Oncol 2003;5:79-88.
11. Brem H, Piantadosi S, Burger PC, Walker M, Selker R, Vick NA, *et al.* Placebo-controlled trial of safety and efficacy of intraoperative controlled delivery by biodegradable polymers of chemotherapy for recurrent gliomas. Lancet 1995;345:1008-12.
12. Patel MA, Kim JE, Ruzevick J, Li G, Lim M. The future of glioblastoma therapy: synergism of standard of care and immunotherapy. Cancers 2014;6:1953-85.
13. Woodworth GF, Dunn GP, Nance EA, Hanes J, Brem H. Emerging insights into barriers to effective brain tumor therapeutics. Front Oncol 2014;4:1-14.
14. Bao S, Wu Q, McLendon RE, Hao Y, Shi Q, Hjelmeland AB, *et al.* Glioma stem cells promote radioresistance by preferential activation of the DNA damage response. Nature 2006;444:756-60.
15. Beier D, Schulz JB, Beier CP. Chemoresistance of glioblastoma cancer stem cells-much more complex than expected. Mol Cancer 2011;10:1-11.
16. Sarkaria JN, Kitange GJ, James CD, Plummer R, Calvert H, Weller M, *et al.* Mechanisms of chemoresistance in malignant glioma. Clin Cancer Res 2008;14:2900-8.
17. Zhang J, Stevens MF, Laughton CA, Madhusudan S, Bradshaw TD. Acquired resistance to temozolomide in glioma cell lines: molecular mechanisms and potential translational applications. Oncology 2010;78:103-14.
18. Blakeley J, Grossman SA. Chemotherapy with cytotoxic and cytostatic agents in brain cancer. In: Aminoff MJ, Boller F, Swaab DF, editors. Handbook of Clinical Neurology. Elsevier; 2012. p. 229-54.
19. Lin SH, Kleinberg LR. Carmustine wafers: localized delivery of chemotherapeutic agents in CNS malignancies. Expert Rev Anticancer Ther 2008;8:343-59.
20. Chamberlain MC. Temozolomide: therapeutic limitations in the treatment of adult high-grade gliomas. Expert Rev Neurother 2010;10:1537-44.
21. Krupa P, Rehak S, Diaz-Garcia D, Filip S. Nanotechnology-new trends in the treatment of brain tumors. Acta Med 2014;57:142-50.
22. Invernici G, Cristini S, Alessandri G, Navone SE, Canzi L, Tavian D, *et al.* Nanotechnology advances in brain tumors: the state of the art. Recent Pat Anticancer Drug Discovery 2011;6:58-69.
23. Rempe R, Cramer S, Qiao R, Galla HJ. Strategies to overcome the barrier: use of nanoparticles as carriers and modulators of barrier properties. Cell Tissue Res 2014;355:717-26.
24. Chang J, Paillard A, Passirani C, Morille M, Benoit JP, Betbeder D, *et al.* Transferrin adsorption onto PLGA nanoparticles governs their interaction with biological systems from blood circulation to brain cancer cells. Pharm Res 2012;29:1495-505.
25. Nuijens JH, Van Berkel PHC, Schanbacher FL. Structure and biological actions of lactoferrin. J Mammary Gland Biol Neoplasia 1996;1:285-95.
26. Ward PP, Paz E, Conneely OM. Multifunctional roles of lactoferrin: a critical overview. Cell Mol Life Sci 2005;62:2540-8.
27. Moreno-Exposito L, Illescas-Montes R, Melguizo-Rodriguez L, Ruiz C, Ramos-Torrecillas J, de Luna-Bertos E. Multifunctional capacity and therapeutic potential of lactoferrin. Life Sci 2018;195:61-4.
28. Jayasinghe S, Siriwardhana A, Karunaratne V. Natural iron sequestering agents: their roles in nature and therapeutic potential. Int J Pharm Pharm Sci 2015;7:8-12.
29. Huang RQ, Ke WL, Qu YH, Zhu JH, Pei YY, Jiang C. Characterization of lactoferrin receptor in brain endothelial capillary cells and mouse brain. J Biomed Sci 2007;14:121-8.
30. Ji B, Maeda J, Higuchi M, Inoue K, Akita H, Harashima H, *et al.* Pharmacokinetics and brain uptake of lactoferrin in rats. Life Sci 2006;78:851-5.
31. Fillebeen C, Descamps L, Dehouck M, Fenart L, Benaıssa M, Spik G, *et al.* Receptor-mediated transcytosis of lactoferrin through the blood-brain barrier. J Biol Chem 1999;274:7011–7.

32. Qiao R, Jia Q, Huwel S, Xia R, Liu T, Gao F, *et al.* Receptor-mediated delivery of magnetic nanoparticles across the blood-brain barrier. ACS Nanol 2012;6:3304-10.
33. Fang JH, Lai YH, Chiu TL, Chen YY, Hu SH, Chen SY. Magnetic core-shell nanocapsules with dual-targeting capabilities and co-delivery of multiple drugs to treat brain gliomas. Adv Healthc Mater 2014;3:1250-60.
34. Talukder MJ, Takeuchi T, Harada E. Characteristics of lactoferrin receptor in bovine intestine: higher binding activity to the epithelium overlying Peyer's patches. J Vet Med A Physiol Pathol Clin Med 2003;50:123-31.
35. Sanchez L, Calvo M, Brock JH. Biological role of lactoferrin. Arch Dis Child 1992;67:657-61.
36. Krishna AD, Mandraju RK, Kishore G, Kondapi AK. An efficient targeted drug delivery through apotransferrin loaded nanoparticles. PLoS One 2009;4:e7240.
37. Lakshmi YS, Kumar P, Kishore G, Bhaskar C, Kondapi AK. Triple combination MPT vaginal microbicide using curcumin and efavirenz loaded lactoferrin nanoparticles. Sci Rep 2016;6:25479.
38. Kumari S, Kondapi AK. Lactoferrin nanoparticle mediated targeted delivery of 5-fluorouracil for enhanced therapeutic efficacy. Int J Biol Macromol 2017;95:232-7.
39. Ahmed F, Ali MJ, Kondapi AK. Carboplatin loaded protein nanoparticles exhibit improve anti-proliferative activity in retinoblastoma cells. Int J Biol Macromol 2014;70:572-82.
40. Mosmann T. Rapid colorimetric assay for cellular growth and survival: application to proliferation and cytotoxicity assays. J Immunol Methods 1983;65:55-63.
41. Wike Hooley JL, Haveman J, Reinhold HS. The relevance of tumour pH to the treatment of malignant disease. Radiother Oncol 1984;2:343-66.
42. Weiss RB, Issell BF. The nitrosoureas: carmustine (BCNU) and lomustine (CCNU). Cancer Treat Rev 1982;9:313-30.
43. Chang CH, Horton J, Schoenfeld D, Salazer O, Perez-Tamayo R, Kramer S, *et al.* Comparison of postoperative radiotherapy and combined postoperative radiotherapy and chemotherapy in the multidisciplinary management of malignant gliomas. Cancer 1983;52:997-1007.
44. Selker RG, Shapiro WR, Burger P, Blackwood MS, Arena VC, Gilder JC, *et al.* The brain tumor cooperative group NIH trial 87-01:a randomized comparison of surgery, external radiotherapy, and carmustine versus surgery, interstitial radiotherapy boost, external radiation therapy, and carmustine. Neurosurgery 2002;51:343-57.
45. De Vita VT, Carbone PP, Owens AH, Gold GL, Krant MJ, Edmonson J. Clinical trials with 1, 3-bis(2-chloroethyl)-1-nitrosourea, NSC-409962. Cancer Res 1965;25:1876-81.
46. O'Driscoll BR, Kalra S, Gattamaneni HR, Woodcock AA. Late carmustine lung fibrosis. Age at treatment may influence severity and survival. Chest 1995;107:1355-7.
47. Bota DA, Desjardins A, Quinn JA, Affronti ML, Friedman HS. Interstitial chemotherapy with biodegradable BCNU (gliadel) wafers in the treatment of malignant gliomas. Ther Clin Risk Manag 2007;3:707-15.
48. Subach BR, Witham TF, Kondziolka D, Lunsford LD, Bozik M, Schiff D. Morbidity and survival after 1,3-bis(2-chloroethyl)-1-nitrosourea wafer implantation for recurrent glioblastoma: a retrospective case-matched cohort series. Neurosurgery 1999;45:17-22.
49. McGovern PC, Lautenbach E, Brennan PJ, Lustig RA, Fishman NO. Risk factors for postcraniotomy surgical site infection after 1,3-bis (2-chloroethyl)-1-nitrosourea (gliadel) wafer placement. Clin Infect Dis 2003;36:759-65.
50. Weber EL, Goebel EA. Cerebral edema associated with gliadel wafers: two case studies. Neurol Oncol 2005;7:84-9.
51. Engelhard HH. Tumor bed cyst formation after BCNU wafer implantation: report of two cases. Surg Neurol 2000;53:220-4.
52. Kleinberg LR, Weingart J, Burger P, Carson K, Grossman SA, Li K, *et al.* Clinical course and pathologic findings after gliadel and radiotherapy for newly diagnosed malignant glioma: implications for patient management. Cancer Invest 2004;22:1-9.
53. Shome D, Poddar N, Sharma V, Sheorey U, Maru GB, Ingle A, *et al.* Does a nanomolecule of carboplatin injected periocularly help in attaining higher intravitreal concentrations? Invest Ophthalmol Vis Sci 2009;50:5896-900.
54. Olivi A, Grossman SA, Tatter S, Barker F, Judy K, Olsen J, *et al.* Dose escalation of carmustine in surgically implanted polymers in patients with recurrent malignant glioma: a new approaches to brain tumor therapy CNS consortium trial. J Clin Oncol 2003;21:1845-9.
55. Sharma A, Sharma US. Liposomes in drug delivery: progress and limitations. Int J Pharm 1997;154:123-40.
56. Alexis F, Pridgen E, Molnar LK, Farokhzad OC. Factors affecting the clearance and biodistribution of polymeric nanoparticles. Mol Pharm 2008;5:505-15.
57. Masserini M. Nanoparticles for brain drug delivery. ISRN Biochem 2013;2013:1-18.
58. Ferroni L, Gardin C, Puppa DA, Sivolella S, Brunello G, Scienza R, *et al.* Novel nanotechnologies for brain cancer therapeutics and imaging. J Biomed Nanotechnol 2015;11:1899-912.
59. Hemant K, Raizaday A, Sivadasu P, Uniyal S, Kumar SH. Cancer nanotechnology: nanoparticulate drug delivery for the treatment of cancer. Int J Pharm Pharm Sci 2015;7:40-6.
60. Sonavane G, Tomoda K, Makino K. Biodistribution of colloidal gold nanoparticles after intravenous administration: effect of particle size. Colloids Surf B 2008;66:274-80.
61. Etame AB, Smith CA, Chan WC, Rutka JT. Design and potential application of PEGylated gold nanoparticles with size-dependent permeation through brain microvasculature. Nanomedicine 2011;7:992-1000.
62. Hanada S, Fujioka K, Inoue Y, Kanaya F, Manome Y, Yamamoto K. Cell-based *in vitro* blood-brain barrier model can rapidly evaluate nanoparticles brain permeability in association with particle size and surface modification. Int J Mol Sci 2014;15:1812-25.
63. Williams PM, Oatley-Radcliffe DL, Hilal N. Feed solution characterization. In: Hilal N, Ismail AF, Matsuura T, Oatley-Radcliffe D. editors. Membrane characterization. Elsevier; 2017. p. 379-404.
64. Uskokovic V. Dynamic light scattering based microelectrophoresis: main prospects and limitations. J Dispers Sci Technol 2012;33:1762-86.
65. Gatenby RA, Gillies RJ. Why do cancers have high aerobic glycolysis? Nat Rev Cancer 2004;4:891-9.
66. Webb BA, Chimenti M, Jacobson MP, Barber DL. Dysregulated pH: a perfect storm for cancer progression. Nat Rev Cancer 2011;11:671-7.
67. Kitamura I, Kochi M, Matsumoto Y, Ueoka R, Kuratsu J, Ushio Y. Intrathecal chemotherapy with 1,3-bis(2-chloroethyl)-1-nitrosourea encapsulated into hybrid liposomes for meningeal gliomatosis: an experimental study. Cancer Res 1996;56:3986-92.
68. Chen PY, Liu HL, Hua MY, Yang HW, Huang CY, Chu PC, *et al.* Novel magnetic/ultrasound focusing system enhances nanoparticle drug delivery for glioma treatment. Neurol Oncol 2010;12:1050-60.
69. Tapeinos C, Battaglini M, Ciofani G. Advances in the design of solid lipid nanoparticles and nanostructured lipid carriers for targeting brain diseases. J Controlled Release 2017;264:306-32.
70. Zhang F, Xu CL, Liu CM. Drug delivery strategies to enhance the permeability of the blood-brain barrier for treatment of glioma. Drug Des Dev Ther 2015;9:2089-100.
71. Bhujbal SV, de Vos P, Niclo SP. Drug and cell encapsulation: alternative delivery options for the treatment of malignant brain tumors. Adv Drug Delivery Rev 2014;67-68:142-53.

PLAGIARISM REPORT

ANALYSIS OF NEURONAL SURVIVAL IN THE PRESENCE OF VARIOUS STRESS CONDITIONS AND TARGETED DELIVERY

by Athmakur Hari Kiran

Submission date: 20-Jun-2019 11:30AM (UTC+0530)
Submission ID: 1145473636
File name: (9.08M)
Word count: 26406
Character count: 161850

ANALYSIS OF NEURONAL SURVIVAL IN THE PRESENCE OF VARIOUS STRESS CONDITIONS AND TARGETED DELIVERY

ORIGINALITY REPORT

4%	2%	3%	4%
SIMILARITY INDEX	INTERNET SOURCES	PUBLICATIONS	STUDENT PAPERS

PRIMARY SOURCES

1	Farhan Ahmed, Mohammad Javed Ali, Anand K. Kondapi. "Carboplatin loaded protein nanoparticles exhibit improve anti-proliferative activity in retinoblastoma cells", International Journal of Biological Macromolecules, 2014 Publication	<1%
2	stemcellres.biomedcentral.com Internet Source	<1%
3	Submitted to Jawaharlal Nehru Technological University Student Paper	<1%
4	Submitted to National University of Singapore Student Paper	<1%
5	Submitted to University of Hull Student Paper	<1%
6	Submitted to University of Hong Kong Student Paper	<1%
7	www.oncotarget.com Internet Source	